Molecular Characterization of the Organellar-Type Alkali Cation/Proton Exchanger NHE6

by

Alina Ilie

Department of Physiology
Faculty of Medicine
McGill University
Montreal

August 2010

A thesis submitted to the Faculty of Graduate Studies and Research in partial fulfillment of the requirements for the degree of Doctor of Philosophy

ABSTRACT

Mammalian alkali cation/proton exchangers, more commonly known as sodium/proton exchangers (NHEs) are a family of transmembrane proteins that mediate an electroneutral exchange of Na^+ (or K^+) and protons across cellular membranes, thereby regulating intracellular pH and volume homeostasis. Eleven different isoforms have been identified, which differ in their tissue distribution, subcellular localization, and function. The organellar-type NHE6 isoform is widely distributed in tissues, but is enriched in brain, heart, and muscle.

In order to elucidate the native distribution of NHE6 and to identify some of the mechanisms underlying its trafficking and function, a rabbit polyclonal antibody was generated. Utilizing this antibody in polarized human SH-SY5Y neuroblastoma cells, endogenous NHE6 was detected in transferrin receptor-containing vesicles in the soma and neurite processes. In mouse hippocampal organotypic slice cultures, NHE6 was detected within the soma, as well as dendritic shafts and spines of CA1 pyramidal cells. Ultrastructural analysis of mouse hippocampus and cortex revealed the presence of NHE6 positive signals predominantly in dendrites, occasionally adjacent to postsynaptic densities, and to a minor extent in some presynaptic terminals.

N-glycosylation of proteins is involved in different aspects of protein function, such as folding, trafficking, stability and activity. To identify the glycosylation site(s) and their potential role in NHE6 function, mutagenesis analysis in combination with different biochemical assays and confocal microscopy were used. Our results revealed that asparagine 128 is the sole target for the N-glycosylation of the transporter. Furthermore, glycosylation was involved in promoting efficient export of the exchanger to the cell surface and for optimal transport activity within recycling endosomes.

The NHEs have been shown to be regulated in part through the interaction of the cytosolic C-terminal domain with numerous interacting partners, depending on the isoform. In order to identify novel interacting proteins involved in the regulation of NHE6, a yeast two-hybrid screen of a human brain cDNA library was conducted using the C-tail of NHE6 as bait. Two of the clones identified encoded the receptor for activated protein kinase C 1 (RACK1), a scaffolding protein involved in numerous protein interactions and biological functions. Direct interaction of these two proteins was confirmed *in vitro* and *in vivo*. Depletion of RACK1 by siRNA resulted in increased total cellular expression and cell surface abundance of NHE6.

Recently mutations in NHE6 have been linked to X-linked mental retardation, with a phenotype closely resembling that of Angelman syndrome. One of the mutations resulted in deletion of two residues (Glu255/Ser256) in the predicted transmembrane domain seven. To investigate the molecular mechanisms underlying the phenotype observed, we generated epitope-tagged variants of NHE6 bearing the deletion and showed that they display deficient processing and maturation, as well as markedly reduced stability in cells. Furthermore, the mutant protein is mislocalized in cells and targeted to an ill-defined acidic compartment. Preliminary results show that depletion of NHE6 in neurons resulted in decreased dendritic branching and disappearance of dendritic spines. We propose that the mutant protein is non-functional; thereby vesicular trafficking is impaired, resulting in deficient dendritic spine growth and maintenance.

RÉSUMÉ

Les échangeurs de Na^+/H^+ (NHEs) sont des protéines transmembranaires qui catalysent l'échange électroneutre de Na^+ (ou K^+) et de protons à travers les membranes cellulaires, régulant ainsi le pH intracellulaire et l'homéostasie du volume cellulaire. Jusqu'à présent, on été identifié onze isoformes, qui diffèrent dans leur distribution tissulaire, localisation subcellulaire, et leur fonction. L'isoforme NHE6 est largement distribué dans les tissus, mais il est plus exprimé dans le cerveau, le cœur et les muscles.

Afin de déterminer la distribution native du NHE6 et d'identifier certains des mécanismes sous-jacents de son trafic et de sa fonction, on a crée un anticorps polyclonal. En utilisant celui-ci pour le marquage des cellules polarisées SH-SY5Y de neuroblastome, le NHE6 endogène a été détecté dans des vésicules contenant le récepteur de la transferrine, dans le corps cellulaire (soma) et au niveau des neurites. Dans des cultures cellulaires de l'hippocampe, le NHE6 a été détecté dans le soma et dans les dendrites ainsi que dans les épines des cellules pyramidales CA1

L'analyse ultrastructurale de l'hippocampe et du cortex de souris a révélé la présence des signaux positifs de NHE6 principalement dans les dendrites, parfois à côté de la région post-synaptique hyperdense, et dans une moindre mesure dans certaines terminaisons présynaptiques.

La N-glycosylation des protéines est impliquée dans de différents aspects de la fonction des protéines, comme le pliage, le trafic, la stabilité et l'activité. Pour identifier les sites de glycosylation et leur rôle potentiel dans la fonction de NHE6, ont a utilisé la mutagenèse, en combinaison avec différents dosages biochimiques et la microscopie confocale. Nos résultats ont révélé que l'asparagine 128 est la seule cible de la N-glycosylation du transporteur. En outre, nous avons démontré que la glycosylation est nécessaire pour l'exportation efficace de l'échangeur à la surface cellulaire, ainsi que pour une l'activité optimal dans les endosomes de recyclage.

Afin d'identifier des nouvelles protéines impliquées dans la régulation de NHE6, nous avons utilisé un système de double-hybride de levure. On a dentifiés deux clones qui codent le récepteur de la protéine kinase C (RACK1), une protéine d'échafaudage impliquée dans les interactions entre protéines. L'interaction directe de ces deux protéines a été confirmée *in vitro* et *in vivo.* L'utilisation de siRNA contre RACK1 conduit à une augmentation de l'expression cellulaire et de la densité sur la surface cellulaire du NHE6.

Récemment, des mutations dans NHE6 ont été liées à un syndrome ressemblant à celui du syndrome d'Angelman. Une de ces mutations conduit a la suppression de deux résidus (Glu255/Ser256) dans le domaine sept transmembranaire. Pour étudier les mécanismes moléculaires sous-jacents au phénotype observé, nous avons généré des variantes de NHE6 portant la suppression, qui on montré une maturation inadéquate, ainsi qu'une stabilité réduite dans les cellules. En outre, la protéine mutante est mal-localisée dans les cellules et se trouve dans un compartiment acide mal défini. Des résultats préliminaires montrent que l'utilisation de siRNA contre NHE6 entraine une baisse de ramification dendritique, ainsi que la disparition d'épines dendritiques dans des neurones. Nous proposons que la protéine mutante n'est pas fonctionnelle, et que le trafic vésiculaire intracellulaire est altéré, ce qui peut entraîner une déficience dans le développement de dendrites.

ACKNOWLEDGMENTS

I would like to start by thanking my supervisor, Dr. John Orlowski for accepting me to work in his lab. I am deeply grateful for all his support and guidance during these years, as well as for giving me the freedom to ask my own questions and find my own answers, and for his essential contribution in my formation as a rigorous scientist. Working in the family-like environment of the JO lab was a truly pleasant experience.

I also would like to thank the members of my supervisory committee, Drs. Ursula Stochaj, Julie Desbarats and John Hanrahan for their advice and support during my research.

I would like to extend my gratitude to all the members of the JO lab, past and present for all their help and friendship; Dr. Viktoria Lukashova who taught me most of the techniques in the lab; Annie Boucher, not only for her technical support, but also for her help and advice on a personal level; Hans Zaun, the most altruistic person I have met; my bench neighbor Tush for trying to cheer me up when I was under the weather; my friend Albena Davidova; and the newest member of our lab, Cassandra McEwan, for all her positive energy and friendship. I would also like to acknowledge the members of the Shrier lab for discussions and help with reagents and protocols, in particular Roxana Atanasiu for her generosity and constant support, but also Val, Hung, Perrine, and Christine.

I am indebted to Drs. Gergely Lukacs and Hervé Barriere for their collaboration and help on the pH measurements. Many thanks to Dr. Anne McKinney for her kindness and interesting collaboration; and to Emily Deane, my NHE6 partner in the McKinney lab.

I would also like to thank Dr. Claire Brown for her truly professional support with confocal microscopy, Joanne Ouellete for her technical assistance with the electron microscopy experiments and Ken

McDonald for help with flow cytometry. A special thanks to Domnica for her honesty and full support.

I am grateful to Dr. Richard Tomlinson for his important financial support during my studies.

Finally, I would like to thank my husband Emil, my parents and my brother for all their support, encouragement, and love.

My sincere apologies to all those who made contributions to this thesis and I failed to mention here.

CONTRIBUTIONS OF AUTHORS

Chapter 1:
Alina Ilie, Emily Deane, Viktoria Lukashova, Rebecca Anne McKinney, and John Orlowski. *Subcellular Localization of the Organellar Sodium/Proton Exchanger 6 Isoform Assessed by Light and Electron Microscopy*.
All experiments were designed and performed by A. Ilie, except for the experiments in Figure 6, which were conducted by E. Deane under the supervision of Dr. RA McKinney. V. Lukashova helped with the preparation of samples for electron microscopy of mouse brain. The study was coordinated and supervised by Dr. J. Orlowski.
.

Chapter 2:
Alina Ilie, Hervé Barriere, Gergely Lukacs, and John Orlowski. *Roles of N-Glycosylation in the Function of the Mammalian Sodium/Proton exchanger NHE6.*
All experiments were designed and performed by A. Ilie, except for the experiments in Figure 7, which were designed by Dr. H. Barriere and conducted by Dr. H. Barriere and A. Ilie under the supervision of Dr. G. Lukacs. The study was coordinated and supervised by Dr. J. Orlowski.

Chapter 3:
Alina Ilie, Albena Davidova, and John Orlowski. *RACK1 Binds to the Recycling Endosomal Na^+/H^+ Exchanger NHE6 and Limits its Accumulation at the Cell Surface*
All experiments were designed and performed by A. Ilie. A. Davidova constructed the GST fusion proteins of the RACK1 WD domains. The study was coordinated and supervised by Dr. J. Orlowski.

Chapter 4:
Alina Ilie, Herve Barriere, Emily Deane, Annie Boucher, Rebecca Anne McKinney, Gergely Lukacs and John Orlowski. *Angelman Syndrome-Linked Mutations in the Alkali Cation/Proton Exchanger NHE6 Disrupt its Maturation, Stability, and Trafficking.*
All experiments were designed and performed by A. Ilie, except for the experiments in Figure 8, which were designed and conducted by Dr. H. Barriere and A. Ilie under the supervision of Dr. G. Lukacs; and except for the experiments in Figure 12, which were performed by E. Deane and supervised by Dr. RA McKinney. A. Boucher helped with the construction of the mutant forms of NHE6 and with the endocytosis assay in Figure 4. Dr. J. Orlowski coordinated and supervised the study.

N.B. All these manuscripts are in preparation for publication.

ORIGINAL CONTRIBUTIONS TO KNOWLEDGE

- NHE6 is distributed not only in endosomes, but also along plasma membrane microvillar-like protrusions and filopodia, when expressed in fibroblast cells and examined by electron microscopy.

- Endogenous NHE6 is present in transferrin receptor-containing recycling endosomes in the soma and neurites of human neuroblastoma SH-SY5Y cells in culture.

- Native NHE6 is localized in vesicles within the soma and dendrites, and in particular in dendritic spines of hippocampal and cortical mouse neurons, suggesting its involvement in synapse formation and plasticity.

- NHE6 is N-glycosylated at asparagine 128. Glycosylation of the transporter is involved in its trafficking to the plasma membrane and optimal activity within recycling endosomes. Endosomal targeting and stability of NHE6 are glycosylation-independent.

- The total cellular expression and cell surface abundance of NHE6 are restricted by its interaction with the receptor for activated protein kinase C 1 (RACK1). RACK1 binds directly to residues 520-565 of the cytoplasmic C-tail of NHE6. NHE6 can interact with multiple WD domains of RACK1.

- The double deletion mutant ΔE287-S288 of NHE6, which has been associated with an Angelman-like syndrome, displays deficient maturation and greatly reduced stability upon expression in cells. The total and cell surface abundance, as well as the internalization rate of the mutant are diminished compared to the wild-type protein. The mutant protein is mislocalized in cells and is targeted predominantly to large endomembrane structures, possible aggregates of vesicles that are present mostly along the periphery of the cell and to a lesser extent

intracellularly. These vesicles are highly acidic and do not express the lysosomal marker LAMP-2.

- NHE6/ΔE287-S288 expression in non-neuronal cells impairs the clathrin-mediated recycling endosomal pathway, as evidenced by decreased uptake of transferrin, dispersal of the perinuclear recycling compartment, and disruption of the F-actin cytoskeleton.

- Preliminary results show that depletion of NHE6 in neurons resulted in decreased dendritic branching and disappearance of dendritic spines, indicating an essential role for NHE6 in normal spine morphogenesis.

ABBREVIATIONS

AS	Angelman syndrome
Asn, N	asparagine
ATCC	American type culture collection
ATP	adenosine tri phosphate
CHO	chinese hamster ovary
CHP1/2	calcineurin B homologous protein
CPA	cation proton antiporter
DOCK3	dedicator of cyclokinesis 3
DTT	dithioltreitol
ERK	extracellular signal-regulated kinase
FRIA	fluorescence ratio imaging analysis
GFP	green fluorescent protein
Glu, E	glutamic acid
GST	glutathione S-transferase
HEK 293	human embryonic kidney 293
IgG	immunoglobulin G
IPTG	isopropyl-β-D-thiogalactopyranoside
kDa	kilo-dalton
LE	late endosome
MW	molecular weight
NHE	sodium/proton exchanger
NHERF1/2	sodium/proton exchanger regulatory factor
OD	optical density
PBS	phosphate buffer saline
PFA	paraformaldehyde
PKC	protein kinase C
PSD	post-synaptic density
PVC	pre-vacuolar compartment
PVDF	polyvinylidene difluoride
RACK1	receptor for activated C-kinase 1
SCAMP	secretory carrier membrane protein
SDS	sodium dodecyl sulphate
SDS-PAGE	SDS-polyacrylamide gel electrophoresis
Ser, S	serine
Tfn-R	transferrin receptor
TGN	*trans*-Golgi network
Y2H	yeast two-hybrid
α-MEM	α-minimum essential medium

TABLE OF CONTENTS

LIST OF FIGURES

GENERAL INTRODUCTION

Strict regulation of pH is essential for all living organisms, as changes in pH affect the ionization state of all weak acids and weak bases in cells, which include cellular peptides and proteins. Furthermore, all proteins are dependent on pH to maintain their optimal structure and function (Roos and Boron, 1981).

Because of its important role, cells are equipped with various means to control and maintain optimal pH. Acute changes in pH are prevented by the inherent pH buffering capacity of cells, which is provided by intracellular weak acid and bases, like phosphate groups and side chains of amino acids, as well as by bicarbonate ions. However, these mechanisms are insufficient to counteract the continuous production of metabolic acid equivalents and cells must actively extrude excess protons from the cytosol. This is accomplished by a variety of transporters, including exchangers (antiporters) or co-transporters (symporters), which couple the transport of protons to other substrates. The main families of transporters involved in extrusion of excess protons from cells are the alkali cation/H^+ exchangers, the monocarboxylate transporters and the mammalian Na^+-coupled bicarbonate transporters (Casey et al., 2010). In addition to proton extruding mechanisms, cells also rely on acid-loading transporters to finely control their internal pH and volume. The most important acid-importing transport system is represented by $Cl^-/HCO3^-$ exchangers, which include two distinct families: SLC4A or anion exchangers (AE1-AE3) and SLC26A proteins (Cordat and Casey, 2009). These exchangers use the inward gradient of Cl^- to extrude bicarbonate from the cell, thereby contributing to the control of pH, regulation of fluid movement, and acid/base secretion (Casey et al., 2010).

The present study is focused on the family of alkali cation/H^+ exchangers, also known as Na^+/H^+ exchangers or NHEs. These are secondary active, electroneutral transporters, which mediate the exchange

of Na^+ or K^+ and H^+ down their respective electrochemical gradients. Members of this family are conserved from bacteria to yeast, plants and mammals (Orlowski and Grinstein, 2004). Mammalian NHEs are transmembrane (glycol)phosphoproteins, which differ in their tissue distribution, subcellular localization and drug sensitivity. Eleven different isoforms have been identified up to date in mammals. According to their subcellular localization and structure homology, the NHEs can be subdivided into three general categories: plasma membrane-type NHEs (NHE1 to NHE5), organellar-type NHEs (NHE6-NHE9), as well as bacterial-like NHEs (NHA1 and NHA2) (Casey et al., 2010).

Mammalian NHEs share ~25-70% identity overall, with 40-60% identity amongst the plasma membrane isoforms NHE1-NHE5 and 60-70% amongst the endomembrane isoforms NHE6-NHE9. NHE8 shows the least similarity to the other organellar NHEs, with only ~25% identity (Orlowski and Grinstein, 2007). NHA1 and NHA2 are more distantly related to the NHEs (~13% identity) and show closer homology to the fungal NHA1 and bacterial NhaA Na^+/H^+ antiporters (Brett et al., 2005a) (Fig. 1).

1.1 PHYLOGENETIC ANALYSIS OF Na^+/H^+ EXCHANGERS

Brett et al. (2005) performed an extensive analysis of the evolutionary origins of eukaryotic sodium/proton exchangers (NHEs) in order to better understand their physiological functions. This study revealed that NHEs are members of the larger monovalent cation proton (CPA) superfamily, which consists of three main gene families: CPA1, CPA2 and bacterial NaT-DC (Na^+-transporting carboxylic acid decarboxylase). The CPA2 family is represented by prokaryotic transporters, as well as by the plant CHX and the yeast NHA1/SOD2

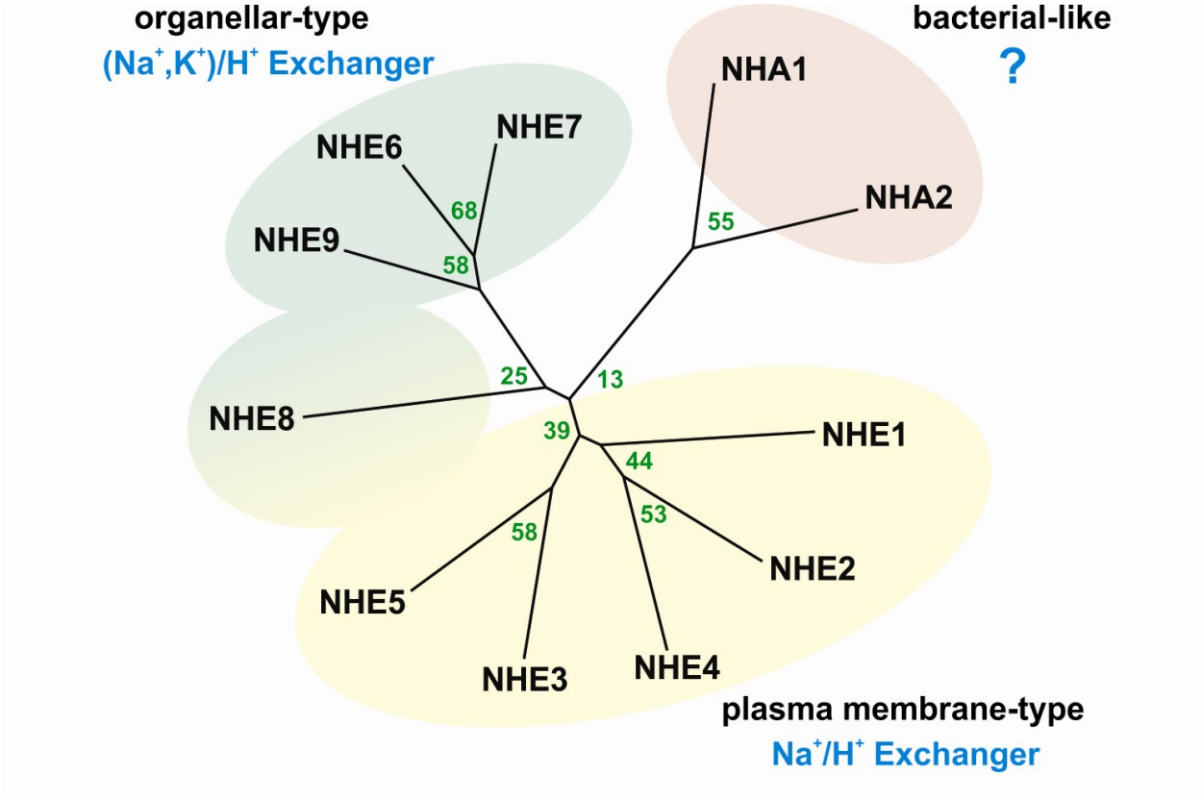

Figure 1. Phylogenetic relationships of human alkali cation/proton exchangers determined by multiple sequence alignments. Adapted from Orlowski and Grinstein (2007).

family of Na^+, K^+/H^+ exchangers. These transporters are localized in the plasma membrane and are important for cytoplasmic Na^+, K^+, and pH homeostasis (Banuelos et al., 2002; Prior et al., 1996; Sychrova et al., 1999). Moreover, Brett et al. identified for the first time a family of new CPA2 genes in animals, which they named NHA based on their similarity to fungal NHA1 and bacterial NhaA transporters. The two human NHA orthologs discovered (NHA1 and NHA2) are most similar to the NHE (SLC9A) genes of the CPA1 family and are found in tandem on chromosome 4.

The CPA1 family evolved from the prokaryotic NhaP genes, and is represented by bacterial NhaP transporters, plant plasma membrane SOS (salt overly sensitive) antiporters, and the eukaryotic NHE transporters (Brett et al., 2005a). The members of the eukaryotic NHE gene family are the best characterized CPA1 transporters and can be divided into two main clades, based on their principal subcellular localization: intracellular and plasma membrane. Based on sequence similarity, the intracellular clade can be further subdivided into three subgroups termed endosomal/TGN, plant vacuolar (present exclusively in the vacuolar membranes of plant cells), and NHE8-like. Moreover, the sperm-specific Na^+/H^+ exchangers required for sperm motility and fertility in mouse (Wang et al., 2003), rat, macaque, and human do not cluster with other mammalian NHE genes and are only distantly similar to the NaT-DC clade (Brett et al., 2005a).

One of the oldest members of the endosomal/TGN clade is the *Saccaromyces cerevisiae* NHX1 (Nass et al., 1997), which is located in prevacuolar/endosomal compartments and is involved in salt tolerance, osmoregulation, pH regulation, and vesicle trafficking (Ali et al., 2004; Bowers et al., 2000; Brett et al., 2005b; Nass and Rao, 1999). Three human orthologs of ScNHX1 have been identified, termed NHE6 (Numata et al., 1998), NHE7 (Numata and Orlowski, 2001), and NHE9 (de Silva et al., 2003). Although experimental evidence is scarce, by analogy with the

yeast NHX1, the human orthologs are thought to regulate organellar pH and volume homeostasis through functional coupling to the H^+ gradient established by the vacuolar H^+-ATPase (Orlowski and Grinstein, 2007).

The role of the NHE8-like clade, which originated from the slime mold *Dictyostelium discoideum*, is even less understood. It has a single ortholog in mammals, NHE8, but no members in plants, suggesting a unique physiological role. The plasma membrane clade of NHE genes contains two subgroups, named recycling and resident (Brett et al., 2005a). The recycling plasma membrane NHEs derive their name from the fact that they cycle between the plasma membrane and endosomes. They seem to be older, as they have members in nematodes and mammals, including the two human paralogs NHE3 (Tse et al., 1992) and NHE5 (Klanke et al., 1995). On the other hand, the resident plasma membrane NHEs have emerged later in evolution, as they are exclusively found in vertebrates and have evolved simultaneously with the Na^+/K^+-ATPase, which creates the Na^+ gradient necessary for their function. The resident plasma membrane group is represented in humans by three paralogs, NHE1 (Sardet et al., 1989), NHE2, and NHE4 (Orlowski et al., 1992).

This detailed phyologenetic analysis of Brett et al. (2005) lead to the novel conclusion that the first eukaryotic NHEs were intracellular transporters, whereas the plasma membrane subgroup appeared more recently in evolution to fulfill functions specific to higher eukaryotes, as it is present exclusively in vertebrates and has no orthologs in yeast or plants.

1.2 STRUCTURAL FEATURES OF Na^+/H^+ EXCHANGERS

Based on hydropathy analysis and computer modeling, all NHEs are predicted to share a common membrane topology, with twelve membrane spanning domains at the N-terminus and a cytoplasmic C-

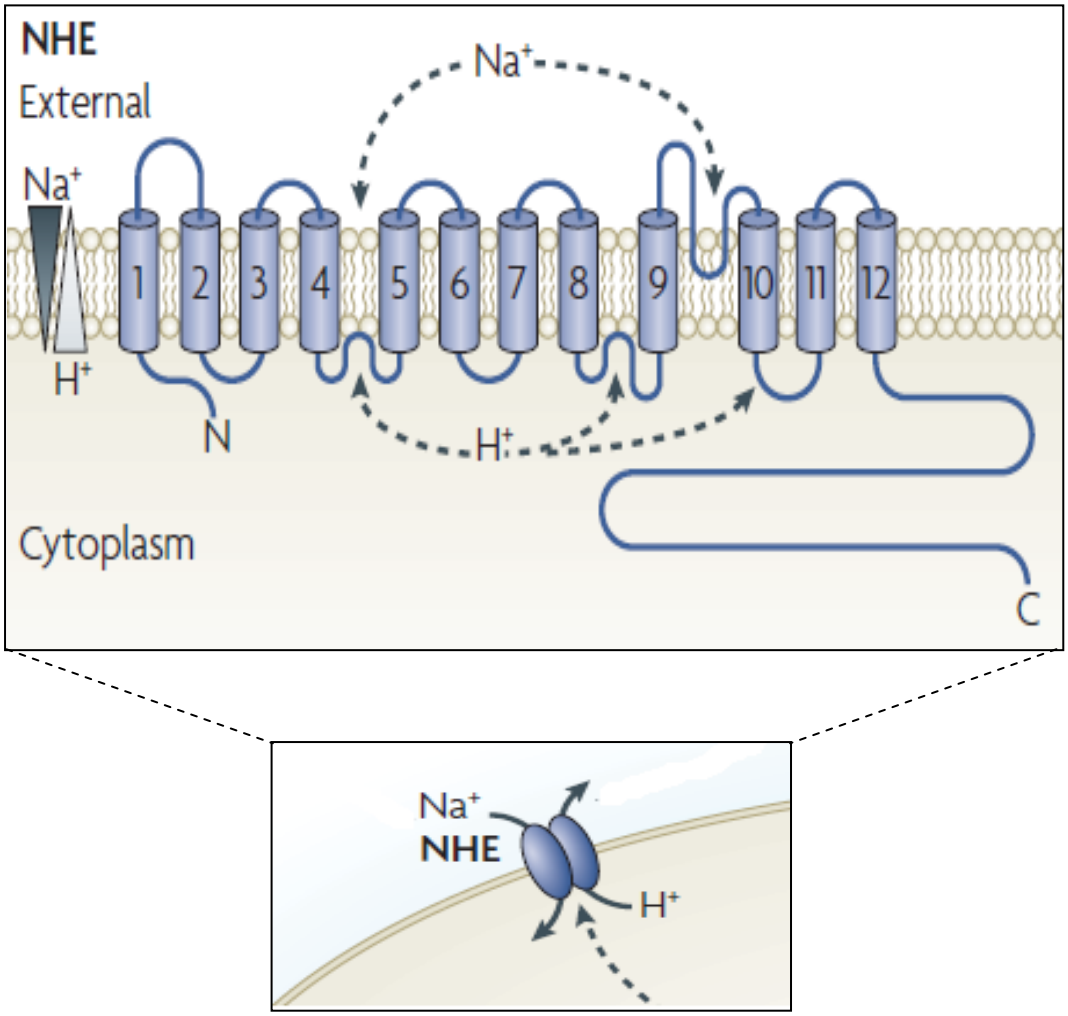

Figure 2. Predicted membrane topology of mammalian alkali/cation proton exchangers. Adapted from Casey JR, Grinstein S, and Orlowski J, Nat Rev Moll Cell Biol, 2010.

terminal domain of varying length (Fig. 2). The N-terminal domain shares a greater similarity among the NHE isoforms, whereas the hydrophilic C-terminus is more divergent and contains consensus phosphorylation sites and binding sites for numerous interacting partners with regulatory functions (Orlowski and Grinstein, 2004).

Using a series of deletion mutants of the C-terminal domain of NHE1, Wakabayashi et al. (1992) established that the ion translocation site is located within the transmembrane N-terminal domain, and that the C-terminus acts as a regulatory domain that determines the set point value and mediates growth factors signals (Wakabayashi et al., 1992). A more refined model of NHE1 topology using cysteine accessibility analysis showed that parts of the second and fourth intracellular loop are accessible to external SH-directed reagents, suggesting that they be part of the ion translocation pore (Wakabayashi et al., 2000). Furthermore, residues within transmembrane helices TM4 and TM9 are essential for the binding of pharmacological antagonists (Khadilkar et al., 2001).

Certain amino acid residues in the transmembrane domain are conserved and essential for the function of all NHE isoforms. This is the case for Glu355 of *Saccharomyces cerevisiae* Nhx1. This residue is conserved in both plasma membrane and organellar NHE and is located in the loop region between transmembrane segments 9 and 10, which is folded within the protein and is predicted to form a re-entrant loop (Sato et al., 2004; Mukherjee et al., 2006). Mutation of Glu355 to alanine resulted in complete loss of Nhx1 function, whereas the conservative substitution to glutamine largely restored function. Similar to the findings in yeast, substitution of the equivalent Glu391 in human NHE1 with glutamine decreased NHE1 function, as measured by the rate of pH recovery from an acute acid load in AP-1 cells expressing the mutant transporter (Murtazina et al., 2001). Other residues (Phe357 and Tyr361) are conserved only among the organellar NHEs and their substitution by the corresponding amino acids from plasma membrane NHE1 resulted in loss

of function, indicating a structural specificity in this region which is important to maintain function (Mukherjee et al., 2006).

In addition, high amino acid conservation was observed in transmembrane regions 3-4, a region important for ion selectivity and drug sensitivity. Residue Leu163 of NHE1 in this region has been shown to be involved in amiloride sensitivity (Counillon et al., 1997; Khadilkar et al., 2001; Yun et al., 1993) and is replaced with the polar amino acid asparagine in organellar NHE isoforms. This might explain, at least in part, the insensitivity of human NHE7 (Numata and Orlowski, 2001) and of *Saccharomyces cerevisiae* Nhx1 (Darley et al., 2000) to amiloride. Furthermore, plant vacuolar NHE orthologs, which are known to be sensitive to amiloride contain an isoleucine residue at this position (Qiu et al., 2003; Venema et al., 2002).

In contrast to the relatively high degree of conservation of the N-terminal domain among NHE isoforms, the C-terminal domain, which is important in the regulation of transport activity, is more variable in length and amino acid sequence. Interestingly, the C-tail is considerably shorter in organellar NHEs (199±46 residues) compared to their plasma membrane counterparts (365±52 residues). Considering that plasma membrane NHEs have evolved more recently, it has been suggested that this increase in C-tail length may correlate with an increased complexity of interactions with regulatory proteins and with the cytoskeleton (Brett et al., 2005a). Although substituted cysteine accessibility analysis predicted that the human NHE1 C-terminal tail is located entirely in the cytosol (Wakabayashi et al., 2000), some studies have suggested that certain epitopes in rat NHE1 (Khan, 2001) and rabbit NHE3 (Biemesderfer et al., 1998) are exposed extracellularly. Likewise, the presence of *N*-linked glycosylation in the C-terminus of *Saccaromyces cerevisiae* Nhx1 predicts that at least some portion of the tail is exposed to the lumen of the prevacuolar compartment (Wells and Rao, 2001). Additionally, topological analysis by protease protection assays of the plant AtNHX1 revealed that

almost the entire C-terminal domain is located in the vacuolar lumen (Yamaguchi et al., 2003).

There is little experimental evidence regarding the tertiary and quaternary structure of mammalian NHEs. The only crystal structure of a cation/proton antiporter solved up to now is that of the *E. coli* Nha transporter (Hunte et al., 2005). The 3.45 Å resolution structure showed the presence of 12 transmembrane segments with N- and C-termini exposed to the cytoplasm. In cross-section, a cytoplasmic and a periplasmic funnel that point toward each other are visible, but are separated by a hydrophobic barrier. A cluster of negatively charged residues at the entry of the cytoplasmic funnel functions probably as the ionic trap and at the same time as the 'pH sensor'. The authors suggest that a pH signal will be detected at this site and will induce a conformational change, resulting in the activation of the exchanger by exposing ionizable residues in another cluster involved in ion translocation (Olkhova et al., 2006; Olkhova et al., 2007; Olkhova et al., 2009) .

Biochemical studies using cross-linkers suggested that NHE1 and NHE3 can form homodimers through interactions between transmembrane regions (Fafournoux et al., 1994) or the cytoplasmic C-domains, which in the case of NHE1 was suggested to control the pH-dependent regulation of the transporter (Hisamitsu et al., 2004). More recently, it has been shown that although individual subunits are active in the acidic pH range, dimerization of NHE1 is required for the functioning of the exchanger in the neutral pH range (Hisamitsu et al., 2007). The model that mammalian NHEs function as homodimers is further supported by the high resolution structure of the *Escherichia coli* Na^+/H^+ antiporter NhaA, which was solved by electron cryomicroscopy and shows that the transporter assembles as a dimer, with each monomer formed by 12 tilted bilayer-spanning helices (Williams, 2000). Additionally, limited kinetic studies in renal brush border membrane vesicles suggested that mammalian NHEs might form tetrameric complexes (Otsu et al., 1993).

1.3 CATION SELECTIVITY AND DRUG SENSITIVITY OF Na^+/H^+ EXCHANGERS

Under physiological conditions, the plasmalemmal NHEs mediate the exchange of extracellular Na^+ for intracellular H^+. Given their hyperbolic dependence on the extracellular Na^+ concentration, plasmalemmal NHEs contain a single binding site for Na^+. Their affinity constants for Na^+ range between 5 and 50 mM, which is well below the normal extracellular Na^+ concentration (~ 150 mM), excluding external Na^+ as a regulatory element (Orlowski and Grinstein, 2004). Other monovalent cations such as Li^+ and $NH4^+$, but not K^+, can also be translocated by plasmalemmal NHEs in exchange for H^+, although less efficiently (Aronson, 1985). On the other hand, organellar NHEs, such as the mammalian NHE7 (Numata and Orlowski, 2001), the yeast ScNhx1 (Brett et al., 2005b), and the plant AtNHX1 (Venema et al., 2002), are able to transport both Na^+ (or Li^+) and K^+ and presumably function as K^+/H^+ exchangers *in vivo*, given that K^+ is the predominant intracellular alkali cation. In contrast to Na^+, some plasmalemmal NHEs show a higher than first-order dependence on intracellular H^+ concentration, indicating the presence of a regulatory H^+ site in addition to the H^+ transport site (Aronson, 1985; Otsu et al., 1992). Indeed, some structural studies showed that the transmembrane domain contains a pH sensor, and the cytoplasmic region controls the pH set-point of the exchanger (Wakabayashi et al., 1992).

Different classes of pharmacological agents have been found to inhibit Na^+/H^+ exchange, including the diuretic compound amiloride and its analogues (Counillon et al., 1993a; Counillon et al., 1993b; Yun et al., 1993), benzoylguanidium-based derivatives (e.g., HOE642 or cariporide, HOE694) (Scholz et al., 1995; Rosskopf et al., 1995), as well as cimetidine, clonidine and harmaline (Orlowski, 1993; Szabó et al., 2000;

Yu et al., 1993; Masereel et al., 2003). While being chemically distinct, these compounds have either a pyrazine, an imidazoline, or a guanidine moiety, therefore bearing some similarity to each other. The sensitivity of NHEs to these inhibitors is isoform-specific, with NHE1 being the most sensitive (Orlowski and Grinstein, 2004).

The sites critical for both drug recognition and cation translocation have been identified within or surrounding transmembrane segments four and nine (Orlowski and Grinstein, 2004). The organellar NHEs are less sensitive to inhibition by amiloride, probably due to structural differences in the regions responsible for drug sensitivity and binding (Darley et al., 2000; Numata and Orlowski, 2001).

1.4 PLASMA MEMBRANE Na^+/H^+ EXCHANGERS

The plasma membrane-type NHEs use the electrochemical gradient of Na^+ generated by the Na^+-K^+-ATPases to preferentially mediate the electroneutral exchange of cytosolic protons for extracellular sodium ions (Casey et al., 2010), with a stoichiometry of 1:1 (Aronson, 1985) or 2:2 (Fuster et al., 2008a). They also can transport lithium ions in exchange for protons, albeit with lower translocation rates than sodium ions (Orlowski and Grinstein, 2007). Five plasma membrane isoforms have been identified in the human genome, which can be subdivided into a resident plasma membrane subgroup, localized exclusively on the cell surface (NHE1, NHE2, and NHE4) and a recycling plasma membrane subgroup, which are present mostly on the plasma membrane, but can cycle between the cell surface and a recycling endosomal compartment (NHE3 and NHE5) (Brett et al., 2005a).

1.4.1 Localization and Physiological Roles of Plasma Membrane Na^+/H^+ Exchangers

NHE1 is the best characterized member of the NHE family and was first cloned in 1989 by Sardet and colleagues (Sardet et al., 1989). It is present at the cell surface of most cell types, with some exceptions, such as renal α- and β-intercalated cells (Biemesderfer et al., 1992) and macula densa cells (Peti-Peterdi et al., 2000). NHE1 is located exclusively on the cell surface and in different cell types accumulates in discrete subdomains of the plasma membrane, such as the lamellipodia of fibroblasts (Grinstein et al., 1993), basolateral membranes of epithelia (Biemesderfer et al., 1992), and intercalated discs and T-tubules of cardiac myocytes (Petrecca et al., 1999).

Recent evidence showed that the NHE1 transcript can undergo alternative splicing to yield a protein that acts as Na^+/Li^+ exchanger but not as a Na^+/H^+ exchanger in human reticulocytes and erythrocytes. This variant is amiloride-insensitive and lacks amino acids Val^{78}-Phe^{176}, corresponding to transmembrane domains II-IV (Zerbini et al., 2003)

NHE1 is considered the housekeeping isoform and is responsible for maintaining cytosolic pH and regulating cell volume. The exchanger is activated when intracellular pH is decreased to critical level, extruding the excess protons and protecting the cell from the deleterious effects of acidification (Slepkov et al., 2007; Orlowski and Grinstein, 2007; Orlowski and Grinstein, 2004). NHE1 is also involved in regulating cell volume after osmotic shrinkage, as Na^+ influx is coupled to water and Cl^- uptake, restoring the cell volume to steady-state levels (Rotin and Grinstein, 1989). NHE1 is also involved in cell proliferation through its control of intracellular pH (Pouysségur et al., 1984; Kapus et al., 1994; Putney and Barber, 2003). NHE1 also plays a structural role as a regulator of cell morphology and focal adhesion assembly by remodelling the actin cytoskeleton and cell shape of fibroblasts. This effect appears to be

independent from the cation translocation function and is mediated via the association of the C-terminal tail with the cytoskeletal-associated proteins ezrin, radixin and moesin (ERM) (Denker et al., 2000). On the other hand, both anchoring to the actin cytoskeleton and the ion exchange activity of NHE1 are required for directional migration of fibroblast cells (Denker and Barber, 2002). Moreover, binding of NHE1 to ERM activated Akt and protected cells from apoptosis, implicating NHE1 as an important cell survival promoter (Wu et al., 2004). However, *in vivo*, the importance of NHE1 in these cellular processes is still under debate, as mice with null mutations in the *Nhe1* gene are viable at birth (Cox et al., 1997; Bell et al., 1999), suggesting the presence of compensatory mechanisms that allow embryogenesis to take place normally. Even though the embryonic development of *Nhe1*$^{-/-}$ mice appears to occur normally, the post-natal growth of these animals is significantly slower and they progressively develop a severe neurodegenerative phenotype, with locomotor ataxia, epileptic-like seizures, and significant mortality prior to weaning (Bell et al., 1999; Cox et al., 1997), indicating the importance of fine pH regulation for neuronal survival and function.

NHE1 has been implicated in the pathogenesis of cardiac and neural ischemia-reperfusion injury, as well as in cancer. During ischemia-reperfusion, the intracellular pH drops and NHE1 is acutely over-activated, resulting in intracellular Na^+ accumulation, which reduces extrusion of Ca^{2+} by the Na^+/Ca^{2+} exchanger or even reverses the exchange activity of this bidirectional transporter. This Ca^{2+} overload ultimately leads to tissue dysfunction (cardiac arrhythmias, altered synaptic transmission) and tissue damage (Karmazyn et al., 1999; White et al., 2000).

NHE1 has also been implicated in pH regulation in tumour cells, where it is necessary for the formation of invadopodia, which are structures allowing tumour cell migration and invasion (Cardone et al., 2005).

In contrast to NHE1, the other mammalian plasma membrane isoforms display a more restricted tissue distribution. NHE2-4 are expressed predominantly in epithelial cells of the kidney and gastrointestinal tract, but low levels are present in other tissues as well (Brant et al., 1995; Malakooti et al., 1999; Orlowski et al., 1992; Tse et al., 1992; Tse et al., 1993b; Wang et al., 1993). High levels of **NHE2** are present in apical membranes of cells in different segments of the kidney, such as cortical ascending limb, macula densa, distal convoluted tubules and connecting tubules (Chambrey et al., 1998; Peti-Peterdi et al., 2000). NHE2 is also present in gastric parietal cells, and is necessary for the long-term viability of parietal cells but is not required for acid secretion by these cells (Schultheis et al., 1998a).

NHE4 resides in the basolateral membrane of renal epithelial cells (Chambrey et al., 2001) and probably fulfills similar functions with NHE1, especially in the macula densa and intercalated cells of the cortical collecting duct, where expression of NHE1 could not be detected (Peti-Peterdi et al., 2000; Biemesderfer et al., 1992). NHE4 is also highly expressed in parietal and chief cells of the stomach (Rossmann et al., 2001) and deletion of the gene in mice resulted in impaired gastric acid secretion, with decreased number of parietal cells, loss of mature chief cells, and increased number of mucous and undifferentiated cells (Gawenis et al., 2005).

The expression of **NHE3** in the kidney is restricted to luminal membranes of discrete segments, such as the proximal tubule and the loop of Henle (Biemesderfer et al., 1997). Furthermore, NHE3 cycles between the plasma membrane and clathrin-associated subapical endosomes (Chow et al., 1999). Apart from its role in the maintenance of intravascular volume and pH homeostasis (Alexander and Grinstein, 2006), NHE3 plays a crucial role in sodium and fluid reabsorption by the proximal tubule, as well as an indirect role in bicarbonate reabsorption (Bobulescu and Moe, 2006). Accordingly, NHE3-null mice exhibit

decreased blood pressure, slight diarrhea and alkalinisation of the intestinal lumen, and sharply reduced bicarbonate and fluid reabsorption in the proximal tubule (Schultheis et al., 1998b). NHE3 is active not only at the plasma membrane, but also in the recycling endosomes where it gets internalized and contributes to luminal acidification (D'Souza et al., 1998; Gekle et al., 1999; Akhter et al., 2002). Its activity in endocytic vesicles has been shown to be crucial *in vivo* for receptor mediated endocytosis of proteins, such as albumin, from the lumen of the proximal tubule and subsequent delivery to the lysosomes (Gekle et al., 2004). The recycling of NHE3 between the plasma membrane and intracellular vesicles also serves as a mean of regulating NHE3 abundance at the cell surface (Orlowski and Grinstein, 2007; Alexander and Grinstein, 2009).

NHE5 is distinguished from the other plasmalemmal isoforms by its predominant expression in neuronal-enriched regions of the central nervous system (Baird et al., 1999; Attaphitaya et al., 1999). It shares high sequence homology with NHE3 (~50% amino acid identity) (Orlowski and Grinstein, 2004). Similar to NHE3, it is localized on the plasma membrane but can be internalized into recycling endosomes by clathrin-mediated endocytosis when stably expressed in Chinese hamster ovary cells (Szaszi et al., 2002). When transiently overexpressed in differentiated PC12 cells or in rat primary hippocampal neurons, NHE5 is distributed to the cell surface, but also in somatodendritic vesicles and synaptic-like vesicles (Szaszi et al., 2002). Its physiological role is unknown, but it has been proposed to regulate the pH of synaptic vesicles, and hence synaptic transmission (Orlowski and Grinstein, 2004). Interestingly, NHE5 is localized to chromosome region 16q22.1 (Klanke et al., 1995) that coincides with a locus linked to a late-onset form of autosomal dominant spinocerebellar ataxia, suggesting that NHE5 is a possible candidate gene in the development of this disease (Flanigan et al., 1996).

1.4.2 Regulation of Plasma Membrane Na^+/H^+ Exchangers

The regulation of NHE1 is complex and involves multiple factors. The transporter contains an internal pH-sensing regulatory site, also known as the H^+ modifier or H^+ sensor, which senses changes in intracellular pH and allosterically regulates the exchange activity, such that the activity increases sharply as the proton concentration rises in the cytosol and then is inhibited when the intracellular pH increases above 7.2 (Casey et al., 2010). In addition to this intrinsic regulation, NHE1 activity can be enhanced by numerous hormones and growth factors, resulting in alkalinisation of the cell and facilitation of certain biological processes. It is believed that many of these factors regulate the exchanger indirectly via phosphorylation of specific residues in the C-tail by multiple kinases. Thus, the p90rsk phosphorylates NHE1 directly at Ser703 (Takahashi et al., 1999), which promotes the binding of the scaffolding protein 14-3-3 (Lehoux et al., 2001). The 14-3-3 protein further acts as a scaffold for the assembly of other signalling molecules, such as MEK (mitogen-activated protein kinase/extracellular signal-regulated kinase kinase) kinases (Fanger et al., 1998). NHE1 is also activated by other kinases, including p160-Rho-associated kinase (ROK), which mediate signals from the integrin receptors that regulate cell adhesion and spreading (Tominaga et al., 1998; Tominaga and Barber, 1998), and Nck-interacting kinase (NIK), which transduces signals from the platelet-derived growth-factor (Yan et al., 2001). The mechanism by which phosphorylation regulates NHE1 activity remains unknown.

NHE1 activity is also controlled via interactions with numerous regulatory proteins, such as the Ca^{2+} binding proteins Ca^{2+}/calmodulin and the calcineurin B homologous proteins. Ca^{2+}/calmodulin binds to either a high affinity or a low affinity inhibitory site in the C-terminus of NHE1 (Wakabayashi et al., 1994). Binding to the high affinity site activates the transporter by abolishing an intramolecular auto-inhibitory interaction,

which usually reduces the affinity of NHE1 for intracellular protons (Wakabayashi et al., 1997). Three other Ca^{2+} binding proteins make up a family of EF-hand motif containing proteins called calcineurin B homologous proteins. These proteins, called CHP-1, -2, and -3 (also known as tescalcin) bind to the juxtamembrane region of the C-terminal segment of NHE1 and activate its transport activity (Pang et al., 2002; Pang et al., 2004; Pang et al., 2001; Zaun et al., 2008).

Although NHE1 does not require the energy of ATP directly to move ions across the membrane, it requires physiological levels of ATP for optimal function (Demaurex et al., 1997). Moreover, optimal activity of NHE1 is dependent on the association between two positively-charged clusters in its cytosolic C-terminus with plasmalemmal phosphatidylinositol 4,5-bisphosphate (PIP2). The dephosphorylation of PIP2 caused by cellular ATP depletion would abrogate this interaction and could thus explain the requirement of NHE1 activity for ATP (Aharonovitz et al., 2000).

The activity of NHE3 is regulated at multiple levels. Numerous hormones and physical factors such as osmolarity control the activity of the transporter via changes in phosphorylation, trafficking to and from the cell surface, interactions with regulatory proteins, and transcription (Hayashi et al., 2002; Alexander and Grinstein, 2009; Donowitz et al., 2009; He and Yun, 2010). For example, hormones that activate cAMP-dependent protein kinase (PKA), like parathyroid hormone, downregulate NHE3 activity through phosphorylation of specific serine residues (Azarani et al., 1995; Azarani et al., 1996; Kurashima et al., 1997; Zhao et al., 1999). Moreover, the activity and apical retention of NHE3 are tightly controlled by tethering to the actin cytoskeleton via PDZ-based adaptor proteins (NHERF1, NHERF2, PDZK1, MAST205, Shank2) and ezrin (Weinman et al., 2005; Thomson et al., 2005; Wang et al., 2006; Han et al., 2006; Cha et al., 2006).

There is limited information available regarding the regulation of the neuronal-enriched isoform NHE5. In Chinese hamster lung fibroblast PS120 cells expressing rat NHE5, the activation of protein kinase A or C, as well as hyperosmolarity, results in the inhibition of NHE5 activity (Attaphitaya et al., 2001). Likewise, inhibition of phosphatidylinositol 3'-kinase causes a pronounced decrease of trafficking and activity of NHE5, while disruption of the F-actin cytoskeleton with cytochalasin D has the opposite effects (Szaszi et al., 2002). In addition, the cell surface abundance of NHE5 is reduced upon its association with the adaptor proteins β-arrestins, which probably act to promote clathrin-mediated endocytosis of the exchanger (Szabó et al., 2005). The activity of NHE5 is also regulated by the scaffolding protein Receptor for Activated C-kinase 1 (RACK1), which binds directly to NHE5 in focal adhesions and activates its transport activity via integrin-dependent and independent pathways (Onishi et al., 2007). A recent study identified secretory carrier membrane protein 2 (SCAMP2) as a novel interacting partner of NHE5, which promotes the cell surface targeting and activity of the transporter in an Arf6-dependent manner (Diering et al., 2009).

1.5 ORGANELLAR Na^+/H^+ EXCHANGERS

The organellar NHEs have distinct tissue distribution and subcellular localization and are represented by multiple isoforms. Although the precise functions and regulatory mechanisms of the mammalian organellar NHEs remain poorly characterized, some valuable insights are provided by studies of their orthologs in yeast (in particular the *Saccharomyces cerevisiae* Nhx1) and plants (especially the *Arabidopsis thaliana* AtNHX1), suggesting that these transporters are essential for vesicular pH regulation and trafficking.

1.5.1 pH Regulation of Cellular Organelles

The pH of intracellular organelles is tightly regulated, and proton concentration can vary up to 100 fold between compartments. The vesicular pH becomes progressively more acidic in the endocytic pathway, from early endosomes (~pH 6.5) to lysosomes (pH < 5.5) (Demaurex, 2002) (Fig. 3). This progressive acidification is essential for the recycling and/or degradation of internalized membrane proteins and fluid-phase solutes, as well as for entry of microbial organisms (Mellman et al., 1986; Yamashiro and Maxfield, 1984; Huynh and Grinstein, 2007). Conversely, in the secretory pathway, the pH becomes more acidic as the cargo is transported to the cell surface, with the pH of the endoplasmic reticulum being near neutral (Kim et al., 1998) with increasing acidification along the Golgi complex, reaching a pH of 6 in the *trans*-Golgi network (Demaurex et al., 1998; Kim et al., 1998). In fact, the pH of secretory granules can be as low as 5.2 (Paroutis et al., 2004). This gradual acidification in the secretory pathway is important for proper post-translational processing, sorting, and transport of newly synthesized proteins (Mellman, 1992; Schoonderwoert et al., 2000; Henkel et al., 2000).

This differential acidification of endosomal compartments is the result of a delicate interplay between H^+ influx and efflux pathway, as well as counterion conductances. Active luminal acidification is mainly generated by the vacuolar-type H^+-translocating ATP hydrolases (V-ATPases) (Jefferies et al., 2008; Marshansky and Futai, 2008). Since the V-ATPase is electrogenic, its activity is dependent on the transmembrane potential, decreasing as the positive charge in the lumen builds up. A recent study suggested that the V-ATPase, in addition to

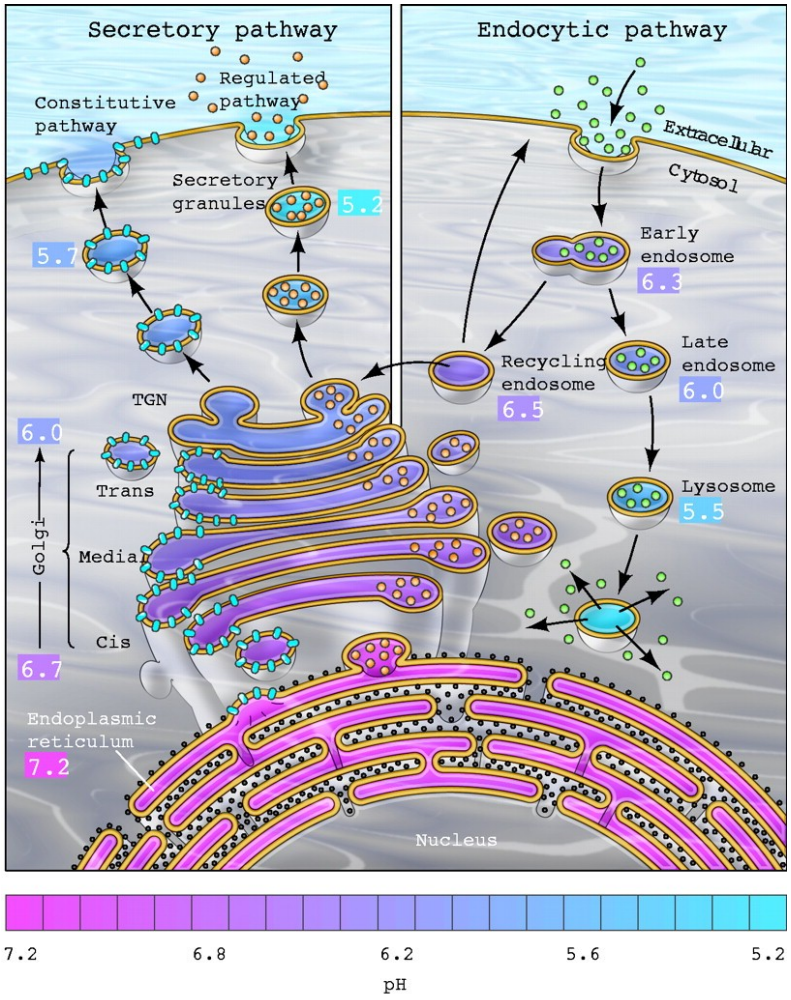

Figure 3. Steady-state pH values of the compartments of secretory and endocytic pathways. From Paroutis, P. et al., Physiology, 2004.

pumping H^+, seems capable of sensing the optimal intravesicular pH and transmitting that signal across the membrane, possible by a conformational change in the a2-subunit, which now becomes competent of recruiting cytoplasmic proteins (like the Arf6 associated guanine-nucleotide-exchange factor ARNO) necessary for protein trafficking between early and late endosomes (Hurtado-Lorenzo et al., 2006).

If the V-ATPase would reach chemical equilibrium, the intraorganellar pH would reach a value of 3. However, measurements showed that along the secretory pathway the intraendosomal pH ranges from 6.7 to 5.5 (Demaurex, 2002), suggesting the existence of regulatory mechanisms. These include various proton leak pathways, including the electrogenic $2Cl^-/1H^+$ exchangers, which contribute significantly to optimal acidification of compartments along the endocytic (Hara-Chikuma et al., 2005a; Hara-Chikuma et al., 2005b; Jentsch, 2007) and secretory pathways (Gentzsch et al., 2003). Furthermore, this mechanism accounts, at least in part, for the rapid alkalinisation of organelles following inhibition of the V-ATPase by macrolide antibiotics such as bafilomycin or concanamycin (Forgac, 2007). In addition to the chloride-proton exchange mechanism, other carrier-mediated H^+ leak pathways that contribute to the differential organellar acidification include a Zn^{2+}-inhibitable H^+ voltage-sensitive conductance in the Golgi complex (Schapiro and Grinstein, 2000), as well as the family of sodium/proton exchangers (NHEs), which are targeted preferentially to membranes of the secretory and endocytic pathways (Numata et al., 1998; Nakamura et al., 2005; Brett et al., 2005a; Orlowski and Grinstein, 2007). Another factor that has been shown to be partially responsible for the variation in intraorganellar pH along the secretory pathway is the gradual increase in the density of proton pumps from the ER to the Golgi, coupled to a decrease in proton permeability (Wu et al., 2001) . Collectively, these observations suggest that the proton leak pathway is the predominant mechanism that contributes to the

regulation of organellar pH, in which most probably the NHEs play an important role.

1.5.2 *Saccharomyces cerevisiae* Nhx1

The most extensively studied organellar NHE is the yeast ScNhx1, which is closely related to human NHE6 (31% identity, 60% similarity). ScNhx1 is localized in the pre-vacuolar compartment (PVC) (equivalent to late endosome) in yeast, where cargo is sorted prior to its delivery to the vacuole/lysosome (Nass and Rao, 1999). Initially, ScNhx1 was proposed to be mainly responsible for conferring salt tolerance by working against the H^+ gradient established by the V-ATPase to sequester Na^+ into the vacuole (Nass and Rao, 1999).

In 2000, Bowers et al. provided evidence that ScNhx1 is involved not only in the regulation of ion homeostasis, but also in the control of vesicle trafficking. Thus, *nhx1* mutants displayed a 'class E' vacuolar protein-sorting phenotype characterized by enlargement of the prevacuolar compartment and missorting of the vacuolar carboxypeptidase Y to the cell surface. Interestingly, the defect in protein trafficking to the vacuole caused by disruption in Nhx1 was considerably more severe than loss of the V-ATPase (Bowers et al., 2000). A later study reported that ScNhx1 directly regulates vesicular trafficking by controlling intracellular pH (Brett et al., 2005b). Indeed, ScNhx1-null cells exhibited sensitivity to the protein synthesis inhibitor hygromycin B and showed abnormal accumulation of the G-protein-coupled receptor Ste3-GFP in the prevacuolar compartment, which could be alleviated by treatment with weak bases, indicating a crucial role of luminal pH for the correct sorting of cargo. Similar to other organellar NHEs, such as the human NHE7 (Numata and Orlowski, 2001) and the plant AtNHX1 (Venema et al., 2002), ScNhx1 can also function as a K^+/H^+ antiporter (Brett et al., 2005b). Little information is available about the molecular mechanisms that govern the regulation of protein trafficking by Nhx1 in

yeast, although one mechanism could be the disruption of K^+-dependent and pH-dependent endosomal processes elicited by Nhx1 malfunction. In this context, it is known that K^+ is an important regulatory co-factor of the Kex2/furin family of endoproteases, which are essential for maturation of newly synthesised proteins in the secretory pathway of yeast and animal cells (Rockwell and Fuller, 2002). Hence, disruptions in intraorganellar K^+ concentration could prevent correct protein processing (Orlowski and Grinstein, 2007).

Another possible mechanism responsible for regulation of protein trafficking by Nhx1 could be by interacting with proteins required for proper trafficking. This hypothesis is supported by a study reporting a direct interaction at the prevacuolar compartment/late endosome between Nhx1 and Gyp6, a GTPase-activating protein for the Ypt/Rab family of small GTPases, which results in inhibition of Nhx1 activity and more acidic vesicles that would be targeted to the vacuole. Once it is delivered to the prevacuolar compartment, Ypt6-GTP displaces Nhx1 on Gyp6, allowing the activation of Nhx1 which promotes retrograde trafficking from the endosome to the Golgi/TGN (Ali et al., 2004).

Recently, Vnx1p, a novel monovalent cation/proton antiporter localized in the vacuolar membrane has been identified in *Saccaromyces cerevisiae* (Cagnac et al., 2007). Although it shares sequence homology with members of the CAX (calcium exchanger) family, Vnx1p does not transport Ca^{2+}. Instead, it functions as a low affinity Na^+/H^+ and K^+/H^+ exchanger and is involved in the regulation of cellular pH and ion homeostasis in yeast.

1.5.3 Plant Intracellular Na^+/H^+ Exchangers

In plants, it is thought that the cation/H^+ exchangers use the proton motive force generated by the H^+-ATPase to extrude cations from the cytosol across the plasma membrane or into intracellular compartments, especially the vacuole, thereby acting to acidify the cytosol (Pardo et al., 2006). The first Na^+/H^+ exchanger cloned in plants was the *Arabidopsis*

thaliana AtNHX1 (Gaxiola et al., 1999). In *Arabidopsis thaliana,* six intracellular NHX transporters have been identified, which can be divided into two main groups, known as class I and class II. Class I comprises isoforms AtNHX1-4, which are localized in the vacuolar membrane (tonoplast) (Pardo et al., 2006). Activity measurements with purified AtNHX1 reconstituted into liposomes showed that the transporter mediated Na^+/H^+ and K^+/H^+ exchange with equal affinity (Venema et al., 2002). Class II is represented by AtNHX5 and AtNHX6, which are only 21-23% similar to class I isoforms, and are localized in endosomal vesicles. Class II exchangers have been shown to use K^+ as their preferred substrate over Na^+ (Venema et al., 2003).

Electrophysiological studies suggest that tonoplast antiporters are involved in the regulation of cytosolic and vacuolar pH and of ion gradients induced by salt stress (Carden et al., 2003). Thus, AtNHX1 is important for maintaining cellular Na^+ and K^+ homeostasis and salt tolerance (Apse et al., 1999). Null mutants of AtNHX1 and plants overexpressing the transporter have substantially altered total antiporter activity, suggesting that AtNHX1 is the major contributor to vacuolar Na^+ and K^+ transport activity, despite the presence of the other isoforms ((Rodriguez-Rosales et al., 2009).

The critical role played by NHX transporters in regulating vacuolar pH is illustrated by the petal color change of *Ipomoea nil* from red to blue during flower opening, which is due to the presence of pH-sensitive anthocyanin pigments in the vacuole and an increase of vacuolar pH from 6.6 to 7.7 during flower opening. This is accompanied by increased protein levels and activities of the V-ATPase, as well as by the *de novo* expression of NHX1, which was still absent 6 hours before the flowers fully opened (Yoshida et al., 2005). Furthermore, plants carrying a recessive mutation in the NHX1 gene displayed only a slight increase in petal vacuolar pH during flower opening, resulting in purple instead of blue

flowers (Yamaguchi et al., 2001), confirming the essential role of NHX1 in the regulation of vacuolar pH.

Plant NHX transporters have been shown to be regulated by different mechanisms. Similar to yeast and mammalian NHEs, the C-terminal region of the *Arabidopsis thaliana* AtNHX1, is essential for regulating antiporter activity. In fact, deletion of the C-tail results in a two-fold increase in Na^+/K^+ selectivity, due to a small decrease in K^+/H^+ transport and a very large increase in Na^+/H^+ activity (Yamaguchi et al., 2003).

An interesting cross-talk between the regulation of plasma membrane and vacuolar NHEs has been described in *Arabidopsis thaliana*, where the tonoplast AtNHX1 is under the regulation of SOS2, a kinase of the salt-overly-sensitive (SOS) pathway, which also activates the plasmalemmal Na^+/H^+ exchanger SOS1 under salt excess (Qiu et al., 2004). Additionally, the activity of the *Arabidopsis thaliana* vacuolar AtNHX1 can be regulated by its interaction with the intraluminal calmodulin-like protein AtCaM15 in a pH- and Ca^{2+}-dependent manner. Coexpression of AtNHX1 and AtCaM15 in purified vacuoles from yeast resulted in an altered ion selectivity of the transporter, as demonstrated by the significant (46%) reduction of the Na^+/K^+ selectivity ratio (Yamaguchi et al., 2005). Under normal physiological conditions, i.e. low vacuolar pH and high Ca^{2+} concentration, AtCaM15 inhibits AtNHX1 through binding to the C-terminal tail of the exchanger. However, during salt stress, the vacuolar pH rises (Gruwel et al., 2001) causing a release of AtCaM15 from the AtNHX1 tail, resulting in the activation of AtNHX1, thus increasing the influx of Na^+ into the vacuole. Such regulation by calmodulin-like proteins was described for ion channels/exchangers (Zielinski, 1998), including the mammalian NHE1 (Wakabayashi et al., 1994; Wakabayashi et al., 1997).

1.5.4 Mammalian Organellar NHEs

The organellar or endomembrane subgroup of NHEs is represented by four isoforms termed NHE6-NHE9. They show low sequence homology with the plasma membrane NHEs (~25% identity) and are expressed widely in tissues, indicating that they perform housekeeping functions within the cell (Orlowski and Grinstein, 2004; Orlowski and Grinstein, 2007).

Tissue distribution and subcellular localization

NHE6 was the first identified human organellar NHE and is ubiquitously expressed, with the highest transcript levels present in brain, skeletal muscle, and heart (Numata et al., 1998). The SLC9A6 gene, which encodes the NHE6 protein, is localized on the X chromosome (Xq26.3) and two alternatively splice variants have been identified to date, termed NHE6-v0 (669 amino acids) (Numata et al., 1998) and NHE6-v1 (701 amino acids) (Miyazaki et al., 2001). The NHE6-v1 variant has been cloned originally from a liver cDNA library (Miyazaki et al., 2001) and contains a stretch of 32 amino acids in the second extracellular loop that is absent in NHE6-v0, but is shared by the other mammalian endomembrane NHEs. PCR analysis performed in our laboratory with end-specific primers lead to identification of both variants in a human brain cDNA library, in similar proportions (60% v1, 40% v0) (Ilie and Orlowski, unpublished data). Thus far no functional differences have been reported between the two splice variants.

Initially NHE6 was postulated to be localized in mitochondria, based on the presence of a putative mitochondrial targeting signal at its N-terminus and the close association of NHE6-GFP-containing vesicles with mitochondria stained using the Mito-tracker dye in transfected HeLa cells (Numata et al., 1998) and was thought to represent a monovalent cation/H^+ exchanger described earlier in this organelle (Garlid et al., 1995). However, other studies indicated that ectopically-expressed NHE6 in COS7 cells was N-glycosylated, targeted to the ER membrane and then

sorted to organellar membranes derived from the ER (Miyazaki et al., 2001). Subsequently, it has been reported that NHE6 colocalizes with transferrin in recycling endosomal compartments and a small fraction (~5%) is present on the plasma membrane in CHO cells transiently expressing a triple HA- and GFP-tagged form of NHE6 (Brett et al., 2002; Ohgaki et al., 2008). A more detailed intracellular distribution analysis indicated that although NHE6 and NHE9 partially overlap when examined in COS7 cells, they tend to be differentially partitioned in early recycling and late recycling endosomes, respectively (Nakamura et al., 2005).

Studies in the vestibular system suggest that the relative distribution of NHE6 may be cell-type specific. In vestibular hair cells, NHE6 and NHE9 are found in intracellular vesicles of the cell bodies, but also in stereocilia, with NHE9 present in all bundles and NHE6 expressed only in hair bundles of a small subset of hair cells, the central flask-shaped cells (Hill et al., 2006).

NHE7 is closely related to NHE6, sharing ~70% amino acid identity. Northern blot analysis revealed that NHE7 is expressed widely in tissues, but is enriched in certain regions of the brain (putamen and occipital lobe), skeletal muscle, and secretory tissues (prostate, stomach, pancreas, pituitary gland, adrenal gland, thyroid gland, salivary gland, and mammary gland) (Numata and Orlowski, 2001). At the intracellular level, NHE7 was found to be predominantly localized in the *trans*-Golgi network (TGN) and associated endosomes when expressed in CHO and MCF-7 cells (Numata and Orlowski, 2001; Lin et al., 2007). Two regions in the C-terminal tail of NHE7, located close to the transmembrane domain (residues 533-559 and 563-568) are required for targeting NHE7 to the TGN (Fukura et al., 2010). A small fraction of NHE7 was detected on the plasma membrane of MCF-7 cells, where it is associated with caveolae/lipid rafts. This association occurs through direct interaction between the cytosolic C-terminal region of NHE7 and caveolin-1. However, NHE7 is endocytosed via a clathrin-

dependent and caveolae-independent mechanism, indicating that NHE7 is also present in non-caveolae lipid rafts (Lin et al., 2007).

NHE8 has little similarity to the other organellar NHEs (~25% amino acid identity with NHE6 and NHE7). The presence of another apical NHE isoform in renal proximal tubules had been suggested by the persistence of Na^+/H^+ activity in mice with genetic deletions of both NHE2 and NHE3. These animals had only a 50% reduction in proximal tubule Na^+-dependent H^+ secretion compared with wild-type mice (Choi et al., 2000). Northern blot analysis shows that NHE8 is ubiquitously expressed, with the highest levels in kidney, testis, skeletal muscle and liver, when examined in mouse tissues (Goyal et al., 2003). In human tissues, the same wide tissue distribution was reported, with the most prominent expression in skeletal muscle and kidney (Nakamura et al., 2005). In situ hybridization studies on mouse kidney found an enrichment of NHE8 signal in renal proximal tubules in the outer medulla (Goyal et al., 2003), although other tissues have not been examined.

When expressed in COS7 cells, NHE8 accumulated mainly in the mid- to trans-Golgi compartments (Nakamura et al., 2005). Immunohistochemical analysis with antibodies that specifically recognize NHE8, detected its presence in the brush border membranes of proximal tubules of rat kidney, where it was predominantly localized at the microvillar surface membrane and to a lesser extent in intermicrovillar coated pits and subapical vesicles (Goyal et al., 2005). Based on these observations, it has been suggested that NHE8 may undergo recycling to and from the apical surface.

Rat NHE8 was detected in brush border membranes of intestinal epithelial cells and there is a higher NHE8 mRNA expression in young compared to adult animals, while NHE2 and NHE3 are expressed at low levels in early life. This study suggests that NHE8 might be important for intestinal Na^+ absorption during early life (Xu et al., 2005). Furthermore,

the expression of NHE8 was higher in younger mice than in adult mice at the level of the stomach (Xu et al., 2008). In rat renal proximal tubules, Northern blot and quantitative real-time PCR showed uniform expression of mRNA in all age groups, but immunoblotting demonstrated the highest NHE8 protein abundance in brush border membrane vesicles of 7- and 14-day old animals, which correlates with the lowest expression of NHE3, suggesting that NHE8 is the principal neonatal apical membrane NHE isoform. Interestingly, the total levels of NHE8 protein in renal cortex were higher in adult animals (Becker et al., 2007).

A very recent study found that epitope-tagged NHE8 is localized predominantly in the *trans*-Golgi network in HeLa cells, but a small fraction was present in multivesicular bodies (Lawrence et al., 2010).

NHE9, the most recently identified NHE, was discovered as a gene linked to attention deficit hyperactivity disorder (ADHD) (de Silva et al., 2003). The study of de Silva and colleagues describes a pericentric inversion in chromosome 3 in a family affected by ADHD, resulting in silencing of DOCK3 (Dedicator Of Cytokinesis 3) and of a new member of the Na^+/H^+ exchanger family, which they called NHE9. Northern blot analysis of human tissues revealed that while NHE9 is ubiquitously expressed, DOCK3 expression is restricted to the brain, implicating one or both of these genes as causative for the disease. Although expressed in the brain, NHE9 was more abundant in the heart and skeletal muscle, followed by the placenta, kidney, and liver. In the brain, the highest levels were detected in the medulla, spinal cord, and cerebral cortex (de Silva et al., 2003). Colocalization studies with different endosomal markers in COS7 cells indicated that NHE9 is localized preferentially in a late recycling endosomal compartment, although some overlap with NHE6-containing endosomes was observed (Nakamura et al., 2005).

Besides ADHD, mutations in NHE9 have been linked to autism and epilepsy. One such mutation changed arginine 423 to a stop codon,

creating a truncation in the final extracellular loop of NHE9 (Morrow et al., 2008).

The data regarding the tissue distribution and intracellular localization of the newly identified bacterial-like **NHA1** and **NHA2** is limited and sometimes conflicting. While one group reported that the expression of NHA2 is restricted to bone, and more specifically to osteoclasts (Pham et al., 2007; Battaglino et al., 2008), other groups found that NHA2 is widely expressed in tissues (Xiang et al., 2007; Fuster et al., 2008b). The intracellular distribution of NHA2 is also under debate. Thus, NHA2 was localized at the plasma membrane in rat pancreatic β cells and transfected polarized dog kidney-derived MDCK cells (Xiang et al., 2007) or in the inner mitochondrial membrane and intracellular vesicles in rat distal tubular kidney cells (Fuster et al., 2008b) and mitochondria of osteoclasts (Battaglino et al., 2008). On the other hand, NHA1 is expressed exclusively in testis (Ye et al., 2006). A very recent study using specific anti-NHA2 antibodies found that NHA2 colocalizes with the late endosomal and lysosomal marker LAMP1 and the V-ATPase a3 subunit, but not with mitochondrial markers. Moreover, NHA2 was highly enriched in the plasma membrane of osteoclasts and is localized at the basolateral membrane of polarized osteoclasts (Hofstetter et al., 2010).

Physiological roles and kinetic properties of organellar NHEs

A particular kinetic characteristic of the organellar NHE is their capability to transport not only Na^+ but also K^+ in exchange for H^+, which contrasts with the plasma membrane NHEs, known to be highly selective for Na^+. As the majority of endomembrane compartments are acidic and potassium is the predominant cytosolic alkali cation, it is largely accepted that organellar NHEs use the electrochemical gradient created by the vacuolar-type ATPases to mediate the exchange of luminal protons for cytosolic potassium, thereby acting as electroneutral alkalinizing molecular

mechanisms (Orlowski and Grinstein, 2007). However, due to technical constraints, the precise cation selectivity and the physiological roles played by organellar NHEs are still ill defined.

A role for NHE6 in the maintenance of apical bile canalicular lumens has been proposed in polarized hepatoma HepG2 cells (Ohgaki et al., 2010). These cells express NHE6-v1, which is localized in recycling endosomes and colocalizes with transcytosing bulk membrane lipids. Silencing by siRNA or overexpression of mCherry-tagged NHE6-v1, but not of the mutant form E287Q/D292N, resulted in reduced retention of bulk membrane lipids and of the bile canalicular resident protein dipeptidyl peptidase IV (DPP IV) at the apical plasma membrane domain. These data indicate that NHE6 is involved in maintaining the polarity of HepG2 cells, albeit the molecular mechanism involved is not clear. One possible mechanism involves the regulation of recycling endosomal pH by NHE6. Indeed, depletion of endogenous NHE6 by siRNA reduced the pH of recycling endosomes from 6.6 to 5.9, whereas overexpression of wild-type NHE6 resulted in alkalinisation of recycling endosomes to pH 7.3. This effect was not observed when the non-functional E287Q/D292N mutant form of NHE6 was expressed in HepG2 cells (Ohgaki et al., 2010).

Lately, NHE6 has received considerable attention, as different mutations in NHE6 have been shown to cause X-linked mental retardation, microcephaly, epilepsy, ataxia, and a happy disposition, a phenotype mimicking Angelman syndrome (Gilfillan et al., 2008). Additionally, a different mutation in NHE6 has been reported very recently and shown to cause a mental retardation syndrome characterized by absence of speech, autistic behavior, epilepsy, late-onset ataxia, as well as neuronal and glial deposition of the microtubule-binding protein tau in cortical and sub-cortical regions (Garbern et al., 2010). This mutation leads to in-frame loss of amino acids Trp338-Thr340 in the predicted transmembrane domain nine of NHE6. These studies implicate a potential role of NHE6 in the regulation of synaptic function.

Endomembrane NHEs have been implicated in regulating ion homeostasis in more specialized types of cells as well. Thus, NHE6 and NHE9 are expressed in stereocilia of vestibular hair cells, which can regulate their pH independently of the cell body. The apical endolymph bathing these cells lacks Na^+ but is highly enriched in K^+. It has been suggested that NHE6 and NHE9 use this high extracellular K^+ concentration to extrude the excess protons generated in the hair bundles by the Ca^{2+}/H^+ exchange activity of the plasma membrane Ca^{2+}-ATPase isoform 2 (PMCA2) (Hill et al., 2006). The activity of PMCA2 is necessary to pump large amounts of Ca^{2+} into the endolymph to generate otoconia, the calcium carbonate crystals embedded in the otolithic membrane which transduces gravity or linear acceleration changes to the hair cells. These data indicate that NHE6 and NHE9 are functionally coupled to PMCA2 and protect the hair bundles from excessive acidification. The ability of NHE6 and NHE9 to mediate both Na^+/H^+ and K^+/H^+ exchange was demonstrated by complementation and cation tolerance growth assays in a yeast strain lacking two endogenous cation/proton exchangers (nhx1Δ nha1Δ). These data showed that the order for cation preference for the two NHE isoforms is K^+, $Na^+ > Li^+ >> Rb^+$ (Hill et al., 2006).

NHE7 most likely fulfills the function of pH and K^+ regulator in the *trans*-Golgi network (TGN). It functions as a nonselective monovalent cation/H^+ exchanger, as it has the capacity to transport both Na^+ and K^+ in exchange for H^+ in stably expressing inducible CHO cells (Numata and Orlowski, 2001). Given that K^+ is the main intracellular alkali cation, the physiological mode of operation is probably as a K^+/H^+ exchanger, making NHE7 not only an important H+ efflux pathway in the TGN, but also a contributor to the regulation of intraluminal K^+ concentration, which could have an effect on the volume homeostasis and hence the morphology of the TGN. The activity of NHE7 was relatively insensitive to amiloride and low concentrations (100 μM) of the amiloride analog benzamil, but it was

blocked significantly by higher concentrations of benzamil (1 mM) and by the unrelated compound quinine (Numata and Orlowski, 2001).

Nakamura and coworkers (2005) were the first to successfully characterize the exchange activity of the mouse NHE8 reconstituted into artificial proteoliposomes. In this system, NHE8 mediated both Na^+/H^+ and K^+/H^+ exchange activity. The Na^+ uptake of proteoliposomes containing the mutant form E220Q/D225N of NHE8 was completely abolished. These two residues had been shown previously to be important for the exchange activity of NHE1 (Fafournoux et al., 1994; Murtazina et al., 2001). Additionally, when overexpressed in COS7 cells, NHE8 dissipated the acidic pH of the Golgi complex, increasing its pH from ~6.5 to ~7.28, indicating that NHE8 mediates proton efflux from the Golgi lumen (Nakamura et al., 2005).

The function of native NHE8 has been characterized in NRK (normal rat kidney polarized epithelial) cells, which express NHE8 on the apical membrane and NHE1 on the basolateral membrane (Zhang et al., 2007). RT-PCR analysis with primers specific for all renal plasma membrane Na^+/H^+ exchangers showed that no other plasma membrane NHEs are present in NRK cells. Apical NHE activity measurements using the pH-sensitive fluorescent dye BCECF, combined with depletion of endogenous NHE8 by siRNA in NRK cells, demonstrated that NHE8 functions as a Na^+/H^+ exchanger, but does not transport K^+. Furthermore, the transporter is highly sensitive to EIPA (Zhang et al., 2007).

The kinetic properties of NHE8 were studied in PS120 cells transiently expressing the transporter. PS120 cells are Na^+/H^+ exchanger-deficient lung Chinese hamster fibroblastic cells and are widely used to study the activity and regulation of different NHE isoforms (Levine et al., 1993; Tse et al., 1993a; Honda et al., 1993). The sodium affinity of rat NHE8 in this system as measured by the Km value is 23 mM (Xu et al., 2008), while rat NHE1, NHE2, and NHE3 have Km values of 10, 50, and

4.7 mM (Orlowski, 1993; Yu et al., 1993). These values indicate that the Na^+ affinity of NHE8 is lower compared to NHE1 and NHE3, but higher compared to NHE2. Moreover, the sensitivity of NHE8 to the amiloride analog HOE694 is similar to NHE2 (K_i 5 μM), as 1 μM had no effect on its activity, while 10 μM significantly inhibited its activity. NHE8 activity was also relatively sensitive to the compound S3226 (as 80 μM inhibited most of its activity) (Xu et al., 2008), which potently inhibits rat NHE3, while NHE1 and NHE2 are relatively insensitive (Schwark et al., 1998).

Very recently, NHE8 has been implicated in the control of protein trafficking and morphology of late endosomes (Lawrence et al., 2010).

Studies in mitochondria, as well as complementation analyses in yeast, showed that NHA2 is a functional Na^+- or Li^+- selective NHE, but does not use K^+ in exchange for protons (Xiang et al., 2007; Fuster et al., 2008b; Battaglino et al., 2008). NHA2 is involved in the regulation of mitochondrial pH and volume, as well as in the later stages of osteoclast differentiation by preventing cells from undergoing apoptosis (Battaglino et al., 2008). However, in NHA2-deficient mice, osteoclast development and activity, as well as the structural parameters of bone were all normal, indicating that the exchanger is not absolutely required for normal bone development *in vivo* (Hofstetter et al., 2010).

Since its transport activity is insensitive to amiloride, but is inhibited by phloretin (which are defining characteristics of Na^+/Li^+ counter-transport activity), it has been suggested that NHA2 is a likely candidate for the sodium-lithium counter-transport activity detected in red blood cells, lymphoblasts, and fibroblasts and linked to hypertension (Xiang et al., 2007).

Regulation of organellar NHEs

Although several reports indicate that organellar NHEs are essential for luminal pH control, thereby affecting vesicular and protein trafficking, the factors and molecular mechanisms governing the regulation and trafficking of mammalian endomembrane NHEs are largely unknown.

A limited number of studies addressed the regulation of the NHE6 isoform. The Angiotensin II receptor AT2 was identified as a NHE6-interacting protein during a yeast two-hybrid screen of a mouse 17-day fetus cDNA library (Pulakat et al., 2005). The interaction between NHE6 and AT2 in transfected MCF-7 cells required the activation of AT2 by angiotensin II, a multifunctional peptide that acts as a vasoconstrictor and a regulator of Na^+ homeostasis by binding to its high affinity receptors AT1 and AT2. However, the physiological significance of this interaction has not been addressed.

Little information is available regarding the regulation of the TGN isoform NHE7. Using the C-terminal tail of NHE7 to screen a human brain cDNA library, Lin et al. (2005) identified secretory carrier membrane proteins 1, -2, and -5 (SCAMPs) as interacting partners for NHE7 (Lin et al., 2005). SCAMPs are transmembrane proteins localized in the Golgi and post-Golgi compartments and the five isoforms identified in mammals are involved in exocytosis (Liu et al., 2002; Guo et al., 2002) and endocytosis (Fernandez-Chacon et al., 2000) of proteins. A deletion mutant of SCAMP2 lacking the TM2 and TM3 regions responsible for NHE7 binding caused both SCAMP2 and NHE7 to redistribute to recycling endosomes. This suggested that SCAMPs regulate the trafficking of NHE7 between the TGN and the recycling endosomal compartment, playing a role in retrieval of NHE7 from the recycling endosomes to the TGN (Lin et al., 2005). SCAMP2 was found to associate with the small GTPase ADP-ribosylation factor Arf6 and with phospholipase D1 (Liu et al., 2005), suggesting its involvement in recruiting important factors involved in vesicle formation and fusion (D'Souza-Schorey and Chavrier,

2006). This finding raises the possibility that NHE7 may form a macromolecular complex that includes SCAMP2 and Arf6, providing a potential link between endomembrane NHEs and vesicle trafficking (Orlowski and Grinstein, 2007).

Several hormones and transcription factors have been implicated in the regulation of NHE8. As mentioned previously, NHE8 levels are higher in brush border membranes of renal proximal tubule and intestinal epithelial cells in young versus mature animals (Xu et al., 2005; Becker et al., 2007). These effects are probably regulated by the thyroid hormone, as the post-natal increase of this hormone has been associated with reduced NHE8 surface expression and decreased activity (Gattineni et al., 2008). Very recent studies showed that during intestinal maturation, NHE8 expression is regulated by the epidermal growth factor (EGF). EGF reduced basal transcription of NHE8, by inhibiting the binding of transcription factor Sp3 to the promoter region of NHE8 (Xu et al., 2010a). Additional regulation of NHE8 during intestinal maturation is provided by glucocorticoids, which inhibit the promoter activity of NHE8 by enhancing the binding of the transcription factor Pax5 to the proximal region of the promoter (Xu et al., 2010b).

Interestingly, NHE9 has been shown to be regulated by neuronal activity. In rat hippocampal cultures, depletion of *NPAS4*, a transcription factor activated in response to depolarization, showed that NHE9 gene expression is significantly enhanced (Morrow et al., 2008). However, the physiological significance of this observation is currently unknown.

1.6 RESEARCH RATIONALE AND OBJECTIVES

Mammalian alkali cation/proton exchangers, also known as sodium/proton exchangers **(**NHEs), are integral membrane proteins that catalyze the exchange of Na^+ (and for some isoforms also K^+) for H^+ down their respective concentration gradients. To date, eleven different isoforms have been identified that are localized not only at the plasma membrane, but also in endomembrane compartments (Orlowski and Grinstein, 2004; Orlowski and Grinstein, 2007; Casey et al., 2010).

The contributions of plasma membrane-type NHEs to cellular 'housekeeping' functions such as maintenance of cytoplasmic pH and systemic electrolyte, acid-base and fluid volume homeostasis are well documented. The discovery of novel NHE isoforms (NHE6-9) localized to discrete compartments along the exocytic and endocytic pathways highlights broader roles for these transporters in cell function. Mutations in some of these organellar transporters give rise to distinct neurological diseases. Thus, there is a need for a better understanding of their structural, functional and regulatory properties.

This research proposal is focused primarily on the organellar-type NHE6 isoform that is postulated to play significant roles in the biogenesis and pH homeostasis of endocytic vesicles in mammalian cells by analogy to its yeast and plant homologues, although the molecular mechanisms are largely unknown (Orlowski and Grinstein, 2004; Orlowski and Grinstein, 2007; Brett et al., 2005a). The central hypothesis is that NHE6 is important for the function and trafficking of discrete recycling endosomal pools in most cells. In neurons, we speculate that NHE6-containing endosomes are required for optimal synapse formation and function.

At the beginning of this project, only limited information was available regarding the subcellular distribution of NHE6 in heterologous systems (Miyazaki et al., 2001; Brett et al., 2002). These studies reported the localization of transiently transfected NHE6 in recycling endosomes,

based on its colocalization with the transferrin receptor. Moreover, NHE6 was shown to be widely expressed in tissues, but the highest expression level was detected in brain, heart, and muscle (Numata et al., 1998). However, nothing was known about its native distribution or the mechanisms regulating its trafficking and function. As such, the main focus of my thesis was to gain insight into the native distribution of NHE6, as well as the molecular mechanisms governing its intracellular trafficking and function.

Given that NHE6, though widely expressed in tissues, is highly enriched in the brain (Numata et al., 1998), we decided to examine its distribution in neuronal cells in culture and in intact brain. To this end, we generated a rabbit polyclonal anti-NHE6 antibody and tested its specificity using biochemical methods and confocal microscopy. This antibody was further used to investigate the expression of NHE6 in mouse, rat, and human brain tissue lysates, as well as its distribution in organotypic hippocampal slice cultures by confocal microscopy. Moreover, to validate the light microscopy data, the subcellular distribution of NHE6 was examined in mouse hippocampus and cortex by transmission electron microscopy (Chapter 1).

The next objective was to identify factors and molecular mechanisms involved in the trafficking of NHE6. As NHE6 is N-glycosylated (Miyazaki et al., 2001) and N-glycosylation is important for the regulation of multiple membrane proteins (Ohtsubo and Marth, 2006), mutational analysis in conjunction with biochemical and light microscopical approaches were used to determine the precise glycosylation site(s) and their role in trafficking of NHE6 in Chapter 2. In order to understand the regulation of NHE6 in the brain, we tried to identify interacting partners of the transporter using the yeast two-hybrid methodology (Chien et al., 1991) to screen a human brain cDNA library. For this assay, the cytoplasmic tail of NHE6 was used as bait, since it is known that this part represents the regulatory domain in other NHE isoforms (Orlowski and

Grinstein, 2004). Chapter 3 presents one of the interacting partners (RACK1) recognized by the yeast two-hybrid assay and the functional consequences of its association with NHE6 in cells.

NHE6 has received considerable attention lately, as mutations in the exchanger have been linked to X-linked mental retardation, microcephaly, epilepsy, and ataxia, a phenotype mimicking Angelman syndrome (Gilfillan et al., 2008). A number of mutations in NHE6 have been identified in different families by Gilfillan et al. (2008), including truncations (R468X, leading to loss of the final transmembrane domain and C-terminus), splice-site mutations (causing skipping of exon 3), frameshift mutations, and a 6 bp deletion, leading to loss of amino-acids E255 and S256 in NHE6-v0. While most of these mutations will probably lead to a completely non-functional protein, the latter is more subtle and in Chapter 4 we investigated the molecular mechanisms responsible for the phenotype observed when amino acids E287 and S288 (corresponding to E255 and S256 in NHE6-v0) were deleted in NHE6-v1.

CHAPTER 1

Subcellular Localization of the Organellar Sodium/Proton Exchanger 6 Isoform Assessed by Light and Electron Microscopy

Alina Ilie, Emily Deane, Viktoria Lukashova, Rebecca Anne McKinney, and John Orlowski.

The organellar-type NHE6 isoform has been recently associated with severe X-linked mental retardation syndromes. In humans, NHE6 is transcribed in most tissues, but is enriched in brain, heart, and skeletal muscle. However, the native localization of the translated protein is not known. This chapter describes the distribution of endogenous NHE6 in neuronal cells, using a combination of biochemical and microscopical techniques. .

ABSTRACT

Recent studies have identified mutations in the solute carrier family 9 gene SLC9A6, which encodes the Na^+/H^+ exchanger NHE6 isoform, that cause severe mental retardation characterized by epilepsy, autism spectrum disorder, ataxia and dystonia as well as other peripheral abnormalities. However, the mechanistic basis for this phenotype remains obscure. In humans, NHE6 is transcribed in most tissues and is particularly abundant in excitable tissues such as brain, skeletal muscle and heart, but detailed information regarding the native distribution of the translated protein, particularly in neural tissue, is wanting. Earlier light microscopy studies using heterologous cell expression systems revealed that NHE6 localizes to a perinuclear recycling endosomal compartment. To characterize its subcellular distribution in finer detail, NHE6 variants containing either internal or external epitope tags were constructed and characterized in transfected nonpolarized cells by both light and electron microscopy. In addition, an isoform-specific rabbit polyclonal antibody was generated that recognizes human, rat and mouse NHE6 and was found to be highly effective for immuno-blotting and immunocytochemistry. In transfected nonpolarized Chinese hamster ovary cells, epitope-tagged NHE6 accumulated in transferrin receptor (Tf-R)-rich recycling endosomes, as expected. However, in addition, a measureable fraction (~10%) was detected at the plasma membrane and, in particular, along small microvillar-like membrane protrusions, some of which may be filopodia. In polarized human SH-SY5Y neuroblastoma cells, endogenous NHE6 also colocalized with Tf-R-containing vesicles in the soma and neurite processes. To further examine its distribution in neurons under more 'native' conditions, confocal imaging was performed using mouse hippocampal CA1 organotypic slice cultures (postnatal day 6; *in vitro* 21 days). Dense populations of NHE6 positive punctae were detected within the soma as well as dendritic shafts and spines of CA1 pyramidal cells.

To corroborate this observation at even higher resolution, the localization of native NHE6 was examined in mouse hippocampus and cortex by transmission electron microscopy (EM). NHE6 positive signals were detected predominately in dendrites, occasionally adjacent to postsynaptic densities (PSD), and to a minor extent in some presynaptic terminals; findings consistent with the light microscopy data. Thus, in both nonpolarized and polarized cells, NHE6 resides not only in intracellular vesicles, but also localizes to distinct plasma membrane protrusions that are cell-type dependent. The predominance of NHE6 in vesicles within dendrites and dendritic spines suggest a role for this transporter in synapse formation and plasticity.

INTRODUCTION

Mammalian alkali/proton antiporters, commonly referred to as Na^+/H^+ exchangers (NHEs), represent a family of at least eleven structurally distinct transmembrane proteins, which show various tissue distribution, subcellular localization, cation selectivity, and function. Nine isoforms (NHE1-9) share ~25-70% amino acid identity and appear to be derived from a more recent common ancestor, while two others termed NHA1 and NHA2 are more distantly related to the NHEs (~13% identity) and show closer homology to the fungal/plant NHA1 and bacterial NhaA Na^+/H^+ antiporters (Orlowski and Grinstein, 2004; Orlowski and Grinstein, 2007; Brett et al., 2005a). The NHE isoforms can be further divided into two general clusters based on their primary structure similarity, principal subcellular location and cation-selectively. NHE1-5 are expressed for the most part in a tissue-specific manner (except NHE1 which is ubiquitous), and all are active at the cell surface (hence termed the plasma membrane-type NHEs) where they selectively catalyze the electroneutral exchange of extracellular Na^+ (and to a lesser extent Li^+) for cytoplasmic H^+. However, isoforms such as the epithelial NHE3 and neuronal NHE5 isoforms can

also enter a recycling endosomal pool (D'Souza et al., 1998; Szaszi et al., 2002).

Amongst the plasma membrane-type NHEs, the ubiquitous NHE1 has been studied most extensively. By comparison, considerably less is known about the NHE6-9 isoforms which are expressed in most tissues and appear to be targeted to discrete, albeit overlapping, compartments along the secretory and endocytic pathways (*i.e.*, organellar-type NHEs) when examined in heterologous expression systems.

NHE6 is concentrated in compartments along the recycling endosomal pathway (Brett et al., 2002; Nakamura et al., 2005; Ohgaki et al., 2008). Human NHE6 also undergoes alternative RNA splicing to form at least two gene products designated NHE6-v0 and NHE6-v1 (Miyazaki et al., 2001). The latter contains an additional 32 amino acids situated between original residues Leu^{143}-Val^{144} and is predicted to reside in the second exoplasmic loop. Thus far, no functional differences between these splice-variants have been reported.

The physiological roles of NHE6 have yet to be elucidated. However, insights can be obtained from studies of the prevacuolar/late endosomal $(Na^+,K^+)/H^+$ exchanger Nhx1 in the yeast *Saccharomyces cerevisiae*. Yeast containing a null mutation of Nhx1 show enhanced acidification and abnormal enlargement of their late endosomal compartment as well as missorting of its cargo; effects that are attenuated by treatment with weak bases (Bowers et al., 2000; Brett et al., 2005b). These data support the notion that endomembrane NHEs serve as a critical alkalinizing mechanism to finely control intraorganellar pH which, by ill-defined mechanisms, modulates endosome biogenesis and trafficking.

The importance of studying NHE6 is further highlighted by very recent genetic findings that have uncovered mutations in human NHE6 that are linked to severe X-linked mental retardation syndromes (Gilfillan et al., 2008; Garbern et al., 2010). Importantly, the sites of NHE6 distribution in the brain have not been studied so far.

In this study, NHE6 variants containing either internal or external epitope tags were constructed and characterized in transfected nonpolarized cells by both light and electron microscopy. In addition, an isoform-specific rabbit polyclonal antibody was generated and used to test NHE6 distribution in neuronal cells in culture and in the brain by confocal laser scanning microscopy and electron microscopy, as well as immunoblotting techniques. Our results show that NHE6 is localized in recycling endosomes and at the plasma membrane along microvillar- and filopodia-like structures in AP-1 cells stably expressing an epitope-tagged form of the exchanger. In polarized human SH-SY5Y neuroblastoma cells, endogenous NHE6 colocalized with transferrin receptor-containing vesicles in the soma and neurite processes. In mouse hippocampal organotypic slice cultures, NHE6 was detected within the soma as well as dendritic shafts and spines of CA1 pyramidal cells by confocal microscopy. Ultrastructural analysis of mouse hippocampus and cortex revealed the presence of NHE6 positive signals predominately in dendrites, occasionally adjacent to postsynaptic densities (PSD), and to a minor extent in some presynaptic terminals; findings consistent with the light microscopy data.

MATERIALS AND METHODS

Reagents

Mouse monoclonal anti-hemagglutinin (HA) antibody was purchased from Covance Inc. (Berkeley, CA); rabbit polyclonal anti-HA was obtained from Abcam Inc. (Cambridge, MA) anti-transferrin receptor antibody was obtained from Zymed Laboratories Inc. (South San Francisco, CA); anti-Flag M2 monoclonal antibody was from Sigma-Aldrich. Horseradish peroxidase-conjugated secondary IgG antibodies were purchased from Jackson ImmunoResearch (West Grove, PA). All

Alexa Fluor® conjugated secondary antibodies were purchased from Molecular Probes (Eugene, OR).

Alpha-Minimum essential medium (α-MEM), fetal bovine serum, penicillin/streptomycin, and trypsin-EDTA were purchased from Invitrogen. All other chemical and reagents were obtained from BioShop Canada (Burlington, ON, Canada) or Fisher Scientific and were of the highest grade available.

Antibody production

To generate a polyclonal antibody specific for NHE6, a recombinant fusion protein of glutathione-S-transferase (GST) and the extreme C-terminal segment of human NHE6 (amino acids 608-669) was constructed by cloning into the BamHI/EcoRI sites of the pGEX-2T vector (Amersham Biosciences). After sequence verification, the plasmid was transformed into the Epicurean Coli BL21-Codon Plus™ strain (Stratagene, Cedar Creek, TX). Individual colonies were cultured overnight, then diluted 1:20 in 1 liter of bacterial growth media, and incubated further at 37°C to reach a sufficient population density. Protein expression was then induced by further incubation with 0.4 mM isopropyl-1-thio-β-D-galactopyranoside (IPTG) at 30°C for 3 hours. The bacterial cultures were centrifuged and the resulting pellets were resuspended in 30 ml of lysis buffer (0.4 mg/ml lysozyme in standard phosphate-buffered saline (PBS), supplemented with protease inhibitors). Bacteria were subsequently lysed by sonication (model 100 Sonic Dismembrator, Fisher) on ice and then cleared by centrifugation at 4°C for 30 min at 13,000 x g. After filtration of the resulting supernatant through a 0.45 μm MILLEX®-HV syringe driven filter unit (Millipore Corporation, Bedford, MA), proteins were purified by incubating the bacterial lysates with glutathione-Sepharose™ beads (GE Healthcare) overnight at 4°C. The purified GST fusion protein bound to glutathione-Sepharose beads was washed six times with PBS, and then eluted with 10 mM glutathione in PBS. The eluted fractions were

concentrated using Amicon® Ultra centrifugal filter devices with a 10 kDa cut off (Millipore, Bedford, MA) at 3,000 X g for 10 min.

Rabbit immunizations with the aforementioned fusion protein were performed at the McGill Animal Resource Centre (Montreal, QC) using standard Canadian Council on Animal Care (CCAC)-approved protocols. In brief, two rabbits received each a total of four injections of the antigen mixed with Freund's Complete Adjuvant. Each rabbit was pre-bled (to collect the pre-immune serum), and the injections were administered roughly three weeks apart. Ten days after each injection, both rabbits were subjected to bleeds of 6 ml of blood/Kg/every three weeks. Exsanguination of the rabbits was performed after completion of the fourth bleed.

The NHE6 antiserum was antigen-purified as follows: the extreme C-terminal region of NHE6 (amino acids 608-669), which was used to generate the antibody, was fused in frame with the maltose binding protein (MBP) by cloning into the EcoRI/BamHI sites of the pMAL-c2X vector (New England Biolabs, Mississauga, ON, Canada). The fusion protein was purified from *E.coli* BL-21 cultures by binding to 50% slurry of amylose resin (New England Biolabs, Mississauga, ON, Canada). The purified fusion protein was run on a 10% SDS-PAGE and then transferred onto a polyvinylidene difluoride (PVDF) membrane (Millipore, Nepean, ON, Canada) overnight. Next day, the membrane strip was incubated with 2 ml of rabbit serum containing the NHE6 antibody at 4°C overnight. After extensive washes with 50 mM TRIS buffer, the antibody was eluted with 50 mM glycine pH 2.5 for 15 minutes, neutralized with 2 M TRIS pH 8.0, and dialyzed overnight at 4°C in PBS. The antiserum was concentrated by using Amicon® Ultra centrifugal filter devices with 5 kDa cut off (Millipore), diluted with equal amounts of glycerol and stored at -20°C.

Cell Culture and Immunoblot Analysis

AP-1 (Chinese hamster ovary cells devoid of plasma membrane Na^+/H^+ exchange activity) (Rotin and Grinstein, 1989) and HeLa cells were maintained in α-Minimum Essential Medium (α-MEM) supplemented with 10% fetal bovine serum, penicillin (100 units/ml), streptomycin (100 µg/ml), and 25 mM $NaHCO_3$ (pH 7.4). SH-SY5Y human neuroblastoma cells were cultured in High Glucose Dulbecco's Modified Eagle Medium (DMEM) supplemented with 10% fetal bovine serum. All cells were incubated in a humidified atmosphere of 95% air, 5% CO_2 at 37 °C.

For western blot analysis, cells were grown in 10-cm dishes and transiently transfected with 5µg of plasmid DNA encoding $NHE6_{HA}$ (NHE6 containing the influenza virus hemagglutinin (HA) epitope at its extreme C-terminus), or $_{3Flag}NHE6_{HA}$ ($NHE6_{HA}$ with a triple Flag epitope inserted in the first extracellular loop, after M53, to detect plasma membrane NHE6) using Lipofectamine™ (Invitrogen) according to the manufacturer's recommended procedure. Forty eight hours post-transfection, cells lysates were obtained by washing cells twice on ice with ice-cold PBS, followed by scraping in 0.5 ml of lysis buffer (1% Triton X-100/PBS supplemented with a tablet of protease inhibitor cocktail, Roche Diagnostics). The lysates were incubated for 30 min on a rocker at 4°C, and then centrifuged at 16,000 x g for 20 min at 4 °C to pellet the nuclei and cellular debris. Ten to twenty micrograms of protein from the resulting supernatants were eluted in SDS-sample buffer (50mM Tris-HCl, pH 6.8, 1% SDS, 50mM dithiothreitol, 10% glycerol, 1% bromophenol blue), and subjected to 10% SDS-PAGE, then transferred to PVDF membranes for Western blotting. The membranes were blocked with 5% non-fat skim milk for 1 hour, then incubated with the specified primary antibodies (mouse monoclonal anti-HA 1:5000 or rabbit polyclonal anti-NHE6 1:1000) in PBS containing 0.1% Tween 20, followed by extensive washes and incubation with goat anti-mouse or anti-rabbit secondary antibodies conjugated to horseradish peroxidase for 1 hour. Immunoreactive bands

were detected using ECL™ Western blotting detection reagents (GE Healthcare).

To examine endogenous expression of NHE6 in brain tissues, commercially available lysates of human whole brain, mouse whole brain (Abcam Inc., Cambridge, MA), and rat cerebrum (BD Biosciences, Oakville, Ontario, Canada) were used. The mouse hippocampus lysate was a generous gift from Dr. Nahum Sonnenberg's laboratory (McGill University, Montreal, Canada).

Cell Fractionation by Differential Gravity Centrifugation

One 10-cm dish of AP-1 cells stably expressing $NHE6_{HA}$ and 6 plates of SH-SY5Y neuroblastoma cells were grown to confluence. Cells were rinsed twice with ice-cold phosphate-buffered saline (PBS) and one time with 1 X Homogenization Buffer (HB) (0.25 M Sucrose, 1 mM EDTA, 20 mM HEPES-NaOH, pH 7.4, supplemented with protease inhibitor cocktail), then collected in 400 µl HB and lysed by passing 15 times through a 26 G ½ needle. The lysates were centrifuged at 700 x g and the supernatants, representing the S0.7 total lysate fraction, were transferred to fresh Eppendorf tubes. An aliquot of this fraction was removed for western blot analysis and the rest was centrifuged at 6000 x g for 10 min. The supernatant called the S6 fraction was transferred to a fresh tube. The remaining pellet, which represents the P6 fraction, was lysed in 100 µl of 1% Triton X-100/PBS, pH 7.4 by rocking overnight at 4°C. The S6 supernatant was centrifuged at 30,000 x g for 30 min and the resulting pellet (which represents the P30 fraction) was lysed in 100 µl of 1% Triton X-100/PBS, pH 7.4 by rocking overnight at 4°C. The remaining S30 supernatant was centrifuged at 100,000 x g for 45 min and the resulting pellet (which represents the P100 fraction) was lysed in 50 µl of 1% Triton X-100/PBS, pH 7.4 by rocking overnight at 4°C. The resulting S100 supernatant represents the cytosolic fraction. Samples of the resulting fractions were resolved by SDS-PAGE and immunoblot analysis using the

affinity-purified rabbit polyclonal NHE6 antibody (1:1000), followed by incubation with a goat anti-rabbit-HRP-conjugated secondary antibody (1:5000). Immunoreactive bands were detected using Western Lightning® Plus-ECL reagents (Perkin Elmer, Inc., Waltham, MA).

Endoglycosidase Treatments

Post-nuclear supernatants of AP1 cells stably expressing $NHE6_{HA}$ were treated with endoglycosidases, according to the manufacturer's recommendations. First, glycoproteins were denatured in 1x denaturing buffer (0.5% SDS, 1% β-mercaptoethanol) at 100°C for 10 min Samples were then divided equally and treated with either Peptide N-glycosidase F (PNGase F) (750 units, New England Biolabs, Mississauga, ON, Canada) or Endo-β-N-acetylglucosaminidase H (Endo H) (750 units, New England Biolabs, Mississauga, ON, Canada). The enzymes were added to 30 µl reactions and incubated overnight at 37°C. Next day, samples were diluted with two-fold concentrated SDS-PAGE sample buffer, boiled for 3 min., briefly centrifuged, and analyzed by SDS-PAGE and western blotting.

Cell Surface Biotinylation

AP-1 cells stably expressing $NHE6_{HA}$ were cultured in 10-cm dishes to sub-confluence, placed on ice and washed three times with ice-cold PBS containing 1 mM $MgCl_2$ and 0.1 mM $CaCl_2$, pH 8.0 (PBS-CM). Next, cells were incubated at 4°C for 30 min with the membrane-impermeable reagent N-hydroxysulfosuccinimydyl-SS-biotin (0.5 mg/ml, Pierce). Cells were washed and incubated twice in quenching buffer (20 mM glycine in PBS-CM) for 7 minutes each on ice to remove unreacted biotin. After two more washes in PBS-CM, the cells were lysed in PBS buffer containing 1% TritonX-100 and protease inhibitor cocktail (Roche) for 30 min on ice, and then centrifuged at 16,000 x g for 20 min at 4°C to remove insoluble cellular debris. A portion of the resulting supernatant was removed and

this represents the total fraction. Increasing fractions of the remaining supernatant were incubated with 100 µl of 50% NeutrAvidin® Agarose Resin slurry (Fisher Scientific, Whitby, ON, Canada) in lysis buffer overnight at 4°C to extract biotinylated membrane proteins. The proteins were then resolved by SDS-PAGE and immunoblot analysis with a monoclonal anti-HA antibody (1:5000). The intensity of the bands was quantified by densitometry from X-ray films exposed in the linear range and analyzed with the FC1000 gel imaging system and software (Alpha Innotech, San Leandro, CA).

Immunofluorescence Confocal Microscopy

AP-1 cells expressing $NHE6_{HA}$ and HeLa cells expressing $_{3Flag}NHE6_{HA}$ were grown in 6-well plates on glass coverslips coated with poly-L-lysine hydrobromide (0.1 mg/ml, Sigma). SH-SY5Y cells were grown on coverslips coated with 2 µg/ml fibronectin (Sigma).

To examine the subcellular localization of NHE6, cells were fixed in 2% paraformaldehyde/PBS for 20 minutes at room temperature, permeabilized with 0.1% saponin/PBS for 20 minutes, and then blocked in 10% goat serum /0.01% saponin/PBS for 1 hour at room temperature. Cells were incubated subsequently with the specified primary antibodies (mouse monoclonal anti-HA 1:2000, anti-Flag 1:3000, anti-Transferrin Receptor 1:200, or rabbit polyclonal anti-NHE6 1:500) overnight at 4°C. Next day, cells were washed four times with 10% goat serum/0.01% saponin/PBS, and then incubated with Alexa Fluor® 568 or Alexa Fluor® 488-conjugated secondary antibodies at a dilution of 1:2000 in 10% goat serum/0.01% saponin/PBS for 1 hour at room temperature. In some cases, membranes were stained using wheat germ agglutinin (WGA) coupled to Alexa Fluor® 594 at a dilution of 1:200 in PBS. After extensive washes with PBS, cover slips were mounted onto glass slides with Aqua Poly/Mount mounting medium (Polysciences Inc., Warrington, PA). Cells were examined by laser scanning confocal microscopy using a Zeiss LSM

510 Meta, and images were analyzed using LSM software and Corel® CorelDraw™ version 13.

Electron microscopy of AP-1 cells

AP-1 cells stably expressing $NHE6_{HA}$ or non-transfected controls were grown on Permanox Lab-Tek® chamber slides (Nalgene, Rochester, NY) to 70-80% confluence, washed in 0.01 M Phosphate Buffered Saline (PBS), and then fixed in 4% paraformaldehyde/0.25% glutaraldehyde/0.1 M Phosphate Buffer (PB). Subsequently, aldehyde groups were blocked for 30 min in 1% sodium borohydride/PBS, and then the samples were washed in PBS, and further blocked for 1 h in 1% BSA/1% FBS/5% goat serum. Cells were permeabilized for 15 min in 0.1% saponin prepared in 1% BSA/1% FBS/5% goat serum/PBS, and then incubated with mouse monoclonal anti-HA antibody (1:200) or no primary antibody (as control) overnight at 4°C in a humid chamber. Next day, cells were washed in PBS, blocked for 10 min in washing buffer (0.1% gelatin stock/0.8% BSA in PBS) and then incubated with goat anti-mouse secondary antibody conjugated to 0.8 nm gold particles (1:50) (Cedarlane, Hornby, Ontario, Canada) overnight at 4°C in a humid chamber. The following day, cells were washed in PBS, fixed for 10 min in 2% glutaraldehyde/PBS, washed and then silver-intensified (silver intensification kit was from GE Healthcare, Baie d'Urfe, QC, Canada), followed by washes in 0.2 M citrate buffer and 0.1 M PB, and post-fixation with 1% osmium tetroxide/0.1 M PB for 1 h at 4°C. Cells were then dehydrated in successive baths of increasing concentrations of ethanol, embedded in Epon (Mecalab, Montreal, Canada) and left to polymerize at 55°C for 48 hours. Ultrathin sections (~60 nm thick) were cut using a Reichert-Jung ultramicrotome, placed onto one-slot, formvar-coated grids, counterstained with uranyl acetate and lead citrate and examined with a Philips 410 electron microscope equipped with a digital camera (Philips Electron Optics Canada, Toronto, ON, Canada).

Detection of NHE6 in Hippocampal Organotypic Slice Cultures

All procedures for animal handling were carried out according to the guidelines of the Canadian Council on Animal Care (CCAC). Transverse hippocampal tissue slices (400 µm) were made from the brains of non-transgenic mice. Slices were mounted onto glass coverslips using chicken plasma and thrombin, and transferred to diagonal flat-bottomed culture tubes containing culture media. Cultures were incubated at 36°C while rotating at a speed of 10 revolutions/hour. Cultures were allowed to mature *in vitro* using the previously described Gähwiler method (Gahwiler et al., 1997) for 21 days.

CA1 pyramidal neurons of slice cultures derived from non-transgenic mice were infected with a Semliki Forest virus strain A7 (SFV A7) expressing a variant GFP construct that undergoes farnesylation (fn-GFP) to facilitate its attachment to cell membranes. SFVA7 selectively targets neurons, thus restricting labeling to this cell type (Lundstrom et al., 2003). Infection was achieved by injecting 1-2 µl of the virus via a glass pipette into the CA1 region, as previously described (Haber et al., 2006). At 16-20 hours after the infection, the cultures were fixed and processed for NHE6 immunohistochemistry.

Cultures were fixed with 4% paraformaldehyde (Sigma Aldrich) dissolved in 0.1 M phosphate buffer (pH 7.4) (PB; Sigma Aldrich) overnight at 4°C. Following fixation, cultures were washed with 0.1 M PB, permeabilized in 0.8% Triton X-100 and blocked with 3 % heat inactivated horse serum (HIHS) (Sigma Aldrich) in PB overnight at 4°C. Cultures were processed for 5 days at 4°C with the primary antigen-purified polyclonal antibody specific for NHE6, diluted 1:250 in 0.4% Triton X-100 and 1.5% HIHS. This long incubation time is needed for the antibody to maximally penetrate the tissue. NHE6 was revealed by indirect immunohistochemistry using anti-rabbit AlexaFluor 594®-conjugated secondary antibody diluted 1:250 in PB with 1.5% HIHS, for two hours at room temperature. Cultures were mounted onto microscope slides using UltraMount® fluorescent mounting medium (Dako) prior to imaging and

subsequent analysis. Control and treated cultures were processed simultaneously.

Confocal Z-stacks were taken using a Leica SP2 laser scanning confocal microscope (beam splitter 488/543/633 nm) equipped with 40x and 63x HCXPL APO oil immersion objectives (numerical apertures 1.25 and 1:4). 512x512 bit images were obtained with Leica confocal software. Optical sections of 0.25-0.3 µm were taken, averaged 3 times to reduce signal-to-noise ratios. Image stacks were deconvolved using Huygens Essential software (Scientific Volume Imaging, Hilversum, Netherlands) and 3D images were compiled as maximum intensity projections using Imaris software (Bitplane Scientific Solutions). Sequential imaging for colocalization of AlexaFluor594-tagged NHE6 with eGFP-labeled CA1 pyramidal neurons was done using 543-nm Helium Neon and 488-nm Argon lasers, respectively.

Electron microscopy of mouse brain

C57BL/16xCD1WT mice were anaesthetized with Equithesin (6.5 mg chloral hydrate and 3 mg sodium pentobarbital in a volume of 0.3 ml, and 0.01 ml of heparin (10 USP/ml), intraperitoneal, per 100 g body weight) and after quick vascular rinse with 0.1% $NaNO_2$, transcardially perfused with 4% paraformaldehyde, 0.1% glutaraldehyde in 0.1 M phosphate buffer (PB), pH 7.4, for 30 min. Perfusion was continued for 30 min with 4% paraformaldehyde in 0.1M PB buffer and 30 min with 10% Sucrose in 0.1M PB. Following tissue extraction, the brains were placed in 30% sucrose in PB overnight at 4°C and next day dissected to obtain prefrontal cortex and hippocampus. Transverse sections (~50 µm thick) were cut on a Vibratome (TPI, St. Louis, MO, USA). Sections were cryoprotected for 1h in 30% sucrose/10% glycerol in 0.1M PB and 1h in 30% sucrose/ 20% glycerol in PB. Three freeze-thaw cycles were performed in isopentane pre-cooled in liquid nitrogen. Sections were treated with 1% sodium borohydride, washed, blocked with 0.5% BSA/0.01 M PBS and treated with rabbit polyclonal anti-NHE6 antibody

(1:200) in 0.01 M PBS supplemented with 0.1% BSA overnight at 4°C. After washes, sections were incubated with 0.8 nm gold-conjugated goat anti-rabbit secondary antibody (1:50) in 0.1% BSA/0.01 M PBS (Cedarlane, Hornby, Ontario, Canada). The signal was amplified using a silver intensification kit (GE Healthcare, Baie d'Urfe, QC, Canada). All sections were then incubated for 1 h in 1% osmium tetroxide/0.1M PB at 4°C. Following dehydration in ascending concentrations of alcohols and propylene oxide, the sections were flat-embedded in Epon. After polymerization, the blocks were trimmed to be able to cut the CA3 and CA1 regions of the hippocampus, and Lamina I, II, III of prefrontal cortex. Ultrathin sections were cut on a Reichert-Jung ultramicrotome using a diamond knife. The ultrathin sections were collected onto one-slot, formvar-coated grids, counterstained with uranyl acetate and lead citrate and examined with a Philips 410 electron microscope equipped with a digital camera (Philips Electron Optics Canada, Toronto, ON, Canada).

RESULTS

The sodium/proton exchanger isoform 6 (NHE6) is a member of the organellar-type subfamily of mammalian alkali/proton exchangers, which is ubiquitously expressed in tissues, but the highest levels of NHE6 mRNA were detected in brain, skeletal muscle, and heart (Numata et al., 1998). Earlier light microscopy studies using heterologous cell expression systems revealed that NHE6 localizes to a perinuclear recycling endosomal compartment (Brett et al., 2002; Nakamura et al., 2005; Ohgaki et al., 2008). To characterize its subcellular distribution in finer detail, NHE6 variants containing either internal or external epitope tags were constructed and characterized in transfected nonpolarized cells by both light and electron microscopy. In addition, an isoform-specific rabbit polyclonal antibody was generated to examine the precise localization of

NHE6 in neuronal cells, which has not been addressed so far in the literature.

First, we tested the expression of a C-terminal HA-epitope tagged form of NHE6 ($NHE6_{HA}$) (Fig. 1.1A) in AP-1 cells, which are a mutagenized derivative of Chinese Hamster Ovary cells devoid of plasma membrane NHE activity (Rotin and Grinstein, 1989). Western blot analysis with anti-HA antibody of lysates obtained from AP-1 cells expressing $NHE6_{HA}$ revealed two bands: a slow migrating fully-glycosylated form (~83 kDa) and a faster migrating core-glycosylated form (~65 kDa). We demonstrate that this migration pattern is due to the N-glycosylation of NHE6 using treatments with specific endoglycosidases, known to differentially cleave the sugars acquired by proteins in the endoplasmic reticulum versus the Golgi apparatus. Endo-β-N-acetylglucosaminidase H (Endo H) removes only high-mannose core-glycosylated residues, which is visible on a gel by a minor shift in the migration of the lower band (Fig. 1.1B). Peptide-N-glycosidase F (PNGase F) is a glycoaminidase that cleaves all asparagine-linked (N-linked) oligosaccharides from glycoproteins, resulting in the complete disappearance of the slower migrating upper band (Fig. 1.1B). The subcellular distribution of the HA-tagged form of NHE6 ($NHE6_{HA}$) was also examined by immunofluorescence confocal microscopy in AP-1 cells. Consistent with earlier findings (Miyazaki et al., 2001; Brett et al., 2002), $NHE6_{HA}$ is present in punctate structures that overlap significantly with the transferrin receptor, a recycling endosomal marker (Figure 1.1 C).

Recycling endosomes are dynamic organelles that shuttle to and from the plasma membrane. Thus, it is conceivable that NHE6 might also be present, at least transiently, at the cell surface. This possibility is supported by an earlier study by Brett and colleagues (2002) who used a cell surface biotinylation assay to show that a minor fraction (~5%) of the total expression of a chimeric NHE6-green fluorescent protein (GFP) construct was present at the plasma membrane when transiently

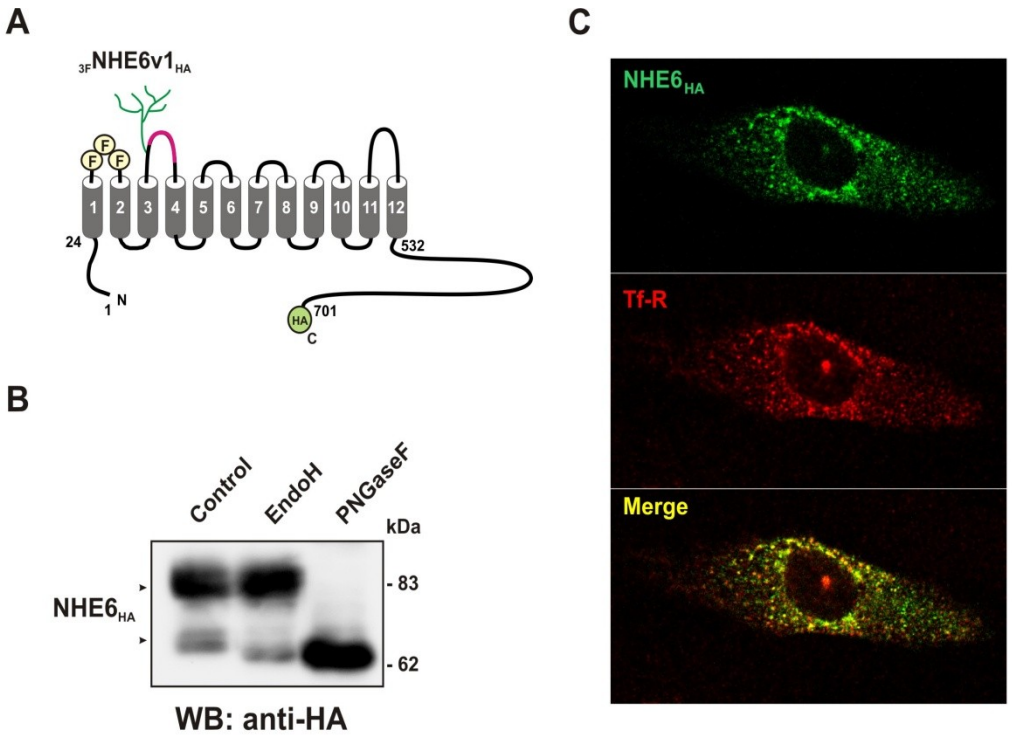

Figure 1.1. Expression of human NHE6-v1 in transiently transfected AP-1 cells.

A. Diagram depicting the predicted transmembrane organization of human NHE6-v1 containing a hemagglutinin (HA)-epitope tag at its C-terminus and a 3x Flag (3F) tag in the first extracellular loop.

B. Western Blot analysis of an HA-tagged form of human NHE6 reveals two bands; a slow migrating fully-glycosylated form (~83 kDa) and a faster migrating core-glycosylated form (~65 kDa). The core-glycosylated residues can be removed by the Endo H glycosidase, whereas all sugars can be removed by the PNGase F glycosidase.

C. $NHE6_{HA}$ colocalizes with the transferrin receptor (Tf-R), a marker of recycling endosomes. AP-1 cells were transfected with $NHE6_{HA}$ and labeled using rabbit polyclonal anti-HA and mouse monoclonal anti-transferrin receptor primary antibodies, followed by anti-rabbit Alexa568 and anti-mouse Alexa488-conjugated secondary antibodies.

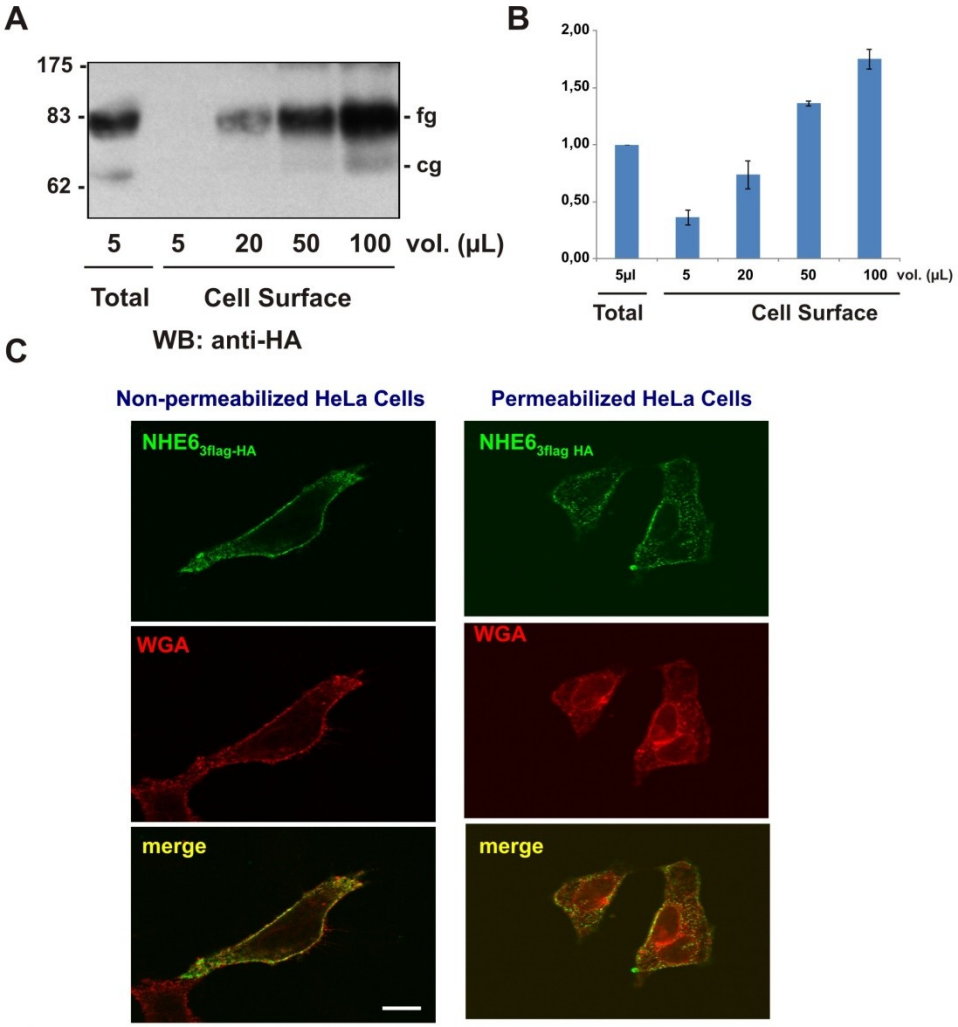

Figure 1.2. NHE6 is present on the cell surface of transfected cells.

A. Plasma membrane $NHE6_{HA}$ levels were detected in stably transfected AP-1 cells using a cell surface biotinylation assay. Total cell lysates were prepared (500 µl) and a portion representing the total fraction was removed. Increasing fractions of the remaining supernatant were incubated with NeutrAvidin® Agarose beads to extract cell surface proteins. A 5 µl aliquot of the original total cell lysate and the cell surface fractions were analyzed by Western blotting with a monoclonal anti-HA antibody. *fg* - fully glycosylated form; *cg* - core glycosylated form.

B. Densitometric quantification of three separate experiments shows that less than 10 % of NHE6 is present on the cell surface. Data points represent mean ± S.D.

C. NHE6 was visualized at the cell surface of transiently transfected HeLa cells using confocal microscopy. To this end, a triple-Flag epitope was inserted into the first extracellular loop of NHE6. $_{3Flag}NHE6_{HA}$ was detected by incubation with anti-Flag primary antibody and Alexa488-conjugated secondary antibody; Alexa594-conjugated wheat germ agglutinin (WGA) was used as a membrane marker. Scale bar represents 10 µM.

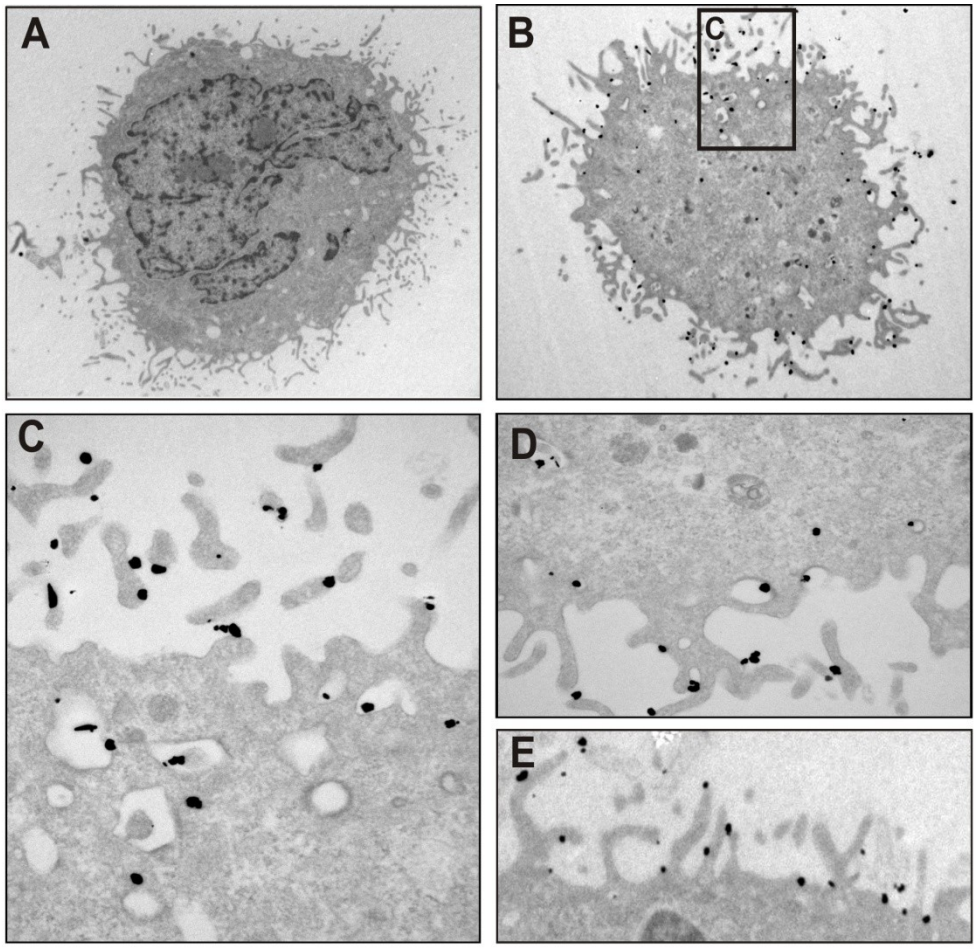

Figure 1.3. Detection of $NHE6_{HA}$ at the plasma membrane and endosomes in transfected AP-1cells by transmission electron microscopy.

AP-1 cells stably expressing human $NHE6_{HA}$ were incubated in the absence (negative control) (A) or presence (B-E) of a mouse monoclonal anti-HA antibody, followed by incubation with a secondary goat anti-mouse anti-IgG antibody conjugated to 0.8 nm gold particles.

overexpressed in CHO cells. A caveat to the use of transiently transfected cells is that they usually contain a high copy number of the exogenous gene which can result in excessive production of the corresponding protein and saturation of the sorting machinery; thereby potentially causing protein mistargeting. By contrast, stable transfections help minimize this concern as they typically contain a low copy number of the introduced gene. Hence, the plasma membrane accumulation of exogenous NHE6 was re-examined in stably transfected CHO/AP-1 cells using the cell surface biotinylation assay. As shown in Fig. 1.2A (*right panel*), western blot analysis of increasing fractions of cell surface biotinylated proteins revealed that less than 10% of the protein can be detected at the plasma membrane; confirming earlier observations. Hence, using the surface biotinylation technique, a minor fraction of NHE6 appears to be retained at the plasma membrane of CHO cells regardless of the mode of transfection. However, an additional limitation of the above analyses is that the N-hydroxysulfosuccinimydyl-SS-biotin reagent, which is normally membrane-impermeant, can penetrate dead cells within the cultures, leading to a false positive result for cell surface expression.

Hence, to validate the subcellular distribution of NHE6 by an alternative approach and to establish the general nature of this expression pattern in nonpolarized cells, NHE6 expression was re-examined in transiently transfected HeLa cells by light microscopy. To visualize cell surface NHE6, a triple-Flag epitope was inserted into the first extracellular loop of NHE6. Surface NHE6 was detected by incubating non-permeabilized cells with an anti-Flag antibody and green Alexa Fluor®488-conjugated secondary antibody. The cell surface was labelled with Alexa Fluor®594-conjugated wheat germ agglutinin (WGA) (Fig. 1.2C, *left panels*). When we labelled permeabilized HeLa cells expressing $_{3Flag}NHE6_{HA}$ under the same conditions, the presence of NHE6 was detected mainly in intracellular punctate structures, corresponding to endosomes, as expected (Fig. 1.2C, *right panels*).

To further verify the immunofluorescence confocal microscopy results, the localization of NHE6 was tested in AP-1 cell stably expressing $NHE6_{HA}$ by transmission electron microscopy. To this end, the cells were incubated in the absence (negative control) or presence of a mouse monoclonal anti-HA antibody, followed by labelling with a secondary goat anti-mouse anti-IgG antibody conjugated to 0.8 nm gold particles and silver-intensification. As shown in Figure 1.3A, no immunogold labelling was detectable in the absence of the anti-HA primary antibody. However, in cells incubated with the anti-HA antibody, lots of staining was observed (Fig. 1.3B), which was localized both in endosomal structures and at the cell surface (Figs. 1.3C-D), particularly in microvillar-like (Fig. 1.3E) and filopodial (1.3D) membrane protrusions. Thus, these ultrastructural images support the localization of NHE6 in endosomes and at the plasma membrane observed by light microscopy.

In order to be able to examine the distribution of native NHE6 at the protein level in cells and tissues, a specific rabbit polyclonal antibody was developed. A recombinant fusion protein consisting of glutathione-S-transferase (GST) linked to isoform-specific C-terminal fragment of NHE6 (amino acids 608-669) was constructed and overexpressed in bacteria, then purified and injected into rabbits using standard Canadian Council on Animal Care (CCAC)-approved protocols (see Materials and Methods for more details). The isolated serum was subjected to antigen-purification to enrich for the NHE6 antibody, as described in the Materials and Methods section.

To test the antibody for NHE isoform specificity, whole cell lysates of AP-1 cells transiently expressing $NHE1_{HA}$, $NHE6_{HA}$, $NHE7_{HA}$, $NHE8_{HA}$, or $NHE9_{HA}$ were fractionated by SDS-PAGE and then subjected to immunoblot analysis using the purified anti-NHE6 antibody. As shown in Figure 1.4A (*upper panel*), two strong immunoreactive signals were detected for NHE6; a slower-migrating, fully-glycosylated form (~83 kDa)

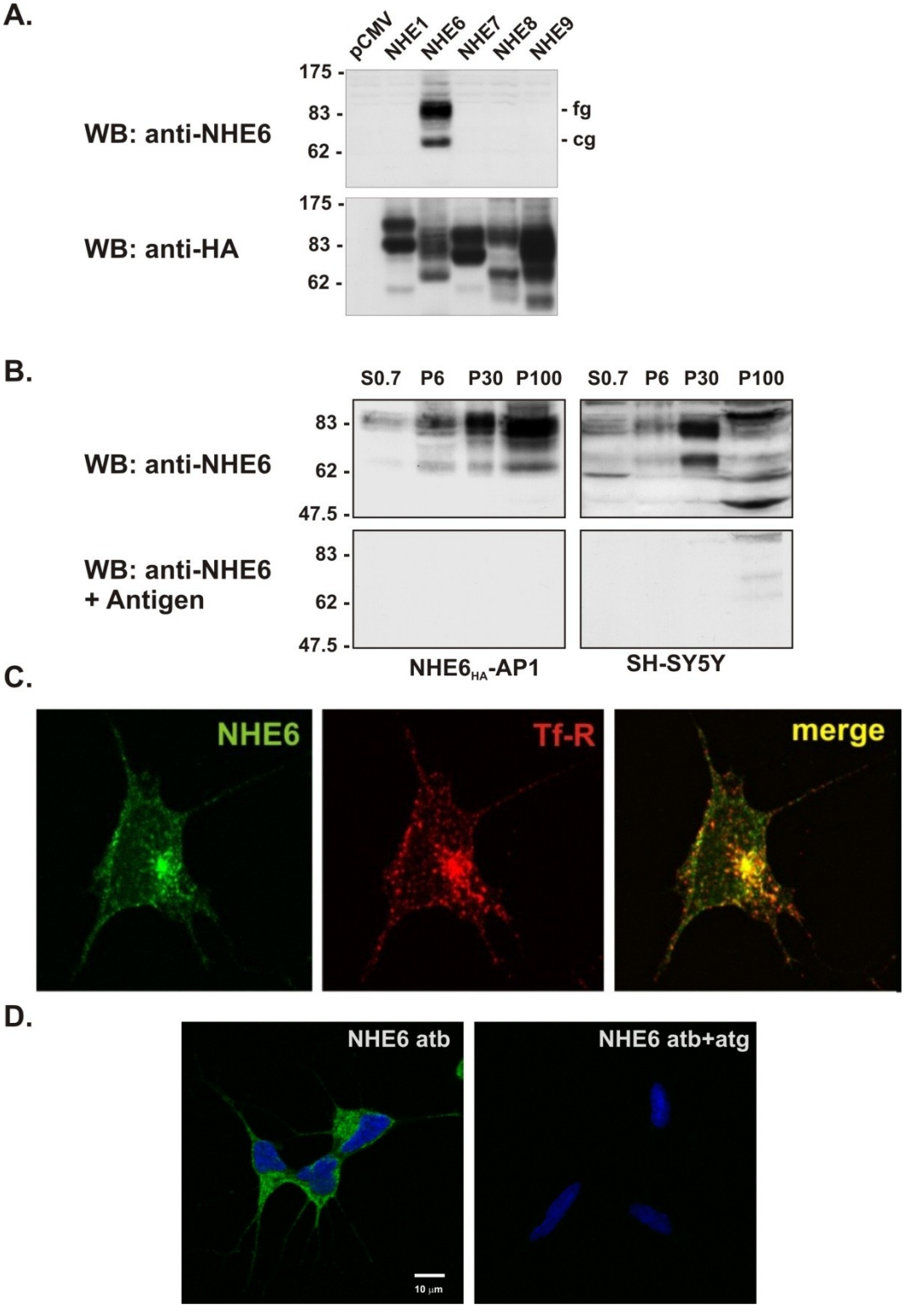
A.
pCMV
NHE1
NHE6
NHE7
NHE8
NHE9
175 -
83 -
62 -
- fg
- cg
WB: anti-NHE6
WB: anti-HA
B.
S0.7
P6
P30
P100
83 -
62 -
47.5 -
WB: anti-NHE6
WB: anti-NHE6
+ Antigen
NHE6HA-AP1
SH-SY5Y
C.
NHE6
Tf-R
merge
D.
NHE6 atb
NHE6 atb+atg
10 µm

Figure 1.4. Characterization of an NHE6 isoform-specific rabbit polyclonal antibody.

A. Lysates of AP-1 cells transiently expressing human $NHE1_{HA}$, $NHE6_{HA}$, $NHE7_{HA}$, $NHE8_{HA}$, and $NHE9_{HA}$ were subjected to SDS-PAGE and immunoblot analysis. In the *upper panel ,* the blot was probed with the anti-NHE6 affinity purified antibody. In the *lower panel* , the immunoblot of HA-epitope tagged constructs of NHE6-9 was reprobed with a mouse monoclonal anti-HA antibody.

B. AP-1 and SH-SY5Y cells were subjected to fractionation and SDS-PAGE, followed by immunoblot analysis with the anti-NHE6 affinity-purified antibody (*upper panels*) or with NHE6 antibody pre-incubated with the immunizing antigen (*lower panels*).

C. Colocalization of native NHE6 with the transferrin receptor (Tf-R) in the soma and neurites of cultured human SH-SY5Y neuroblastoma cells.

D. Control experiment showing that the signal detected with the NHE6 antibody is specific in SH-SY5Y neuroblastoma cells, as no fluorescent signal is observed in the presence of immunizing antigen. The green Alexa Fluor488-conjugated secondary goat anti-rabbit antibody was applied to both samples.

and a faster migrating core-glycosylated form (~65 kDa), which correspond to the expected sizes of NHE6. No signal was detected in lysates of AP-1 cells that were transfected with the plasma membrane-type $NHE1_{HA}$ nor with the closely-related NHE6 paralogs $NHE7_{HA}$, $NHE8_{HA}$ or $NHE9_{HA}$, verifying the selectivity of the antibody for NHE6. As a control, the blots were subsequently stripped and reprobed with an anti-HA monoclonal antibody to verify the expression of the NHE isoforms (Fig. 1.4A*, lower panel*).

To further confirm the NHE6 antibody specificity and to detect native NHE6 in cells, cell fractionation was performed by differential gravity centrifugation, followed by immunoblot analysis. We used AP-1 cells stably expressing $NHE6_{HA}$ (as positive control) and human neuroblastoma SH-SY5Y cells. NHE6 was detected in all examined fractions, but was more abundant in the P30 fraction, in both the stably transfected AP-1 cells and endogenously in the SH-SY5Y neuroblastoma cell line (Fig. 1.4B). To test the specificity of the NHE6 antibody, a parallel gel was run and immunoblotted with the antibody pre-incubated with the immunizing antigen. As shown in Figure 1.4B (*lower panels*), no immunoreactive bands were detected under these experimental conditions, confirming the specificity of the signal obtained with the NHE6 antibody.

Next, the efficacy of the anti-NHE6 antibody was evaluated in cellular localization analyses by dual-immunolabelling confocal microscopy in human neuroblastoma SH-SY5Y cells. As shown in Figure 1.4C, immunoreactive signals for native NHE6 were detected in punctate vesicles in the soma and neurites that overlapped significantly, but not completely, with transferrin receptor-containing endosomes. Additional control experiments showed no detectable signals in SH-SY5Y neuroblastoma cells labelled with the primary NHE6 antibody in the presence of competing immunizing antigen (Fig. 1.4D).

To examine the expression of NHE6 in brain, lysates of rat cerebrum, whole human and mouse brain, as well as isolated mouse hippocampus were separated by SDS-PAGE and immunoblotted with the native NHE6 antibody. As shown in Fig. 1.5, both the core and fully glycosylated forms of NHE6 were detected in all examined tissues. Lysates of AP-1 cells transfected with empty vector and the tagged $NHE6_{HA}$ form were resolved on the same blot as negative and positive controls, respectively. The observation that our antibody can recognize not only human, but also mouse and rat NHE6, highlights the utility of this probe for further analysis of NHE6 expression in brain of different animal models.

The above immunoblot analysis indicates that NHE6 is expressed in the hippocampus. To provide a more refined evaluation of its subcellular distribution in hippocampal CA1 neurons, confocal imaging was performed using hippocampal organotypic slice cultures (postnatal day 6; *in vitro* 21 days). As shown in Figure 1.6C, the immunofluorescence signal for NHE6 was highly punctate within the CA1 area of the hippocampus. The control sample prepared in the absence of the primary antibody was negative (Fig. 1.6A). Furthermore, after incubation of the samples with the primary antibody in the presence of the immunizing antigen, no fluorescent signal was detected (Fig. 1.6B). These controls demonstrate once again the specificity of the NHE6 antibody.

To further characterize the distribution of NHE6 in this region, CA1 excitatory pyramidal neurons were labeled by transfecting them with a Semliki Forest Virus A7 (SFVA7) strain expressing a variant GFP construct that undergoes farnesylation (fn-GFP) to facilitate its attachment to cell membranes (Fig. 1.6D). The advantage of using Fn-GFP is that it only demarcates the plasma membrane, whereas WGA and FM4-64 can stain also intracellular membranes with time. As shown in Figures 1.6E and 1.6F, a maximum intensity projection (stacked optical sections) revealed dense populations of NHE6 positive punctae within the soma and

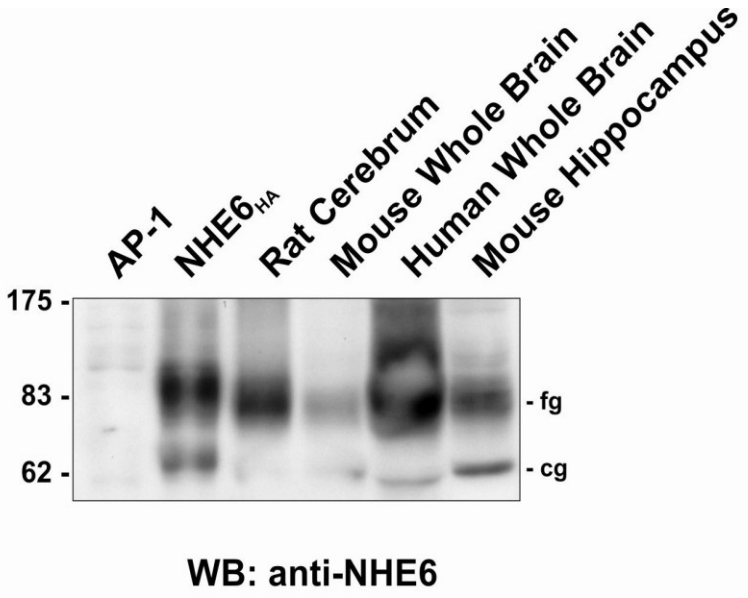

Figure 1.5. Detection of native NHE6 in brain tissue lysates.

Lysates of AP-1 cells transiently transfected with empty vector (AP-1) or $NHE6_{HA}$, as well as lysates of rat cerebrum, mouse whole brain, human whole brain, and mouse hippocampus were subjected to SDS-PAGE and immunoblot analysis with the anti-NHE6 antibody. The fully glycosylated (*fg*), mature form of NHE6, as well as the core-glycosylated form (*cg*) are visible.

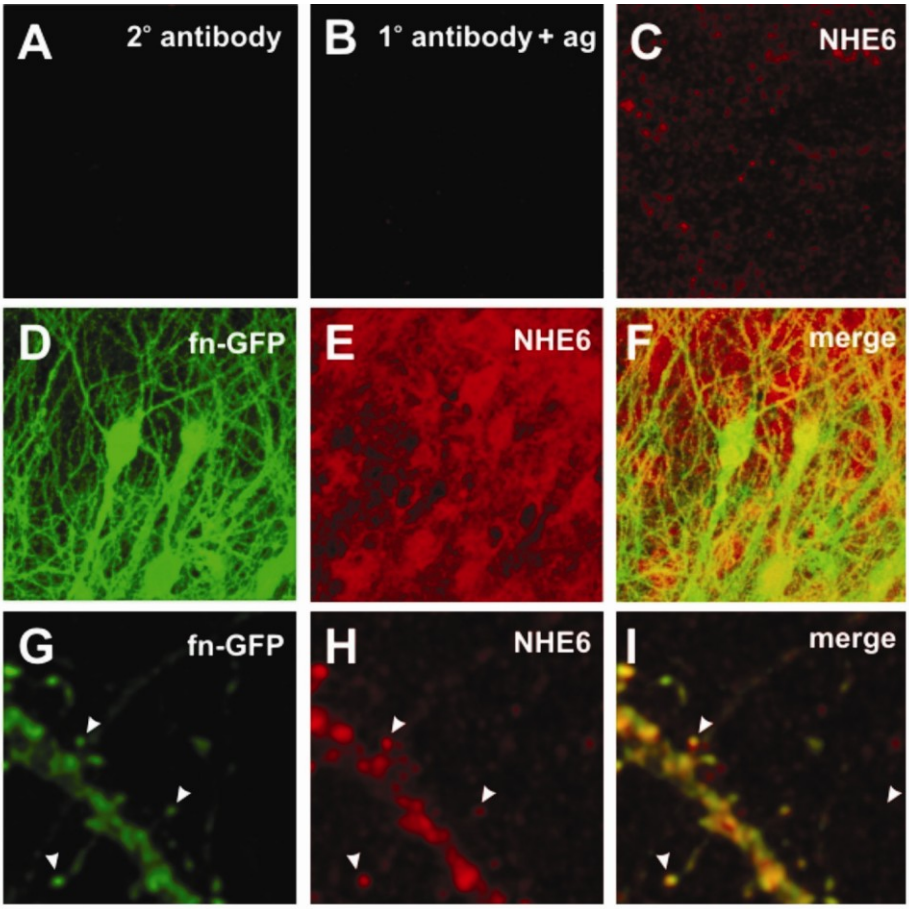

Figure 1.6. Confocal imaging showing the localization of NHE6 in area CA1 of organotypic slice cultures (postnatal day 6, *in vitro* 21 days).

A. Control without 1° antibody showing that the 2nd antibody CY5 was not labeling unspecifically.
B. Control with 1° antibody in the presence of immunizing antigen.
C. Micrograph revealing NHE6 positive punctae are densely located within area CA1 of the hippocampus.
D - F. Micrographs showing a maximum intensity projection of the localization of NHE6 within CA1 excitatory pyramidal neurons which have been labeled by transfecting with a Semliki Forest Virus A7 (SFVA7) strain expressing farnesylated GFP (fn-GFP). **(D)** reveals many pyramidal cells which are labeled with SFVA7. **(E)** NHE6 staining of the area. **(F)** NHE6 positive punctae are located within the soma and dendrites of CA1 pyramidal cells.
G - I. Micrographs of maximum intensity projections of the localization of NHE6 punctae within the postsynaptic specialization, the dendritic spines (*arrowheads*).

dendrites of CA1 pyramidal cells, and most likely interneurons and astrocytes as well. Higher resolution images of isolated dendrites showed that NHE6-containing vesicles are located not only in dendritic shafts, but also in the spines (Fig. 1.6G-I). This is an exciting observation as it suggests a potential role for NHE6-containing vesicles in spine morphogenesis and plasticity.

To further corroborate this observation at even higher resolutions, we examined the localization of native NHE6 in the CA1 and CA3 regions of mouse hippocampus, as well as in mouse prefrontal cortex by transmission electron microscopy (TEM). Following incubations of the tissue samples with the antigen-purified NHE6 antibody, the 0.8 nm gold-conjugated goat anti-rabbit secondary antibody, and silver intensification, both in the CA3 (Fig. 1.7., *upper panels*) and CA1 (Fig. 1.7, *middle panels*) regions of the hippocampus, NHE6 positive signals were detected in dendrites, occasionally adjacent to postsynaptic densities (PSD), which is suggestive of excitatory synapses. Occasionally, some NHE6-positive puncta were observed presynaptically, associated with synaptic boutons (Fig. 1.7, *upper right panel*). In control experiments with no primary antibody, no (or extremely little) staining was observed in the examined sections, confirming the specificity of the signal produced by the NHE6 antibody (Fig. 1.7, *lower panel*).

The same staining pattern was observed in sections of mouse prefrontal cortex, with NHE6 signal being present in dendrites, sometimes associated with postsynaptic densities (Fig. 1.8, *upper panels*). In negative control samples incubated in the absence of primary antibody, very little signal was detected (Fig. 1.8, *lower panel*).

DISCUSSION

The sodium/proton exchanger isoform 6 (NHE6) is a member of the organellar-type subfamily of mammalian alkali cation/proton exchangers,

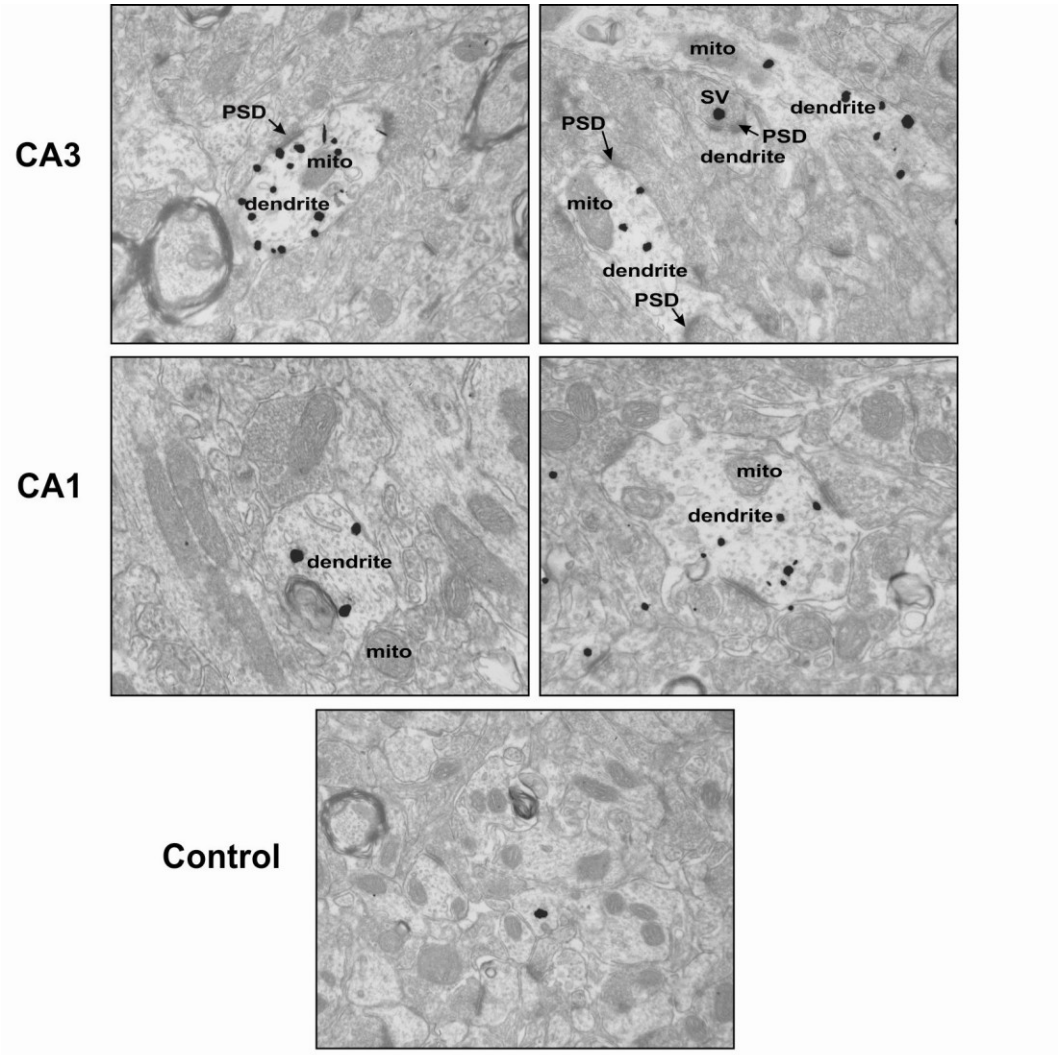

Figure 1.7. Subcellular localization of native NHE6 in areas CA3 (*upper panels*) and CA1 (*middle panels*) of mouse hippocampus by transmission electron microscopy.

C57BL/16xCD1WT mice were anaesthetized with Equithesin intraperitoneally, perfused transcardially with 4% paraformaldehyde, 0.1% glutaraldehyde in 0.1 M phosphate buffer (PB) according to standard protocols. Brains were dissected to obtain prefrontal cortex and hippocampus. Ultrathin sections (50 µm) were treated with rabbit polyclonal anti-NHE6 antibody (1:200) (*upper and middle panels*) or no antibody (*lower panel*) overnight at 4ºC. After washes, sections were treated with 0.8 nm gold-conjugated goat anti-rabbit secondary antibody (1:50). Signal was amplified with a silver intensification kit. Images were examined with a Philips 410 electron microscope equipped with a digital camera. Magnification: x24400.
Abbreviations: SV, *synaptic vesicles*, PSD, *postsynaptic density*, mito, *mitochondria*

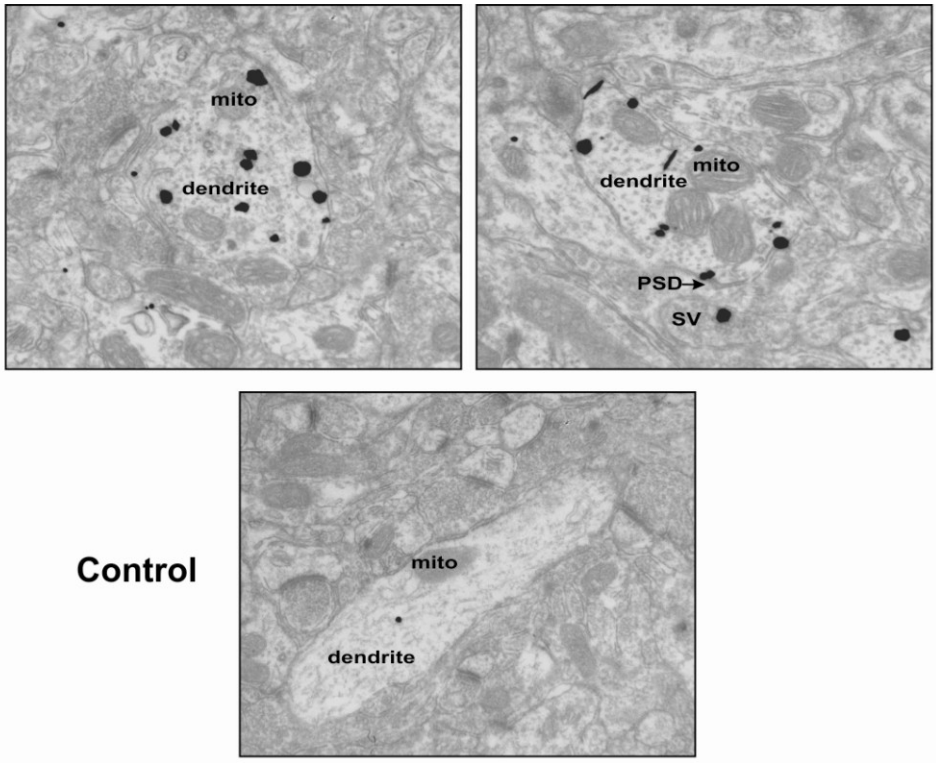

Figure 1.8. Subcellular localization of native NHE6 in mouse prefrontal cortex by transmission electron microscopy.

C57BL/16xCD1WT mice were anaesthetized with Equithesin intraperitoneally, perfused transcardially with 4% paraformaldehyde, 0.1% glutaraldehyde in 0.1 M phosphate buffer (PB) according to standard protocols. Brains were dissected to obtain prefrontal cortex and hippocampus. Cryosections (50 µm thick) were treated with rabbit polyclonal anti-NHE6 antibody (1:200) (*upper panels*) or no antibody as control (*lower panel*) overnight at 4ºC. After washes, sections were treated with 0.8 nm gold-conjugated goat anti-rabbit secondary antibody (1:50). Signal was amplified with a silver intensification kit. Images were examined with a Philips 410 electron microscope equipped with a digital camera. Magnification: x24400.

Abbreviations: SV, *synaptic vesicles*, PSD, *postsynaptic density*, mito, *mitochondria*

which also includes NHE7, 8, and 9. Like other members of this subgroup, NHE6 is ubiquitously expressed in tissues, but the highest mRNA levels are found in brain, skeletal muscle, and heart (Numata et al., 1998). It has been shown that in nonpolarized cultured cells, NHE6 is localized mainly in recycling endosomal compartments (Brett et al., 2002; Nakamura et al., 2005; Ohgaki et al., 2008). However, the precise localization of NHE6 in brain has not been addressed so far in the literature.

To characterize its subcellular distribution in finer detail, NHE6 constructs containing either internal or external epitope tags were generated and characterized in transfected nonpolarized cells by both light and electron microscopy. The expression of an HA-tagged form of NHE6 ($NHE6_{HA}$) in AP-1 cells showed that NHE6 is an N-linked glycoprotein that is localized in recycling endosomes and on the plasma membrane, which is in agreement with previous data from the literature (Miyazaki et al., 2001; Brett et al., 2002). Additionally, electron microscopy was used for the first time to study NHE6 at the ultrastructural level. Our analysis in AP-1 cells stably expressing $NHE6_{HA}$ showed the presence of NHE6 both in endosomal structures and at the cell surface, especially along microvillar-like and filopodial structures. Microvilli are best characterized in epithelial cells with a brush border, where they enlarge the apical surface and increase the absorptive capacity of these cells (Kerjaschki et al., 1984; Danielsen and van, 1995) However, microvilli-like protrusions have been also described in non-epithelial cells, such as leukocytes, where they are involved in cell-to-cell adhesion (von Andrian et al., 1995). Interestingly, several types of membrane protrusions, including microvilli, filopodia, blebs and lamellipodia (or ruffles) have been described on the surface of cultured CHO cells by scanning electron microscopy as early as 1973 (Porter et al., 1973). The number and density of these membrane structures was dependent on the different phases of the cell cycle. The functional differences between microvilli in epithelial versus non-epithelial

cells are reflected by the different membrane protein composition and by different components of the actin cytoskeleton, which is the major organizer of these plasma membrane domains (Condeelis, 1993). In addition, some of the NHE6-containing membrane structures that we visualized by electron microscopy resemble filopodia, which are thin, finger-like structures that are filled with tight parallel bundles of filamentous actin (Mattila and Lappalainen, 2008). Intriguingly, in neurons filopodia are required for directional neurite outgrowth (Zheng et al., 1996) and for the initial neurite formation (Dent et al., 2007). Moreover, dendritic spines develop from filopodia-like precursors (Sekino et al., 2007), and the small GTPase Rac1 induces the proper spine formation by regulating actin dynamics (Luo et al., 1996). Furthermore, using yeast two-hybrid analysis, we identified Rac1 as an NHE6 interacting partner (Ilie A. and Orlowski J., unpublished results). Collectively, these data, corroborated with its presence in dendritic spines (see below), suggest that NHE6 might be involved in the development and/or maintenance of different types of specialized membrane protrusions, such as microvilli/filopodia in CHO cells and dendritic spines in neurons.

In order to study native NHE6, we generated a rabbit polyclonal antibody and showed that it can specifically and selectively recognize NHE6 in different applications, including western blotting and immunofluorescence confocal microscopy. Furthermore, we show that endogenous NHE6, similar to the HA-tagged form, is localized in a transferrin-rich recycling endosomal compartment in SH-SY5Y neuroblastoma cells (Fig. 1.4). Significantly, the SH-SY5Y cell line partially mimics neuronal differentiation by extending dendritic-like projections or neurites into the surrounding area and could serve as another convenient model system for studying the organellar NHEs.

Using the NHE6 antibody, we showed that NHE6 protein is readily detected and abundant in brain lysates in different species, *i.e*. human, mouse, and rat, and more specifically in mouse hippocampus as well (Fig.

1.5). We examined in more detail the distribution of NHE6 in hippocampal area CA1 using immunofluorescence analysis of mouse hippocampal organotypic slices. The advantage of this preparation is that the slices can be maintained in a tissue culture environment that allows nerve cells to continue to differentiate and to develop a tissue architecture that closely mirrors that observed *in situ*. We detected NHE6 within the soma and dendrites of CA1 pyramidal cells; higher resolution images of isolated dendrites showed that NHE6-containing vesicles are present not only in dendritic shafts, but also in dendritic spines (Fig. 1.6). We further confirmed the localization of NHE6 in dendrites of hippocampal and prefrontal cortex neurons by transmission electron microscopy (Figs.1.7-1.8). These results are particularly intriguing in the light of recent findings linking mutations in NHE6 to severe X-linked mental retardation syndromes (Gilfillan et al., 2008; Garbern et al., 2010).

In the study of Gilfillan et al., (2008), different types of mutations in NHE6 lead to a severe mental retardation syndrome, with profound developmental delay, accompanied by microcephaly, epilepsy, ataxia, hyperkinesia, lack of speech, happy demeanor with episodes of unprovoked laughter, and low attention span as well as other peripheral abnormalities. These features closely resemble Angelman syndrome (Angelman, 1961) which arises from defects in the maternally inherited allele of ubiquitin protein ligase E3A (UBE3A/E6-AP) (Lalande and Calciano, 2007). This enzyme regulates multiple downstream effectors, including the Rho-GTPase guanine nucleotide exchanger factor (Rho-GEF) Pbl/ECT2 (Reiter et al., 2006) and calcium/calmodulin kinase type 2 (CaMKII) (van Woerden et al., 2007; Weeber et al., 2003) which have been implicated in neuronal morphogenesis and synaptic function. Furthermore, knockout mice lacking UBE3A exhibit abnormal morphology and reduced density of dendritic spines on cerebellar Purkinje cells and pyramidal neurons in the hippocampus and cortex (Dindot et al., 2008), suggesting that the observed behavioural phenotype results from specific

abnormalities in synaptic development and/or plasticity. Interestingly, in a mouse line that contains a targeted knockout of NHE6 (Deltagen, Inc., San Mateo, CA, http://www.informatics.jax.org), the male mice display hyperactivity and are more prone to epileptic seizures induced by pentylenetetrazol/metrazol, a γ-aminobutyric acid (GABA) antagonist. This milder phenotype might be due to a compensation mechanism by upregulation of NHE9 or other NHEs, but is still consistent with a defect in synaptic transmission.

The above findings raise a number of intriguing questions. Given the similar phenotypes, do NHE6 and UBE3A share a common pathway? If not, do loss-of-function mutations in NHE6 nevertheless give rise to similar dendritic spine abnormalities, and if so, what might be the underlying mechanisms? One hint comes from recent studies demonstrating that the growth and maintenance of dendritic spines in response to excitatory synaptic inputs requires not only dynamic remodeling of the spine actin cytoskeleton (Matus, 2000; Zito et al., 2004; Honkura et al., 2008) and Ca^{2+} signaling (Brunig et al., 2004) but also a local supply of recycling endosomes that can be rapidly mobilized to provide membranes and glutamate receptors (*e.g.*, AMPA-R, NMDA-R) (Matsuzaki et al., 2004; Park et al., 2004) required for long-term potentiation (LTP), an experimental model thought to underlie learning and memory (Matsuzaki, 2007). Manipulations that acutely block trafficking of recycling endosomes in hippocampal neurons causes a rapid decline in dendritic spine size and density, and prevent LTP-induced spine formation (Park et al., 2006). Our discovery of the localization of NHE6 to postsynaptic recycling endosomes of hippocampal and prefrontal cortex neurons neurons suggests an important role for this transporter in normal dendritic spine morphogenesis.

Recently, a novel mutation associated with an X-linked mental retardation syndrome was described in NHE6, consisting of a three amino acid deletion (Trp338-Thr340) in the predicted transmembrane segment nine (Garbern et al., 2010). The afflicted male individuals presented

symptoms that are common with the patients described by Gilfillan et al. (2008), like profound mental retardation, severe language disturbance, and seizures. However, different symptoms were present as well, including autistic behavior, late-onset progressive ataxia (that began in the fourth decade), wide-spread neuronal loss, and most peculiar neuronal and glial inclusions of the microtubule-binding protein tau. The latter is characteristic to adult-onset neurodegenerative disorders (collectively known as tauopathies), which include Alzheimer's disease, progressive supranuclear palsy, corticobasal degeneration, and others. Six different tau isoforms are produced by alternative splicing in the human central nervous system (Goedert et al., 1989). In the normal human brain, splicing of exons 2.3, and 10 is tightly regulated in order to maintain similar levels of the isoforms with three (3R) and four (4R) microtubule-binding domains in the C-terminus of tau (Goedert and Jakes, 1990). In the patients described by Garbern et al. (2010), a clear predominance of the 4R isoform was observed, similar to corticobasal degeneration and progressive supranuclear palsy (Arai et al., 2001), which are disorders of unknown etiology. Contrary to the disorder produced by the NHE6 mutation, corticobasal degeneration and progressive supranuclear palsy appear much later in life, and do not present the severe degeneration of cerebellar Purkinje cells described by Garbern et al. However, the molecular mechanisms underlying these differences are not understood.

In summary, in the present study we showed that NHE6 is distributed in recycling endosomes and at the plasma membrane, especially along membrane protrusions, when expressed in fibroblastic cells. Furthermore, we generated a rabbit polyclonal antibody that specifically recognized NHE6 in the soma and neurites of neuroblastoma cells in culture, as well as in dendrites and in particular dendritic spines of hippocampal and cortical neurons.

CHAPTER 2

Roles of N-Glycosylation in the Function of the Mammalian Sodium/Proton Exchanger NHE6

Alina Ilie, Hervé Barriere, Gergely Lukacs, and John Orlowski

In the previous chapter we characterized the native distribution of NHE6 in cells and also showed that the exchanger is N-glycosylated.

N-glycosylation is a frequent covalent modification that can regulate different aspects of protein function. In this chapter we aimed to identify the sites responsible for the glycosylation of NHE6 and to explore the functional role of this modification on the trafficking and function of the exchanger.

ABSTRACT

The mammalian Na^+/H^+ exchanger NHE6 is an integral membrane glycoprotein that is present in recycling endosomes and thought to play an important role in vesicular pH and biogenesis. The factors that govern its biosynthetic maturation, membrane trafficking and activity are not well understood. Numerous studies have implicated *N*-glycosylation as an important covalent modification that can influence different aspects of protein function, including protein folding, stability, trafficking, and/or activity. However, the significance of this modification for NHE6 function has not been examined. A PROSITE search identified three strong putative glycosylation sites at asparagines 128, 369, and 623 of the NHE6-v0 splice variant. To assess their relevance, these sites were mutated to alanine individually or in combination. Expression of the mutant constructs in CHO cells, as well as endoglycosidase treatments, revealed that Asn128 is the sole site targeted for oligosaccharide modification. The glycosylation-deficient mutant displayed decreased cell surface abundance, but its stability and kinetics of internalization were not appreciably affected. In addition, endosomal compartments containing the glycosylation-deficient mutant were more alkaline compared to wild type. These data suggest a role for glycosylation in promoting efficient export of the transporter to the cell surface and for optimal transport activity within recycling endosomes.

INTRODUCTION

Mammalian alkali cation/proton exchangers, commonly referred to as sodium/proton exchangers (NHEs), are integral membrane (glyco)phosphoproteins that catalyze the countertransport of Na^+ (and for some isoforms also K^+) for H^+ down their respective concentration gradients and play a central role in cellular pH and volume homeostasis (Orlowski and Grinstein, 2004; Orlowski and Grinstein, 2007; Brett et al., 2005a). To date, eleven different isoforms have been isolated. Based on

their primary structure similarity and subcellular localization, the members of this family can be broadly classified into plasma membrane-type (NHE1 to NHE5) and endomembrane- or organellar-type (NHE6 to NHE9) transporters. Structurally, NHEs consist of two major domains: an N-terminal domain composed of 12 predicted transmembrane segments, involved in cation transport, and a smaller C-terminal domain found in the cytoplasm and involved in regulation of the transporter activity (Orlowski and Grinstein, 2004; Orlowski and Grinstein, 2007; Brett et al., 2005a; Bobulescu et al., 2005).

NHE6 is a member of the organellar-type subfamily and is widely expressed, with highest mRNA levels in brain, heart, and skeletal muscle (Numata et al., 1998). At the subcellular level, NHE6 is distributed in a recycling endosomal compartment, but a small fraction is also resident at the plasma membrane (Miyazaki et al., 2001; Brett et al., 2002; Nakamura et al., 2005; Ohgaki et al., 2008). By analogy to its yeast homolog Nhx1 (Bowers et al., 2000; Brett et al., 2005b), human NHE6 is postulated to play significant roles in the biogenesis and pH homeostasis of endocytic vesicles.

Glycosylation represents a frequent co- and post-translational modification of proteins and it has been estimated that more than half of all proteins are glycoproteins (Apweiler et al., 1999). In *N*-glycosylation, the sugar moieties are linked to asparagine (Asn, N) residues present in the consensus glycosylation site Asn-X-Ser/Thr, where X can be any amino acid, except proline (Bause, 1983). The effects of *N*-glycosylation on protein function are varied and include the facilitation of protein folding, trafficking, and activity. NHE6 has been shown to be *N*-glycosylated (Miyazaki et al., 2001), but the precise site(s) of glycan attachment and their effects, if any, on NHE6 function are unknown. Using a PROSITE search, three strong putative N-glycosylation sites were identified in the NHE6-v0 variant: two reside in predicted extracellular loops (N128 and N369), and the third one is localized within the cytoplasmic C-terminus, at

N623. While the latter site is theoretically inaccessible to the glycosylation machinery within the secretory pathway, recent analyses of the endosomal Na^+/H^+ exchanger Nhx1 of *Saccharomyces cerevisiae* identified two glycosylation sites within its predicted cytoplasmic C-terminus, suggesting that at least a segment of the hydrophilic tail domain is positioned within the endosomal lumen. Hence, to study the effect of N-linked glycosylation on the regulation of NHE6 trafficking and stability, the critical asparagines of the consensus sites were mutated to alanines. Endoglycosidase treatments and immunoblotting analysis revealed that Asn128 is the sole target for the *N*-glycosylation of the transporter. Loss of glycosylation diminished NHE6 abundance at the cell surface. This effect is attributed to a reduction in the rate of processing and insertion into the plasma membrane as neither its half-life nor its rate of internalization into recycling endosomes were affected. Interestingly, endosomes containing the glycosylation-deficient mutant were more alkaline compared to wild-type controls, suggesting an impairment in NHE6 activity. Our data reveal that glycosylation is involved in the regulation of NHE6 function and trafficking to the plasma membrane.

MATERIALS AND METHODS

Reagents

Mouse monoclonal primary antibodies were obtained from commercial sources, as follows: anti-hemagglutinin (HA) antibody from Covance Inc. (Berkeley, CA); anti-Flag M2 from Sigma-Aldrich (Oakville, ON); anti-myc from Upstate Biotechnology Inc. (Lake Placid, NY); anti-glyceraldehyde 3-phosphate dehydrogenase (GAPDH) from Abcam (Cambridge, MA), and anti-transferrin receptor from Zymed (South San Francisco, CA). Rabbit polyclonal anti-HA antibody was purchased from Abcam (Cambridge, MA).

Horseradish peroxidase-conjugated secondary IgG antibodies, as well as FITC-conjugated goat anti-mouse secondary Fab were purchased from Jackson ImmunoResearch Laboratories (West Grove, PA). All Alexa Flour® conjugated secondary antibodies were purchased from Molecular Probes (Eugene, OR).

Alpha-Minimum essential medium (α-MEM), fetal bovine serum, penicillin/streptomycin, and trypsin-EDTA were purchased from Invitrogen. G418 sulfate was obtained from Wisent Inc. (St-Bruno, QC, Canada). All other chemical and reagents were obtained from BioShop Canada (Burlington, ON, Canada), Sigma or Fisher Scientific and were of the highest grade available.

Recombinant DNA Constructs and Mutagenesis

The cloning of human isoform NHE6-v0 used in the experiments described in this chapter was described previously (Numata et al., 1998). NHE6-v0 was engineered to include the influenza virus hemagglutinin (HA) (YPYDVPDYAS) epitope at its extreme C-terminus and cloned into the mammalian expression vector pCMV (Virdee and Orlowski, unpublished results). This construct, named $NHE6_{HA}$, was used as a template to substitute the three putative N-glycosylation sites (Asn128, 369, and 623) identified in NHE6 by a PROSITE search, to Ala. The mutations were introduced by PCR using the commercially available QuikChange™ site-directed mutagenesis kit (Stratagene, Cedar Creek, TX) according to the manufacturer's recommended protocol. The following mutants were obtained: single substitutions NN127/128AA (henceforth termed N128A), NN368/369AA (henceforth termed N369A), N623A, double substitutions NN127/128AA_NN368/369AA, NN368/369AA_N623A, NN127/128AA_N623A, and the triple substitution NN127/128AA_NN368/369AA_N623A. All constructs were sequenced to verify the fidelity of the sequences.

The $NHE6_{HA}$ wild-type and N128A constructs were also inserted into the *HindIII*/*XbaI* sites of the mammalian expression vector pcDNA3.1 (Invitrogen) and used as templates to introduce a triple Flag (3X DYKDDDDK) epitope in the first extracellular loop. First, PCR was used to engineer a *NotI* restriction site in the first extracellular loop, after M53, followed by the introduction of annealed primers representing the 3xFlag epitope, which generated a construct termed $_{3Flag}NHE6_{HA}$. All constructs were sequenced to insure that no mutations were introduced during the PCR.

Cell Culture and cDNA Transfection

CHO (Chinese hamster ovary) and AP-1 (CHO cells devoid of plasma membrane Na^+/H^+ exchange activity (Rotin and Grinstein, 1989) cells were maintained in α-Minimum Essential Medium (α-MEM) supplemented with 10% fetal bovine serum, penicillin (100 units/ml), streptomycin (100 µg/ml), and 25 mM $NaHCO_3$ (pH 7.4). Cells were incubated in a humidified atmosphere of 95% air, 5% CO_2 at 37ºC.

To generate AP-1 cells stably expressing $NHE6_{HA}$ wild-type or N128A mutant, cells were grown to subconfluence in a 6-well plate and transfected with plasmid DNA (1µg/well) using Lipofectamine™ reagent according to the manufacturer's instructions. Twenty-four hours after transfection, cells were split (1:50) into 10-cm dishes and selected for stably expressing clones in α-MEM culture medium supplemented with G418 sulfate (600 µg/ml) over a 3-week period.

Immunoblot Analysis

AP-1 cells were grown in 10-cm dishes and transiently transfected with 5µg of plasmid DNA encoding $NHE6_{HA}$ wild-type or mutant constructs using Lipofectamine™ (Invitrogen) according to the manufacturer's recommended procedure. Twenty-four hours post-transfection, cell lysates were obtained by washing cells twice on ice with ice-cold PBS,

followed by scraping in 0.4 ml of lysis buffer containing 0.5% Triton X-100/PBS supplemented with a tablet of protease inhibitor cocktail (Roche Diagnostics). Lysates were incubated for 30 min on a rocker at 4ºC, and then centrifuged for 20 min at 4°C to pellet the nuclei and cellular debris. Twenty micrograms of protein from the resulting supernatants were eluted in SDS-sample buffer (50 mM Tris-HCl, pH 6.8, 1% SDS, 50 mM dithiothreitol, 10% glycerol, 1% bromophenol blue), and subjected to 10% SDS-PAGE, then transferred to polyvinylidene fluoride (PVDF) membranes (Millipore, Nepean, Ontario, Canada) for Western blotting. The membranes were blocked with 5% non-fat skim milk for 1 hour, then incubated with mouse monoclonal anti-HA primary antibody (1:5000), in PBS containing 0.1% Tween 20, followed by extensive washes and incubation with goat anti-mouse-horseradish peroxidase (HRP)-conjugated secondary antibody (1:5000) for 1 h.

Immunoreactive bands were detected using ECL™ Western blotting detection reagents (GE Healthcare, Baie d'Urfe, QC, Canada).

Endoglycosidase Treatments

Post-nuclear supernatants of AP-1 cells transiently expressing $NHE6_{HA}$ wild-type or N128A, N369A, and N623A mutants were obtained 24 h post-transfection and treated with endoglycosidases, according to the manufacturer's recommendations. First, glycoproteins were denatured in 1x denaturing buffer (0.5% SDS, 1% β-mercaptoethanol) at 100°C for 10 min. Samples were then divided equally and treated with no enzyme (control), Peptide N-glycosidase F (PNGase F) (750 units, New England Biolabs, Mississauga, ON, Canada) or Endo-β-N-acetylglucosaminidase H (Endo H) (750 units, New England Biolabs, Mississauga, ON, Canada). The enzymes were added to 30 µl reactions and incubated overnight at 37°C. Next day, samples were diluted with two-fold concentrated SDS-PAGE sample buffer, boiled for 3 min, briefly centrifuged, and analyzed by

SDS-PAGE and western blotting with mouse monoclonal anti-HA antibody.

Cell Surface Biotinylation

AP-1 cells stably expressing $NHE6_{HA}$ wild-type or N128A mutant constructs were cultured in 10-cm dishes to sub-confluence, placed on ice and washed three times with ice-cold PBS containing 1 mM $MgCl_2$ and 0.1 mM $CaCl_2$, pH 8.0 (PBS-CM). Next, cells were incubated at 4°C for 30 min with the membrane-impermeable reagent N-hydroxysulfosuccinimydyl-SS-biotin (0.5 mg/ml) (ThermoScientific, Rockford, IL). Cells were washed and incubated twice in quenching buffer (20 mM glycine in PBS-CM) for 7 min each on ice to remove unreacted biotin. After two more washes in PBS-CM, the cells were lysed in 0.5 ml PBS buffer containing 0.5% TritonX-100 and protease inhibitor mixture for 30 min on ice, and then centrifuged at 16,000 x g for 20 min at 4°C to remove insoluble cellular debris. A fraction of the resulting supernatant was removed and this represents the total fraction. Increasing fractions of the remaining supernatant, representing 1%, 4%, 10%, 20%, and 60% of the original lysate, were incubated with 100 µl of 50% NeutrAvidin® Agarose Resin slurry (Fisher Scientific, Whitby, ON, Canada) in lysis buffer overnight at 4°C to extract biotinylated membrane proteins. An aliquot representing 1% of the original total cell lysate and the cell surface fractions were resolved by 10% SDS-PAGE and analyzed by Western blotting with a monoclonal anti-HA antibody.

Measurement of NHE6 Stability

To determine the stability of wild-type and mutant NHE6, AP-1 cells stably expressing $NHE6_{HA}$ wild-type or the N128A glycosylation-deficient mutant were treated with cycloheximide (100 µg/ml) in α-MEM supplemented with 10% FBS and penicillin/streptomycin for up to 24 hours to inhibit new protein synthesis. At appropriate time points, cells were

lysed, protein concentrations were measured, and equal quantities of proteins were subjected to SDS-PAGE and immunoblotting with a mouse monoclonal anti-HA antibody. Equal protein loading was verified by immunoblot analysis of the same membranes with rabbit polyclonal anti-GAPDH antibody. The intensity of the bands was quantified by densitometry of X-ray films exposed in the linear range and analyzed using ImageJ software.

Fluorescence-based Endocytosis Assay

AP-1 cells grown in 10-cm dishes were transiently transfected with 5 µg of pcDNA3 (mock) or $_{3Flag}NHE6_{HA}$ wild-type or mutant N128A cDNA constructs. Twenty-four hours post-transfection, cells were transferred to 12 well-plates and further grown for 24 hours. Cells were chilled on ice, washed with ice-cold PBS supplemented with 0.1 mM $CaCl_2$ and 1 mM $MgCl_2$ (PBS-CM, pH 7.4), blocked in 10% goat serum/PBS-CM, and then incubated with a mouse monoclonal anti-Flag antibody (1:3000) (Sigma) on ice for 1 h. Internalization of the bound antibody was initiated by incubating the cells with warm (37ºC) α-MEM for the indicated time points and terminated by placing the plates on ice. Cell were washed and labeled with goat anti-mouse HRP-conjugated secondary antibody (1:1000) (GE Healthcare, Baie d'Urfe, QC, Canada). After extensive washes with PBS-CM, cells were treated on ice with Amplex® Red reagent (Invitrogen). Aliquots were transferred to 96-well plates and fluorescence readings were taken with a POLARstar OPTIMA (BMG Labtech, Inc, Offenburg, Germany) plate reader using 544-nm excitation and 590-nm emission wavelengths. All experiments were performed in triplicates and repeated at least three times. Results were expressed as a percentage of the fluorescence recorded prior to internalization, after subtraction of the value measured with mock-transfected cells. Results are shown as mean ± standard error of the mean (SEM).

Immunocytochemistry

To examine the subcellular localization of NHE6 wild-type (wt) and N128A mutant, AP-1 cells stably expressing NHE6-N128A$_{HA}$ were grown in 10-cm dishes and transiently transfected with NHE6-wt$_{Flag}$ or NHE6-wt$_{myc}$. Twenty-four hours post-transfection, the cells were transferred to 2 µg/ml fibronectin (Sigma) -coated glass coverslips and grown for 24 more h. Cells were fixed in 2% paraformaldehyde/PBS for 20 min, followed by permeabilization in 0.1% saponin/PBS for 20 min and blocking for 1 h in 10% goat serum/PBS at room temperature. Cells were subsequently incubated with rabbit polyclonal anti-HA (1:1000) and mouse monoclonal anti-Flag (1:2000) or anti-myc (1:1000) primary antibodies in 10% goat serum/0.01% saponin/PBS over night at 4ºC, followed by goat anti-rabbit Alexa Fluor® 488- and anti-mouse Alexa Fluor® 568-conjugated secondary antibodies (1:2000) for 1 h at room temperature. After extensive washes with PBS, cells were mounted onto glass slides using Aqua Poly/Mount mounting medium (Polysciences Inc., Warrington, PA).

To examine their colocalization with transferrin receptor, NHE6$_{HA}$ wild-type or N128A mutant were transfected into CHO cells, and transferred to fibronectin-coated glass coverslips 24 h later. After 24 more hours in culture, cells were fixed in 2% paraformaldehyde, permeabilized, and incubated with rabbit polyclonal anti-HA (1:2000) and mouse monoclonal anti-transferrin receptor (1:500) primary antibodies over night at 4ºC. Next day, cells were labeled with goat anti-rabbit Alexa Fluor® 488- and anti-mouse Alexa Fluor® 568-conjugated secondary antibodies (1:2000) for 1 h at room temperature, washed and mounted.

Cells were examined by laser scanning confocal microscopy using a Zeiss LSM 510 Meta, and images were analyzed using LSM software and Corel® CorelDraw™ version 13.

Analysis of Trafficking by Single-Cell Fluorescence Ratio Imaging (FRIA)

AP-1 cells were transfected with $NHE6_{HA}$ wild-type bearing a triple Flag at position M53 or N128 and cell surface resident protein was labeled on ice with anti-Flag monoclonal antibody (1:1000 dilution, Sigma-Aldrich) and FITC-conjugated goat anti-mouse secondary Fab (1:1000 dilution, Jackson ImmunoResearch Laboratories, West Grove, PA). Cells were then washed in PBS supplemented with 1 m M $MgCl_2$ and 0.1 mM $CaCl_2$ (PBS-CM) and chased for the indicated time points in growth medium at 37°C. FRIA was performed on an Axiovert 100 inverted fluorescence microscope (Carl Zeiss MicroImaging, Toronto, ON, Canada) at room temperature equipped with a Hamamatsu ORCA-ER 1394 (Hamamatsu, Japan) cooled CCD camera and a Planachromat (63x NA 1.4) objective essentially as described previously (Barriere et al., 2007; Barriere and Lukacs, 2008). Image acquisition and FRIA were performed with MetaFluor software (Molecular Devices, Downingtown, PA). Images were acquired at 490±5 and 440±10 nm excitation wavelengths, using a 535±25-nm emission filter. In each experiment, the pH of 100–1000 vesicles was determined. Mono- or multipeak Gaussian distributions of vesicular pH values were obtained with Origin 7.5 software (OriginLab, Northampton, MA).

Calibration curves have been performed like previously described (Barriere and Lukacs, 2008; Barriere et al., 2009). Briefly, in situ calibration was performed by clamping the vesicular pH between 4 and 7.5 in K+-rich medium (135 mM KCl, 10 mM NaCl, 20 mM Hepes or 20 mM MES, 1 mM $MgCl_2$, and 0.1 mM $CaCl_2$) with 10 μM nigericin, 10 μM monensin, 0.4 μM bafilomycin and 20 μM carbonyl cyanide m-chlorophenyl hydrazone (CCCP) and recording the fluorescence ratios.

RESULTS

NHE6 is N-glycosylated at Asn128

N-glycosylation of proteins is known to facilitate the optimal functioning of many molecular and cellular processes, including protein folding and sorting, receptor activation, signal transduction, endocytosis and cell adhesion (Haltiwanger and Lowe, 2004; Ohtsubo and Marth, 2006). The NHE6 isoform is subject to N-glycosylation (Miyazaki et al., 2001), but the significance, if any, of glycans for NHE6 function has not been investigated.

As shown in Figure 2.1A, the organellar-type NHE contain a variable number of sequences that conform to the canonical motif for N-glycosylation, N-X-S/T, where X can be any amino acid except proline (Jones et al., 2005). However, the degree of conservation of these sites is not very high, except for one site (NLS) which is present in all organellar-type NHEs. NHE6-v0 contains three putative N-linked glycosylation sites at positions 128 (^{128}NVT), 369 (^{369}NLS), and 623 (^{623}NSS) (Fig. 2.1B). In order to identify the actual site(s) responsible for the glycosylation of NHE6, the putative glycosylated Asn residues in NHE6-v0 were substituted for alanine either individually or in combination using site-directed mutagenesis. The obtained constructs, bearing an HA tag at their extreme C-terminus were expressed in Chinese hamster ovary AP-1 cells and analyzed by Western blotting with a mouse monoclonal anti-HA antibody. As shown in Figure 2.2A, wild-type $NHE6_{HA}$ migrated as two bands: a slower migrating, higher molecular weight band (~ 83kDa), which corresponds to the fully glycosylated, mature form of the protein; and a faster migrating, lower molecular weight band (~ 65kDa), characteristic for the core-glycosylated form. However, the single substitution mutant N128A, as well as the double and triple mutants that contain the N128A substitution migrated as a single band, at the level of ~65 kDa. Furthermore, the single N369A and N623A mutants, as well as the double

A.

```
NHE6v0          MARRGWRRAPLRRGVGSSPRARRLMRPLWLLLAVGVFDWAGASD-GGGGEARAMDEEIVS  59
NHE6v1          MARRGWRRAPLRRGVGSSPRARRLMRPLWLLLAVGVFDWAGASD-GGGGEARAMDEEIVS  59
NHE7            MEPGDAARPGSGRATGAPP-PRLLLLPLLLGWGLRVAAAASASSSGAAAEDSSAMEELAT  59
NHE8            MGEKMAEEERFPNTTHEG------------FNVTLHTTLVVTTKLVLPTPGKPILPVQT  47
NHE9            MER-----------------------------------------------QSRVMS  9

NHE6v0          IHVPSDVN-NVTLSCEVQSSPTTLLV--------------------------------TF  146
NHE6v1          IHVPSDVN-NVTLSCEVQSSPTTLLVNVSGKFYEYMLKGEISSHELNNVQDNEMLRKVTF  178
NHE7            TPATSGRD-KSLSCTQEDRAFSTLLVNVSGKFFEYTLKGEISPGKINSVEQNDMLRKVTF  178
NHE8            EFK------KLANWKEEE-------------------------------------MF  121
NHE9            TAPTDIESGTVYDCVKLTFSPSTLLVNITDQVYEYKYKREISQHNINPHQGNAILEKMTF  129

NHE6v0          VTGQLAG-DFYFTDCLLFGAIVSATDPVTVLAIFHELQVDVELYALLFGESVLNDAVAIV  265
NHE6v1          VTGQLAG-DFYFTDCLLFGAIVSATDPVTVLAIFHELQVDVELYALLFGESVLNDAVAIV  297
NHE7            IMGQLSD-KFYYTDCLFFGAIISATDPVTVLAIFNELHADVDLYALLFGESVLNDAVAIV  297
NHE8            IS------KLNMTDSFAFGSLISAVDPVATIAIFNALHVDPVLNMLVFGESILNDAVSIV  235
NHE9            HAGQLKNGDFHFTDCLFFGSLMSATDPVTVLAIFHELHVDPDLYTLLFGESVLNDAVAIV  249

NHE6v0          LSSSIVAYQPAGDNSHTFDVTAMFKSIGIFLGIFSGSFAMGAATGVVTALVTKFTKLREF  325
NHE6v1          LSSSIVAYQPAGDNSHTFDVTAMFKSIGIFLGIFSGSFAMGAATGVVTALVTKFTKLREF  357
NHE7            LSSSIVAYQPAGLNTHAFDAAAFFKSVGIFLGIFSGSFTMGAVTGVN-ANVTKFTKLHCF  356
NHE8            LTNTAEGLTRK-NMSDVSGWQTFLQALDYFLKMFFGSAALGTLTGLISALVLKHIDLRKT  294
NHE9            LTYSISIYSPK-ENPNAFDAAAFFQSVGNFLGIFAGSFAMGSAYAIITALLTKFTKLCEF  308

NHE6v0          QLLETGLFFLMSWSTFLLAEAWGFTGVVAVLFCGITQAHYTYNNLSTESQHRTKQLFELL  385
NHE6v1          QLLETGLFFLMSWSTFLLAEAWGFTGVVAVLFCGITQAHYTYNNLSTESQHRTKQLFELL  417
NHE7            PLLETALFFLMSWSTFLLAEACGFTGVVAVLFCGITQAHYTYNNLSVESRSRTKQLFEVL  416
NHE8            PSLEFGMMIIFAYLPYGLAEGISLSGIMAILFSGIVMSHYTHHNLSPVTQILMQQTLRTV  354
NHE9            PMLETGLFFLLSWSAFLSAEAAGLTGIVAVLFCGVTQAHYTYNNLSSDSKIRTKQLFEFM  368

NHE6v0          LHIRVGVDSDQE-----------HLGV--------------------PENER-RTTKAES  531
NHE6v1          LHIRVGVDSDQE-----------HLGV--------------------PENER-RTTKAES  563
NHE7            LNIRVGVEEPSEEDQNEHHWQYFRVGVDPDQDPPPNNDSFQVLQGDGPDSARGNRTKQES  594
NHE8            MDIEDAKAHRRN-------------------------------------KKDVNLS  492
NHE9            LQIRVGVDLDEN------------LKEDPSS------------QHQEANNLDKNMTKAES  522

NHE6v0          ILNDGDISLTYGDSTVNTEPATSSAPR-------RFMGNSSEDALDRELAFGDHELVIRG  644
NHE6v1          ILNDGDISLTYGDSTVNTEPATSSAPR-------RFMGNSSEDALDRELAFGDHELVIRG  676
NHE7            ILTEGDLTLTYGDSTVTANGSSSSHTASTSLEGSRRTKSSSEEVLERDLGMGDQKVSSRG  714
NHE8            RIQMKTLTNKWYEEVR-------------------QGPSGSEDDEQELL----------  581
NHE9            IVNQDELAINYQEQASSPCSPPARLGLD---QKASPQTPGKENIYEGDLGLGGYELKLEQ  637
```

B.

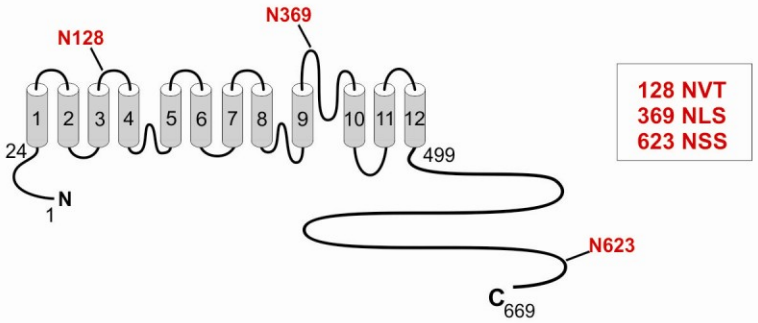

Figure 2.1. Predicted N-glycosylation sites in organellar-type NHEs.

A. Alignment of NHE organellar-type isoforms using Clustal W2. Consensus *N*-linked glycosylation sites are shown in red and were identified using PROSITE.
B. Putative N-glycosylation sites in NHE6. A PROSITE search identified three strong putative N-glycosylation sites in NHE6-v0 at Asn 128, 369, and 623.

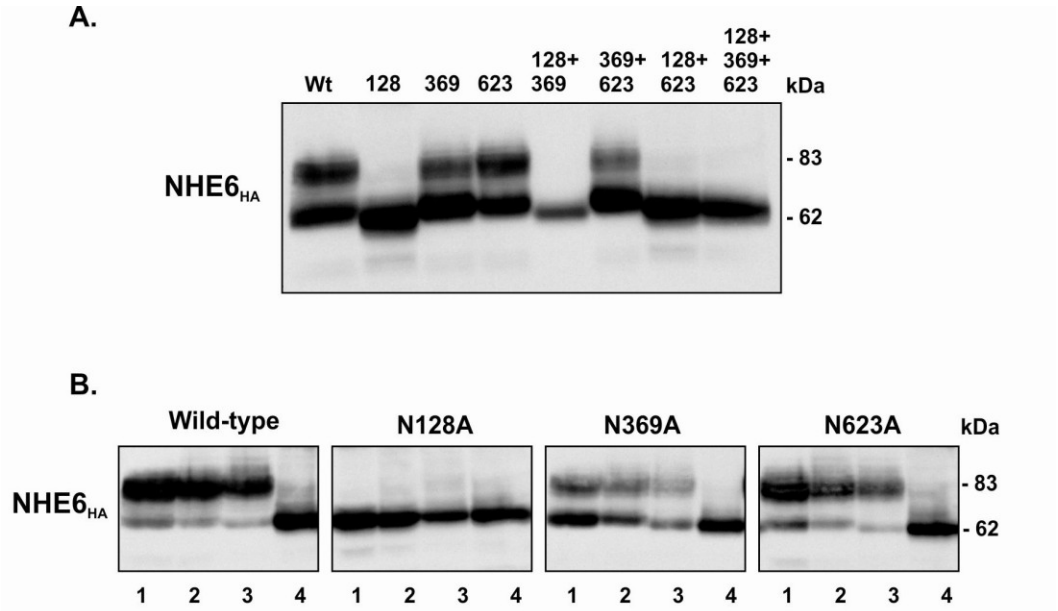

Figure 2.2. NHE6 is N-glycosylated at Asn 128.

A. AP-1 cells were transiently transfected with $NHE6_{HA}$ wild-type (*Wt*) or the following mutants: single substitutions NN127/128AA (*128*), NN368/369AA (*369*), N623A (*623*), double substitutions NN127/128AA_NN368/369AA (*128+369*), NN368/369AA_N623A (*369+623*), NN127/128AA_N623A (*128+623*), and the triple substitution NN127/128AA_NN368/369AA_N623A (*128+369+623*). Cell lysates were obtained 24 hours post-transfection and subjected to SDS-PAGE and western blot analysis with a mouse monoclonal anti-HA antibody.

B. AP-1 cells transiently expressing $NHE6_{HA}$ wild-type or the NN127/128AA, NN368/369AA, and N623A mutants were subjected to endoglycosidase treatments. Post-nuclear lysates were obtained 24 hours post-transfection. An aliquot of the initial lysate was removed and the rest was denaturated and divided into three parts, which were incubated over night with no enzyme, EndoH, and PNGaseF, respectively. Aliquots of the initial lysate (*lane 1*) and of the no-enzyme (*lane 2*), EndoH (*lane 3*), and PnGase F (*lane 4*)-treated samples were resolved by SDS-PAGE and immunoblot analysis with mouse monoclonal anti-HA antibody.

substitution N369A/N623A mutant showed the same migration pattern as the wild-type protein. These results suggested that N128 is the sole site responsible for glycosylation of NHE6.

To verify that this migration pattern is indeed due to the N-glycosylation of NHE6, the wild-type and single substitution mutants (N128A, N369A, and N623A) were evaluated for their sensitivity to cleavage by specific endoglycosidases endo-β-N-acetylglucosaminidase H (Endo H) and peptide-N4 (N-acetyl-β-glucosaminyl) asparagine amidase F (peptide-N-glycosidase F or PNGase F) known to differentially cleave the sugars acquired by proteins in the endoplasmic reticulum (*i.e.*, Endo H cleaves only high mannose and some hybrid types of N-linked oligosaccarides; often called core-glycosylation) versus the Golgi apparatus (*i.e.*, PNGase F cleaves all N-linked carbohydrates, including high mannose, hybrid, and complex oligosaccharides). To this end, lysates of AP-1 cells transiently expressing $NHE6_{HA}$ wild-type or the single substitution mutants were subjected to Endo H and PNGase F treatments. Endo H cleaves between the two N-acetylglucosamine subunits directly proximal to the Asn residue causing a shift in the mobility of the immature form (Fig. 2.2B, *lane 3*). PNGase F cleaved all the oligosaccharides from NHE6-v0, resulting in the complete disappearance of the slower migrating mature form (Fig. 2.2B, *lane 4*). This migration pattern was observed for the wild-type protein, as well as for the N369A and N623A mutants, confirming that these constructs undergo complex glycosylation. On the contrary, no shift in the migration of the N128A mutant was observed upon treatment with either Endo H or PNGase F, demonstrating that no *N*-glycosylation was acquired and confirming that Asn128 is the unique site responsible for glycosylation of NHE6.

Endosomal targeting of NHE6 is glycosylation-independent

Previous studies have shown that NHE6 is localized mainly in a transferrin-containing endosomal compartment in cells (Brett et al., 2002; Ohgaki et al., 2008; Nakamura et al., 2005).

To verify the correct localization of the glycosylation-deficient mutant N128A in recycling endosomes, CHO cells were transfected with $NHE6_{HA}$ wild-type or mutant N128A and colocalization with endogenous transferrin receptor, a known marker for recycling endosomes, was examined by immunofluorescence confocal microscopy. As expected, a significant degree of colocalization of wild-type $NHE6_{HA}$ and transferrin receptor was observed (Fig. 2.3, *upper panels*). The N128A mutant displayed a high degree of colocalization with transferrin receptor as well (Fig. 2.3, *lower panels*), similar to the wild-type protein, supporting the hypothesis that the endosomal targeting of NHE6 is glycosylation-independent.

Glycosylation is involved, but not essential for cell-surface trafficking of NHE6

NHE6 is mainly localized in intracellular compartments, but ~ 10% can be detected at the cell surface (Brett et al., 2002), (Figs. 1.2A,B). To investigate whether glycosylation is essential for exit from the Golgi and for transport to the plasma membrane, we performed cell surface biotinylation in AP-1 cells stably expressing $NHE6_{HA}$ wild-type or N128A mutant. Total cell lysates were prepared and a portion representing the total fraction was removed. Increasing fractions of the remaining supernatant, representing 1%, 4%, 10%, 20%, and 60% of the original lysate, were incubated over night with NeutrAvidin® Agarose beads to extract cell surface proteins. An aliquot representing 1% of the original total cell lysate and the cell surface fractions were resolved by SDS-PAGE and analyzed by Western blotting with a monoclonal anti-HA antibody. As shown in Figure 2.4A, unglycosylated NHE6, similar to the wild-type, was

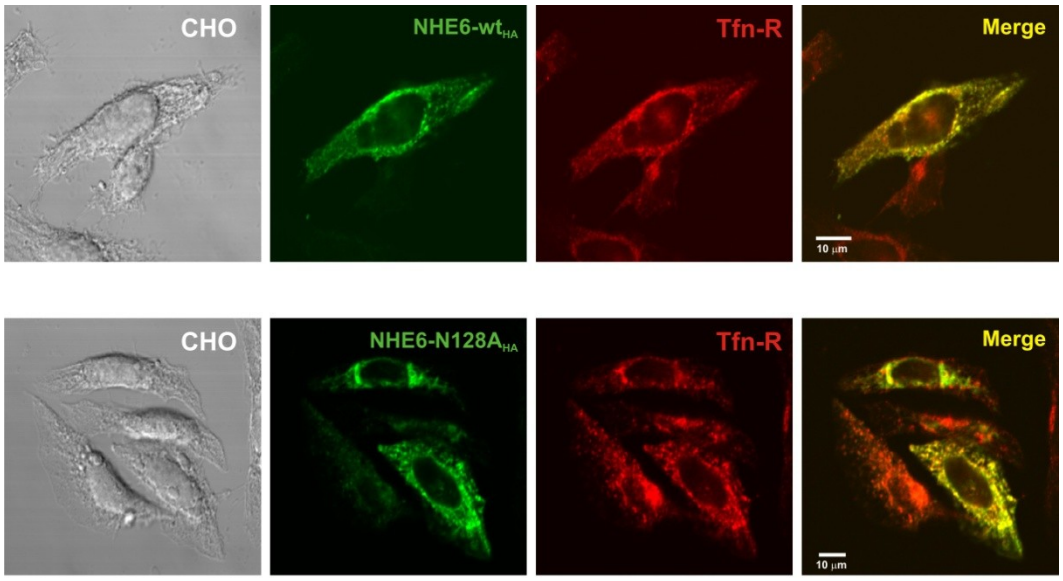

Figure 2.3. NHE6$_{HA}$ wild-type and N128A mutant colocalize with transferrin receptor in transfected CHO cells.

CHO cells were transfected with NHE6$_{HA}$ wild-type or N128A mutant and transferred to fibronectin-coated glass coverslips 24 hours later. After 24 more hours, cells were fixed in 2% paraformaldehyde and incubated with rabbit polyclonal anti-HA and mouse monoclonal anti-transferrin receptor primary antibodies, followed by goat anti-rabbit Alexa Fluor® 488- and anti-mouse Alexa Fluor® 568-conjugated secondary antibodies.

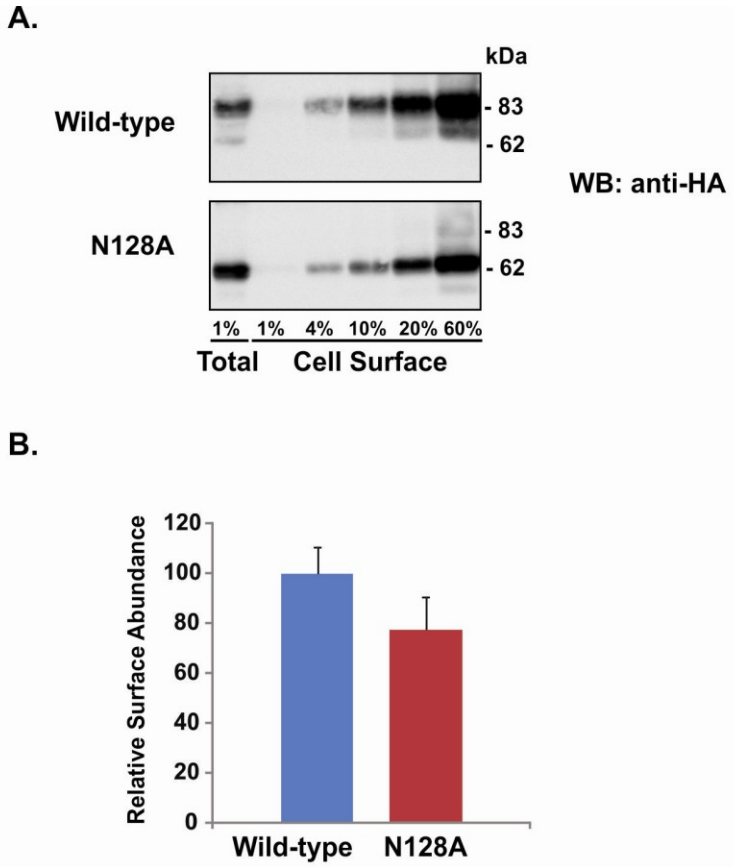

Figure 2.4. Glycosylation-deficient mutant of NHE6 is present on the cell surface.

A. Plasma membrane $NHE6_{HA}$ levels were detected in AP-1 cells stably expressing $NHE6_{HA}$ wild-type (*upper panel*) or the N128A mutant (*lower panel*) using a cell surface biotinylation assay. Total cell lysates were prepared (500 µl) and a portion representing the total fraction was removed. Increasing fractions of the remaining supernatant, representing 1%, 4%, 10%, 20%, and 60% of the original lysate, were incubated with NeutrAvidin® Agarose beads to extract cell surface proteins. An aliquot representing 1% of the original total cell lysate and the cell surface fractions were analyzed by Western blotting with a monoclonal anti-HA antibody.

B. Densitometric quantification of 3 separate experiments using the 10% fraction point normalized to the amount present in the lysate. Data points represent mean ± SEM.

clearly retained by avidin, indicating that a significant portion of the mutant protein reaches the plasma membrane. Comparative densitometric analysis of the cell surface abundance of wild-type and N128A mutant using the 10% fraction was performed by dividing the surface protein by the total protein present in the lysate. The relative surface abundance obtained this way was ~25% lower for the unglycosylated mutant compared to its wild-type counterpart (Fig. 2.4B), suggesting that glycosylation facilitates, but is not essential for, NHE6 accumulation at the cell surface. This may indicate that the glycosylation-deficient mutant is internalized at a faster rate and/or that the half-life and/or transport to the cell surface are decreased when compared to the fully glycosylated protein.

To further verify the cell surface expression data by an alternate method and to test the hypothesis that glycosylation affects the internalization rate of NHE6, plasmalemmal NHE6 was measured using a cell-based enzyme-linked immunosorbent assay (ELISA). To this end, AP-1 cells were transiently transfected with $NHE6_{HA}$ wild-type and mutant N128A constructs bearing a triple Flag epitope in the first extracellular loop at position M53 ($_{3Flag}NHE6_{HA}$). First, the total expression of the two constructs was verified by immunoblotting with a mouse monoclonal anti-HA antibody. As shown in Figure 2.5A, the wild-type construct underwent complex glycosylation, whereas the mutant protein migrated as a single band, demonstrating that no glycans were attached to it. Significantly, the total expression for both constructs was similar, if not identical. In order to verify the cell surface expression of wild-type and N128A mutant, the amount of $_{3Flag}NHE6_{HA}$ present at the plasma membrane relative to total protein expression was measured using a cell-based ELISA. This assay measures the loss of cell surface immunoreactivity of epitope-tagged plasma membrane proteins (Barriere et al., 2006). Forty-eight hours after transfection, the cells were placed on ice and cell-surface resident NHE6 was labelled with a mouse monoclonal anti-Flag antibody, followed by

internalization at 37ºC for different time points (5, 15, and 30 min). The remaining cell surface protein was measured after incubation with a HRP-conjugated secondary antibody and the Amplex® Red fluorescent substrate. The amount of $_{3Flag}NHE6_{HA}$ present at the plasma membrane was measured before initiating the internalization (i.e., at 0 time point) and normalized to total protein. As demonstrated in Figure 2.5B, the surface levels of N128A mutant $_{3Flag}NHE6_{HA}$ were ~30% lower compared to the wild-type protein, supporting the biotinylation data and the hypothesis that glycosylation plays a role in the steady-state abundance of NHE6 at the cell surface. However, the rate of internalization of the glycosylation-deficient mutant was very similar to the wild-type protein (Fig. 2.5C), suggesting that glycans are not required for the proper endocytosis of NHE6. By inference, these data suggest that efficient protein processing along the biosynthetic pathway and transport to the cell surface may be impaired.

Glycosylation is not important for the stability of NHE6

In order to test if glycosylation is important for the stability of NHE6, AP-1 cells stably expressing $NHE6_{HA}$ wild-type or N128A mutant were treated with 100 µg/ml cycloheximide 2, 4, 8, or 24 hours to block new protein synthesis. Cell lysates were obtained at the indicated time points and equal amounts of proteins were resolved by SDS-PAGE and analyzed by western blotting with a mouse monoclonal anti-HA antibody. As shown in Figure 2.6, the half-life of the mutant $NHE6_{HA}$ N128A was indistinguishable from wild-type, suggesting that the stability of NHE6 is glycosylation-independent.

Glycosylation seems to be important for the function of NHE6

To test the hypothesis that glycosylation might regulate the function of NHE6, we monitored the vesicular pH (pH_v) of NHE6-containing vesicles by fluorescence ratio image analysis (FRIA), essentially as described for

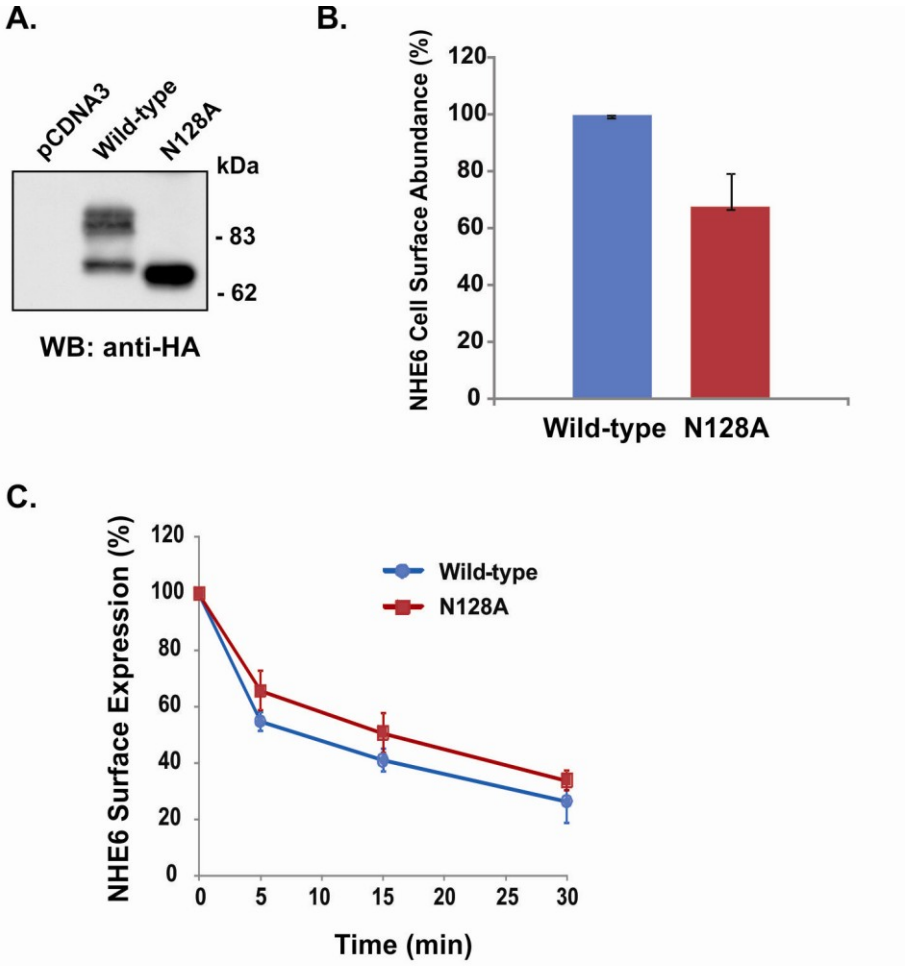

Figure 2.5. Mutation of glycosylation site in $_{3Flag}NHE6_{HA}$ results in decreased cell surface targeting, but has no effect on its internalization kinetics.

A. Western blot showing the expression of $_{3Flag}NHE6_{HA}$ wild-type and N128A glycosylation-deficient mutant in AP-1 cells after 48 hours of transfection.

B. Cell surface abundance of $_{3Flag}NHE6_{HA}$ wild-type and N128A mutant was measured in AP-1 cells at 48 hours-postransfection using a cell-based enzyme-linked immunosorbent assay (ELISA) and normalized to total cellular protein. Data represent mean ± SEM of four independent experiments.

C. Internalization kinetics of $_{3Flag}NHE6_{HA}$ wild-type and N128A mutant was determined in AP-1 cells after 48 hours of transfection by cell-based ELISA. Data are shown as mean ± SEM of four independent experiments.

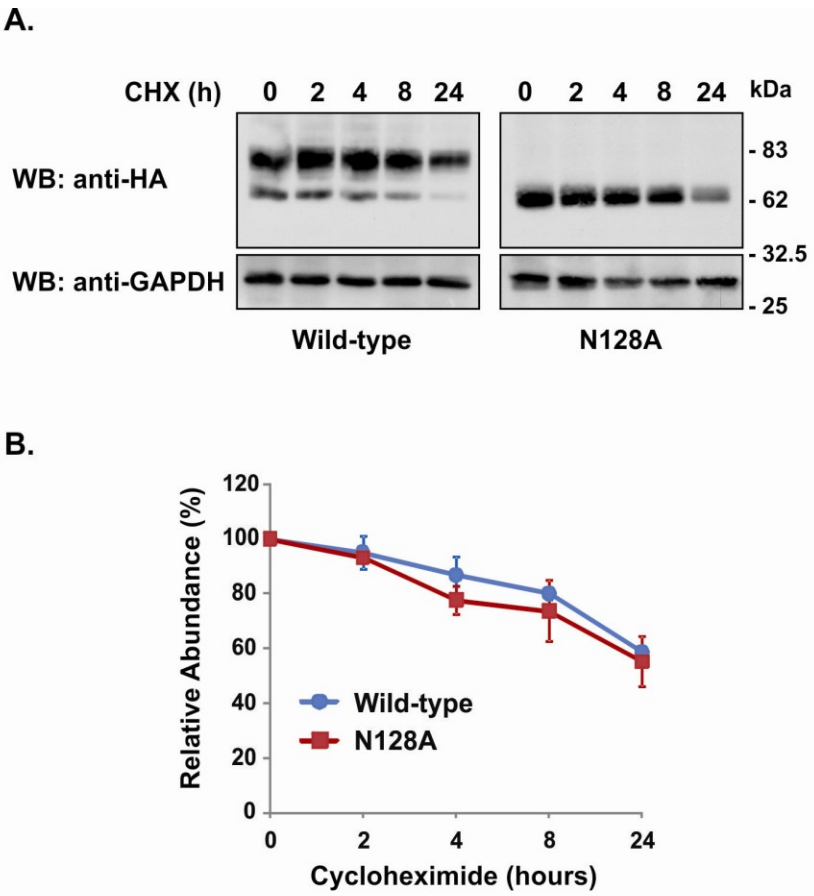

Figure 2.6. Stability of glycosylation-deficient mutant is not affected.

A. AP-1 cells stably expressing $NHE6_{HA}$ wild-type (*left panels*) or N128A mutant (*right panels*) were treated with 100 µg/ml cycloheximide to block new protein synthesis for the indicated time points. Cell lysates were prepared and equal amounts of proteins were separated by SDS-PAGE and analyzed with a mouse monoclonal anti-HA antibody. GAPDH was used as loading control.

B. Western blots from three individual experiments were quantified by densitometry of X-ray films exposed in the linear range and analyzed using ImageJ software. Data represent mean ± SEM.

CD4TIUb (Barriere et al., 2009; Barriere et al., 2007) . AP-1 cells were transfected with $NHE6_{HA}$ bearing a triple Flag epitope at position M53 in the first extracellular loop or at position N128 in the second extracellular loop to disrupt glycosylation. As shown in Fig. 2.7A by western blot with a monoclonal anti-HA antibody, the M53 construct displays the expected banding pattern, with a slower migrating, fully-glycosylated form and a faster migrating, core-glycosylated form, as previously demonstrated in Figure 2.2. Insertion of the triple Flag epitope in the glycosylation site, at Asn128 disturbs the normal glycosylation of the protein, which now migrates as a single band on a SDS-PAGE (Fig. 2.7A). Forty-eight hours post-transfection, $_{3Flag}NHE6_{HA}$ present on the cell surface was labeled on ice with primary mouse monoclonal anti-Flag antibody, followed by the pH-sensitive probe, FITC-conjugated Fab secondary antibody. Cells were then incubated in cell culture media at 37ºC for 30 min or 60 min and analyzed by FRIA. After 30 min of internalization, $_{3Flag}NHE6_{HA}$_M53 was detected in an acidic compartment (pH~ 6.07), which corresponds to the sorting endosomal and/or perinuclear recycling endosomal compartments, whereas after 60 min it was present in a late recycling endosomal pool which is more alkaline, as suggested by the higher pH of 6.5. On the other hand, the $_{3Flag}NHE6_{HA}$_N128 construct was detected in more alkaline compartments after 30 min (pH ~6.85) and 60 min (pH~6.6) of endocytosis (Fig. 2.7B). These data suggest that the lack of NHE6 glycosylation impairs endosomal pH homeostasis, either by a direct effect on NHE6 activity or possibly by disturbing some critical protein-protein interactions essential for the proper regulation of endosomal pH. Determination of the precise mechanism will require further experimentation.

DISCUSSION

In this study we have identified the *N*-glycosylation site of NHE6-v0 and defined a role for this post-translational modification in the transport of NHE6 to the cell surface and possible for its function. Using site-directed

mutagenesis and biochemical assays, we showed that Asn128 is the unique site responsible for N-glycosylation of NHE6. The glycosylation-deficient mutant was targeted correctly to a transferrin-enriched recycling endosomal compartment, similar to its wild-type counterpart, as shown by immunofluorescence confocal microscopy, suggesting that proper endosomal localization of NHE6 does not require glycosylation. The stability and the internalization rate of the unglycosylated mutant protein were also unaffected, but its cell surface abundance was decreased compared to the wild-type fully glycosylated protein, suggestive of the involvement of N-glycans in NHE6 trafficking to the plasma membrane. FRIA experiments showed an alkalinization of glycosylation deficient NHE6-containing endosomes, suggesting a possible role for glycosylation in regulating the function of NHE6.

N-glycosylation represents a frequent modification of proteins that influences a myriad of molecular and cellular events, including protein folding, trafficking and stability, receptor activation, signal transduction, endocytosis and cell adhesion (Ohtsubo and Marth, 2006). Some proteins are completely reliant on glycosylation for function, others display partial dependence (*e.g.* become temperature-sensitive for folding), while others appear totally indifferent to oligosaccharide modification (Helenius and Aebi, 2001; Soroka et al., 2008). In some cases, protein function is glycan-dependent in one cell type but not another (Helenius and Aebi, 2001).

Earlier studies of the yeast *Saccharomyces cerevisiae* homolog of NHE6, named Nhx1, showed that the transporter is localized to a late endosomal/prevacuolar compartment and is also *N*-glycosylated (Wells and Rao, 2001; Nass et al., 1997; Nass and Rao, 1998). Nhx1 contains six putative consensus sites for *N*-linked glycosylation; three are present in loop regions of the N-terminal transmembrane domain and were predicted to face the lumen of the prevacuolar compartment, while the other three are located in the C-terminal tail and predicted to reside in the

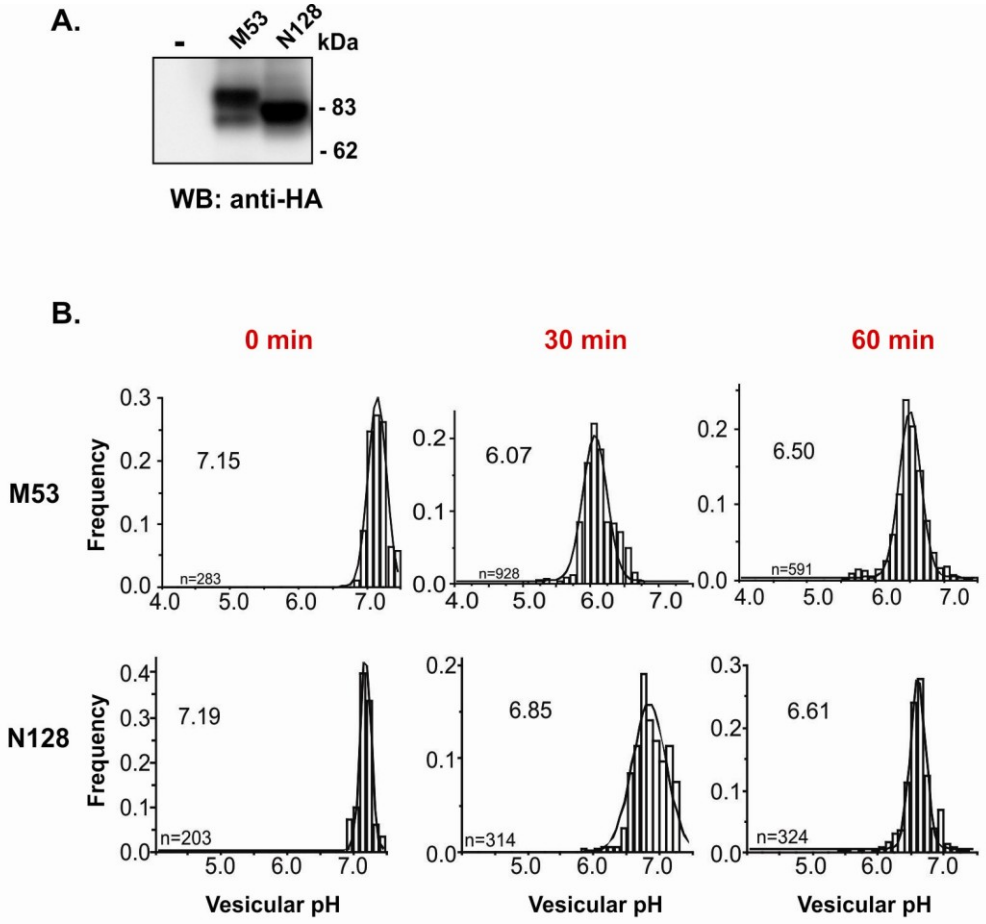

Figure 2.7. Fluorescence ratio imaging analysis (FRIA) of the internalization kinetics of $_{3Flag}NHE6_{HA}$_M53 and $_{3Flag}NHE6_{HA}$_N128 in AP-1 cells.

A. AP-1 cells were transfected with $NHE6_{HA}$-wt bearing a triple Flag epitope at M53 ($_{3Flag}NHE6_{HA}$_M53) or N128 ($_{3Flag}NHE6_{HA}$_N128) and cell lysates were obtained 48 h post-transfection. Proteins were separated by SDS-PAGE and the expression of the transfected constructs was analyzed by western blotting with a mouse monoclonal anti-HA antibody.

B. $_{3Flag}NHE6_{HA}$_M53 and $_{3Flag}NHE6_{HA}$_N128 were expressed in AP-1 cells and endosomal delivery was assessed two days post-transfection. Anti-Flag M2 primary antibody (1/2000) and FITC-conjugated Fab secondary antibody (1/1000) were bound to the cells for 1 h on ice. The temperature was raised to 37°C for 30 or 60 min and the vesicular pH (pHv) was measured by FRIA. The mean (± SEM) pHv and the number of vesicles analyzed in a single experiment are indicated.

cytosol. Mutational analysis showed that two Asn residues (N515 and N550) in the C-terminus are subject to *N*-linked glycosylation. However, loss of *N*-linked glycosylation did not appreciably affect the function of Nhx1, in as much as yeast expressing the glycosylation-deficient mutant displayed normal sodium-tolerant growth. Notwithstanding, the presence of *N*-linked glycans in the C-terminus of Nhx1 predicts a surprising membrane topology, with at least some portion of the Nhx1 tail being exposed to the lumen of the prevacuolar compartment (Wells and Rao, 2001). By contrast, our data indicate that Asn623 in NHE6-v0 is not glycosylated, supporting the topological membrane model postulated for mammalian Na^+/H^+ isoforms, whereby the C-terminal domain is located in the cytosol (Orlowski and Grinstein, 2004; Brett et al., 2005a; Orlowski and Grinstein, 2007).

The effect of glycosylation on mammalian plasma membrane-type NHEs has also been investigated. The ubiquitously expressed plasma membrane-type Na^+/H^+ exchanger NHE1 contains three consensus sites for *N*-linked glycosylation at asparagines 75, 370, and 410, but only Asn 75 is utilized. However, N-glycosylation was not found to be important for the transport function and pharmacological properties of NHE1. In addition, NHE1 also undergoes O-linked glycosylation in the first extracellular loop which is rich in serine and threonine residues (Counillon et al., 1994). The same study also showed that rat NHE3 was not glycosylated when expressed in fibroblast cells. However, subsequent studies using tunicamycin, an antibiotic that blocks *N*-glycosylation, showed that endogenous NHE3 is *N*-glycosylated in cultured pig kidney LLC-PK_1 cells (Soleimani et al., 1996), but the glycosylation sites were not defined. Treatment with tunicamycin significantly decreased NHE3 activity in these cells and inhibited the trafficking of NHE3 from the endoplasmic reticulum to the plasma membrane. In addition, a threefold increase in NHE3 mRNA expression was observed in the presence of tunicamycin, leading the authors to propose that the glycosylated form of the exchanger

regulates the expression of NHE3 mRNA through a feed-back loop that is inhibited in the presence of underglycosylated NHE3. However, the mechanism was not defined further and other indirect pharmacological effects are possible.

Glycosylation has also been found to have differential effects on members within other ion carrier families. For instance, isoforms of the Kv1 voltage-gated potassium channel family contain a single *N*-glycosylation consensus site in the linker between their first two transmembrane domains. Mutation of this site in the Kv1.2 channel decreased cell surface level by ~40%, whereas the stability and folding of the unglycosylated mutated protein was not altered, similar to our results with NHE6 (Watanabe et al., 2007). Furthermore, the single channel conductance was not affected, but the activation kinetics of the channel was diminished (Watanabe et al., 2007). On the other hand, preventing *N*-glycosylation of Kv1.4 decreased its stability and plasma membrane abundance of Kv1.4 (Watanabe et al., 2004).

Thus, the effects of glycosylation on trafficking and protein stability appear to be isoform specific. The fact that the glycosylation-deficient mutant is still able to reach the plasma membrane, even though its levels are reduced, implies that other glycosylation-independent regulatory mechanisms are involved in trafficking NHE6 to the cell surface, like interactions with scaffolding proteins, as it has been shown for Kv1 channels (Tiffany et al., 2000) or phosphorylation of the exchanger, as it is the case for NMDA receptors (Scott et al., 2001).

N-glycosylation is essential for the trafficking and function of numerous other membrane proteins, including the G-protein coupled protease-activated receptor-1 (PAR1), which is the main effector of thrombin signalling. *N*-linked glycosylation of the N-terminus is important for transport to the cell surface, whereas *N*-glycosylation of the second extracellular loop is important for ligand-induced receptor activation and endocytosis (Soto and Trejo, 2010). Additionally, the importance of *N*-

linked glycosylation of proteins is further highlighted by studies showing that defects in *N*-linked glycosylation are linked to impaired cell surface expression of membrane proteins like rhodopsin and the sulphonylurea receptor, leading to severe diseases such as retinitis pigmentosa and persistent hyperinsulinemic hypoglycaemia, respectively (Conti et al., 2002; Zhu et al., 2004).

Our data showed that the cell surface levels of unglycosylated NHE6 is reduced, but its internalization rate does not differ from the fully glycosylated wild-type NHE6. As the quantity of protein on the cell surface membrane depends on the rate of both its delivery to this location and endocytosis of the protein, we concluded that glycosylation of NHE6 is important for its delivery to the cell surface. Similar data were published for CFTR (cystic fibrosis transmembrane conductance regulator)(Glozman et al., 2009). Although the cell surface level of glycosylation-deficient CFTR was severely reduced, the internalization rates of glycosylation-deficient and wild-type CFTR were similar, but the recycling of mutants was significantly inhibited.

Transport of unglycosylated mutants to the cell surface was recorded for other membrane proteins, including the cold-sensitive TRPM8 (transient receptor potential melastatin-like) channels, where a single asparagine (Asn934) was identified as the only acceptor for *N*-linked glycans. Mutation of this site to glutamine did not abolish the transport of the channel to the cell surface nor its ability to form functional channels. However, cell surface expression of the glycosylation-deficient mutant was reduced, leading the authors to suggest that glycosylation either increases the efficiency of transport to the membrane and/or prolong the stability of the channels once it reaches the plasma membrane (Erler et al., 2006). By contrast, *N*-glycosylation of the organic solute transporter α subunit is not necessary for its association with its β subunit or for plasma membrane location and function of the transporter in HepG2 cells (Soroka et al., 2008).

In conclusion, we show that glycosylation of NHE6-v0 participates in its accumulation at the cell surface and its regulation of recycling endosomal pH homeostasis.

CHAPTER 3

RACK1 Binds to the Recycling Endosomal Na^+/H^+ Exchanger NHE6 and Limits its Accumulation at the Cell Surface

Alina Ilie, Albena Davidova, and John Orlowski

In the previous chapters we described the native distribution of NHE6 in neuronal cells and identified the site responsible for the N-glycosylation of the exchanger, as well as the role of this post-translational modification in the trafficking and function of the exchanger. To identify novel interacting partners involved in the regulation of NHE6, we performed a yeast two-hybrid analysis using the C-terminal cytosolic portion of the transporter to screen a human brain cDNA library. One of the proteins identified in this screen was the receptor for activated C-kinase 1 (RACK1). In this chapter we confirm the interaction between these two proteins and examine its functional consequences.

ABSTRACT

The ubiquitously expressed mammalian Na^+/H^+ exchanger NHE6 isoform resides mainly in transferrin rich endosomes, where it is postulated to modulate vesicular pH homeostasis and biogenesis. However, the molecular mechanisms that govern its trafficking, regulation, and function are largely unknown. To this end, the cytoplasmic C-terminal portion of NHE6 was used to screen a human brain cDNA library for interacting partners by yeast two-hybrid methodology. Two of the clones identified encoded the receptor for activated protein kinase C (RACK1), a scaffolding protein involved in numerous protein interactions and biological functions. Direct interaction of these two proteins was confirmed *in vitro* by GST fusion protein pull-down assays. Further analyses delimited the RACK1-binding site of NHE6 to amino acids 520-565 and showed that NHE6 can bind to multiple WD domains of RACK1. NHE6 and RACK1 also formed a complex in intact cells, as revealed by co-immunoprecipitation assays and dual-immunolabelling fluorescence confocal microscopy. Depletion of RACK1 by siRNA resulted in increased total cellular expression and cell surface abundance of NHE6. These data suggest an important role for RACK1 in restricting the expression and accumulation of NHE6 at the plasma membrane.

INTRODUCTION

Mammalian alkali cation/proton exchangers, commonly referred to as sodium/proton exchangers (NHEs), are integral membrane (glyco)phosphoproteins that catalyze the countertransport of Na^+ (and for some isoforms also K^+) for H^+ down their respective concentration gradients and play a central role in cellular pH and volume homeostasis. Structurally, NHEs are composed of an N-terminal membrane spanning domain responsible for ion transport, and a more divergent C-terminal tail

facing the cytosol, which is important in regulating the transporters activity and trafficking (Orlowski and Grinstein, 2004).

To date, eleven different NHE isoforms have been identified (Casey et al., 2010). According to their subcellular localization and structure homology, the NHEs can be subdivided into three general categories: plasma membrane-type NHEs (NHE1 to NHE5), organellar-type NHEs (NHE6-NHE9), as well as bacterial-like NHEs (NHA1 and NHA2) (Brett et al., 2005a; Orlowski and Grinstein, 2007).

The organellar isoform NHE6 is widely expressed in tissues (Numata et al., 1998). At the cellular level, NHE6 resides mainly in a recycling endosomal compartment (Brett et al., 2002; Nakamura et al., 2005), but a small portion of the protein (~10%) can reach the plasma membrane (Fig. 1.2). It has been postulated that NHE6 might play significant roles in the biogenesis and pH homeostasis of endocytic vesicles in mammalian cells (Orlowski and Grinstein, 2007). However, virtually nothing is known about the factors and mechanisms that regulate the transporter's trafficking and function.

In order to identify putative interacting partners for NHE6, a yeast two-hybrid screen was conducted using the entire C-terminal portion of NHE6 to screen a human brain cDNA library. Two of the positive clones were found to encode almost the entire protein portions of the receptor for activated protein kinase C (RACK1) (clone1: V69 to R317, clone 2: S63 to R317). Here we confirm the interaction between NHE6 and RACK1 by biochemical, cellular and immunological methods and investigate the functional consequences of this interaction on NHE6 expression and trafficking. Our results suggest that RACK1 is involved in regulating the expression and cell surface accumulation of NHE6 in cells.

MATERIALS AND METHODS

Materials

The following primary antibodies were obtained from commercial sources: mouse monoclonal and rabbit polyclonal anti-hemagglutinin (HA) (Covance Inc., Berkeley, CA); monoclonal and polyclonal anti-glyceraldehyde 3-phosphate dehydrogenase (GAPDH) (Abcam Inc., Cambridge, MA); mouse monoclonal anti-β-tubulin (Sigma-Aldrich); mouse monoclonal anti- RACK1 (BD Transduction Laboratories, San Diego, CA); rabbit polyclonal anti-RACK1 (Santa Cruz Biotechnology, Santa Cruz, CA); mouse monoclonal and rabbit polyclonal anti-myc antibodies (Upstate Biotechnology, Lake Placid, NY). Horseradish peroxidase-conjugated secondary IgG antibodies were purchased from Jackson ImmunoResearch (West Grove, PA). All Alexa Flour® conjugated secondary antibodies were purchased from Molecular Probes (Eugene, OR).

Alpha-Minimum essential medium (α-MEM), High Glucose Dulbecco's Modified Eagle Medium (DMEM), fetal bovine serum, penicillin/streptomycin, and Lipofectamine™ were purchased from Invitrogen. FuGENE® 6 was from Roche Diagnostics (Mannheim, Germany). [^{35}S]methionine was obtained from PerkinElmer Life Sciences. G418 sulfate was purchased from Wisent Inc. (St-Bruno, QC, Canada).

All other chemical and reagents were obtained from BioShop Canada (Burlington, ON, Canada) or Fisher Scientific and were of the highest grade available.

Yeast two-hybrid screening

The C-terminal portion of human NHE6 (corresponding to amino acids A499-A669) was amplified by PCR using the following primers: forward, 5'-GAG GCC GAA TTC GCA ATG CTG TCA TGC TTG- 3'

(*EcoRI* site is underlined) and reverse, 5'-GTC GAC GGA TCC GGC TGG ACC ATG TCT CG (*BamHI* is underlined). After gel-purification, the fragment was cloned in frame with the *GAL4* 1-147 DNA-binding domain of the pAS2-1 vector (BD Biosciences) carrying the TRP1 gene. This construct was used as a bait to screen 3.5 x 10^6 independent clones of a human brain cDNA library cloned in frame with the *GAL4* 768-881 activation domain in the pACT2 vector (BD Biosciences) carrying the LEU2 gene. The two constructs were co-transformed into the yeast *Saccharomyces cerevisiae* strain AH109 (*MATa, trp1-901, leu2-3, 112, ura3-52, his3-200, gal4*Δ*, gal80*Δ*, LYS2::GAL1*$_{UAS}$*-GAL1*$_{TATA}$*-HIS3, GAL2*$_{UAS}$*-GAL2*$_{TATA}$*-ADE2, ura3::MEL1*$_{UAS}$*-MEL1*$_{TATA}$*-lacZ*) using the lithium acetate method (Gietz et al., 1997). To ensure that the plasmids encoding the bait and the library do not activate the reporter gene *lac*Z on their own, the two constructs were transformed separately into the yeast strain AH109 and the resulting colonies were subjected to the β-galactosidase filter assay. Only white colonies were obtained in the presence of the chromogenic substrate X-Gal (5-bromo-4-chloro-3-indolyl-β-D-galacto-pyranoside), suggesting that the reporter gene was not activated. As additional positive controls, AH109 yeast cells were co-transformed with the plasmids pCL1 (encoding the wild-type full-length GAL4 transcription factor) or pTD1-1 (encoding the SV40 large T-antigen $_{(84\text{-}708)}$) and pVA3-1 (containing the murine p53 $_{(72\text{-}390)}$ gene). As negative control, AH109 yeast cells were co-transformed with plasmids encoding two proteins that are known not to interact, namely the SV40 large T-antigen$_{(84\text{-}708)}$ (pTD1-1) and human lamin C$_{(66\text{-}230)}$ (pLAM5'-1) All plasmids used were from BD Biosciences.

Positive transformants were selected under high stringency conditions on selection media (SD/-Ade/-His/-Leu/-Trp) and subjected to the β galactosidase filter assay. Growth- and β-galactosidase double positive clones were extracted from yeast and transformed into *E. coli* DH5α cells; DNA was isolated, sequenced and identified using the BLAST

search program. A total of 283 positive clones were isolated and sequenced.

Two of the positive clones were found to encode significant portions (clone1: S63 to R317, clone 2: V69 to R317) of RACK1 (receptor for activated C kinase 1, also called guanine nucleotide binding protein (G protein), beta polypeptide 2-like 1).

Gene Construction and Plasmids

Full-length human RACK1 was purchased from ATCC (Manassas, VA) and amplified by PCR using primers containing restriction sites for *EcoRV* at the 5' end and *HindIII* at the 3' end. The resulting PCR amplicons were sub-cloned in frame with the *myc* tag (EQKLISEEDL) of the mammalian expression vector pCMV-Tag3B (Stratagene, La Jolla, CA). Full-length RACK1 was also inserted into the mammalian expression vector pcDNA3.1 (Invitrogen), after PCR amplification with primers containing *HindIII* and *XbaI* restriction sites at 5' and 3' ends, respectively.

The cloning of human isoform NHE6-v0 used in the experiments described in this chapter was described previously (Numata et al., 1998). NHE6-v0 was engineered to include the influenza virus hemagglutinin (HA) (YPYDVPDYAS) epitope at its extreme C-terminus and cloned into the mammalian expression vector pCMV (Virdee and Orlowski, unpublished results). The $NHE6_{HA}$ wild-type construct was also inserted into the *HindIII*/*XbaI* sites of the mammalian expression vector pcDNA3.1 (Invitrogen) and used as templates to introduce a triple Flag (3X DYKDDDDK) epitope in the first extracellular loop. First, PCR was used to engineer a *NotI* restriction site in the first extracellular loop, after M53, followed by the introduction of annealed primers representing the 3xFlag epitope, which generated a construct termed $_{3Flag}NHE6_{HA}$. All constructs were sequenced to verify their fidelity.

Cell Culture and cDNA Transfection

CHO (Chinese hamster ovary), AP-1 (a chemically-mutagenized derivative of CHO cells devoid of plasma membrane Na^+/H^+ exchange activity) (Rotin and Grinstein, 1989), and HEK293 cells were maintained in α-Minimum Essential Medium (α-MEM) supplemented with 10% fetal bovine serum, penicillin (100 units/ml), streptomycin (100 µg/ml), and 25 mM $NaHCO_3$ (pH 7.4). HEK-GRIP cells were a generous gift from Dr. G. Lukacs (McGill University) and were cultured in High Glucose Dulbecco's Modified Eagle Medium (DMEM) supplemented with 10% fetal bovine serum and 500 µg/ml G418 sulfate. SH-SY5Y human neuroblastoma cells were cultured in DMEM supplemented with 10% fetal bovine serum. All cells were incubated in a humidified atmosphere of 95% air, 5% CO_2 at 37°C.

To generate AP-1 or HEK293 cells stably expressing $NHE6_{HA}$, cells were grown to subconfluence in a 6-well plate and transfected with plasmid DNA (1µg/ml) using Lipofectamine™ reagent according to the manufacturer's instructions. Twenty-four hours after transfection, cells were split (1:50) into 10-cm dishes and selected for stably expressing clones in α-MEM culture medium supplemented with G418 sulfate (600 µg/ml) over a 3-week period.

Construction of Glutathione S-Transferase (GST) Fusion Protein and *In Vitro* Binding Assay

GST fusion proteins of segments of the C-terminal region of NHE6 were produced by PCR amplification using primers containing *BamHI* at the 5′ terminus and *EcoRI* at the 3′ terminus. These PCR products were subcloned in-frame into the bacterial expression vector pGEX-2T (Amersham Biosciences). Inserts were sequenced to verify their fidelity, and then the plasmid constructs were transformed into the Epicurian Coli® BL21-CodonPlus™ strain (Stratagene, Cedar Creek, TX). The same methodology was used to construct GST-fusion proteins of full-length

RACK1 and of each of the seven WD domains of RACK1 separately (WD1 to WD7).

Individual colonies were cultured overnight, then diluted 1:25 in 50 ml of bacterial growth media, and incubated further at 37 °C with vigorous shaking to obtain a sufficient population density (OD_{600}~0.6). Protein expression was then induced with 0.4 mM isopropyl 1-thio-β-galactopyranoside (IPTG), and cultures were incubated at 30°C for 3 hours. The bacterial cultures were centrifuged, and the resulting pellets were resuspended in 500 µl of GST-lysis buffer (1 mM EDTA, 0.5% Nonidet P-40) and protease inhibitors in standard phosphate-buffered saline (PBS). Bacteria were subsequently lysed by sonication (model 100 Sonic Dismembrator, Fisher) on ice and cleared by centrifugation at 4°C for 30 min. GST-NHE6 fusion proteins were then purified by incubating bacterial cell lysates with glutathione-Sepharose™ beads (GE Healthcare) for several hours at 4°C. The purified GST fusion proteins bound to glutathione-Sepharose beads were washed six times with GST-lysis buffer and then incubated with either 2.5 µl of *in vitro* translated full-length ^{35}S-labeled RACK1 or cell lysates of Chinese hamster ovary (CHO) cells over-night at 4°C.

RACK1 cloned into the pcDNA3.1 vector was synthesized *in vitro* using a transcription-translation coupling reaction in rabbit reticulocyte lysates (Promega, Madison, WI) in the presence of [^{35}S]methionine. To obtain cell lysates, CHO cells cultured in 10-cm dishes were washed twice with ice-cold PBS, followed by addition of 500 µl of ice-old cell lysis buffer (1% Triton, protease inhibitors cocktail (Roche) in PBS, pH 7.4), scraping and incubating on a rocker at 4°C for 1 h. Cell lysates were then cleared of debris by centrifuging at 16,000 x g for 20 min at 4°C. GST-NHE6 fusion protein complexes were washed four times with GST-lysis buffer and eluted in Laemmli buffer (50 mM Tris-HCl, pH 6.8, 2% SDS, 10% glycerol, 0.1% bromophenol blue, and 100 mM DTT). Proteins were separated by SDS-PAGE and then transferred to polyvinylidene fluoride

membranes (Millipore, Nepean, Ontario, Canada) for Western blotting. Membranes were blocked with 5% nonfat powdered milk in PBS for 1 h, followed by incubation with a monoclonal anti-RACK1 antibody (1:2000) (BD Transduction Laboratories™) in 5% milk/PBS/Tween 0.1% for 1 hour and a goat anti-mouse secondary antibody conjugated to horseradish peroxidase at a dilution of 1:5000 (Jackson ImmunoResearch, West Grove, PA). Immunoreactive bands were detected using Western Lightning ®Plus-ECL reagents (Perkin Elmer, Inc., Waltham, MA). Expression of the GST constructs was verified by either running a parallel gel stained with Coomassie Blue (CB) dye, or by staining the membrane with Ponceau red after western blotting.

To identify the NHE6 binding site(s) in RACK1, GST-fusion proteins of full-length RACK1 and of the individual WD domains (WD1 to 7), were bound to glutathione-Sepharose™ beads and incubated over night with lysates obtained from HEK293 cells stably expressing $NHE6_{HA}$. The beads were washed, and then the proteins were eluted with Laemmli buffer and resolved by SDS-PAGE. Bound NHE6 was identified by Western blotting with a monoclonal anti-HA antibody.

Co-immunoprecipitation

Co-immunoprecipitation experiments of NHE6 and RACK1 were performed in CHO cells cultured in 10-cm dishes and transfected with either 10 µg of empty pCMV vector (as negative control) or 5 µg of both $NHE6_{HA}$ and $_{myc}$RACK1 using Lipofectamine™ reagent (Invitrogen) according to the manufacturer's instructions. Thirty hours post-transfection, cell lysates were prepared by washing the cells twice with ice-cold PBS and scraping them into 500 µl of cell lysis buffer (0.5% Nonidet-P40, 0.25% sodium deoxycholate, and protease inhibitors in PBS, pH 7.4). Cell lysates were rocked at 4°C for 30 min and centrifuged for 20 min at 16,000 x g to pellet cellular debris. Supernatants were pre-cleared with 100 µl of a 50% slurry of protein G-Sepharose beads™ (GE

Healthcare) in cell lysis buffer for 1 h at 4°C. The beads were removed by brief centrifugation and a fraction of the cell lysate was removed for immunoblotting. Five µg of polyclonal anti-HA or anti-myc antibodies were added to the remaining cell lysates and incubated with gentle rocking at 4°C for 4 h. Subsequently, 100 µl of 50% protein G-Sepharose™ slurry beads was added to each tube and incubated with the immunoprecipitates overnight. Next day, the beads were washed four times with cell lysis buffer; the proteins were eluted with Laemmli buffer and then subjected to SDS-PAGE and transferred to polyvinylidene fluoride membranes. Proteins were detected by Western blotting with primary monoclonal anti-myc (1:1000 dilution) and anti-HA (1:5000 dilution) antibodies, followed by goat anti-mouse HRP-conjugated secondary antibody (1:5000 dilution). Protein bands were visualized using Western Lightning ®Plus-ECL detection reagents.

A similar protocol was used to detect the formation of complexes between $NHE6_{HA}$ and endogenous RACK1 in HEK293 cells transiently or stably expressing $NHE6_{HA}$. HEK293 cells were grown in 10-cm dishes and transfected with 8 µg pCMV or 8 µg $NHE6_{HA}$ using Lipofectamine reagent. Cells were lysed 30 hours post-transfection and pre-cleared for 1 h on Protein A Agarose beads (Invitrogen). Lysates were subjected to immunoprecipitation overnight at 4°C with anti-IgG (as negative control) or anti-HA polyclonal antibodies. Next day, 100 µl of a 50% slurry Protein A Agarose beads was added and incubated with the immunoprecipitates for 3 h. Subsequently, the beads were washed and the proteins eluted in Laemmli buffer, then resolved on a SDS-PAGE, transferred to polyvinylidene fluoride membranes, and immunoblotted with anti-RACK1 (1:1500) and anti-HA (1:5000) monoclonal antibodies.

HEK293 cells stably expressing $NHE6_{HA}$ were lysed and pre-cleared for 1.5 h on Protein G-Sepharose beads (GE Healthcare). Lysates were subjected to immunoprecipitation overnight at 4°C with the following polyclonal antibodies: anti-RACK1, non-specific IgG, anti-HA, and anti-

NHE6. Next day, 100 µl of 50% slurry Protein G-Sepharose beads was added and incubated with the immunoprecipitates for 3.5 h. Subsequently, the beads were washed and the proteins eluted in Laemmli buffer, then resolved on a SDS-PAGE gel, transferred to polyvinylidene fluoride membranes, and immunoblotted with the monoclonal anti-RACK1 or anti-HA antibodies.

Measurement of Endocytosis by Cell-based Enzyme-Linked Immunosorbent Assay (ELISA)

HEK-GRIP cells were plated into 6-well plates and transfected with 100 nM of non-targeting siRNA pool #1 (scrambled siRNA) or SMARTpool® RACK1 siRNA (Dharmacon) using Dharmafect1 transfection reagent (Dharmacon) according to the manufacturer's recommended protocol. After 24 h, the transfection reaction mix was removed and 2 µg per well of pcDNA3 (as negative control) or $_{3Flag}NHE6_{HA}$ were transfected into the cells using FuGENE® 6 (Roche Diagnostics, Mannheim, Germany). After 24 h, the cells were transferred into 12-well plates and further grown for 24 h for the fluorescence-based endocytosis assay, which was done 72 h after the siRNA transfection and 48 h after the NHE6 cDNA transfection. Cells were chilled on ice, washed with ice-cold PBS supplemented with 0.1 mM $CaCl_2$ and 1 mM $MgCl_2$ (PBS-CM), pH 7.4, blocked in 10% goat serum/PBS-CM, and then incubated with an anti-Flag monoclonal antibody (1:3000 dilution) (Sigma) on ice for 1 hour. After extensive washes with PBS-CM, internalization of the bound antibody was initiated by incubating the cells with warm (37ºC) α-MEM for the indicated time points and terminated by placing the plates on ice. Cells were washed with PBS-CM and labeled with anti-mouse secondary HRP-conjugated antibody (1:1000 dilution) (GE Healthcare). After extensive washes with PBS-CM, cells were incubated on ice with Amplex® Red reagent (Invitrogen). Aliquots were transferred to 96-well plates and fluorescence readings were taken with a POLARstar OPTIMA

plate reader (BMG Labtech, Inc, Offenburg, Germany) using 544-nm excitation and 590-nm emission wavelengths. All experiments were performed in triplicates and repeated at least three times. The internalization kinetics results were expressed as a percentage of the fluorescence recorded prior to internalization, after subtraction of the value measured with pcDNA3 (mock) - transfected cells and normalization for total protein concentration. Results are shown as mean ± standard error of the mean (SEM).

Cell Surface Biotinylation

AP-1 cells stably expressing $NHE6_{HA}$ were cultured in 6-well plates and transfected with 100 nM non-targeting siRNA pool #1 (scrambled siRNA) or SMARTpool® RACK1 siRNA (Dharmacon) using Dharmafect1 transfection reagent (Dharmacon) according to the manufacturer's recommended protocol.

HEK-GRIP cells were grown in 6-well plates and transfected with 100 nM scrambled or RACK1 siRNA and $_{3Flag}NHE6_{HA}$ using the same protocol described for the fluorescence-based endocytosis assay.

Seventy two hours after the siRNA transfection, cells were placed on ice and washed three times with ice-cold PBS containing 1 mM $MgCl_2$ and 0.1 mM $CaCl_2$ (PBS-CM), pH 8.0. Next, cells were incubated on ice for 30 min with the membrane-impermeable reagent N-hydroxysulfosuccinimydyl-SS-biotin (0.5 mg/ml, Pierce). Cells were washed with PBS-CM and incubated twice in quenching buffer (20 mM glycine in PBS-CM) for 7 minutes each on ice to remove unbound biotin. After two more washes in PBS-CM, the cells were lysed in lysis buffer (0.5% Nonidet-P40, 0.25% sodium deoxycholate, and protease inhibitors in PBS, pH 7.4) for 30 min on ice, and then centrifuged at 16,000 x g for 20 min at 4°C to remove insoluble cellular debris. A portion of the resulting supernatant was removed and this represented the total fraction. Protein concentration in the lysates was determined using Bio-Rad DC

protein assay reagents (Bio-Rad Laboratories, Hercules, CA). Equal amounts of proteins were incubated with 100 µl of 50% NeutrAvidin® Agarose Resin slurry (Fisher Scientific, Whitby, ON, Canada) in lysis buffer with gentle rocking overnight at 4°C to extract biotinylated membrane proteins. The proteins were then resolved by SDS-PAGE and immunoblot analysis. The surface and total $NHE6_{HA}$ was detected with a monoclonal anti-HA antibody (1:5000) and RACK1 was detected with an anti-RACK1 monoclonal antibody (1:2000). Equal protein loading was checked with either a monoclonal anti-GAPDH antibody (1:70000) or a monoclonal anti-β-tubulin antibody (1:5000). The intensity of the bands was quantified by densitometry from X-ray films exposed in the linear range and analyzed using ImageJ software.

Measurements of Protein Stability

To determine the stability of NHE6 in the presence of RACK1 siRNA, AP-1 cells stably expressing $NHE6_{HA}$ or HEK-GRIP cells transiently expressing $_{3Flag}NHE6_{HA}$ were grown in 6 well-plates and transfected with scrambled or RACK1 siRNA's using the same protocol described for the cell surface biotinylation assay.

Seventy two hours after the siRNA transfection, cells were treated with cycloheximide (150 µg/ml) in complete media (α-MEM supplemented with 10% FBS and penicillin/streptomycin for the AP-1 cells and high-glucose DMEM containing 10% FBS and 500 µg/ml G418 sulfate for HEK-GRIP cells) for up to 24 h to inhibit new protein synthesis. At appropriate time points, cells were lysed, protein concentrations were measured, and equal quantities of protein were subjected to SDS-PAGE and immunoblotting with anti-HA, anti-RACK1 and anti-β-tubulin monoclonal antibodies. The intensity of the bands was quantified by densitometry from X-ray films exposed in the linear range and analyzed using ImageJ software.

Immunofluorescence Confocal Microscopy

SH-SY5Y human neuroblastoma cells were cultured on glass coverslips coated with 10 µg/ml fibronectin (Sigma). To examine the subcellular localization of endogenous NHE6 and RACK1, cells were fixed in 2% paraformaldehyde/PBS pH 7.4 for 20 minutes, permeabilized with 0.1% saponin/PBS pH 7.4 for 20 min, and then blocked in 10% goat serum /0.01%saponin/PBS pH 7.4 for 1 h at room temperature. Cells were incubated subsequently with anti-NHE6 rabbit polyclonal (1:300) and anti-RACK1 (1:600) monoclonal primary antibodies overnight at 4°C. Next day, cells were washed four times with 10% goat serum/0.01% saponin/PBS pH 7.4, and then incubated with goat anti-mouse Alexa Fluor® 488 and goat anti-rabbit Alexa Fluor® 568-conjugated secondary antibodies at a dilution of 1:2000 in 10% goat serum/0.01% saponin/PBS, pH 7.4, for 1 h at room temperature. After extensive washes with PBS, cover slips were mounted onto glass slides using Aqua Poly/Mount mounting medium (Polysciences Inc., Warrington, PA).

Cells were examined by laser scanning confocal microscopy using a Zeiss LSM 510 Meta microscope, and images were analyzed and presented using LSM software and Corel® CorelDraw™ version X3.

RESULTS

Identification of RACK1 as an NHE6 interacting partner

Numerous studies have shown the importance of the C-terminal region of plasma membrane NHEs for the regulation of these transporters (Orlowski and Grinstein, 2004). However, little is known about the mechanisms that regulate NHE6 trafficking and function. In an attempt to decipher these mechanisms, we used yeast two-hybrid methodology (Chien et al., 1991) to screen a human brain cDNA library for NHE6 interacting partners. To this end, the cytosolic C-terminal portion of NHE6 (amino acids 499-669) was fused to the *Gal4* DNA binding domain and the

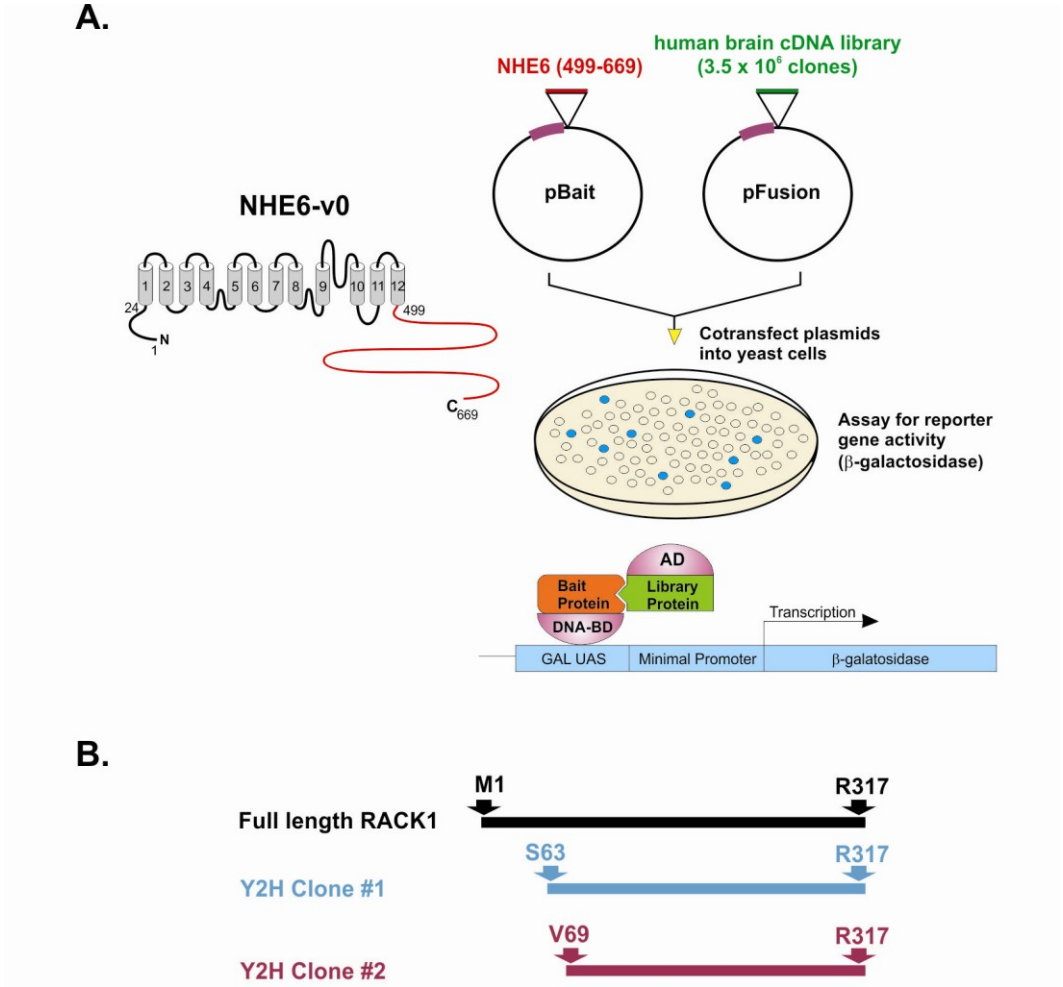

Figure 3.1. RACK1 was identified as an interacting partner of NHE6 in a yeast two-hybrid screen.

A. The C-terminal tail of NHE6 (amino acids 499-669) was used as bait to screen a human brain cDNA library by yeast two-hybrid methodology.

B. Two clones representing portions of the coding sequence of RACK1 have been identified as interacting partners of NHE6: clone #1 spans the length of the protein between amino acids S63 and R317, and clone #2 between amino acids V69 and R317.

resultant chimeric protein was used as bait to screen 3.5 x 10^6 clones of a human brain cDNA library (Fig 3.1A). To identify positive clones, transformants were subjected to selection under high stringency conditions, including both growth selection on media lacking essential amino acids (SD/-Ade/-His/-Leu/-Trp) and color-selection using a β-galactosidase filter assay. Growth- and β-galactosidase double positive clones were extracted from yeast and transformed into *E. coli* DH5α cells. A total of 283 positive clones were isolated, sequenced, and identified using the BLAST search program.

Two independent clones encoding portions of RACK1 located in the coding region and spanning almost the entire protein were identified in this screen (Fig 3.1B). RACK1 is a 317-amino acid scaffolding protein, which has been implicated in numerous cellular functions due to its ability to interact with a variety of proteins (McCahill et al., 2002). One of the RACK1 clones identified in our screen spans amino acids Ser63 to Arg317, while the second clone starts at Val69 and spans the rest of the coding region (Fig. 3.1B).

NHE6 and RACK1 interact *in vitro*

To confirm the interaction between RACK1 and NHE6, we performed *in vitro* protein-binding pull-down studies. A purified GST (glutathione-S-transferase) fusion protein containing the C-terminal tail of NHE6 (amino acids 499-669) was incubated with ^{35}S-labeled RACK1 synthesized *in vitro* using rabbit reticulocyte lysates. Protein complexes were separated by SDS-PAGE and RACK1 bound to NHE6 was detected by western blotting with anti-RACK1 antibody. As shown in Figure 3.2A, a specific band representing RACK1 bound to the NHE6-C terminus was obtained. To further confirm this result, purified GST alone or a GST fusion protein containing the C-terminal tail of NHE6 were incubated with Chinese hamster ovary (CHO) cell lysates and the isolated GST protein complexes were analyzed for the presence of endogenous RACK1 by

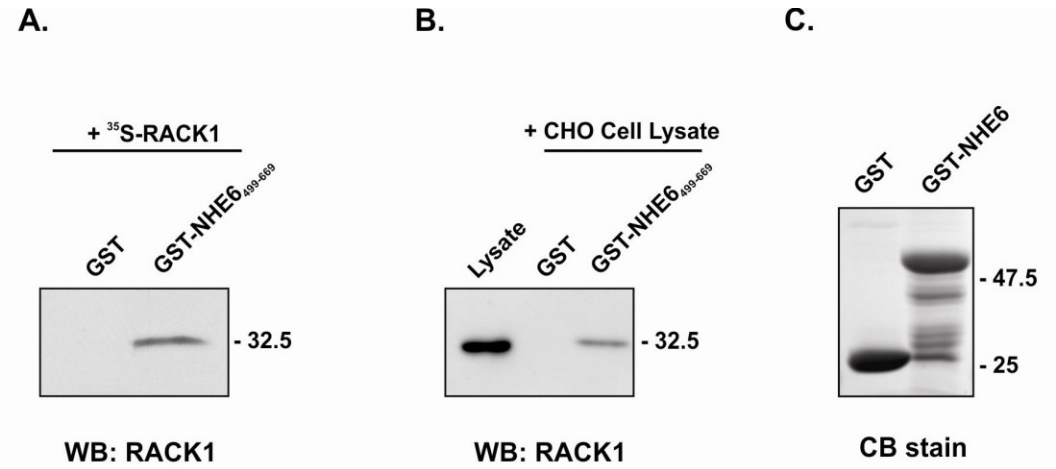

Figure 3.2. RACK1 binds to NHE6 C-terminus *in vitro*.

A. *In vitro* binding assay. GST (as negative control) or a purified GST fusion protein containing the C-terminus of NHE6 (499-669) bound to glutathione-Sepharose™ beads were incubated with ^{35}S-labeled RACK1 protein synthesized *in vitro* in rabbit reticulocyte lysates using a transcription-translation coupling reaction in the presence of [^{35}S]methionine. Proteins were separated by SDS-PAGE, and transferred to polyvinylidene fluoride membranes which were immunoblotted with an anti-RACK1 antibody.

B. Glutathione S-Transferase (GST) pull-down assay. GST (as negative control) or a purified GST fusion protein containing the C-terminus of NHE6 (499-669) bound to glutathione-Sepharose™ beads were incubated with CHO cell lysates, subjected to SDS-PAGE and immunoblotted with a monoclonal anti-RACK1 antibody. Input represents 2% of total lysate incubated with the GST constructs.

C. To verify the expression of the GST constructs, a parallel gel was stained with Coomassie Blue (CB) dye.

immunoblotting. As shown in Figure 3.2B, RACK1 was able to bind to the GST-NHE6 construct, but did not bind to GST alone. These data confirm our yeast two-hybrid screen results; namely that RACK1 can bind directly to the C-terminal domain of NHE6.

NHE6 and RACK1 form a complex in mammalian cells

In order to verify if full-length NHE6 associates with RACK1 in living cells, CHO cells were transiently transfected with either empty vector (pCMV) or full-length $NHE6_{HA}$ and $_{myc}$RACK1. Cell lysates were obtained 30 h post-transfection and incubated with either an anti-myc antibody to immunoprecipitate $_{myc}$RACK1 or an anti-HA antibody to precipitate $NHE6_{HA}$. Aliquots of the initial lysates and the immunoprecipitates were analyzed by SDS-PAGE and Western blotting. As shown in Fig. 3.3A, each of the lysates expressed similar amounts of $_{myc}$RACK1, as well as similar amounts of $NHE6_{HA}$, which migrated as two bands, namely a slower migrating band representing the fully glycosylated form and a faster migrating band, which represents the core-glycosylated form of the protein. When lysates were immunoprecipitated with the anti-myc antibody, $NHE6_{HA}$ was detected in the complex by immunoblotting with an anti-HA antibody, as shown in Fig. 3.3B (*upper panel*). In Fig. 3.3B it seems like RACK1 interacts mainly with the core-glycosylated form of NHE6. However, in the cell lysates shown in Fig. 3.3A, NHE6 is present mostly in the core-glycosylated form as well, because the cells were lysed twenty-four hours post-transfection, which was insufficient for the complete maturation of NHE6.

In the reciprocal experiment, when the immunoprecipitation was done in the presence of the anti-HA antibody, $_{myc}$RACK1 was found to be present in the same complex with NHE6, as shown by western blotting with an anti-myc antibody (Fig. 3.3B*, lower panel*).

To further confirm the interaction between NHE6 and RACK1 in intact cells and to address the concern that the binding might be due to

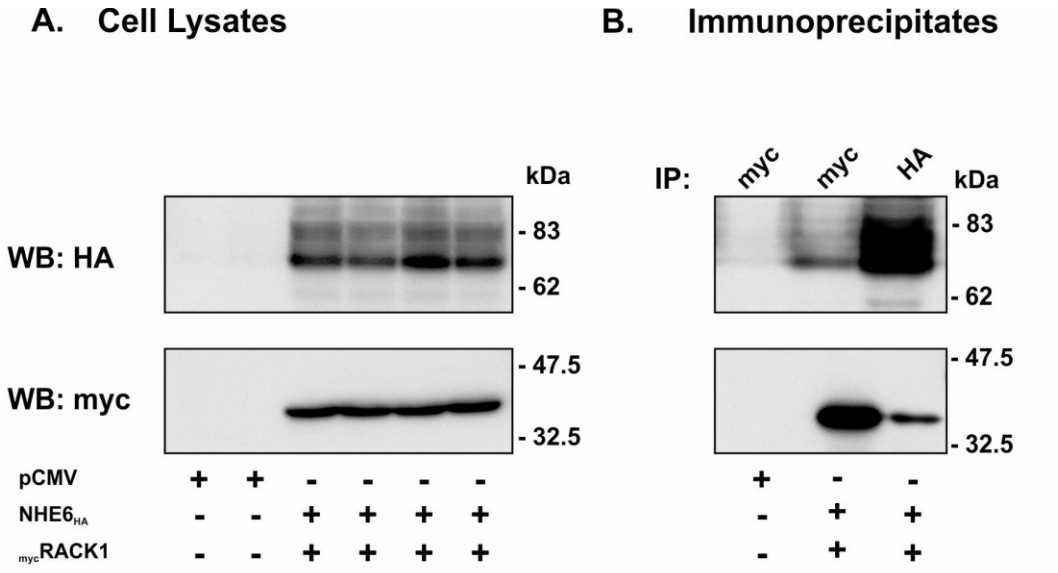

Figure 3.3. NHE6 and RACK1 form a complex in transfected CHO cells.

CHO cells were transfected with $NHE6_{HA}$ and $_{myc}$RACK1, or empty vector (pCMV), and lysed 30 hours post-transfection. Cell lysates were pre-cleared for 1 hour on Protein G-Sepharose beads™ , followed by immunoprecipitation for 4 hours at 4°C with anti-myc or anti-HA rabbit polyclonal antibodies. Subsequently, a 50% slurry of Protein G-Sepharose beads was added and incubated with the immunoprecipitates overnight. Next day, aliquots of the initial lysates (*panel A*) as well the immunoprecipitated proteins (*panel B*) were resolved by SDS-PAGE, transferred to polyvinylidene fluoride membranes, and immunoblotted with the indicated mouse monoclonal antibodies.

the overexpression of $_{myc}$RACK1, we performed co-immunoprecipitation experiments of $NHE6_{HA}$ with endogenous RACK1 in HEK293 cells transiently or stably expressing $NHE6_{HA}$. It was not possible to perform these experiments with endogenous NHE6 due to its very low expression level in these cells, which was not detectable in cell lysates by immunoblotting with our endogenous anti-NHE6 antibody.

Lysates of HEK293 cells transiently expressing $NHE6_{HA}$ were incubated overnight with isotype control IgG antibody or with anti-HA antibody. Endogenous RACK1 could be detected only in the immunoprecipitates obtained with the anti-HA antibody (upper panel of Figure 3.4A). Both $NHE6_{HA}$ and RACK1 were expressed at similar levels in all the samples, as shown in the lower panels of Figure 3.4A. Similar results were obtained in HEK293 cells stably expressing $NHE6_{HA}$; *i.e.* RACK1 was co-immunoprecipitated with $NHE6_{HA}$ specifically by the anti-HA or anti-NHE6 antibodies, but not by the isotype specific IgG control antibody (Fig. 3.4B).

To further demonstrate the association between native NHE6 and RACK1, the subcellular distribution of the proteins was verified by immunofluorescence confocal microscopy in SH-SY5Y human neuroblastoma cells. This cell line was chosen because we showed previously (Fig. 1.4) that we could detect native NHE6 in these cells by immunofluorescence microscopy using our polyclonal anti-NHE6 antibody. Cells cultured on fibronectin-coated glass cover slips were fixed and dual immunolabelled with antibodies recognizing endogenous NHE6 and RACK1, followed by red Alexa Fluor® 568 and green Alexa Fluor® 488-conjugated secondary antibodies, respectively. As shown in Figure 3.5, RACK1 and NHE6 partially colocalize in SH-SY5Y cells, which was expected considering that RACK1 has numerous other interacting partners.

Collectively, the biochemical data and the confocal microscopy data confirmed that NHE6 and RACK1 are able to interact in living cells.

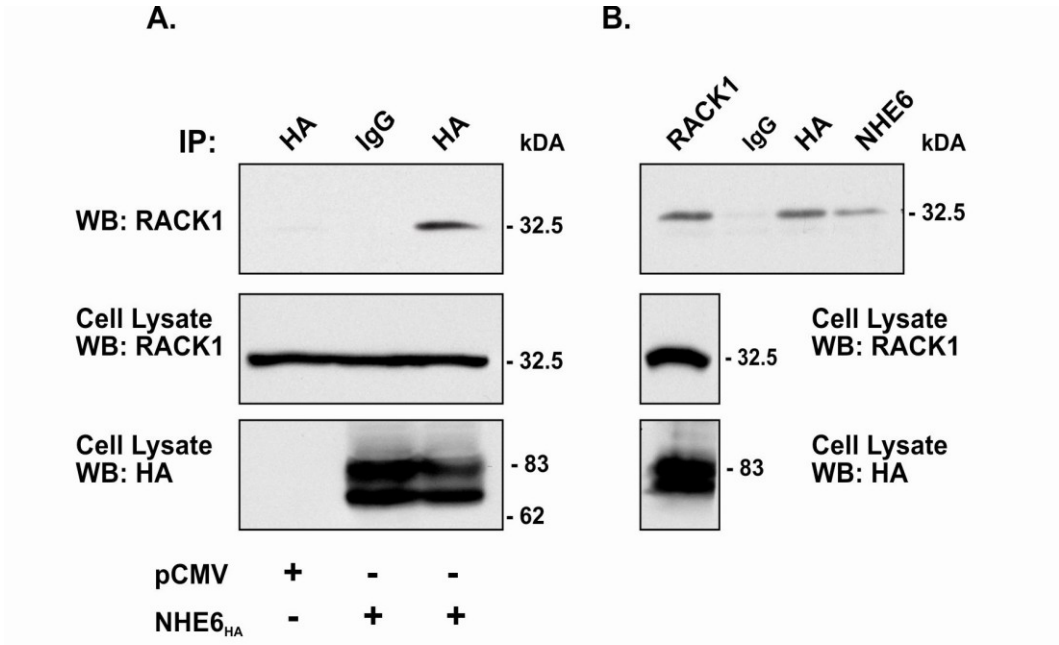

Figure 3.4. $NHE6_{HA}$ interacts with endogenous RACK1 in HEK293 cells transiently (*panel A*) or stably (*panel B*) expressing $NHE6_{HA}$.

A. HEK293 cells transiently transfected with pCMV or $NHE6_{HA}$ were lysed 30 hours post-transfection and pre-cleared for 1 hour on Protein A agarose beads. Lysates were subjected to immunoprecipitation overnight at 4°C with anti-IgG (as negative control) or anti-HA polyclonal antibodies. Next day, a 50% slurry of Protein A agarose beads was added and incubated with the immunoprecipitates for 3 hours. Subsequently, the beads were washed and the proteins eluted in Laemmli buffer, then resolved by SDS-PAGE, and detected by immunoblotting with the indicated monoclonal antibodies.

B. HEK293 cells stably expressing $NHE6_{HA}$ were lysed and pre-cleared for 1.5 hours on Protein G-Sepharose beads. Lysates were subjected to immunoprecipitation overnight at 4°C with the indicated polyclonal antibodies (RACK1, control IgG, HA, and NHE6, respectively). Next day, a 50% slurry of Protein G-Sepharose beads was added and incubated with the immunoprecipitates for 3 hours. Subsequently, the beads were washed and the proteins eluted in Laemmli buffer, then separated by SDS-PAGE, and analyzed by immunoblotting with the indicated monoclonal antibodies.

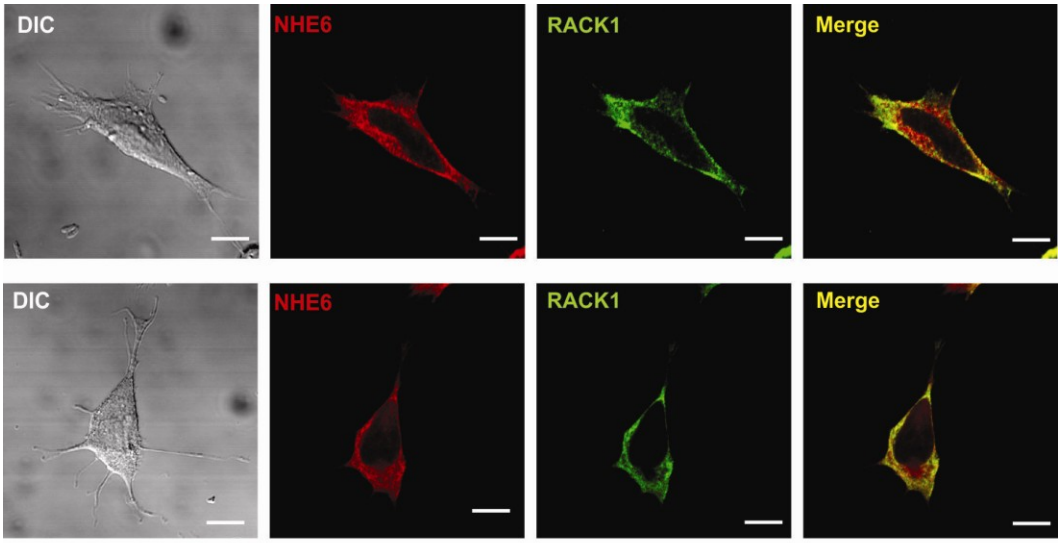

Figure 3.5. Endogenous NHE6 and RACK1 partially colocalize in SH-SY5Y human neuroblastoma cells.

SH-SY5Y neuroblastoma cells were grown on fibronectin-coated cover slips, fixed in 2% paraformaldehyde/PBS, permeabilized, then labeled with rabbit polyclonal anti-NHE6 and mouse monoclonal anti-RACK1 antibodies, followed by anti-rabbit Alexa568 and anti-mouse Alexa488-conjugated secondary antibodies. Cells were mounted on glass slides and imaged with a confocal Zeiss LSM510 Meta microscope. The scale bar in the panels represents 10 μM.

Mapping of the RACK1-binding domain of NHE6

In order to delineate the binding region for RACK1 within the C-terminus of NHE6, protein binding pull-down assays were performed. GST fusion proteins containing the full-length (amino acids 488-669) or different fragments spanning the entire C-terminus of NHE6 were produced in *E. coli* and extracted from the bacterial lysates using glutathione-Sepharose™ beads. The beads were incubated with CHO cell lysates, bound proteins were separated by SDS-PAGE, and endogenous RACK1 bound to the NHE6 tail fragments was detected by immunoblotting with an anti-RACK1 antibody. As shown in Figure 3.6 (*upper panel*), RACK1 was found to bind only to the full-length C-tail (amino acids 499-669) and to the fragment containing amino acids 520-565 of NHE6. From this assay, we could conclude that the RACK1 binding site is restricted to ~45 amino acids that are located close to the juxtamembrane region of the cytoplasmic C-terminus of NHE6.

Mapping of the NHE6-binding region of RACK1

RACK1 is a well-known scaffolding protein that interacts with a wide variety of different proteins implicated in an array of cellular functions (McCahill et al., 2002). It consists of seven Trp-Asp (WD) domain repeats, which form a seven-bladed propeller structure (McCahill et al., 2002; Coyle et al., 2009) and offers numerous binding sites for its interacting partners (Fig. 3.7A). To determine the WD domain(s) of RACK1 involved in binding to NHE6, we constructed GST-fusion proteins expressing either the full-length RACK1 or each of the seven WD repeats separately. After purification from *E. coli* bacterial lysates and binding to glutathione-Sepharose™ beads, these GST-fusion proteins were incubated with HEK293 cell lysates stably expressing $NHE6_{HA}$. $NHE6_{HA}$ bound to RACK1 was identified by immunoblotting with an anti-HA antibody. The results from this pull-down assay show that NHE6 can bind to multiple sites in

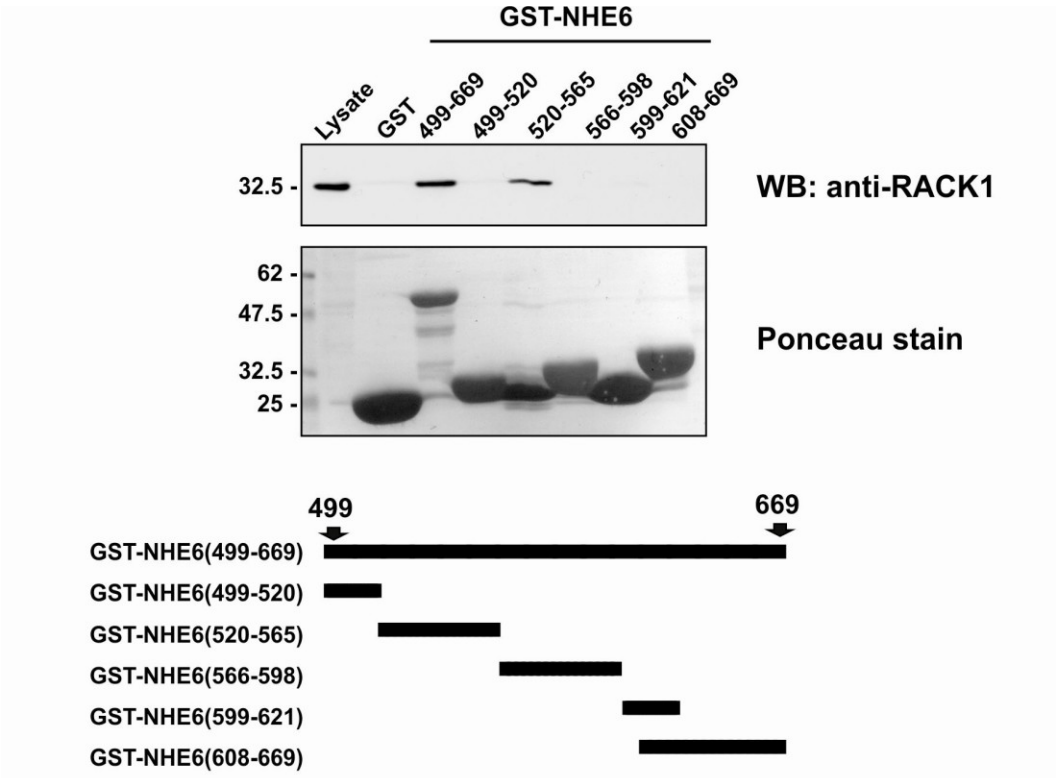

Figure 3.6. Mapping of the RACK1-binding region in NHE6.

Protein binding pulldown assays were used to identify the binding region for RACK1 within the C-terminus of NHE6. GST fusion proteins containing the full-length (amino acids 499-669) or different fragments of the C-terminus of NHE6 were produced in *E.coli* and extracted from the bacterial lysates using glutathione-Sepharose™ beads. The beads were incubated with CHO cell lysates, bound proteins were separated by SDS-PAGE, transferred to polyvinylidene fluoride membranes, and RACK1 was detected by immunoblotting with an anti-RACK1 antibody (*upper panel*). To verify the expression of the GST fusion proteins, the membrane was stained with Ponceau red after blotting (*lower panel*).

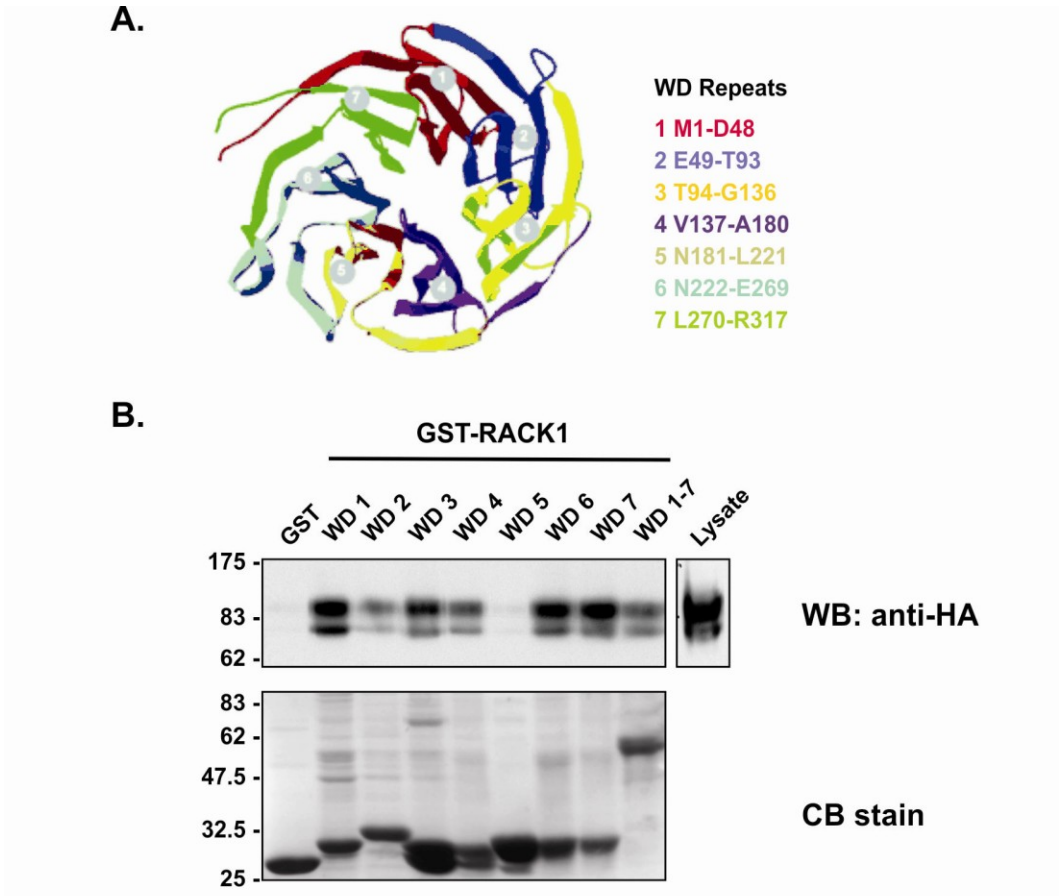

Figure 3.7. Mapping of the NHE6-binding domain of RACK1.

A. RACK1 model showing the seven WD repeats that form a seven-bladed propeller structure (from McCahill *et al.*, 2002).

B. Protein binding pulldown assays were used to identify the domains of RACK1 that NHE6 binds to. GST fusion proteins containing the separate WD domains of RACK1 or the full-length RACK1 were generated in *E.coli* and purified from the bacterial lysates using glutathione-Sepharose™ beads. The beads were incubated with HEK293 cell lysates stably expressing $NHE6_{HA}$, bound proteins were separated by SDS-PAGE, transferred to a polyvinylidene fluoride membrane, and NHE6 was detected by immunoblotting with an anti-HA antibody (*upper panel*). To verify the expression of the RACK1-GST fusion proteins, a parallel gel was stained with Coomassie Blue (*lower panel*).

RACK1, including WD domains 1, 2, 3, 4, 6, and 7, but not WD5 (Fig. 3.7B).

RACK1 regulates NHE6 expression and cell surface abundance

Having confirmed that NHE6 and RACK1 form a complex in cells, we next sought to decipher the functional significance of this interaction. As RACK1 was already shown to regulate the trafficking to the cell surface of specific G protein-coupled receptors (Parent et al., 2008), we hypothesized that RACK1 is important for trafficking of NHE6. To test this hypothesis, we used a fluorescence-based antibody-cell surface binding and internalization assay. HEK-GRIP cells were transfected with either RACK1 siRNA or scrambled RACK1 siRNA as a control, followed by transient transfection with $_{3Flag}NHE6_{HA}$. The efficiency of RACK1 knock down in our system was approximately 40% (Figs. 3.8A, 3.8B). Surface NHE6 was labelled on ice with anti-Flag antibody, followed by internalization of the Flag-labelled surface NHE6 in cell culture medium at 37ºC for increasing periods of time (0, 5, 10, and 15 minutes). Remnant cell surface $_{3Flag}NHE6_{HA}$ protein was detected using a goat anti-mouse HRP-conjugated secondary antibody and the fluorescent substrate Amplex® Red (Invitrogen). Interestingly, the total level of $_{3Flag}NHE6_{HA}$ was elevated in the presence of RACK1 siRNA, as shown by immunoblotting with anti-HA antibody (Fig. 3.8A). Furthermore, the abundance of NHE6 on the cell surface is significantly increased (more than double) when RACK1 level is diminished by siRNA (Fig. 3.8C). However, the internalization kinetics of NHE6 is not changed after depletion of RACK1 by siRNA (Figure 3.8D), suggesting that RACK1 is not involved in the regulation of NHE6 endocytosis.

To further validate these observations by an alternative approach, we measured the levels of NHE6 present at the plasma membrane following perturbation of RACK1 expression using cell surface biotinylation. To this end, HEK-GRIP cells were transfected with RACK1

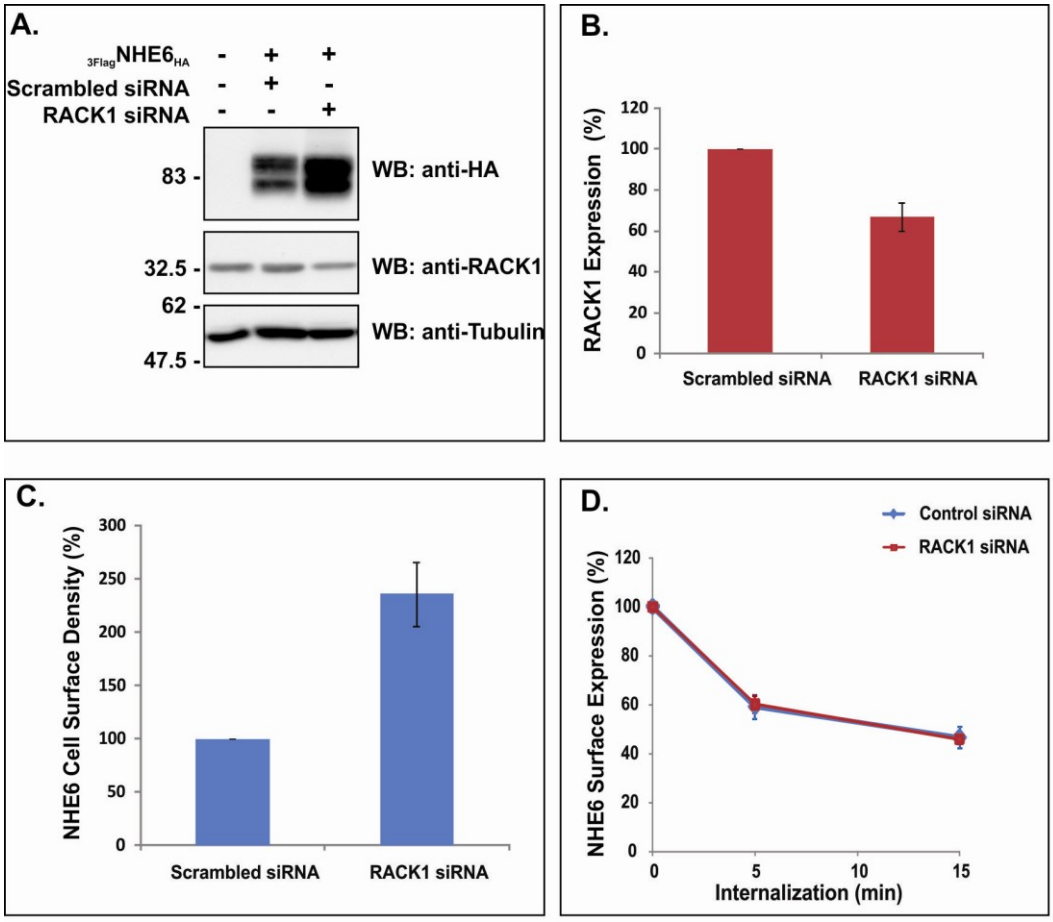

Figure 3.8. RACK1 knock-down increases cells surface expression of NHE6 but does not affect its internalization kinetics in HEK-GRIP cells.

A. Representative Western Blot showing expression of $_{3Flag}NHE6_{HA}$ and of endogenous RACK1 after treatment of HEK-GRIP cells with scrambled or RACK1 siRNA for 72 hours. Tubulin was used as a loading control.

B. RACK1 abundance in the presence of scrambled or targeting siRNA was quantified by densitometry in all five experiments and normalized to the level of tubulin present in each sample.

C. Cell surface density of NHE6 in the presence of RACK1 siRNA was measured using a cell-based enzyme-linked immunosorbent assay (ELISA) and expressed as percentage of surface NHE6 in the presence of a scrambled siRNA and normalized for total cellular protein.

D. Kinetics of NHE6 endocytosis measured in HEK-GRIP cells expressing $_{3Flag}NHE6_{HA}$ in the presence of RACK1 siRNA, using a cell-based enzyme-linked immunosorbent assay (ELISA). Data points represent mean ± SEM of five different experiments, each done in triplicate.

siRNA or a scrambled siRNA, as well as with $_{3Flag}NHE6_{HA}$. Cells were then subjected to cell surface biotinylation on ice and plasma membrane proteins were recovered on NeutrAvidin® Agarose beads. Samples of the total lysate and the fraction representing cell surface proteins were resolved by SDS-PAGE. Equal amounts of proteins were loaded onto the gels, as shown by immunoblotting with an anti-tubulin antibody (Fig. 3.9A). Surface and total NHE6 levels were detected by western blotting with an anti-HA antibody. As shown in Fig. 3.9A, total and cell surface amounts of NHE6 were significantly elevated in the presence of RACK1 siRNA. To get a quantitative measure of this increase, western blots from four different experiments were analyzed by densitometry using ImageJ. Although RACK1 expression was suppressed only by approximately 40%, cell surface level of NHE6 was increased almost 100%, whereas total amount was elevated by ~60% (Fig. 3.9B).

In order to assess that the aforementioned results are not influenced by the triple Flag epitope that is present in the first extracellular loop of $_{3Flag}NHE6_{HA}$ and to verify if the increased levels of NHE6 caused by RACK1 depletion are cell-type specific, we repeated the biotinylation assay in AP-1 cells stably expressing $NHE6_{HA}$, which contains a single HA-epitope at its C-terminus. Given that RACK1 is highly conserved among species, it was expected that the anti-human RACK1 siRNA would efficiently deplete RACK1 in hamster AP-1 cells as well. Indeed, in the presence of anti-human RACK1 siRNA, approximately 60% of RACK1 knock-down was observed in AP-1 cells stably expressing $NHE6_{HA}$ (Figs. 3.9C,D). The data obtained are very similar to those described in HEK-GRIP cells transiently expressing $_{3Flag}NHE6_{HA}$, i.e. depletion of RACK1 resulted in elevated levels of both total and surface NHE6 (Figs. 3.9C,D).

Collectively, these data suggests that RACK1 binding to NHE6 might regulate its transcription/translation and/or stability, and possibly its trafficking to the plasma membrane in at least two different cell types.

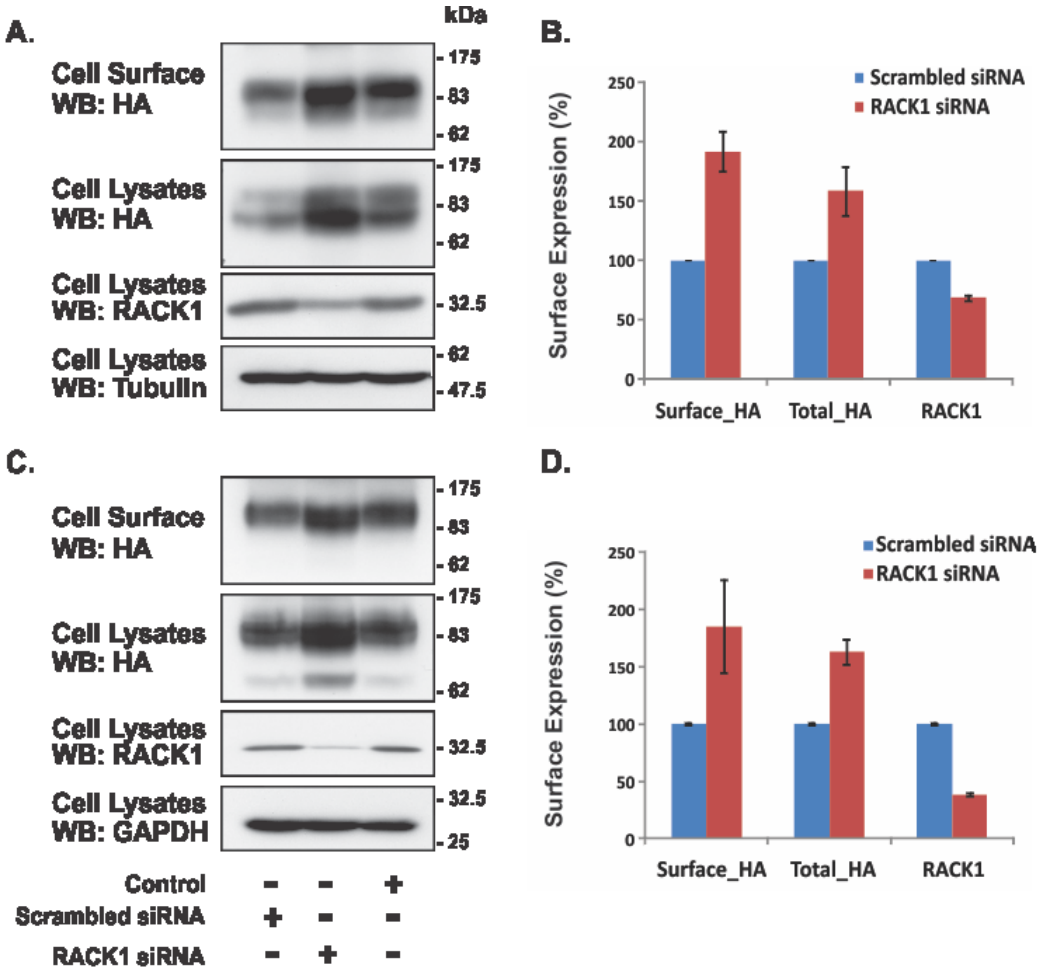

Figure 3.9. RACK1 depletion increases total and cell surface expression of NHE6 in HEK-GRIP cells transiently expressing $_{3Flag}$NHE6$_{HA}$ (A-B) and in AP-1 cells stably expressing NHE6$_{HA}$ (C-D).

HEK-GRIP cells (**A**) or AP-1 cells stably expressing NHE6$_{HA}$ (**C**) were transfected with RACK1 siRNA, a scrambled siRNA, or left un-transfected (Control). Next day, the HEK-GRIP cells were transfected with $_{3Flag}$NHE6-v1$_{HA}$. Forty eight hours later, the cells were subjected to cell surface biotinylation, lysed, and equal amounts of proteins were loaded onto NeutrAvidin® Agarose beads overnight. Next day, the beads were washed to remove unbound proteins, proteins were eluted in Laemmli buffer and separated by SDS-PAGE. Surface NHE6, as well as total NHE6 were detected by immunoblotting with a monoclonal anti-HA antibody. The level of RACK1 knock-down was assessed by immunoblotting with a monoclonal anti-RACK1 antibody. Equal amounts of proteins were loaded onto the gels, as shown by immunoblotting with a monoclonal anti-tubulin antibody.

Quantification by film densitometry of surface and total NHE6, as well as RACK1 level in HEK-GRIP cells (**B**) and AP-1 cells (**D**). Data are shown as mean ± SEM of four different experiments.

To determine if the increased amount of NHE6 observed in the presence of RACK1 siRNA is due to an increased stability of NHE6, HEK-GRIP cells were transfected with RACK1 siRNA or a scrambled siRNA, in combination with $_{3Flag}NHE6_{HA}$. Cells were then subjected to cycloheximide treatment (150 µg/ml) over a 24 h period to stop new protein synthesis. Cell lysates were obtained and equal amounts of proteins were separated by SDS-PAGE, as shown by immunoblotting with an anti-β-tubulin antibody. $_{3Flag}NHE6_{HA}$ and endogenous RACK1 were detected by immunoblotting with anti-HA and anti-RACK1 antibodies, respectively. As shown in Figure 3.10A, the amount of NHE6 is increased in the presence of RACK1 siRNA both before the application of cycloheximide (0 time point) and after 24 h of treatment with cycloheximide. However, the proportion of NHE6 lost due to the cycloheximide treatment is similar in the cells treated with scrambled siRNA and RACK1 siRNA (Fig. 3.10B), suggesting that RACK1 is not implicated in the regulation of NHE6 stability.

DISCUSSION

The mammalian alkali cation/proton exchanger NHE6 is widely expressed and localizes mainly to a recycling endosomal compartment (Brett et al., 2002; Nakamura et al., 2005), but a small fraction can traffic to the cell surface (Fig. 1.2). However, virtually nothing is known about the mechanisms that regulate NHE6 trafficking and function. In this study, we have identified RACK1 as an interacting partner for NHE6 by yeast two-hybrid screening of a human brain cDNA library. This interaction was confirmed by *in vitro* studies using GST fusion protein binding pull-down assays and by co-immunoprecipitation experiments of cell lysates. This association was further corroborated by dual-immunolabeling confocal microscopy of endogenous NHE6 and RACK1 in human neuroblastoma

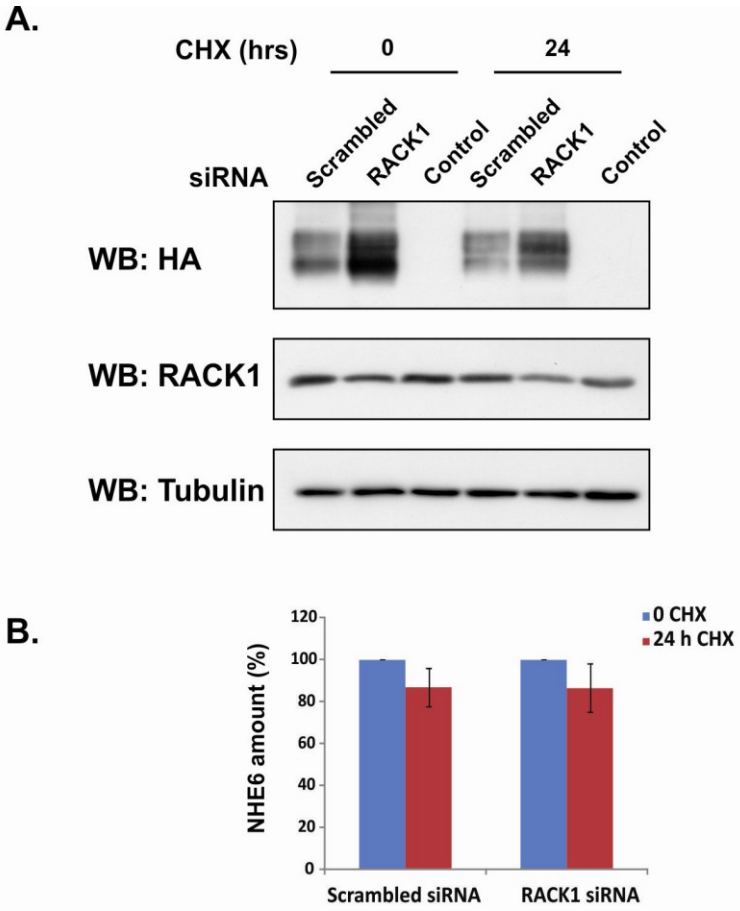

Figure 3.10. RACK1 knock-down has no effect on the stability of NHE6.

A. HEK-GRIP cells were transfected with RACK1 siRNA, a scrambled si RNA, or left un-transfected. After 24 hours, the cells were transfected with $_{3Flag}NHE6_{HA}$ and after 48 hours, subjected to cycloheximide treatment (150 µg/ml) for 24 hours to stop new protein synthesis. Cells were lysed and equal amounts of proteins were separated by SDS-PAGE. NHE6 was detected by immunoblotting with a monoclonal anti-HA antibody. The level of RACK1 knock-down was assessed by immunoblotting with a monoclonal anti-RACK1 antibody, and equal protein loading was verified with a monoclonal anti-ß-tubulin antibody.

B. Quantification of $_{3Flag}NHE6_{HA}$ levels after 24 hours of cycloheximide treatment. The amount at the 0 time point was normalized to 100% for each scrambled and RACK1 siRNA-treated samples. Data represent mean ± SEM of three different experiments.

cells. Collectively, these data indicated that RACK1 interacts directly with the C-terminal region of NHE6 in mammalian cells.

Mapping of the RACK1-binding region of NHE6 by GST pull-down assays revealed that the binding region encompasses amino acids 520-565 of the C-terminal region of NHE6. Interestingly, RACK1 has also been found to interact with other NHE isoforms, including the brain-enriched NHE5 (Onishi et al., 2007), NHE7 and NHE9 (Ohgaki et al., 2008). NHE5 binds to RACK1 directly in focal adhesions and activates its transport activity via integrin-dependent and independent pathways when stably overexpressed in AP-1 cells (Onishi et al., 2007). With respect to NHE9, the site of interaction with RACK1 was mapped to amino acids 528-577 of NHE9 (Ohgaki et al., 2008). This region is highly homologous to the corresponding region in NHE6 (*i.e.*, amino acids 537 to 588) which overlaps the site delineated in our study. Furthermore, we show that NHE6 can bind to multiple WD domains of RACK1, with the exception of WD5, which was previously shown to be the binding site for integrin-β (Liliental and Chang, 1998).

RACK1 is a multi-functional protein first cloned in 1989 from both a chicken liver cDNA library and a B-lymphoblastoid cell line (Guillemot et al., 1989). The name RACK1 was given to the protein to describe its function as an intracellular receptor for activated protein kinase C (Mochly-Rosen et al., 1991; Ron et al., 1994).

RACK1 is a 36-kDa scaffolding protein that belongs to the tryptophan-aspartate (WD) superfamily, containing seven internal Trp-Asp 40 (WD40) repeats, which are predicted to form a seven-blade propeller structure, with each blade made up of β-sheets (Steele et al., 2001). This predicted structure was confirmed by Coyle et al., (2009), who solved the crystal structure at 2.1-Å of the yeast orthologue of RACK1 (Ascp1). RACK1 shows a high degree of homology and 42% identity with the β subunit of G-proteins (McCahill et al., 2002).

RACK1 has since been shown to interact with numerous other proteins, including Src kinase (Chang et al., 1998), the integrin β receptor (Liliental and Chang, 1998), the NMDA receptor (Yaka et al., 2002), and many others (Sklan et al., 2006), thus integrating signals from different pathways.

RACK1 was previously shown to stimulate the export to the cell surface of membrane proteins, such as specific G-protein coupled receptors (GPCRs), including the thromboxane A2 receptor, the angiotensin II type I receptor, and CXCR4 (Parent et al., 2008). When RACK1 was knocked down in cells using siRNA, these receptors were retained in the endoplasmic reticulum. Interestingly, RACK1 depletion had no effect on the trafficking to the plasma membrane of other GPCRs, including the β2-adrenergic receptor and the prostaglandin D2 receptor (Parent et al., 2008). To determine if RACK1 regulates the trafficking to the plasma membrane of NHE6, we investigated the effects of RACK1 depletion upon cell surface expression of the exchanger. Our data show significantly elevated levels of NHE6 on the cell surface when endogenous RACK1 was depleted, suggesting that RACK1 might be involved in the retention of NHE6 to intracellular compartments. Interestingly, the total cellular amount of NHE6 was also markedly elevated, suggesting that RACK1 might regulate the stability of NHE6. Indeed, RACK1 has been previously shown to promote the proteasomal-dependent degradation of several interacting partners, notably the hypoxia-inducible factor 1 (HIF-1) (Liu and Semenza, 2007) and the C-type lectin-like receptor CLEC-2 which plays important roles in platelet activation (Ruan et al., 2009). However, under our experimental conditions involving the use of cycloheximide, the stability of NHE6 was not markedly affected following depletion of endogenous RACK1 by siRNA, suggesting that RACK1 is not a significant factor in regulating the stability of NHE6.

Alternatively, knockdown of RACK1 might stimulate the biosynthesis of NHE6 by an indirect mechanism. This hypothesis would

be compatible with other known actions of RACK1. Studies in eukaryotes have demonstrated that RACK1 is a highly conserved core 40S ribosomal protein (the 33rd ribosomal protein of the eukaryotic 40S subunit) (Ceci et al., 2003; Gerbasi et al., 2004) and, by cryo-EM analysis, is located close to the mRNA exit channel (Sengupta et al., 2004). In the yeast *Saccharomyces cerevisiae*, genetic ablation of the RACK1 ortholog Asc1p (52% sequence identity to human RACK1) significantly upregulates the abundance of a small subset of proteins (only 27 out of 1500 proteins) (Gerbasi et al., 2004), suggesting that Asc1p/RACK1 might act as a selective translational repressor. Although we cannot exclude an indirect effect of RACK1 siRNA knock-down upon the abundance of NHE6 transcript levels, our data are more readily explained by RACK1 regulation of NHE6 translation. Speculatively, certain physiological states that require a down-regulation of NHE6 could lead to the recruitment to ribosome-associated RACK1 of specific translational repressors that could decrease translation of NHE6.

Considering the fact that RACK1 is present in two separate pools in cells, *i.e.* one ribosome-associated, and one cytosolic (Ceci et al., 2003), Coyle et al. (2009) showed that RACK1 can perform both ribosome localization-dependent and -independent functions in yeast. This observation comes to support our results, which suggest that RACK1 is involved in regulating both expression and trafficking of NHE6.

We also have to mention that our data contradict the results of Ohgaki et al. (2008), which show that depletion of RACK1 in HeLa cells decreased the cell surface levels of NHE6, but have no effect on the total amount of NHE6. Although these differences are difficult to reconcile, they might be explained by the different cell types used. In our experiments, we used both HEK-GRIP and AP-1 cells, and our results are consistent in both cell lines. In addition, we can exclude non-specific effects exerted by our RACK1 siRNA pool, as levels of house-keeping genes, like tubulin and GAPDH are not affected by depletion of endogenous RACK1. On the

other hand, Ohgaki et al. (2008) were able to detect native NHE6 with a specific polyclonal anti-NHE6 antibody. Although HeLa cells and HEK293 cells express similar levels of NHE6 mRNA (Nakamura et al., 2005), we were not able to detect endogenous NHE6 using our polyclonal anti-NHE6 antibody in HEK cells, so our experiments were done with HA-tagged NHE6.

In conclusion, in the present study we have identified RACK1 as an interacting partner of NHE6 and showed that RACK1 is involved in the regulation of expression and cell surface abundance of NHE6.

CHAPTER 4

Angelman Syndrome-Linked Mutations in the Alkali Cation/Proton Exchanger NHE6 Disrupt its Maturation, Stability, and Trafficking.

Alina Ilie, Hervé Barriere, Emily Deane, Annie Boucher, Rebecca Anne McKinney, Gergely Lukacs and John Orlowski

In the previous chapters we described the native distribution of NHE6 in neuronal cells and identified N-glycosylation and the interaction with RACK1 as important regulatory factors for the expression, trafficking, and function of the exchanger. To gain further insight into the physiological roles of NHE6, in this chapter we investigate the mechanisms responsible for the Angelman syndrome-like phenotype caused by a 6 base-pair deletion that results in the loss of amino acids E287 and S288 in transmembrane domain seven of the exchanger.

ABSTRACT

Mutations in the mammalian Na^+/H^+ exchanger NHE6 have been recently shown to cause X-linked mental retardation, microcephaly, epilepsy, and ataxia; a phenotype mimicking Angelman syndrome. A number of mutations in NHE6 have been identified in different families, including a 6 base-pair deletion that results in the loss of amino acids E287 and S288 in transmembrane domain seven. However, the consequences of this mutation on transporter function are unknown. To better understand the nature of this defect, the disease-causing mutation (ΔES) as well as single (E287Q, E287A and S288A) and double (E287Q-S288A) amino acid substitutions were engineered in a HA-epitope tagged form of the NHE6-v1 splice-variant, and the effects on its biosynthesis, post-translational maturation, membrane trafficking and function were assessed. In transfected Chinese hamster ovary AP-1 cells, Western blot analyses showed that mutant constructs of E287 displayed decreased abundance and impaired post-translational modification, suggesting that this acidic residue is essential for the correct maturation of the protein. Furthermore, the stability of the protein containing a mutation of E287 is significantly reduced compared to the wild-type. Moreover, the cell surface level and the internalization rate of the ΔES mutant were diminished. The ΔES mutant protein was mislocalized in cells and accumulated predominantly in large endomembrane structures, possible aggregates of vesicles, mostly along the periphery of the cell. These are highly acidic, ill-defined compartments, as they do not express the classical lysosomal marker LAMP-2. Additionally, the cells expressing the double deletion mutant were round and the normal architecture of the actin cytoskeleton was disrupted. The impairment of the clathrin-mediated recycling endosomal pathway, as evidenced by decreased uptake of transferrin and dispersal of the perinuclear recycling compartment in ΔES-expressing cells, in conjunction with the decreased dendritic branching and disappearance of dendritic spines when NHE6 is depleted in neurons,

suggest an important role for NHE6 in normal recycling of vesicles, which is necessary for dendritic spine maintenance and growth.

INTRODUCTION

Angelman syndrome (AS) is a severe neurological disorder, characterized by severe developmental delay with minimal or no use of words, movement or balance disorder, hyperkinetic behavior, epileptic seizures, and a sociable disposition, with frequent bursts of laughter (Clayton-Smith and Laan, 2003). Different underlying genetic mechanisms for this disease have been uncovered, including a deletion or rearrangement of chromosome 15 at locus 15q11-q13 (60-75% of patients), paternal uniparental disomy (2-5% of cases), mutations in the imprinting center (2-5%), or mutations in the ubiquitin ligase UBE3A gene in 10% of affected individuals (Lalande and Calciano, 2007; Van Buggenhout and Fryns, 2009). So far, the genetic defect remained elusive for 5-26% of patients showing a typical Angelman syndrome phenotype (Van Buggenhout G. and Fryns, 2009). One important insight into the underlying genetic defect in these patients was contributed by the discovery of mutations in the mammalian sodium-proton exchanger NHE6 in patients with Angelman-like phenotype, which have normal UBE3A and lack any of the other mutations typically found in patients with AS (Gilfillan et al., 2008).

NHE6 is a member of the organellar-type subfamily of the alkali cation/proton exchanger family, more commonly termed sodium/proton exchangers (NHEs). NHEs are transmembrane proteins essential for the regulation of intracellular pH and volume homeostasis and display various tissue distribution and subcellular localization (Orlowski and Grinstein, 2007).

NHE6 shows ubiquitous tissue distribution, but the highest mRNA levels are present in excitable tissues, such as the brain, heart, and skeletal muscle (Numata et al., 1998). At the subcellular level, NHE6 is

distributed in a recycling endosomal compartment, but a small fraction can also reach the plasma membrane (Brett et al., 2002; Miyazaki et al., 2001; Nakamura et al., 2005; Ohgaki et al., 2008). By analogy with its yeast homolog Nhx1 (Bowers et al., 2000; Brett et al., 2005b), human NHE6 is postulated to play significant roles in the biogenesis and pH homeostasis of endocytic vesicles.

Two different splice variants of NHE6 have been described so far, termed NHE6-v0 (Numata et al., 1998) and NHE6-v1 (Miyazaki et al., 2001). We identified both isoforms in a human brain cDNA library (Clontech) in similar proportions, by using PCR with specific NHE6 5' and 3' end-primers.

Different mutations (*i.e.,* deletions, premature stop codon, frameshift) in NHE6 in four separate families have been shown to cause X-linked mental retardation, microcephaly, epilepsy, ataxia, lack of speech and a happy disposition; a phenotype that closely mimics Angelman syndrome (Gilfillan et al., 2008). More recently, another mutation in NHE6 has been reported that elicits a subset of the symptoms present in the NHE6-associated Angelman-like syndrome (*i.e.*, mental retardation syndrome, absence of speech, epilepsy, and ataxia), but is distinguished by the additional manifestation of autistic behavior as well as neuronal and glial deposition of the microtubule-binding protein tau in cortical and sub-cortical regions (Garbern et al., 2010). This mutation results in the in-frame loss of three amino acids at position 338-340 (Trp-Ser-Thr) in the predicted transmembrane segment nine of NHE6-v0 (amino acids 370-372 in the longer NHE6-v1 splice-variant).

A number of mutations in NHE6 have been identified in different families by Gilfillan et al. (2008), including truncations (R468X, leading to loss of the final transmembrane domain and C-terminus), splice-site mutations (causing skipping of exon 3), frameshift mutations, and a 6 bp deletion, leading to loss of amino-acids E255 and S256 in NHE6-v0 (corresponding to E287 and S288 in NHE6-v1) (Fig. 4.1A). While most of

these mutations will probably lead to a non-functional protein and a null-phenotype in males, the internal deletion mutation ΔE287-S288 is more subtle. Hence, we investigated the molecular mechanisms responsible for the phenotype observed when amino acids E287 and S288 were deleted in NHE6-v1. These amino acids are highly conserved in all NHE isoforms and the corresponding glutamic acid residue is important for ion transport in NHE1 (Fafournoux et al., 1994; Murtazina et al., 2001) and NHE8 (Nakamura et al., 2005). However, so far there are no experimental tools available to accurately measure the ion transport properties of mammalian NHE6. Here we tested the hypothesis that amino acids E287 and S288 are important for the maturation, stability, and trafficking of NHE6-v1.

MATERIALS AND METHODS

Reagents

Mouse monoclonal anti-hemagglutinin (HA) antibody was purchased from Covance Inc. (Berkeley, CA); polyclonal and monoclonal anti-glyceraldehyde-3-phosphate dehydrogenase (GAPDH) antibodies were obtained from Abcam Inc. (Cambridge, MA); mouse monoclonal anti-Flag M2 and rabbit polyclonal anti-Flag antibodies were from Sigma. Mouse monoclonal anti-EEA1 was purchased from BD Biosciences Pharmingen (San Diego, CA). Mouse monoclonal anti-LAMP2 antibody developed by B.L. Granger and S. Uthayakumar was obtained from the Developmental Studies Hybridoma Bank, which is maintained by the University of Iowa, Department of Biology, Iowa City, IA 52242.

Horseradish peroxidase-conjugated secondary IgG antibodies, as well as FITC-conjugated goat anti-mouse secondary Fab were purchased from Jackson ImmunoResearch Laboratories (West Grove, PA). All Alexa Flour® conjugated secondary antibodies were purchased from Molecular Probes (Eugene, OR).

Alpha-Minimum essential medium (α-MEM), fetal bovine serum, penicillin/streptomycin, and trypsin-EDTA were purchased from Invitrogen.

All other chemical and reagents were obtained from BioShop Canada (Burlington, ON, Canada), Sigma or Fisher Scientific and were of the highest grade available.

Recombinant DNA Constructs and Mutagenesis

The full length human NHE6-v1 isoform was cloned from a human brain Matchmaker™ cDNA library (Clontech) using PCR methodology and was engineered to contain the influenza virus hemagglutinin (HA) (YPYDVPDYAS) epitope at its extreme C-terminal end. This construct termed $NHE6_{HA}$ (wild-type) was inserted into the *HindIII*/*XbaI* sites of the mammalian expression vector pCDNA3 (Invitrogen). This construct was used as a template to engineer the following mutations by PCR mutagenesis: double deletion of amino acids E287 and S288 (ΔE287/S288), the conservative double substitution E287Q/S288A, and the single mutations E287A, E287Q, and S288A. These amino acids correspond to amino acids E255 and S256 in the NHE6-v0 isoform, which have been described to be mutated in patients affected by a severe X-linked mental retardation syndrome (Gilfillan et al., 2008).

The same template ($NHE6_{HA}$) was also used to introduce a triple Flag (3X DYKDDDDK) epitope in the first extracellular loop. First, PCR was used to engineer a *NotI* restriction site in the first extracellular loop of $NHE6_{HA}$, after M53, followed by the introduction of annealed primers representing the 3xFlag epitope, which generated a construct termed $_{3Flag}NHE6_{HA}$. This construct was further used as a template to introduce the ΔE287/S288, E287Q/S288A, E287Q, and S288A mutations using PCR mutagenesis. All constructs were sequenced to insure that no additional mutations were introduced during the PCR.

GFP- and mCherry (ChFP) -C-terminal-tagged forms of $_{3Flag}$NHE6-v1 wild-type and ΔE287/S288 mutant were constructed by insertion between the *XhoI*/*HindIII* restriction sites of the pAcGFP1-N1 vector (BD Biosciences Clontech, Palo Alto, CA).

Cell Culture and Immunoblot Analysis

Chinese hamster ovary cells devoid of plasma membrane Na^+/H^+ exchange activity (AP-1cells) (Rotin and Grinstein, 1989) and HeLa cells were maintained in α-Minimum Essential Medium (α-MEM) supplemented with 10% fetal bovine serum, penicillin (100 units/ml), streptomycin (100 µg/ml), and 25 mM $NaHCO_3$ (pH 7.4). HEK-GRIP cells were cultured in High Glucose Dulbecco's Modified Eagle Medium (DMEM) supplemented with 10% fetal bovine serum, 3.7 g/l $NaHCO_3$, and 500 µg/ml G418 sulfate. Cells were incubated in a humidified atmosphere of 95% air, 5% CO_2 at 37ºC.

For western blot analysis, AP-1 cells were grown in 10-cm dishes and transiently transfected with 5µg of plasmid DNA encoding $NHE6_{HA}$ wild-type or mutant constructs using Lipofectamine™ (Invitrogen) according to the manufacturer's recommended procedure. Forty eight hours post-transfection, cell lysates were obtained by washing cells twice on ice with ice-cold PBS, followed by scraping in 0.5 ml of lysis buffer containing 1% Triton X-100/PBS supplemented with a tablet of protease inhibitor cocktail (Roche Diagnostics). Lysates were incubated for 30 min on a rocker at 4ºC, and then centrifuged for 20 min at 4°C to pellet the nuclei and cellular debris. Ten to twenty micrograms of protein from the resulting supernatants were eluted in SDS-sample buffer (50 mM Tris-HCl, pH 6.8, 1% SDS, 50 mM dithiothreitol, 10% glycerol, 1% bromophenol blue), and subjected to 9% SDS-PAGE, then transferred to polyvinylidene fluoride (PVDF) membranes (Millipore, Nepean, Ontario, Canada) for Western blotting. The membranes were blocked with 5% non-fat skim milk for 1 hour, then incubated with the specified primary antibodies (mouse monoclonal HA 1:5000, rabbit polyclonal GAPDH 1:5000 or mouse monoclonal GAPDH 1:50000) in PBS containing 0.1% Tween 20, followed by extensive washes and incubation with goat anti-mouse or anti-rabbit-horseradish peroxidase (HRP)-conjugated secondary antibodies for

1 h. Immunoreactive bands were detected using Western Lightning ™ Plus-ECL blotting detection reagents (Perkin Elmer Inc., Waltham, MA).

Cell Surface Biotinylation

AP-1 cells stably expressing $NHE6_{HA}$ wild-type or mutant constructs were cultured in 10-cm dishes to sub-confluence, placed on ice and washed three times with ice-cold PBS containing 1 mM $MgCl_2$ and 0.1 mM $CaCl_2$, pH 8.0 (PBS-CM). Next, cells were incubated at 4°C for 30 min with the membrane-impermeable reagent N-hydroxysulfosuccinimydyl-SS-biotin (0.5 mg/ml) (ThermoScientific, Rockford, IL). Cells were washed and incubated twice in quenching buffer (20 mM glycine in PBS-CM) for 7 minutes each on ice to remove unreacted biotin. After two more washes in PBS-CM, the cells were lysed in PBS buffer containing 1% TritonX-100 and protease inhibitor mixture for 30 min on ice, and then centrifuged at 16,000 x g for 20 min at 4°C to remove insoluble cellular debris. A fraction of the resulting supernatant was removed and this represents the total fraction. The remaining supernatant was incubated with 100 µl of 50% NeutrAvidin® Agarose Resin slurry (Fisher Scientific, Whitby, ON, Canada) in lysis buffer overnight at 4°C to extract biotinylated membrane proteins. The proteins were then resolved by SDS-PAGE and analyzed by western blotting.

Stability of NHE6 Wild-Type and Mutants

To determine the stability of wild-type and mutant NHE6, AP-1 cells were grown in 10-cm dishes and transfected with $NHE6_{HA}$ wild-type or mutant constructs. Sixteen hours post-transfection, the cells were transferred to 6-well plates and further grown for twenty four hours. To inhibit new protein synthesis, cells were treated with cycloheximide (150 µg/ml) in α-MEM supplemented with 10% FBS and penicillin/streptomycin for up to 24 hours. At appropriate time points, cells were lysed, protein concentrations were measured, and equal quantities of protein were

subjected to SDS-PAGE and immunoblotting with a mouse monoclonal anti-HA antibody. The intensity of the bands was quantified by densitometry of X-ray films exposed in the linear range and analyzed with the FC1000 gel imaging system and software (Alpha Innotech, San Leandro, CA).

Fluorescence-based Endocytosis Assay

AP-1 and HEK-GRIP cells were transiently transfected with 5 µg of $_{3Flag}NHE6_{HA}$ wild-type or mutant cDNA constructs. Twenty four hours post-transfection, cells were transferred to 12 well-plates and further grown for 24 hours. Cells were chilled on ice, washed with ice-cold PBS supplemented with 0.1 mM $CaCl_2$ and 1 mM $MgCl_2$ (PBS-CM, pH 7.4), blocked in 10% goat serum/PBS-CM, and then incubated with a mouse monoclonal anti-Flag antibody (1:3000) (Sigma) on ice. Internalization of the bound antibody was initiated by incubating the cells with warm (37ºC) α-MEM for the indicated time points and terminated by placing the plates on ice. Cell were washed and labeled with goat anti-mouse HRP-conjugated secondary antibody (1:1000) (GE Healthcare). After extensive washes with PBS-CM, cells were treated on ice with Amplex® Red reagent (Invitrogen). Aliquots were transferred to 96-well plates and fluorescence readings were taken with a POLARstar OPTIMA (BMG Labtech, Inc, Offenburg, Germany) plate reader using 544-nm excitation and 590-nm emission wavelengths. All experiments were performed in triplicates and repeated at least three times. Results were expressed as a percentage of the fluorescence recorded prior to internalization, after subtraction of the value measured with mock-transfected cells. Results are shown as mean ± standard error of the mean (SEM).

Analysis of Trafficking by Single-Cell Fluorescence Ratio Imaging (FRIA)

AP-1 cells were transfected with $_{3Flag}NHE6_{HA}$ wild-type or ΔE287/S288 and cell surface resident protein was labeled on ice with anti-Flag monoclonal antibody (1:1000 dilution, Sigma-Aldrich) and FITC-conjugated goat anti-mouse secondary Fab (1:1000 dilution, Jackson ImmunoResearch Laboratories, West Grove, PA). Cells were then washed in PBS supplemented with 1 m M $MgCl_2$ and 0.1 mM $CaCl_2$ (PBS-CM) and chased for the indicated time points in growth medium at 37°C. FRIA was performed on an Axiovert 100 inverted fluorescence microscope (Carl Zeiss MicroImaging, Toronto, ON, Canada) at room temperature equipped with a Hamamatsu ORCA-ER 1394 (Hamamatsu, Japan) cooled CCD camera and a Planachromat (63x NA 1.4) objective essentially as described previously (Barriere et al., 2007; Barriere and Lukacs, 2008). Image acquisition and FRIA were performed with MetaFluor software (Molecular Devices, Downingtown, PA). Images were acquired at 490±5 and 440±10 nm excitation wavelengths, using a 535±25-nm emission filter. In each experiment, the pH of 100–1000 vesicles was determined. Mono- or multipeak Gaussian distributions of vesicular pH values were obtained with Origin 7.5 software (OriginLab, Northampton, MA).

Calibration curves have been performed like previously described (Barriere and Lukacs, 2008; Barriere et al., 2009). Briefly, in situ calibration was performed by clamping the vesicular pH between 4 and 7.5 in K+-rich medium (135 mM KCl, 10 mM NaCl, 20 mM Hepes or 20 mM MES, 1 mM $MgCl_2$, and 0.1 mM $CaCl_2$) with 10 μM nigericin, 10 μM monensin, 0.4 μM bafilomycin and 20 μM carbonyl cyanide m-chlorophenyl hydrazone (CCCP) and recording the fluorescence ratios.

Immunofluorescence Confocal Microscopy

To examine the subcellular localization of NHE6, AP-1 cells were grown in 10-cm dishes and co-transfected or transfected separately with

$_{3Flag}$NHE6-v1$_{GFP}$ wild-type and $_{3Flag}$NHE6-v1$_{ChFP}$ ΔE287/S288 mutant. Twenty-four hours post-transfection, the cells were transferred to 1.5 µg/ml fibronectin (Sigma) -coated glass coverslips and grown for 24 more h. Cells were fixed in 2% paraformaldehyde/PBS for 20 min at room temperature and mounted onto glass slides using Aqua Poly/Mount mounting medium (Polysciences Inc., Warrington, PA)

To examine the internalization of NHE6 into transferrin-containing endosomes, AP-1 cells were grown in 10-cm dishes and transfected with $_{3Flag}$NHE6$_{HA}$ wild-type or ΔE287/S288 mutant. Twenty-four hours post-transfection, the cells were transferred to fibronectin-coated glass coverslips and grown for 24 more h. For the zero time point, cells were serum-depleted for one hour, incubated with 10 µg/ml Alexa Fluor® 488-conjugated transferrin for 45 min in serum-free media at 37ºC, and then placed on ice. Cells were then labelled for one hour on ice with mouse monoclonal anti-Flag antibody (1:2000) in PBS-CM/10 mM Glucose/10 mM HEPES, ph 7.4, washed 3 times with PBS supplemented with 1 m M $MgCl_2$ and 0.1 m M $CaCl_2$ (PBS-CM), and then incubated on ice with goat anti-mouse Alexa Fluor® 568-conjugated secondary antibody (1:1300). After extensive washes with PBS, cells were fixed in 2% paraformaldehyde/PBS for 20 min at room temperature and mounted onto glass slides. For the 60 minutes endocytosis time point, after serum depletion, cells were labeled on ice with the primary anti-Flag and secondary Alexa Fluor® 568-conjugated antibodies, and then chased with serum free media at 37ºC for 1 h. For transferrin labelling, the chasing media contained 10 µg/ml Alexa Fluor® 488-conjugated transferrin during the last 45 minutes of chase. Cells were subsequently fixed and mounted.

For colocalization studies, AP-1 cells were transfected with $_{3Flag}$NHE6$_{HA}$ wild-type or ΔE287/S288 mutant and transferred to glass coverslips coated with 1.5 µg/ml fibronectin. Forty-eight hours after transfection, cells were incubated for 2 h with rabbit polyclonal anti-Flag antibody at 37ºC, chased for 30 min in culture media, and then fixed in 2%

paraformaldehyde/PBS for 20 min at room temperature, followed by permeabilization with 0.1% saponin/PBS for 20 min, and blocking in 10% goat serum /0.01% saponin /PBS for 1 h. Subsequently the cells were incubated with mouse monoclonal anti-EEA1 (1:600) or anti-LAMP-2 (1:50) antibodies for 2 h at room temperature. Next, cells were washed four times with 10% goat serum/0.01% saponin/PBS, and then incubated with anti-mouse Alexa Fluor® 488 and anti-rabbit Alexa Fluor® 568 at a dilution of 1:2000 in 10% goat serum/0.01% saponin/PBS for 1 h at room temperature. After extensive washes with PBS, cover slips were mounted onto glass slides with Aqua Poly/Mount mounting medium (Polysciences Inc., Warrington, PA).

To visualize the cytoskeleton, CHO cells expressing $NHE6_{HA}$ wild-type or ΔE287/S288 mutant, were fixed in 2% paraformaldehyde/PBS for 20 min at room temperature, followed by permeabilization with 0.1% saponin/PBS for 20 min, and blocking in 10% goat serum /0.01% saponin /PBS for 1 h. Subsequently the cells were incubated with mouse monoclonal anti-HA antibody (1:1000) and rhodamine-phalloidin (Invitrogen) (1:500) for 2 h at room temperature, followed by anti-mouse Alexa Fluor® 488 (1:2000) for 1 h and 4', 6'-diamidino-2-phenylindole (DAPI) (Sigma) for 15 min at room temperature. After extensive washes with PBS, cells were mounted onto glass slides.

Cells were examined by laser scanning confocal microscopy using a Zeiss LSM 510 Meta, and images were analyzed using LSM software and Corel® CorelDraw™ version 13.

Flow Cytometry

To measure transferrin uptake by flow cytometry, AP-1 cells were transfected with GFP alone or $NHE6\text{-}v1_{GFP}$. Forty-eight hours after transfection, the cells were serum-depleted for 1.5 h, and then incubated with Alexa Fluor® 633-conjugated transferrin for 20 min at 37ºC, followed by washes to remove unbound transferrin. Cells were analyzed by flow

cytometry using the 633 nm laser of a FACSAria Sorter (Becton Dickinson, San Jose, CA) to excite the Alexa Fluor 633 fluorophore. A gate was set around the GFP-positive cells and the amount of transferrin- Alexa 633 taken up by 10^4 of these cells was measured using the BD FACSDiva software.

HeLa cells were cultured in 6-well plates and transfected with 100 nM siRNA pool #1 (scrambled siRNA) or SMARTpool® NHE6 siRNA (Dharmacon, Lafayette, CO) using Dharmafect1 transfection reagent (Dharmacon) according to the manufacturer's recommended protocol. Seventy-two hours post-transfection, the cells were serum-starved for 1.5 h and then incubated with Alexa Fluor® 633-conjugated transferrin for 20 min at 37ºC. 10^5 cells were analyzed by flow cytometry.

To measure apoptosis by flow cytometry, AP-1 cells were transfected with GFP alone, $_{3Flag}NHE6_{GFP}$ wild-type or ΔE287/S288 mutant. Forty-eight hours after transfection, cells were labeled with Annexin V-APC (5 µl/test) (eBioscience, San Diego, CA) and propidium iodide (PI) (5 µl/test from 50 µg/ml stock solution) (Becton Dickinson, San Jose, CA), according to the manufacturer's recommended protocol. Cells were examined by flow cytometry using a FACSAria Sorter (Becton Dickinson, San Jose, CA) and analyzed with the BD FACSDiva software running the FACSAria Sorter. Annexin V-APC was excited by the 633 nm red laser and PI by the 488 nm argon laser. Ten thousand GFP-positive cells were analyzed for each individual construct transfected. PI-Annexin V double negative cells represent viable cells. PI only positivity is a marker of nuclei, devoid of plasma membrane; Annexin V only positive cells indicate early apoptotic cells, whereas PI-Annexin V double positive cells represent late apoptotic-necrotic cells.

Real-time PCR (RT-PCR)

HeLa cells were grown in 6-well plates and transfected with 100 nM siRNA pool #1 (scrambled siRNA) or SMARTpool® NHE6 siRNA

(Dharmacon) using Dharmafect1 transfection reagent (Dharmacon) according to the manufacturer's recommended protocol. Total RNA was extracted with TRIzolreagent (InvitrogenCanada Inc.). Real-time PCRs were performed using IQ SYBR Green Supermix (Bio-Rad Laboratories Inc., ON) and analyzed with Gene Expression Analysis for iCycler iQ® Real-Time PCR Detection System (BioRad).

RESULTS

The NHE6-v0 residues Glu255 and Ser256 are conserved in all NHE isoforms

Two different splice variants of NHE6 have been described so far, termed NHE6-v0 (Numata et al., 1998) and NHE6-v1 (Miyazaki et al., 2001). We cloned the full-length NHE6-v1 isoform from a human brain cDNA library and introduced the influenza virus hemagglutinin (HA) epitope at its extreme terminus. Because the NHE6-v1 isoform contains a stretch of 32 amino acids in the second extracellular loop that are absent in NHE6-v0, Glu255 and Ser256 from the NHE6-v0 isoform correspond to Glu287 and Ser288 in NHE6-v1. These amino acids are highly conserved in all NHE isoforms (Fig. 4.1B).

Processing of mutant NHE6 is deficient

To investigate the importance of the E287-S288 residues to NHE6 function, the following mutations were engineered in the HA-epitope tagged form of NHE6-v1 ($NHE6_{HA}$): deletion of amino acids E287 and S288 (ΔE287/S288), the conservative double substitution E287Q/S288A, and the single substitutions E287Q, E287A, and S288A.

Wild-type and mutant HA-tagged forms of NHE6-v1 were transiently transfected in Chinese hamster ovary AP-1 cells and their expression was evaluated by immunoblotting with an anti-HA antibody 48 hours after transfection. As shown previously, wild-type $NHE6_{HA}$ migrated

A.

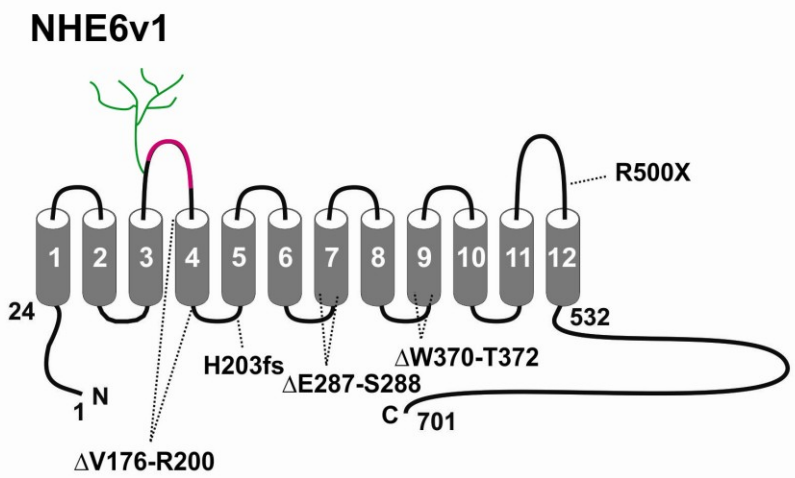

B.

NHE1	LVFGESLLNDAVTVVLYHLFEEFANYE... .HVGIVDIFL GFLSFFVVAL
NHE2	LVFGESLLNDAVTVVLYNLFKSFCQMK... .TIETIDVFA GIANFFVVGI
NHE3	IVFGESLLNDAVTVVLYNVFESFVALGG.. DNVTGVDCVK GIVSFFVVSL
NHE4	MIFGEALLNDGITVVLYNMLIAFTKMHKF. EDIETVDILA GCARFIVVGL
NHE5	IVFGESLLNDAVTVVLYKVCNSFVEMGS.. ANVQATDYLK GVASLFVVSL
NHE6v0	LLFGESVLNDAVAIVLSSSIVAYQPAGDNS HTFDVTAMFK SIGIFLGIFS
NHE6v1	LLFGESVLNDAVAIVLSSSIVAYQPAGDNS HTFDVTAMFK SIGIFLGIFS
NHE7	LLFGESVLNDAVAIVLSSSIVAYQPAGLNT HAFDAAAFFK SVGIFLGIFS
NHE8	LVFGESILNDAVSIVLTNTA EGLTRKNMS.DVSGWQTFLQ ALDYFLKMFF
NHE9	LLFGESVLNDAVAIVLTYSISIYSPK.ENP NAFDAAAFFQ SVGNFLGIFA

Figure 4.1. Mutations in NHE6 identified by Gilfillan et al. (2008) in patients with Angelman-like syndrome (*panel A*) and alignment of human NHE isoforms (*panel B*).
The glutamic acid and serine residues (E255/S256 in NHE6-v0) deleted in patients with severe mental retardation syndrome reported by Gilfillan et al. (2008) are shown in red in *panel B* and are highly conserved.

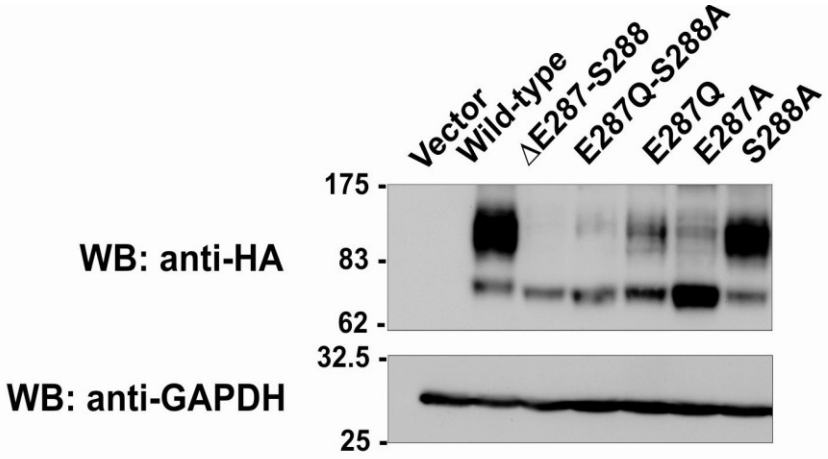

Figure 4.2. Expression of wild-type and mutant NHE6-v1 in transfected AP-1 cells.

AP-1 cells were transfected with empty vector, NHE6-v1 wild-type, and the indicated mutant forms of NHE6. Total cell lysates were prepared 48 hours post-transfection and analyzed by Western blotting with a mouse monoclonal anti-HA antibody (*upper panel*). The same membrane was immunoblotted with a mouse monoclonal anti-GAPDH antibody as a control for protein loading (*lower panel*).

as two bands: a slower migrating, higher molecular weight band representing the mature fully-glycosylated form of the protein; and a faster migrating, lower molecular weight band, characteristic for the immature core-glycosylated form (Fig. 4.2). On the contrary, all constructs where E287 is mutated either conservatively to glutamine (E287Q) or non-conservatively to alanine (E287A) showed reduced abundance and impaired post-translational modification, as the proteins mostly remain in the unglycosylated or core-glycosylation state. Interestingly, the defect is the most severe in the double deletion mutant, whereas the S288A mutant behaves similar to the wild-type, suggesting that Glu287 plays an essential role in the proper processing of NHE6.

Stability of mutant NHE6 is decreased

One possible mechanism that could account for the low abundance of several of the NHE6 mutants is decreased structural stability resulting in more rapid degradation. In order to test this hypothesis, wild-type and mutant HA-tagged forms of NHE6-v1 were expressed in AP-1 cells and their expression levels were monitored after inhibiting *de novo* protein synthesis with cycloheximide for 2, 4, 8, or 24 hours. Cell lysates were obtained at the indicated time points and proteins were resolved by SDS-PAGE and analyzed by western blotting with a mouse monoclonal anti-HA antibody. As shown in Figs. 4.3A and B, the wild-type protein is very stable, even after 24 hours of treatment with cycloheximide. A very similar pattern was observed for the S288A mutant (Fig. 4.3A). On the other hand, the double deletion mutant had almost completely disappeared already after 4 hours of cycloheximide treatment (Fig. 4.3A, B). The other mutants of E287 also display greatly reduced half-lives compared to the wild-type protein (Figs. 4.3A), suggesting an essential role of E287 in the stability of NHE6-v1.

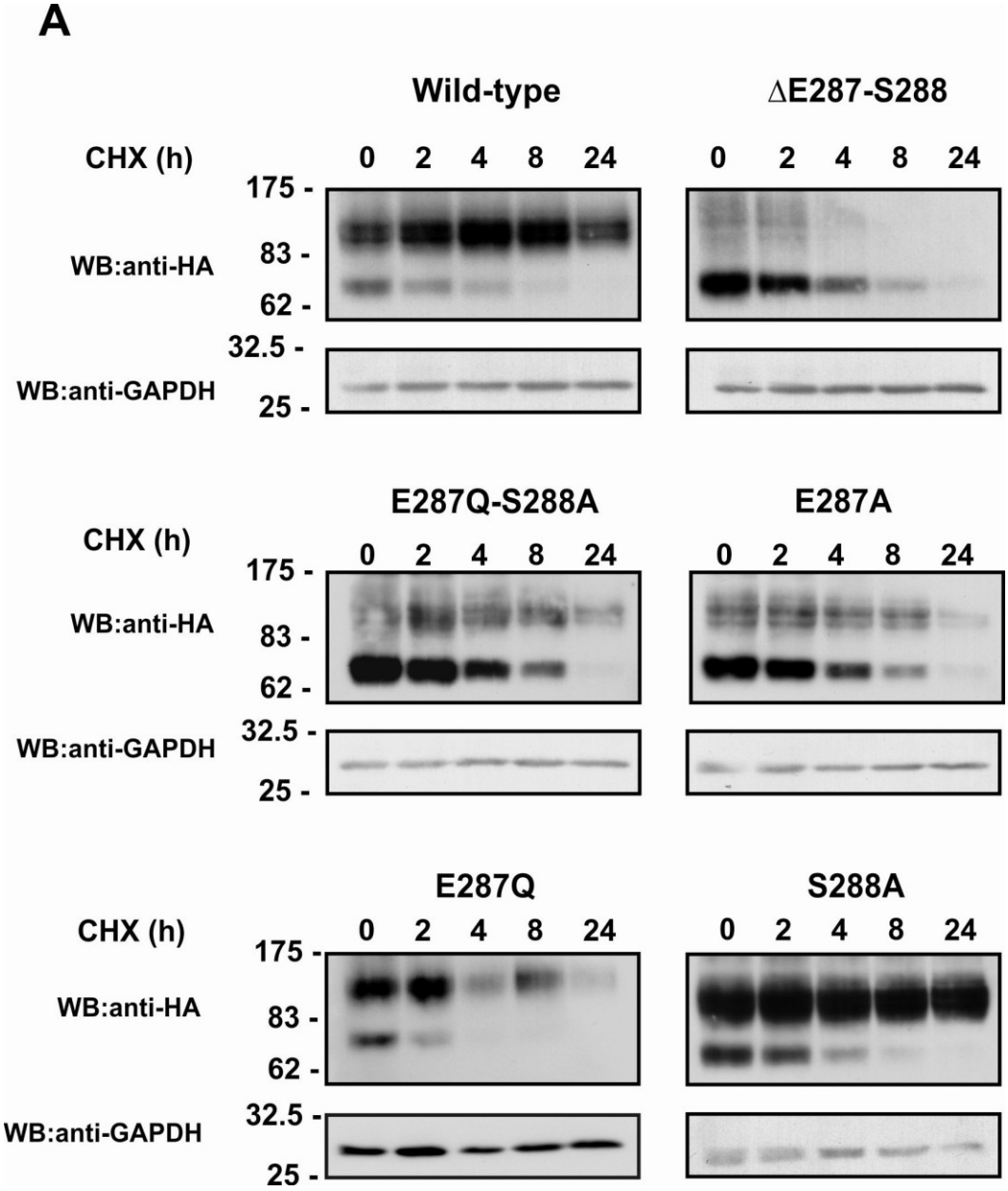
A
Wild-type
ΔE287-S288
CHX (h)
0 2 4 8 24
0 2 4 8 24
175 -
83 -
62 -
WB:anti-HA
32.5 -
25 -
WB:anti-GAPDH
E287Q-S288A
E287A
CHX (h)
0 2 4 8 24
0 2 4 8 24
175 -
83 -
62 -
WB:anti-HA
32.5 -
25 -
WB:anti-GAPDH
E287Q
S288A
CHX (h)
0 2 4 8 24
0 2 4 8 24
175 -
83 -
62 -
WB:anti-HA
32.5 -
25 -
WB:anti-GAPDH

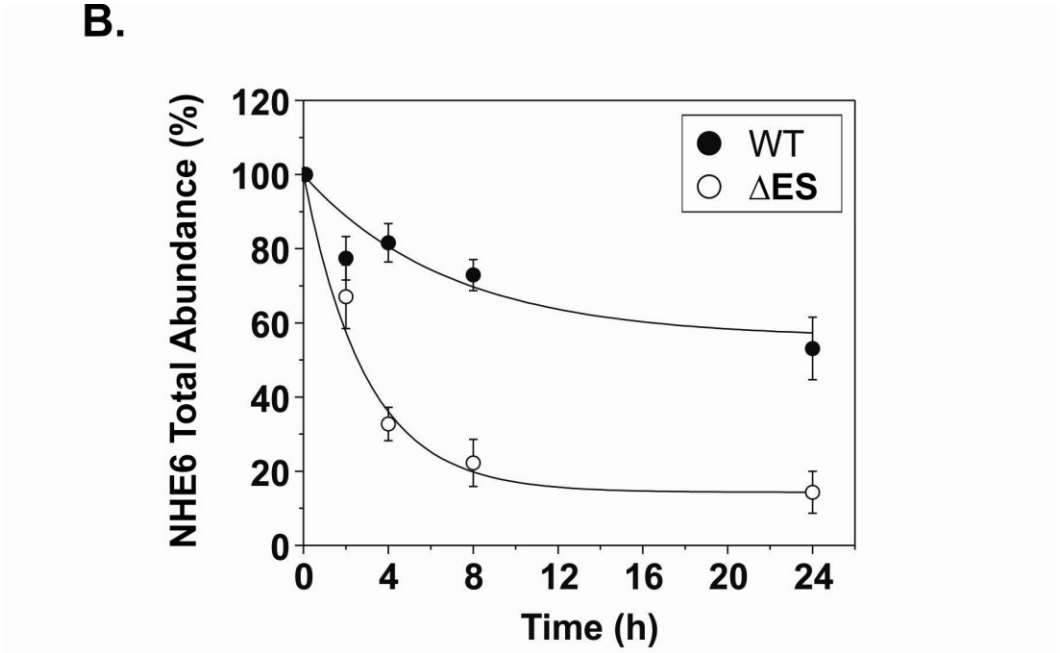

Figure 4.3. Stability of wild-type and mutant NHE6-v1 in transfected AP-1 cells.

A. AP-1 cells expressing $NHE6_{HA}$ wild-type, ΔES, E287Q-S288A, E287A , E287Q and S288A were treated with 150 µg/ml cycloheximide for the indicated time points, lysed and analysed by immunoblotting with a mouse monoclonal anti-HA antibody. Equal amounts of proteins were loaded, as shown by immunoblotting of the same membranes with an anti-GAPDH antibody. **B**. Quantitative analysis by densitometry of NHE6 wild-type (WT) and mutant (ΔES) protein abundance as a function of time in the presence of cycloheximide . Error bars represent the mean ± SEM of three separate experiments.

Mutant NHE6 displays lower surface expression and slower internalization rate

Previous studies have shown that wild-type NHE6 is predominantly localized in an intracellular endosomal compartment (Miyazaki et al., 2001; Brett et al., 2002; Nakamura et al., 2005; Ohgaki et al., 2008), but can also traffic to the plasma membrane (Brett et al., 2002, Fig. 1.2). To assess whether the mutant proteins maintain this normal sorting pattern, $NHE6_{HA}$ wild-type and mutant ΔE287-S288 constructs bearing a triple Flag epitope in the first extracellular loop at position M53 ($_{3Flag}NHE6_{HA}$) were engineered and transfected into AP-1 and HEK-GRIP cells (Fig. 4.4A). The cell surface expression of these constructs was verified using a cell-based enzyme-linked immunosorbent assay (ELISA). Two different cell-types were used in order to test if the observed effects are cell-type dependent. Forty-eight hours after transfection, the cells were placed on ice and the cell-surface resident NHE6 was labelled with primary mouse monoclonal anti-Flag and secondary HRP-conjugated antibodies, followed by detection with the Amplex® Red fluorescent substrate. As shown in Fig. 4.4B, the cell surface levels of ΔE287-S288 are lower compared to the wild-type protein (70% of wild-type in AP-1 cells, and 50% in HEK-GRIP cells).

We next assessed whether the kinetics of internalization of the double deletion mutant was altered compared to the wild-type protein. To test this hypothesis, $_{3Flag}NHE6_{HA}$ wild-type and mutant were transiently expressed in AP-1 and HEK-GRIP cells, and their internalization was examined using a fluorescence-based endocytosis assay. This assay measures the loss of cell surface immunoreactivity of epitope-tagged plasma membrane protein by use of an enzyme-linked immunosorbent assay (Barriere et al., 2006). Forty-eight hours after transfection, the cells were placed on ice and incubated with a mouse monoclonal anti-Flag antibody to label cell surface NHE6, followed by internalization at 37 ºC for different time points (5, 10, 15, and 30 min). The remaining cell surface

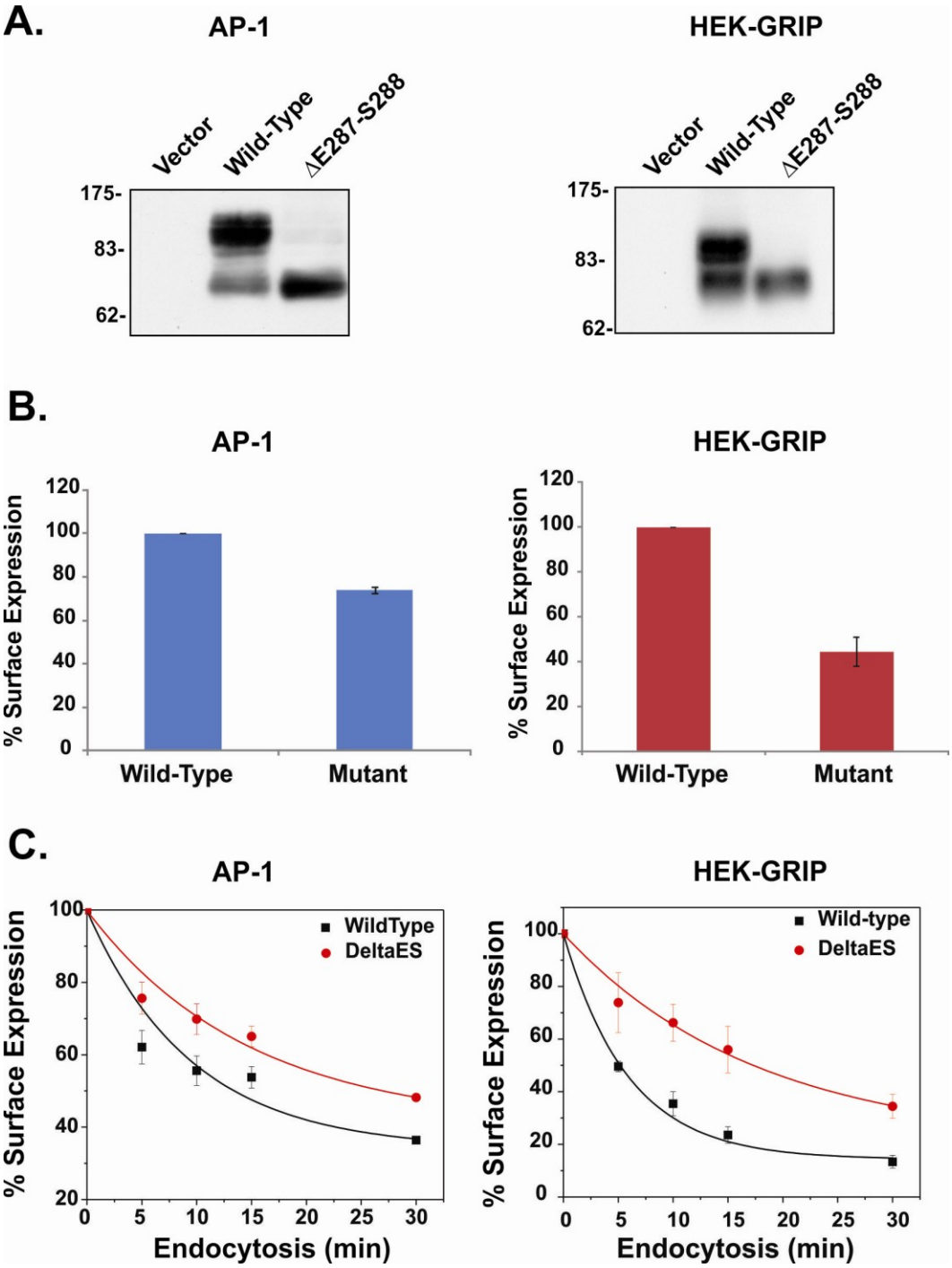
A.
AP-1
HEK-GRIP
Vector
Wild-Type
ΔE287-S288
175-
83-
62-
B.
AP-1
HEK-GRIP
% Surface Expression
120
100
80
60
40
20
0
Wild-Type
Mutant
C.
AP-1
HEK-GRIP
% Surface Expression
WildType
DeltaES
Wild-type
DeltaES
100
80
60
40
20
0
5
10
15
20
25
30
Endocytosis (min)

Figure 4.4. Surface expression and internalization of NHE6-v1 wild-type and ΔE287-S288 mutant proteins in AP-1 cells *(left panels)* and HEK-GRIP cells (*right panels*) using a cell based enzyme-linked immunosorbent assay (ELISA).

A. Western Blot showing expression of $_{3Flag}$NHE6v1$_{HA}$ wild-type and ΔE287-S288 mutant proteins in AP-1 and HEK-GRIP cells.

B. Cell surface density of mutant ΔE287-S288 NHE6 was measured using cell based ELISA and expressed as percentage of the wild-type protein normalized for total cellular protein. AP-1 and HEK-GRIP cells were transfected with empty vector, $_{3Flag}$NHE6$_{HA}$ wild-type or ΔE287-S288. Forty-eight hours post-transfection, surface NHE6 was labeled on ice using a mouse monoclonal anti-Flag antibody, followed by internalization of the Flag-labeled NHE6 at 37ºC for the indicated time points. Remaining cell surface NHE6 was labeled with a goat anti-mouse HRP-conjugated secondary antibody and detected using the fluorescent Amplex® Red substrate.

C. Kinetics of endocytosis measured using the cell-based ELISA. Data points represent mean ± SEM of four different experiments, each done in triplicate.

protein was measured after incubation with a HRP-conjugated secondary antibody and the Amplex® Red fluorescent substrate. As shown in Fig. 4.4C, the wild-type protein was rapidly sequestered both in AP-1 cells (~40% internalized after 5 min) and in HEK-GRIP cells (~50% internalized after 5 min). However, the ΔE287-S288 mutant was internalized at a much slower rate (~25% after 5 min in both AP-1 and HEK-GRIP cells).

Intracellular distribution of mutant NHE6 is altered

To further validate the subcellular distribution of the NHE6 ΔE287-S288 mutant protein, AP-1 cells were transiently transfected (48 h) with wild-type NHE6 construct containing green fluorescent protein (GFP) at its C-terminus ($_{3Flag}NHE6_{GFP}$) and/or ΔE287-S288 mutant containing cherry fluorescent protein (ChFP)-tagged at its C-terminus ($_{3Flag}NHE6_{ChFP}$ ΔES) and visualized by confocal microscopy. As expected, the wild-type protein was distributed to small punctate vesicles, many of which coalesced in a region near the Golgi and nucleus; often referred to as the perinuclear recycling compartment (Fig. 4.5A, *upper panels*). On the other hand, the double deletion mutant accumulated in small as well as large endomembrane structures, possible aggregates of vesicles, that are dispersed predominantly along the periphery of the cell and to a lesser extent intracellularly, but rarely did the vesicles concentrate in the perinuclear region (Fig. 4.5A, *lower panels*). Interestingly, when the wild-type and mutant proteins were co-expressed, in most cells they showed partial colocalization (Fig. 4.5B). Parenthetically, it was also noted that the morphology of cells expressing the ΔE287-S288 mutant often appeared rounded and less elongated compared to wild-type NHE6 transfected cells. Furthermore, the normal architecture of the actin cytoskeleton was disrupted in mutant-expression cells, although the underlying molecular basis for this phenomenon is unknown (Fig. 4.6).

To define the identity of the $_{3Flag}NHE6_{HA}$ wild-type and ΔE287-S288-containing compartments, AP-1 cells transiently expressing these

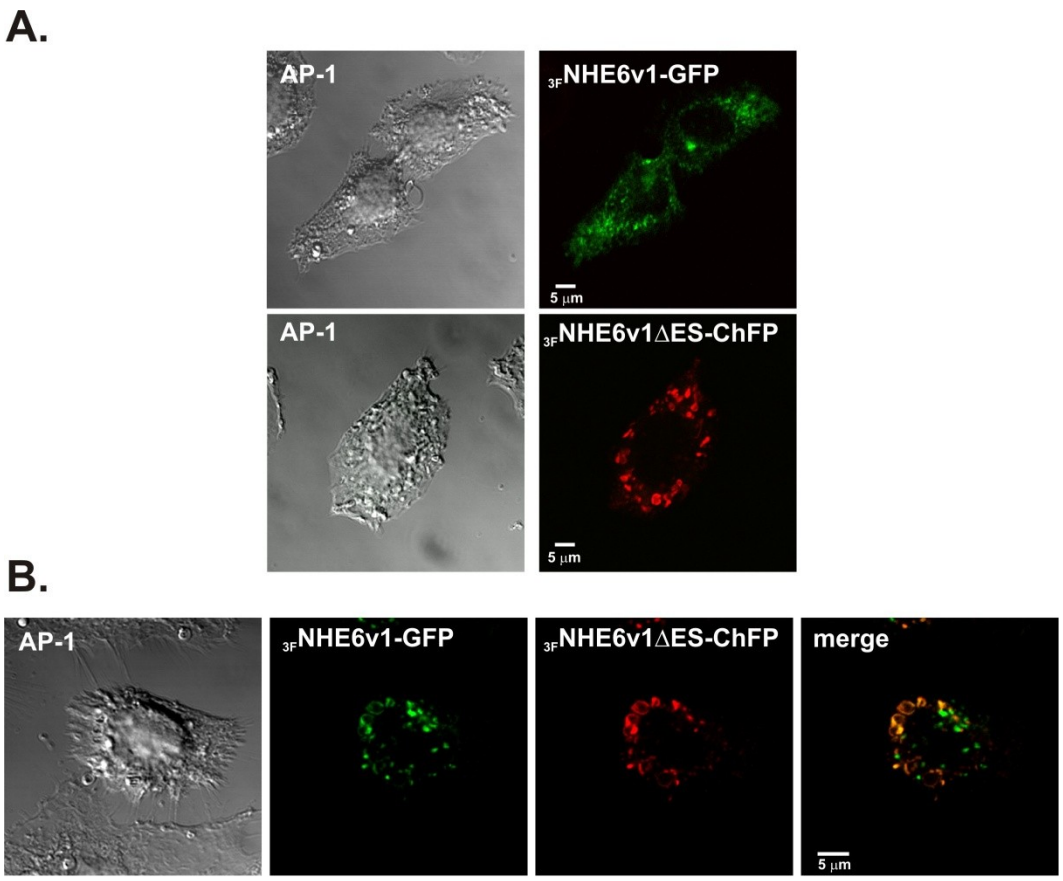

Figure 4.5. Localization of GFP-tagged $_{3F}$NHE6-v1 wild-type and mCherry (ChFP)-tagged $_{3F}$NHE6-v1 ΔES mutant in AP-1 cells by confocal microscopy.

AP-1 cells were grown on fibronectin-coated glass coverslips and transiently transfected with $_{3F}$NHE6v1-GFP wild-type and $_{3F}$NHE6v1ΔES-ChFP either individually (*panel A*) or together (*panel B*). Forty-eight hours after transfection, cells were fixed in 2% paraformaldehyde, mounted onto glass slides, and examined by confocal microscopy.

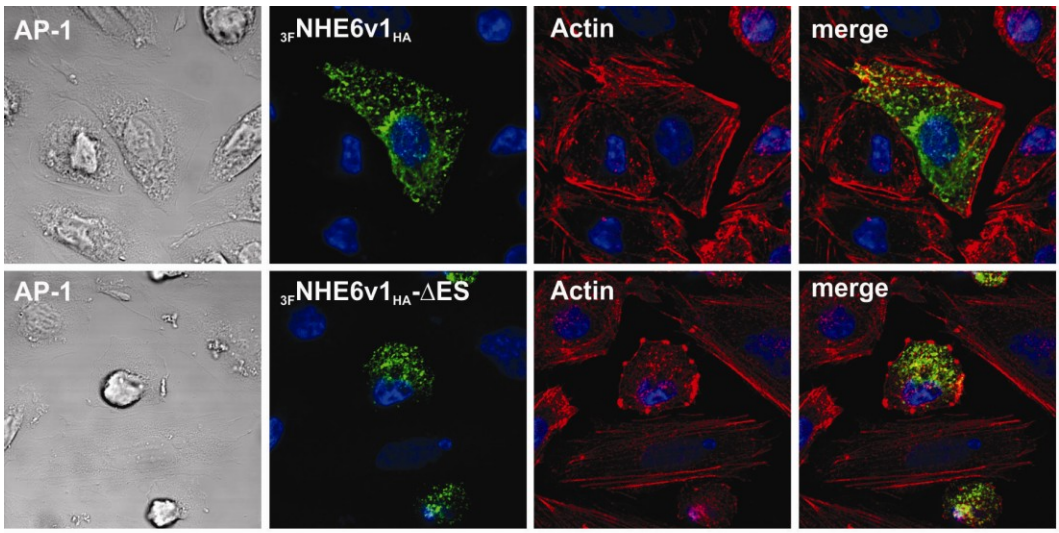

Figure 4.6. The actin cytoskeleton is disrupted in CHO cells expressing $NHE6_{HA}$ ΔES. CHO cells were grown on fibronectin-coated glass coverslips and transiently transfected with $NHE6_{HA}$ wild-type (*upper panels*) or $NHE6_{HA}$ ΔES (*lower panels*). Twenty-four hours after transfection, cells were fixed in 2% paraformaldehyde, followed by labeling of $NHE6_{HA}$ with a mouse monoclonal anti-HA antibody and goat anti-mouse Alexa488-conjugated secondary antibody. The actin cytoskeleton was labeled with rhodamin-phalloidin and the nuclei with DAPI. Cells were then mounted and examined by confocal microscopy.

constructs were incubated for 45 min with Alexa Fluor® 488-conjugated transferrin, a marker of recycling endosomes. The cells were then placed on ice and incubated with primary mouse monoclonal anti-Flag antibody and Alexa Fluor® 568-conjugated goat anti-mouse secondary antibody to label $_{3Flag}NHE6_{HA}$ at the cell surface. The cells were subsequently incubated at 37 ºC for 60 min to allow internalization of the cell surface pool of immunolabelled $_{3Flag}NHE6_{HA}$. Confocal microscopy analyses of these cells revealed the presence of both wild-type and ΔE287-S288 $_{3Flag}NHE6_{HA}$ at the cell surface before the initiation of endocytosis (Fig. 4.7 A, B, *upper panels*). After 60 min of internalization at 37ºC, the vast majority of wild-type $_{3Flag}NHE6_{HA}$ was detected in the transferrin–containing recycling endosomal pool, as expected (Fig. 4.7A, *lower panels*). Interestingly, the initial Alexa488-transferrin uptake in cells expressing the ΔE287-S288 mutant (at the 0 min time point prior to internalization) was clearly diminished compared to neighbouring wild-type cells (Fig. 4.7B). Furthermore, after 60 min of internalization, the ΔE287-S288 mutant was present in vesicles that were dispersed through the cell and showed only partial colocalization with transferrin-containing endosomes (Fig. 4.7B, *lower panel*).

In an attempt to further characterize the nature of the ΔE287-S288 compartment, additional dual immunolabelling studies were performed with other endosomal markers. As shown in Figure 4.8, the distribution of ΔE287-S288 was largely distinct from the early endosomal marker EEA1, though some minor overlap was observed. ΔE287-S288 also displayed little, if any, colocalization with the lysosomal marker LAMP-2. These data suggested that mutant ΔE287/S288 NHE6 accumulates in a discrete, albeit ill-defined, vesicular compartment.

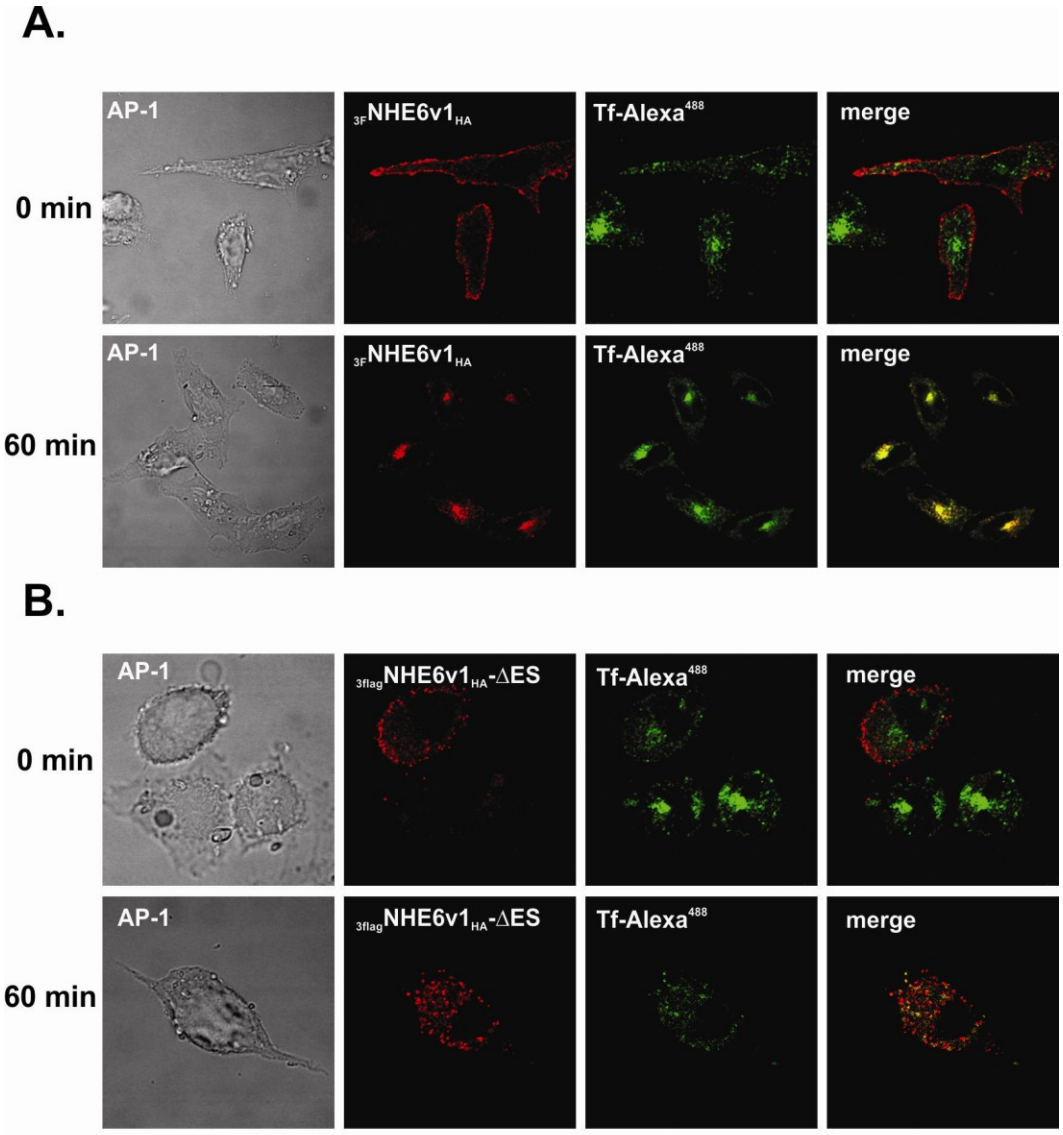

Figure 4.7. Internalization and colocalization with transferrin-Alexa488 of $_{3Flag}NHE6_{HA}$ wild-type and mutant ΔE287/S288 in AP-1 cells by confocal immunofluorescence microscopy.

AP-1 cells grown on fibronectin-coated glass coverslips were transfected with $_{3Flag}NHE6_{HA}$ wild-type (*panel A*) or mutant ΔE287/S288 (*panel B*), serum-depleted and incubated with Alexa488-conjugated transferrin for 45 min. Cells were then placed on ice and incubated with primary mouse monoclonal anti-Flag antibody and Alexa568-conjugated secondary antibody, and either fixed in 2% paraformaldehyde immediately (*0 min* time point) or after incubation at 37ºC for 1 h (*60 min* time point).

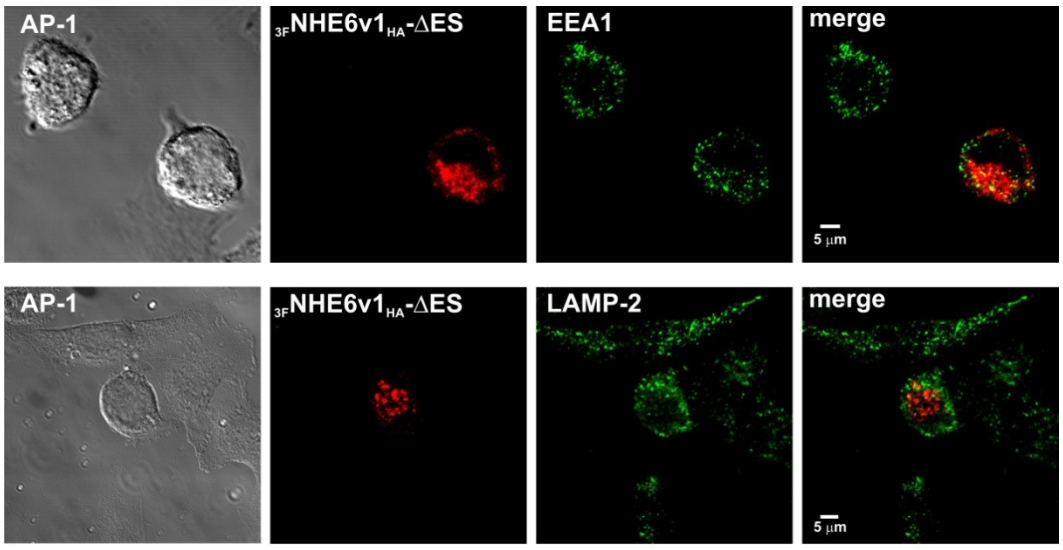

Figure 4.8. Lack of colocalization of $_{3Flag}NHE6_{HA}$ ΔE287-S288 with the early endosomal marker EEA1 (*upper panels*) and the lysosomal marker LAMP-2 (*lower panels*) by immunofluorescence confocal microscopy.

AP-1 cells were grown on fibronectin-coated glass coverslips and transfected with $_{3Flag}NHE6_{HA}$ ΔE287-S288. Forty-eight hours post-transfection, the cells were incubated with rabbit polyclonal anti-Flag antibody, fixed in 2% paraformaldehyde, and labeled with mouse monoclonal anti-EEA1 or anti-LAMP2 antibodies, followed by goat anti-mouse Alexa488- and anti-rabbit Alexa568-conjugated secondary antibodies. Cells were mounted onto glass slides and examined by confocal microscopy.

Mutant NHE6 is targeted to an acidic compartment

In view of the altered protein stability and missorting of the ΔE287-S288 mutant, we next examined whether the pH homeostasis of ΔE287-S288-containing vesicles was altered. Numerous studies have indicated that intraorganellar pH is an important determinant of proper membrane trafficking and fusion (Johnson et al., 1993; van Weert et al., 1995; Weisz, 2003a; Weisz, 2003b). To test this hypothesis, the vesicular pH (pH_v) of NHE6-containing vesicles was measured by fluorescence ratio image analysis (FRIA), as described previously for other cargo (Barriere et al., 2007; Barriere et al., 2009). AP-1 cells were transfected with $_{3Flag}$NHE6-v1$_{HA}$ wild-type or ΔE287-S288 mutant. Forty-eight hours post-transfection, wild-type or mutant NHE6 on the cell surface were labeled on ice with primary mouse monoclonal anti-Flag antibody, followed by the pH-sensitive fluorophore, FITC-conjugated Fab secondary antibody. Cells were then incubated in culture media at 37 ºC for 30 min or 60 min and analyzed by FRIA. After 30 min of internalization, NHE6 wild type was predominantly targeted to an acidic compartment of ~pH 6.0, a value characteristic of both early/sorting and perinuclear recycling endosomes (Fig. 4.9). This was followed by its trafficking to a more alkaline compartment of ~pH 6.5 at 60 min which is typical of peripheral recycling endosomes as they shuttle back to the cell surface. By contrast, the ΔE287-S288 mutant was progressively sorted to highly acidic vesicle with an average luminal pH of ~5.0; levels typical found in late endosomes/ lysosomes.

NHE6 ΔE287/S288-expressing cells do not seem to undergo apoptosis

As mentioned earlier, AP-1 cells expressing mutant $_{3Flag}$NHE6$_{HA}$ ΔE287/S288 generally displayed an abnormal morphology compared to those expressing the wild-type transporter. The most striking difference is that a large proportion of the mutant-expressing cells are rounded; a

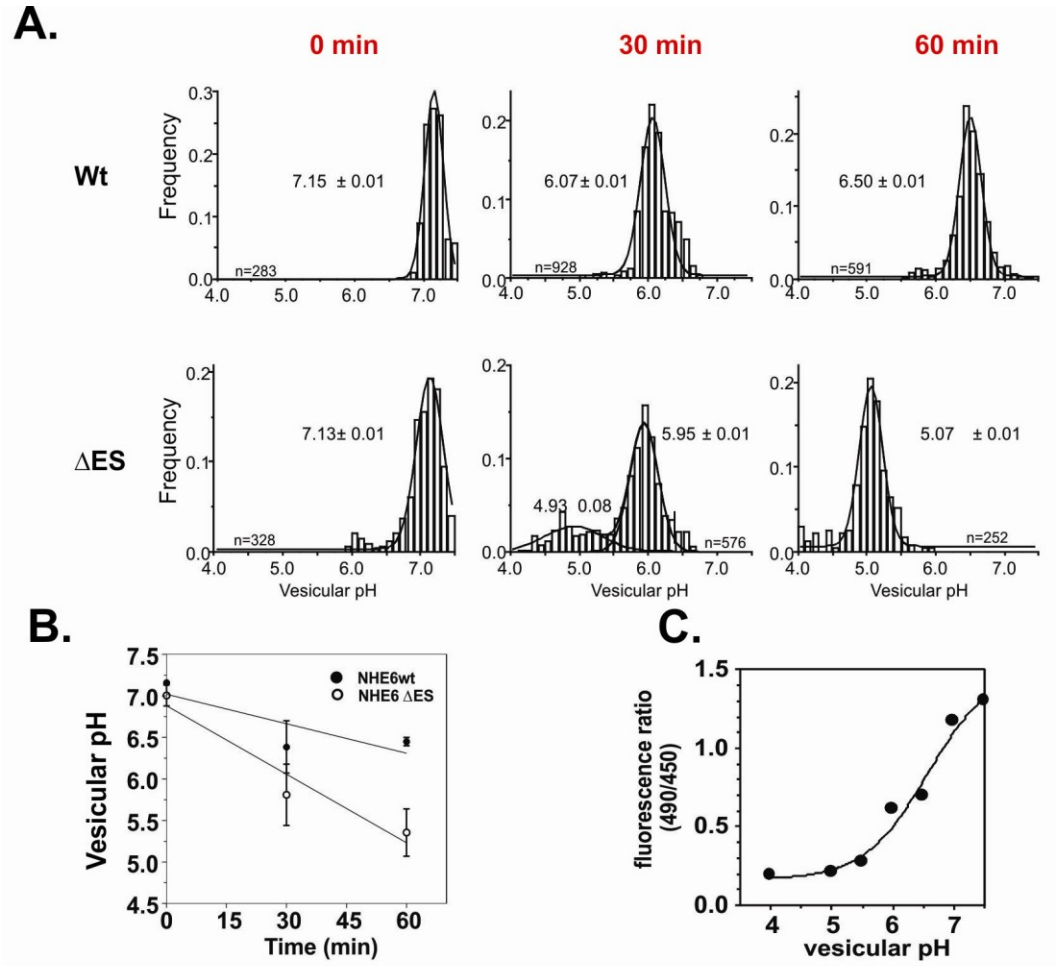

Figure 4.9. Monitoring internalized NHE6 cargoes sorting by vesicular pH (pHv) measurement.

A. NHE6-wt and ΔES and were transiently transfected in AP-1 cells and endosomal delivery was assessed two days post-transfection. Anti-Flag M2 primary antibody (1/2000) and FITC-conjugated Fab secondary antibody (1/1000) were bound to the cells for 1 h on ice. The temperature was raised to 37°C for 30 or 60 min and the pHv was measured by fluorescence ratio imaging (FRIA). The mean (± SEM) pHv and the number of vesicles analyzed in a single experiment are indicated.

B. The mean pHv from 100 to 1000 vesicles analyzed from 2 independent experiments, each done in duplicate.

C. FITC-FITC calibration curve. In situ calibration was performed by clamping the vesicular pH between 4 and 7.5 in K+-rich medium and recording the fluorescence ratios.

feature that is often observed is cells undergoing apoptosis (Hacker, 2000). In order to test this hypothesis, AP-1 cells were transfected with GFP-tagged NHE6-v1$_{HA}$ wild-type or ΔE287/S288. Forty-eight hours post-transfection, the cells were incubated in the presence of Annexin V-APC and propidium iodide and analyzed by flow cytometry to determine the fraction of apoptotic cells. Annexin V is a Ca^{2+} -dependent phospholipid-binding protein with high affinity for phosphatidylserine (PS) (Andree et al., 1990), which is normally present in the inner leaflet of the plasma membrane. Propidium iodide (PI) is a fluorescent molecule that binds to double-stranded DNA but cannot cross the intact plasma membrane of viable cells. During the early stages of apoptosis, PS is translocated to the outer leaflet of the plasma membrane, where it is now accessible for binding to Annexin V. However, the integrity of the plasma membrane is maintained, so PI cannot penetrate inside the cells. As such, Annexin V positive and PI negative cells are considered to be early apoptotic. In the later stages of apoptosis, as well as in necrosis, the plasma membrane becomes leaky, allowing PI to enter the cells and to bind to DNA, so Annexin V+PI double positive cells are late apoptotic or necrotic (Vermes et al., 1995). Ten thousand GFP-positive cells were analyzed and a slightly higher proportion of apoptotic cells was detected among the ΔE287-S288-expressing cells compared to cells expressing wild-type $_{3Flag}$NHE6$_{GFP}$, but this difference was not statistically significant (Fig. 4.10). Considering that the analysis was done 48 hours after transfection, it is possible that many mutant-expressing cells that underwent apoptosis were lost already. To get a more comprehensive understanding of this phenomenon, it will be necessary to repeat the analysis at earlier time points after transfection.

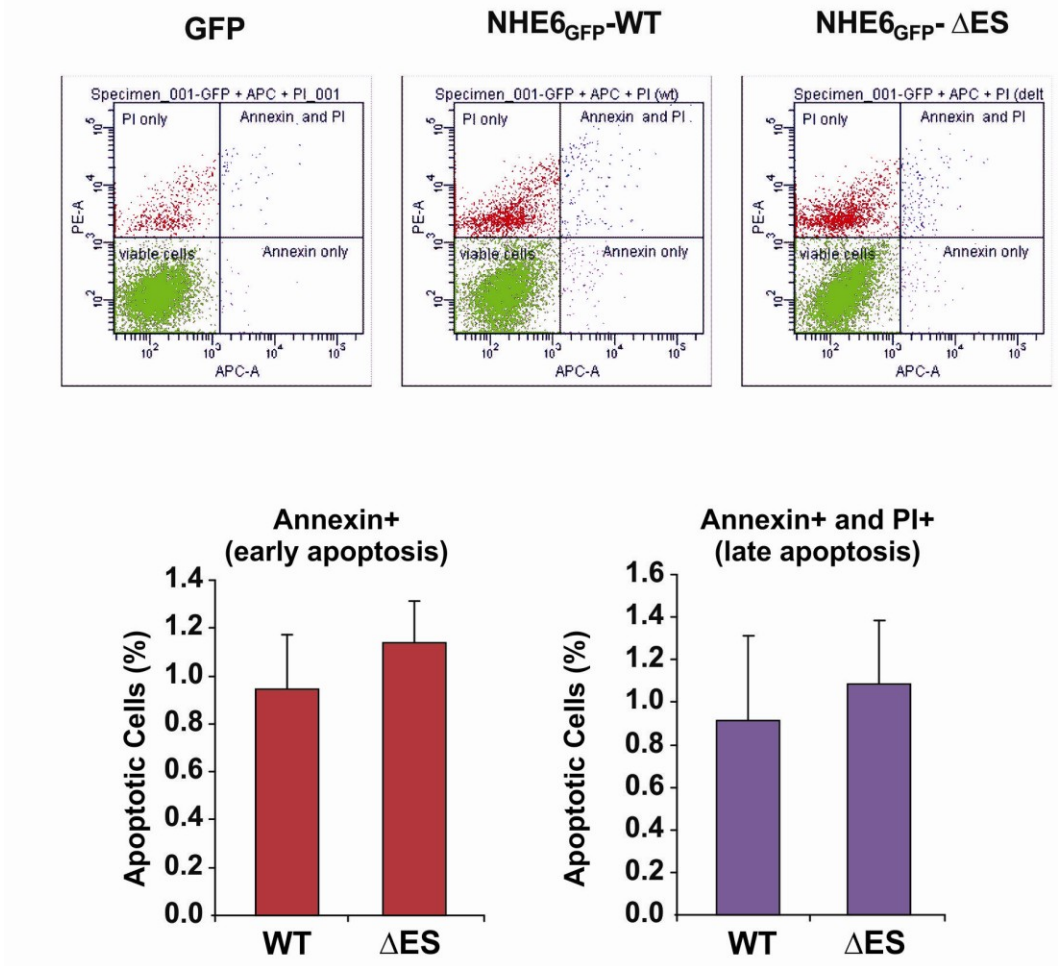

Figure 4.10. Analysis of apoptosis by flow cytometry.
AP-1 cells were transfected with GFP alone, $NHE6_{GFP}$ wild-type or ΔE287/S288 mutant. Forty-eight hours after transfection, cells were labeled with Annexin V-APC and propidium iodide (PI) and examined by flow cytometry. PI-Annexin V double negative cells represent viable cells. PI only positivity is a marker of dead cells; Annexin V positive cells indicate early apoptotic cells, whereas PI-Annexin V double positive cells represent late apoptotic cells (*upper panels*). Data of triplicates are shown as mean ± SEM (*lower panels*).

DISCUSSION

Mutations in the organellar-type NHE6 have been linked recently to an X-linked mental retardation syndrome, which resembles the phenotype of Angelman syndrome (Gilfillan et al., 2008). The authors describe a range of mutations in NHE6 in different families, including truncations (R468X, leading to loss of the final transmembrane domain and the C-terminus), splice-site mutations (causing skipping of exon 3), frameshift mutations, and a 6 bp in frame-deletion, leading to loss of amino-acids E255 and S256 in NHE6-v0. While most of these mutations will probably lead to a completely non-functional protein, the latter is more subtle and we investigated the molecular mechanisms responsible for the phenotype observed when amino acids E287 and S288 were deleted in NHE6-v1.

Two different splice variants of NHE6 have been described so far, termed NHE6-v0 (Numata et al., 1998) and NHE6-v1 (Miyazaki et al., 2001). We identified both variants in a human brain cDNA library in similar proportions. Because the NHE6-v1 isoform contains a stretch of 32 amino acids in the second extracellular loop that are absent in NHE6-v0, Glu255 and Ser256 from the NHE6-v0 isoform correspond to Glu287 and Ser288 in NHE6-v1. We engineered the double deletion mutation (ΔE287-S288), as well as substitution mutations (E287Q-S288A, E287Q, E287A, and S288A) into NHE6-v1$_{HA}$ and showed that mutation or loss of E287, but not S288, resulted in defective maturation, as revealed by dramatic impairments in the addition of complex N-glycans to the protein. In spite of deficient maturation, the mutant proteins were detected on the cell surface, as shown by ELISA and microscopy. Additionally, the stability of the ΔE287-S288 mutant is greatly reduced and its internalization rate is slower compared to its wild-type counterpart. Fluorescence ratio imaging analysis combined with immunofluorescence confocal microscopy showed that in contrast to wild-type NHE6-v1 which is predominantly in transferrin-enriched recycling endosomes, the double deletion mutant showed only minor colocalization with transferrin and with the early endosomal marker

EEA1 and instead accumulated in highly acidic vesicles that do not appear to be lysosomes as they are LAMP-2 negative. These ill-defined vesicles might be autophagosomes, but this determination will require further experimentation.

While our study was ongoing, Roxrud *et al*. (2009) reported that the stability of a GFP-tagged variant of the ΔE255-S256 NHE6-v0 mutant is reduced compared to the wild-type protein, when expressed in HeLa cells. However, curiously both their wild-type and ΔES GFP-tagged constructs migrated as a single band of ~65-70 kDa, which is way below the expected molecular weight of the fully glycosylated, mature form of NHE6 tagged to GFP (~110 kDa). This raises doubts about the fidelity of their constructs, which might be truncated forms of NHE6, and makes any further interpretation of their data difficult.

Despite the fact that the physiological roles of human NHE6 are not fully understood, insight can be gained from studies of the *Saccharomyces cerevisiae* prevacuolar/late endosomal $(Na^+,K^+)/H^+$ exchanger Nhx1. This transporter is 31% identical and 60% similar to human NHE6, and is important for trafficking of proteins out of the prevacuolar compartment. Yeast containing a null mutation of Nhx1 show enhanced acidification and abnormal enlargement of their prevacuolar/late endosomal compartment as well as missorting of its cargo; effects that could be attenuated by treatment with weak bases (Brett et al., 2005b; Bowers et al., 2000). These data support the idea that endomembrane NHEs serve as a critical alkalinizing mechanism to finely control intraorganellar pH, which modulates endosome biogenesis and trafficking.

The involvement of mammalian NHE6 in cargo trafficking is supported by experiments showing that depletion of endogenous NHE6 in HeLa cells by siRNA (Fig. 4.11A) resulted in consistently reduced uptake of transferrin-Alexa633 by ~25%, as measured by flow cytometry (Fig. 4.11B). Conversely, overexpression of NHE6-GFP in AP-1 cells resulted in a consistent increase of transferrin-Alexa633 uptake (Fig. 4.11C),

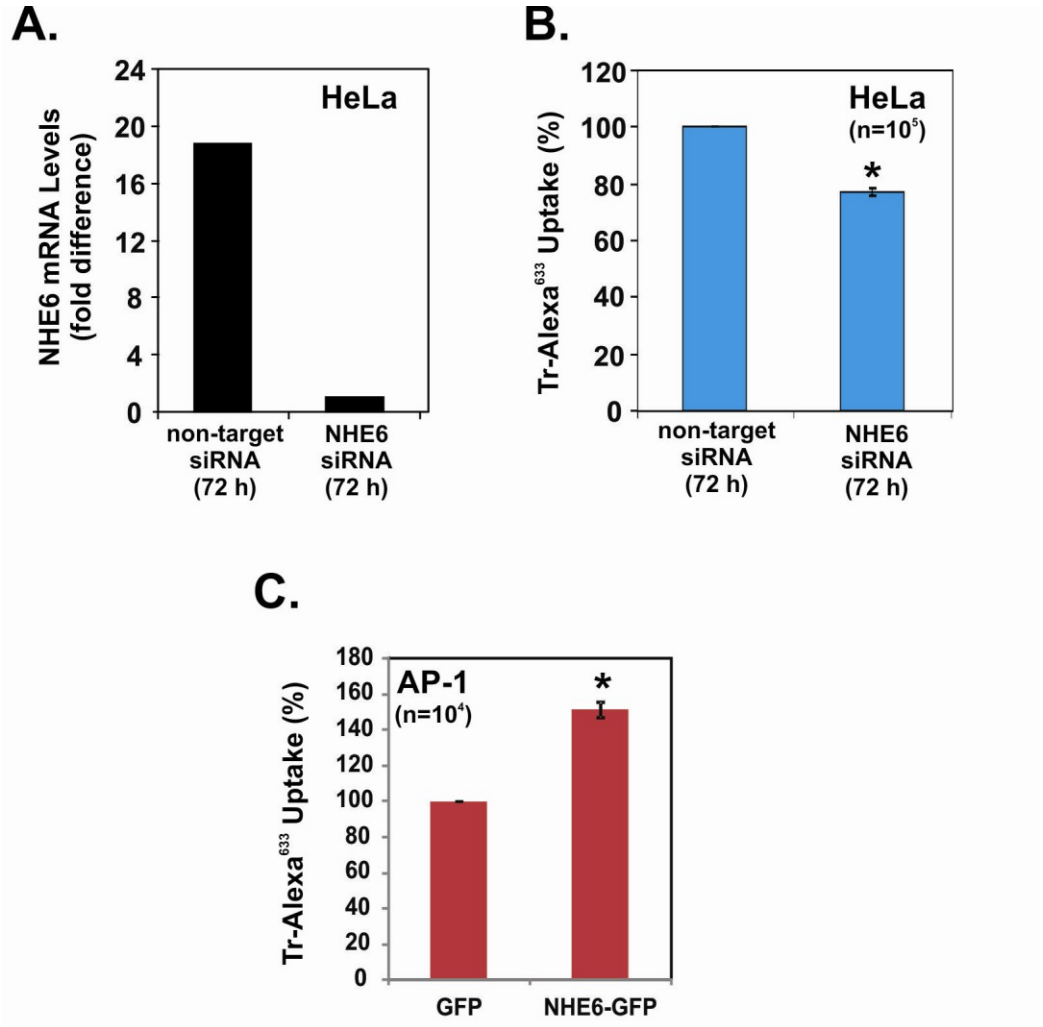

Figure 4.11. Effect of NHE6 knockdown (*panel B*) and overexpression (*panel C*) on transferrin uptake by flow cytometry.

A. HeLa cells were transfected with non-target siRNA or NHE6 siRNA, lysed 72 h post-transfection with TRIzol® Reagent (Invitrogen) and subjected to quantitative PCR analysis.

B. HeLa cells transfected for 72 h with non-target siRNA or NHE6 siRNA were serum-depleted for 1.5 h, incubated with Alexa 633-conjugated transferrin for 20 min. 10^5 cells were analyzed by flow cytometry. Data represent mean ± SEM of three independent experiments.

C. AP-1 cells were transfected with GFP alone or NHE6-$v1_{GFP}$, serum-depleted for 1.5 h, and incubated with Alexa 633-conjugated transferrin for 20 min. 10^4 GFP- positive cells were analyzed by flow cytometry. Data represent mean ± SEM of three independent experiments.

suggesting that NHE6 function is important for transferrin trafficking. Interestingly, the uptake of transferrin in ΔE287-S288-expressing cells was consistently lower when compared to wild-type NHE6-v1-expressing cells, and the perinuclear recycling endosomal compartment is not visible, indicating that the function of the double deletion mutant is compromised.

The mechanism by which the two amino-acid deleted form of NHE6 can cause an Angelman syndrome-like phenotype still remains obscure. Patients carrying mutations in NHE6 displayed pronounced developmental delays accompanied by microcephaly, epilepsy, ataxia, hyperkinesia, lack of speech, happy demeanor with episodes of unprovoked laughter, and low attention span as well as other peripheral abnormalities (Gilfillan et al., 2008). These symptoms are very similar to Angelman syndrome (AS), a severe neurodevelopmental disorder which arises from defects in the ubiquitin protein ligase E3A (UBE3A/E6-AP) gene (Lalande and Calciano, 2007). This enzyme is imprinted in certain brain regions, being only maternally expressed particularly in the hippocampus, cerebellum, olfactory bulb, and visual cortex (Jiang et al., 1998; Yashiro et al., 2009; Albrecht et al., 1997), while its expression is bi-allelic in the other organs. UBE3A was initially designated as E6-associated protein (E6-AP) based on its ability to bind to the E6 protein of human papilloma virus and degrade p53 (Huibregtse et al., 1993). UBE3A is characterized by a 350 amino acid C-terminal HECT (homologous to the E6-AP carboxyl terminus) domain and functions as an E3 ubiquitin protein-ligase, defining target specificity and catalyzing the transfer of activated ubiquitin to substrates (Scheffner et al., 1993). The majority of UBE3A mutations identified in patients with AS are predicted to disrupt the catalytic activity of the enzyme (Cooper et al., 2004). The importance of UBE3A in the development of AS has been supported by targeted inactivation of the gene in mouse models (Miura et al., 2002; Jiang et al., 1998). In both models, upon inheritance of the maternal, but not the paternal, defective gene, mice display features of AS, including microcephaly, impaired motor

function and long-term potentiation, deficits in context-dependent and spatial learning, and inducible seizures. These findings support the hypothesis that loss of UBE3A activity in the brain results in accumulation of substrate proteins, leading to the neurological abnormalities that characterize AS. Additionally, UBE3A knockout mice exhibit thinner dendrites as well as reduced spine length and density on cerebellar Purkinje cells and pyramidal neurons in the hippocampus and cortex (Dindot et al., 2008), suggesting that the observed behavioural phenotype stems from specific abnormalities in synaptic development and/or plasticity. Recent studies revealed the essential role of UBE3A in experience-dependent maturation of the visual cortex (Yashiro et al., 2009). Some important insight into the mechanism underlying the synaptic dysfunction induced by disruption of UBE3A has been contributed by the study of Greer and colleagues (2010), showing that the expression of UBE3A is induced by neuronal activity and the enzyme regulates synaptic function by ubiquitinating and degrading the synaptic protein Arc. In the absence of functional UBE3A, the levels of Arc increase in neurons, leading to excessive internalization of AMPA receptors at synapses and impaired synaptic function (Greer et al., 2010). Given the similar phenotypes produced by mutations in UBE3A and NHE6, an obvious question would be if the two proteins operate along the same pathway and if NHE6 is actually a substrate or an interacting partner of UBE3A.

It is interesting that in the study of Greer and colleagues (2010), the authors suggest that the neurological defects present in AS are ultimately the result of impaired recycling of glutamate receptors at the synapse. Considering that NHE6 is highly expressed in brain (Numata et al., 1998), that it regulates cargo trafficking (Fig. 4.11) and that it is localized in dendritic spines (Fig. 1.6), it is tempting to speculate that NHE6 is important for the recycling of post-synaptic neurotransmitter receptors and that its absence or dysfunction will impair the normal trafficking of recycling endosomes involved in spine development, maintenance and

plasticity. Consistent with this notion, NHE6/ΔE287-S288 expression in non-neuronal cells impairs the clathrin-mediated recycling endosomal pathway, as evidenced by decreased uptake of transferrin, dispersal of the perinuclear recycling compartment, and disruption of the F-actin cytoskeleton. Additional preliminary data in support of this hypothesis was also recently obtained in neurons. Depletion of endogenous NHE6 by siRNA in CA1 pyramidal neurons of mouse hippocampal slice cultures caused a marked reduction in dendritic branching and almost complete disappearance of dendritic spines (Fig. 4.12), clearly indicating an essential role for NHE6 in normal spine morphogenesis.

Our hypothesis is further supported by data from the literature, demonstrating that the growth and maintenance of dendritic spines in response to excitatory synaptic inputs requires a local supply of recycling endosomes that can be rapidly mobilized to provide membranes and glutamate receptors (Park et al., 2004; Park et al., 2006) required for long-term potentiation (LTP). Recent studies have also uncovered a critical role for postsynaptic recycling endosomes in the growth and maintenance of dendritic spines in response to stimuli that induce long-term potentiation in the hippocampus. Blocking of recycling endosomal transport in hippocampal neurons resulted in a significant decline in the number of dendritic spines and prevented new spine formation in response to activation of synaptic NMDA receptors (Park et al., 2006).

In conclusion, our data suggest an important role for NHE6 in the biogenesis and functioning of the recycling endosomal pathway. Further studies are necessary to elucidate the molecular mechanisms responsible for the phenotype caused by disruption of NHE6 in the brain.

Acknowledgments

We thank Dr. Tian-Tian Wang for help with the quantitative RT-PCR assay.

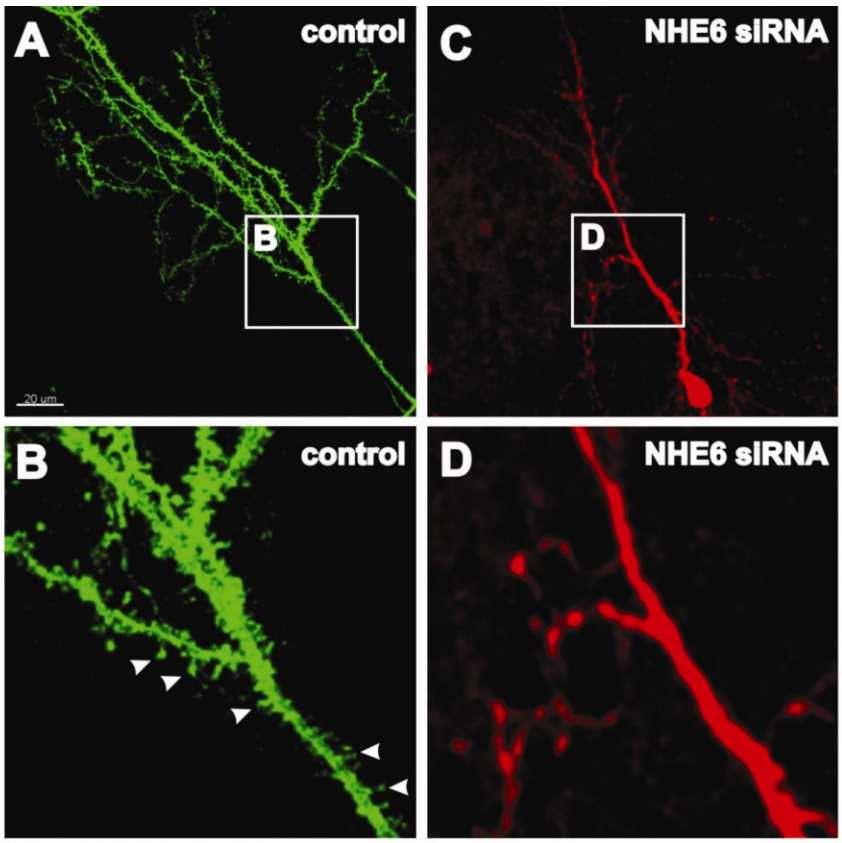

Figure 4.12. Effect of siRNA knockdown of NHE6 on morphology of dendrites in CA1 pyramidal neurons in mouse organotypic hippocampal slice cultures.

Mouse organotypic hippocampal slice cultures were transfected with Dharmacon® siGENOME® anti-NHE6 or negative control siRNA (100 nM), and mCherry expression vector (22.5 µg/mL) using DharmaFECT®Duo transfection reagent in serum-free media. Slices were injected in multiple locations in area CA1 and then bath applied with solution before being returned to culture tubes with serum-containing media. Cultures were incubated at 37°C for 72 hours before fixation in 4% paraformaldehyde.

GENERAL DISCUSSION AND CONCLUSION

The main focus of this project was to gain insight into the native distribution of NHE6, as well as the molecular mechanisms governing its intracellular trafficking and function.

NHE6 represents an organellar- or endomembrane-type NHE and is widely expressed in tissues, but the highest transcript levels are found in excitable organs, such as brain, heart, and muscle (Numata et al., 1998). Human NHE6 also undergoes alternative RNA splicing to form at least two gene products designated NHE6-v0 (Numata et al., 1998) and NHE6-v1 (Miyazaki et al., 2001). The latter contains an additional 32 amino acids situated between original residues Leu^{143}-Val^{144} and is predicted to reside in the second exoplasmic loop. Thus far, no functional differences between these splice-variants have been reported. We identified both variants in a human brain cDNA library in similar proportions.

At the beginning of this project, only limited information was available regarding the subcellular distribution of NHE6 in heterologous systems (Miyazaki et al., 2001; Brett et al., 2002). These studies reported the localization of transiently transfected NHE6 in recycling endosomes, based on its colocalization with the transferrin receptor. However, nothing was known about the native distribution, the mechanisms regulating trafficking or the physiological roles of this transporter. The importance of studying the native distribution of NHE6 in the brain is highlighted by recent findings linking mutations in this endosomal transporter to severe X-linked mental retardation syndromes (Gilfillan et al., 2008; Garbern et al., 2010). As such, the first objective was to examine the localization of NHE6 in neuronal cells. To this end, a rabbit polyclonal antibody was generated. Despite the close sequence homology between the endomembrane-type isoforms NHE6, NHE7, and NHE9, our antibody specifically and selectively recognized NHE6 in different applications,

including western blotting and immunofluorescence confocal microscopy. This antibody was able to detect native NHE6 in a transferrin-rich recycling endosomal compartment in SH-SY5Y neuroblastoma cells, similar to its distribution in overexpressing systems. Moreover, we showed that the NHE6 protein is abundant in brain lysates in different species, *i.e*. human, mouse, and rat, and more specifically in mouse hippocampus. Examination of the distribution of NHE6 in hippocampal area CA1 revealed the presence of the exchanger within the soma and dendrites of CA1 pyramidal cells; higher resolution images of isolated dendrites showed that NHE6-containing vesicles are present not only in dendritic shafts, but also in dendritic spines. We further confirmed the localization of NHE6 in dendrites of hippocampal and prefrontal cortex neurons by transmission electron microscopy. These data, in conjunction with our preliminary findings showing reduced dendritic branching and almost complete disappearance of dendritic spines when endogenous NHE6 was depleted in pyramidal hippocampal neurons, are highly suggestive of an important role of the exchanger for synaptic growth and plasticity.

Having established that endogenous NHE6 is localized in recycling endosomes in neurons, the next objective was to identify some of the factors and molecular mechanisms that regulate its trafficking and function. As NHE6 is a glycoprotein (Miyazaki et al., 2001) and N-glycosylation has been implicated in the regulation of protein folding, trafficking, stability, and function (Ohtsubo and Marth, 2006), we examined the potential significance of this frequent post-translational modification with respect to NHE6 function. We identified asparagine 128 (N128) as the unique site responsible for glycan modification of NHE6 and demonstrated a role for N-glycosylation in promoting efficient export of the transporter to the cell surface, as well as for optimal transport activity within recycling endosomes.

This is the first report addressing the potential regulatory effect of N-glycosylation on a member of the organellar-type NHEs. So far, the effect of glycosylation has been investigated only on mammalian plasma membrane-type NHEs. Thus, N-glycosylation was found not to be important for the transport function and pharmacological properties of NHE1. The glycosylation status of the NHE3 isoform is controversial, with studies reporting either that the exchanger is not glycosylated in fibroblastic cells (Counillon et al., 1994), or, on the contrary, that it undergoes N-glycosylation in epithelial cells (Soleimani et al., 1996). Although the precise glycosylation sites were not identified, treatment with tunicamycin (an antibiotic that inhibits N-glycosylation) significantly decreased NHE3 activity in these cells and inhibited the trafficking of NHE3 from the endoplasmic reticulum to the plasma membrane. Collectively, these data suggest that glycans exert isoform-specific regulatory effects among the different members of the mammalian NHE family. Interestingly, in Nhx1, the yeast homolog of NHE6, mutational analysis showed that two asparagine residues (N515 and N550) in the C-terminus are subject to *N*-linked glycosylation, predicting a surprising membrane topology, with at least some portion of the Nhx1 tail being exposed to the lumen of the prevacuolar compartment (Wells and Rao, 2001). By contrast, our data indicate that Asn623 (the consensus N-glycosylation site located in the C-terminus of human NHE) does not undergo glycan modification in NHE6-v0, supporting the topological membrane model postulated for mammalian Na^+/H^+ isoforms, whereby the C-terminal domain is located in the cytosol (Orlowski and Grinstein, 2004; Brett et al., 2005a; Orlowski and Grinstein, 2007).

The NHEs have been shown to be regulated in part through the interaction of the cytosolic C-terminal domain with numerous interacting partners, depending on the isoform (Orlowski and Grinstein, 2004; Orlowski and Grinstein, 2007). However, the regulatory interacting

partners of NHE6 are unknown, with one exception, *i.e*. the angiotensin II receptor AT2, which can bind to the C-tail of NHE6 (Pulakat et al., 2005); the physiological consequences of this interaction are unknown. Using yeast two-hybrid methodology to screen a human brain cDNA library with the C-tail of NHE6 as bait, we identified novel interacting proteins potentially involved in the regulation of NHE6. Two of the clones identified encoded the receptor for activated protein kinase C 1 (RACK1), a scaffolding protein involved in numerous protein interactions and biological functions (McCahill et al., 2002). The physiological consequences of this interaction were further analyzed. First, direct interaction of these two proteins was confirmed *in vitro* by GST fusion protein pull-down assays. NHE6 and RACK1 also formed a complex in intact cells, as revealed by co-immunoprecipitation assays and dual-immunolabelling fluorescence confocal microscopy. Interestingly, RACK1 has also been found to interact with other NHE isoforms, including the plasma-membrane type NHE5 isoform (Onishi et al., 2007), as well as the organellar-type isoforms NHE7 and NHE9 (Ohgaki et al., 2008). NHE5 binds to RACK1 directly in focal adhesions and activates its transport activity via integrin-dependent and independent pathways when stably overexpressed in AP-1 cells (Onishi et al., 2007).

Depletion of RACK1 by siRNA resulted in significantly elevated levels of NHE6 on the cell surface, suggesting that RACK1 might be involved in the retention of NHE6 to intracellular compartments. In addition, the total cellular amount of NHE6 was also markedly elevated in the presence of RACK1 siRNA, and this was not due to increased stability of NHE6, suggesting that RACK1 might regulate the biosynthesis of NHE6 by an indirect mechanism. Although we cannot exclude an indirect effect of RACK1 siRNA knock-down upon the abundance of NHE6 transcript levels, our data are more readily explained by RACK1 regulation of NHE6 translation. We propose that certain physiological states that require a down-regulation of NHE6 could lead to the recruitment to ribosome-

associated RACK1 of specific translational repressors that could decrease translation of NHE6. This hypothesis is supported by studies in eukaryotes showing that RACK1 is a highly conserved core 40S ribosomal protein (Ceci et al., 2003; Gerbasi et al., 2004). Considering the fact that RACK1 is present in two separate pools in cells, *i.e.* one ribosome-associated, and one cytosolic (Ceci et al., 2003), Coyle et al. (2009) showed that RACK1 can perform both ribosome localization-dependent and -independent functions in yeast. This observation comes to support our results, which suggest that RACK1 is involved in regulating both expression and trafficking of NHE6. However, further experimentation is required to determine the mechanism by which RACK1 represses the expression of NHE6. The first step to address this query would be to test if the transcript levels of the exchanger are affected when RACK1 is depleted in cells.

As mentioned previously, mutations in NHE6 have been linked to severe mental retardation syndromes. Different mutations (*i.e.,* deletions, premature stop codon, frameshift) in NHE6 in four separate families have been shown to cause X-linked mental retardation, microcephaly, epilepsy, ataxia, lack of speech and a happy disposition; a phenotype that closely mimics Angelman syndrome (Gilfillan et al., 2008). More recently, another mutation in NHE6 has been reported that leads to a mental retardation phenotype similar to the Angelman-like syndrome, but is distinguished by the additional manifestation of autistic behavior. Furthermore, deposition of the microtubule-binding protein tau has been observed in cortical and sub-cortical regions of these patients (Garbern et al., 2010).

One of the mutations described in the study of Gilfillan et al., (2008) was a 6 bp deletion, leading to loss of amino-acids E255 and S256 in NHE6-v0 (corresponding to E287 and S288 in NHE6-v1). In order to understand the mechanisms underlying the severe phenotype induced by this mutation, we generated epitope-tagged variants of the double deletion

mutant (ΔES) and expressed them in cells. Our results showed that the mutant protein failed to undergo proper maturation and displayed a greatly reduced stability compared to the wild-type protein. Furthermore, the mutant protein was mislocalized in cells. In contrast to wild-type NHE6, which was detected predominantly in transferrin-enriched recycling endosomes, the double deletion mutant showed only minor colocalization with transferrin and with the early endosomal marker EEA1 and instead accumulated in highly acidic vesicles and large endomembrane structures that could be conglomerates of vesicles. These vesicles do not appear to be lysosomes as they do not express the lysosomal marker LAMP-2. These ill-defined vesicles might be autophagosomes, but this determination will require further experimentation.

The physiological roles of mammalian NHE6 are largely unknown. However, some indications can be obtained from studies of the prevacuolar/late endosomal $(Na^+,K^+)/H^+$ exchanger Nhx1 in the yeast *Saccharomyces cerevisiae*. Yeast containing a null mutation of Nhx1 show increased acidification and abnormal enlargement of their late endosomal compartment, as well as missorting of its cargo; effects that are attenuated by treatment with weak bases (Bowers et al., 2000; Brett et al., 2005b). These data support the notion that endomembrane NHEs serve as a critical alkalinizing mechanism to finely control intraorganellar pH which, by poorly known mechanisms, modulates endosome biogenesis and trafficking.

We provide the first evidence for the implication of mammalian NHE6 in cargo trafficking, as depletion of endogenous NHE6 in HeLa cells by siRNA resulted in consistently reduced uptake of transferrin by approximately 25%. Additionally, overexpression of NHE6-GFP in AP-1 cells resulted in a consistent increase of transferrin uptake, suggesting that NHE6 is involved in transferrin trafficking. Interestingly, the uptake of transferrin in the double deletion mutant expressing cells was consistently lower when compared to wild-type NHE6-expressing cells, and the

perinuclear recycling endosomal compartment was not detectable, indicating that the function of the double deletion mutant is compromised. This hypothesis is further supported by studies showing that mutations of the corresponding glutamic acid residue in NHE1 (Murtazina et al., 2001) and NHE8 (Nakamura et al., 2005) completely abolish their activity.

The mechanisms by which mutations in NHE6 can cause an Angelman syndrome-like phenotype still remain to be deciphered. It has been suggested that the neurological defects present in Angelman syndrome are ultimately the result of impaired recycling of glutamate receptors at the synapse. Considering that NHE6 is highly expressed in brain (Numata et al., 1998), that it regulates cargo trafficking and that it is localized in dendritic spines, it is tempting to speculate that the exchanger is important for the recycling of post-synaptic neurotransmitter receptors and that its absence or dysfunction will impair the normal trafficking of recycling endosomes, thereby affecting spine development, maintenance and plasticity. In addition to the cellular phenotype induced by the double deletion mutant in cells (*i.e.* impaired transferrin uptake, disruption of the perinuclear recycling compartment and of the actin cytoskeleton), more preliminary data in support of this hypothesis were recently obtained in neurons. Depletion of endogenous NHE6 by siRNA in CA1 pyramidal neurons of mouse hippocampal slice cultures resulted in a significant reduction of dendritic branching and almost complete disappearance of dendritic spines, clearly indicating an essential role for NHE6 in normal spine morphogenesis.

Our hypothesis is further supported by data from the literature, demonstrating that the growth and maintenance of dendritic spines in response to excitatory synaptic inputs requires a local supply of recycling endosomes that can be rapidly mobilized to provide membrane constituents and glutamate receptors (Park et al., 2004; Park et al., 2006) required for long-term potentiation (LTP). Hence, our data suggest an important role for NHE6 in the biogenesis and functioning of the recycling

endosomal pathway, which is required for the normal development and/or maintenance of dendritic spines. Further studies are necessary to elucidate the molecular mechanisms responsible for the phenotype caused by disruption of NHE6 in the brain.

Moreover, our study opens new avenues for further analyses of other cellular functions requiring the activity of NHE6. For example, our yeast two-hybrid screen revealed numerous candidate interacting partners of NHE6, which are involved in various cellular activities, including cytoskeleton dynamics, signaling, scaffolding, solute carriers, and cell metabolism (see Appendix). Among these candidates, of particular interest are the small GTPase Rac1 and the cyclin-dependent kinase 5 (CDK5), which are important regulators of actin cytoskeletal remodeling and membrane transport in neurons and other cell types (Ng et al., 2002; Nakayama et al., 2000; Samuels et al., 2007; Dhariwala and Rajadhyaksha, 2008). Interestingly, these two proteins are critical for normal dendritic arborization, spine growth, and plasticity. Furthermore, their dysfunction has been linked to various neurological diseases, such as mental retardation (Newey et al., 2005), Alzheimer's (Maccioni et al., 2001), Parkinson's (Neystat et al., 2001), and Huntington's (Luo et al., 2005) disease. Moreover, CDK5 and Rac1 form a complex in neuronal growth cones (Nikolic et al., 1998). Thus, it is possible that NHE6, Rac1, and CDK5 are involved in the same pathway and are critical for actin remodeling and membrane trafficking in neurons and other cell types.

In conclusion, the present work expands the general knowledge of the mammalian Na^+/H^+ exchanger family, by defining some of the factors governing the regulation and function of the organellar-type isoform NHE6. Furthermore, it provides some insight into the complex molecular mechanisms underlying severe X-linked mental retardation syndromes

and opens avenues for further research that will eventually lead to the understanding of the physiological roles played by NHE6.

REFERENCES

Aharonovitz,O., Zaun,H.C., Balla,T., York,J.D., Orlowski,J., and Grinstein,S. (2000). Intracellular pH regulation by Na^+/H^+ exchange requires phosphatidylinositol 4,5-bisphosphate. J. Cell Biol. *150*, 213-224.

Akhter,S., Kovbasnjuk,O., Li,X., Cavet,M., Noël,J., Arpin,M., Hubbard,A.L., and Donowitz,M. (2002). Na^+/H^+ exchanger 3 is in large complexes in the center of the apical surface of proximal tubule-derived OK cells. Am. J. Physiol. Cell Physiol. *283*, C927-C940.

Albrecht,U., Sutcliffe,J.S., Cattanach,B.M., Beechey,C.V., Armstrong,D., Eichele,G., and Beaudet,A.L. (1997). Imprinted expression of the murine Angelman syndrome gene, Ube3a, in hippocampal and Purkinje neurons. Nat. Genet. *17*, 75-78.

Alexander,R.T. and Grinstein,S. (2006). Na^+/H^+ exchangers and the regulation of volume. Acta Physiol (Oxf) *187*, 159-167.

Alexander,R.T. and Grinstein,S. (2009). Tethering, recycling and activation of the epithelial sodium-proton exchanger, NHE3. J. Exp. Biol. *212*, 1630-1637.

Ali,R., Brett,C.L., Mukherjee,S., and Rao,R. (2004). Inhibition of sodium/proton exchange by a Rab-GTPase-activating protein regulates endosomal traffic in yeast. J. Biol. Chem. *279*, 4498-4506.

Andree,H.A., Reutelingsperger,C.P., Hauptmann,R., Hemker,H.C., Hermens,W.T., and Willems,G.M. (1990). Binding of vascular anticoagulant alpha (VAC alpha) to planar phospholipid bilayers. J. Biol. Chem. *265*, 4923-4928.

Angelman,H. (1961). Syndrome of coloboma with multiple congenital abnormalities in infancy. Br. Med. J. *1*, 1212-1214.

Apse,M.P., Aharon,G.S., Snedden,W.A., and Blumwald,E. (1999). Salt tolerance conferred by overexpression of a vacuolar Na^+/H^+ antiport in *Arabidopsis*. Science *285*, 1256-1258.

Apweiler,R., Hermjakob,H., and Sharon,N. (1999). On the frequency of protein glycosylation, as deduced from analysis of the SWISS-PROT database. Biochim. Biophys. Acta *1473*, 4-8.

Arai,T., Ikeda,K., Akiyama,H., Shikamoto,Y., Tsuchiya,K., Yagishita,S., Beach,T., Rogers,J., Schwab,C., and McGeer,P.L. (2001). Distinct isoforms of tau aggregated in neurons and glial cells in brains of patients with Pick's disease, corticobasal degeneration and progressive supranuclear palsy. Acta Neuropathol. *101*, 167-173.

Aronson,P.S. (1985). Kinetic properties of the plasma membrane Na-H exchanger. Annu. Rev. Physiol. *47*, 545-560.

Attaphitaya,S., Nehrke,K., and Melvin,J.E. (2001). Acute inhibition of brain-specific Na^+/H^+ exchanger isoform 5 by protein kinases A and C and cell shrinkage. Am. J. Physiol. *281*, C1146-C1157.

Attaphitaya,S., Park,K., and Melvin,J.E. (1999). Molecular cloning and functional expression of a rat Na^+/H^+ exchanger (NHE5) highly expressed in brain. J. Biol. Chem. *274*, 4383-4388.

Azarani,A., Goltzman,D., and Orlowski,J. (1995). Parathyroid hormone and parathyroid hormone-related peptide inhibit the apical Na^+/H^+ exchanger NHE-3 isoform in renal cells (OK) via a dual signalling cascade involving protein kinase A and C. J. Biol. Chem. *270*, 20004-20010.

Azarani,A., Goltzman,D., and Orlowski,J. (1996). Structurally diverse N-terminal peptides of parathyroid hormone (PTH) and PTH-related peptide (PTHRP) inhibit the Na^+/H^+ exchanger NHE3 isoform by binding to the

PTH/PTHRP receptor type I and activating distinct signaling pathways. J. Biol. Chem. *271*, 14931-14936.

Baird,N.R., Orlowski,J., Szabó,E.Z., Zaun,H.C., Schultheis,P.J., Menon,A.G., and Shull,G.E. (1999). Molecular cloning, genomic organization, and functional expression of Na^+/H^+ exchanger isoform 5 (NHE5) from human brain. J. Biol. Chem. *274*, 4377-4382.

Banuelos,M.A., Ruiz,M.C., Jimenez,A., Souciet,J.L., Potier,S., and Ramos,J. (2002). Role of the Nha1 antiporter in regulating K^+ influx in Saccharomyces cerevisiae. Yeast *19*, 9-15.

Barriere,H., Bagdany,M., Bossard,F., Okiyoneda,T., Wojewodka,G., Gruenert,D., Radzioch,D., and Lukacs,G.L. (2009). Revisiting the Role of CFTR and Counterion Permeability in the pH Regulation of Endocytic Organelles. Mol. Biol. Cell.

Barriere,H. and Lukacs,G.L. (2008). Analysis of endocytic trafficking by single-cell fluorescence ratio imaging. Curr. Protoc. Cell Biol. *Chapter 15*, Unit.

Barriere,H., Nemes,C., Du,K., and Lukacs,G.L. (2007). Plasticity of polyubiquitin recognition as lysosomal targeting signals by the endosomal sorting machinery. Mol. Biol. Cell *18*, 3952-3965.

Barriere,H., Nemes,C., Lechardeur,D., Khan-Mohammad,M., Fruh,K., and Lukacs,G.L. (2006). Molecular basis of oligoubiquitin-dependent internalization of membrane proteins in Mammalian cells. Traffic. *7*, 282-297.

Battaglino,R.A., Pham,L., Morse,L.R., Vokes,M., Sharma,A., Odgren,P.R., Yang,M., Sasaki,H., and Stashenko,P. (2008). NHA-oc/NHA2: A mitochondrial cation-proton antiporter selectively expressed in osteoclasts. Bone *42*, 180-192.

Bause,E. (1983). Structural requirements of N-glycosylation of proteins. Studies with proline peptides as conformational probes. Biochem. J. *209*, 331-336.

Becker,A.M., Zhang,J., Goyal,S., Dwarakanath,V., Aronson,P.S., Moe,O.W., and Baum,M. (2007). Ontogeny of NHE8 in the rat proximal tubule. Am. J. Physiol Renal Physiol *293*, F255-F261.

Bell,S.M., Schreiner,C.M., Schultheis,P.J., Miller,M.L., Evans,R.L., Vorhees,C.V., Shull,G.E., and Scott,W.J. (1999). Targeted disruption of the murine *Nhe1* locus induces ataxia, growth retardation, and seizures. Am. J. Physiol. *276*, C788-C795.

Biemesderfer,D., DeGray,B., and Aronson,P.S. (1998). Membrane topology of NHE3. Epitopes within the carboxyl-terminal hydrophilic domain are exoplasmic. J. Biol. Chem. *273*, 12391-12396.

Biemesderfer,D., Reilly,R.F., Exner,M., Igarashi,P., and Aronson,P.S. (1992). Immunocytochemical characterization of Na^+-H^+ exchanger isoform NHE-1 in rabbit kidney. Am. J. Physiol. *263*, F833-F840.

Biemesderfer,D., Rutherford,P.A., Nagy,T., Pizzonia,J.H., Abu-Alfa,A.K., and Aronson,P.S. (1997). Monoclonal antibodies for high-resolution localization of NHE3 in adult and neonatal kidney. Am. J. Physiol. *273*, F289-F299.

Bobulescu,I.A., Di,S.F., and Moe,O.W. (2005). Na^+/H^+ exchangers: physiology and link to hypertension and organ ischemia. Curr. Opin. Nephrol. Hypertens. *14*, 485-494.

Bobulescu,I.A. and Moe,O.W. (2006). Na^+/H^+ exchangers in renal regulation of acid-base balance. Semin. Nephrol. *26*, 334-344.

Bowers,K., Levi,B.P., Patel,F.I., and Stevens,T.H. (2000). The sodium/proton exchanger Nhx1p is required for endosomal protein

trafficking in the yeast Saccharomyces cerevisiae. Mol. Biol. Cell *11*, 4277-4294.

Brant,S.R., Yun,C.H.C., Donowitz,M., and Tse,C.-M. (1995). Cloning, tissue distribution, and functional analysis of the human Na^+/H^+ exchanger isoform, NHE3. Am. J. Physiol. *269*, C198-C206.

Brett,C.L., Donowitz,M., and Rao,R. (2005a). Evolutionary origins of eukaryotic sodium/proton exchangers. Am. J. Physiol Cell Physiol *288*, C223-C239.

Brett,C.L., Tukaye,D.N., Mukherjee,S., and Rao,R. (2005b). The Yeast Endosomal $Na^+(K^+)/H^+$ Exchanger Nhx1 Regulates Cellular pH to Control Vesicle Trafficking. Mol. Biol. Cell *16*, 1396-1405.

Brett,C.L., Wei,Y., Donowitz,M., and Rao,R. (2002). Human Na^+/H^+ exchanger isoform 6 is found in recycling endosomes of cells, not in mitochondria. Am. J. Physiol. Cell Physiol. *282*, C1031-C1041.

Brunig,I., Kaech,S., Brinkhaus,H., Oertner,T.G., and Matus,A. (2004). Influx of extracellular calcium regulates actin-dependent morphological plasticity in dendritic spines. Neuropharmacology *47*, 669-676.

Cagnac,O., Leterrier,M., Yeager,M., and Blumwald,E. (2007). Identification and characterization of Vnx1p, a novel type of vacuolar monovalent cation/H+ antiporter of Saccharomyces cerevisiae. J. Biol. Chem. *282*, 24284-24293.

Carden,D.E., Walker,D.J., Flowers,T.J., and Miller,A.J. (2003). Single-cell measurements of the contributions of cytosolic Na(+) and K(+) to salt tolerance. Plant Physiol *131*, 676-683.

Cardone,R.A., Casavola,V., and Reshkin,S.J. (2005). The role of disturbed pH dynamics and the Na^+/H^+ exchanger in metastasis. Nat. Rev. Cancer *5*, 786-795.

Casey,J.R., Grinstein,S., and Orlowski,J. (2010). Sensors and regulators of intracellular pH. Nat. Rev. Mol. Cell Biol. *11*, 50-61.

Ceci,M., Gaviraghi,C., Gorrini,C., Sala,L.A., Offenhauser,N., Marchisio,P.C., and Biffo,S. (2003). Release of eIF6 (p27BBP) from the 60S subunit allows 80S ribosome assembly. Nature *426*, 579-584.

Cha,B., Tse,M., Yun,C., Kovbasnjuk,O., Mohan,S., Hubbard,A., Arpin,M., and Donowitz,M. (2006). The NHE3 juxtamembrane cytoplasmic domain directly binds ezrin: dual role in NHE3 trafficking and mobility in the brush border. Mol. Biol. Cell *17*, 2661-2673.

Chambrey,R., St John,P.L., Eladari,D., Quentin,F., Warnock,D.G., Abrahamson,D.R., Podevin,R.A., and Paillard,M. (2001). Localization and functional characterization of Na+/H+ exchanger isoform NHE4 in rat thick ascending limbs. Am. J. Physiol. Renal Physiol. *281*, F707-F717.

Chambrey,R., Warnock,D.G., Podevin,R.A., Bruneval,P., Mandet,C., Bélair,M.F., Bariéty,J., and Paillard,M. (1998). Immunolocalization of the Na^+/H^+ exchanger isoform NHE2 in rat kidney. Am. J. Physiol. Renal Physiol. *275*, F379-F386.

Chang,B.Y., Conroy,K.B., Machleder,E.M., and Cartwright,C.A. (1998). RACK1, a receptor for activated C kinase and a homolog of the beta subunit of G proteins, inhibits activity of src tyrosine kinases and growth of NIH 3T3 cells. Mol. Cell Biol. *18*, 3245-3256.

Chien,C.-T., Bartel,P.L., Sternglanz,R., and Fields,S. (1991). The two-hybrid system: A method to identify and clone genes for proteins that interact with a protein of interest. Proc. Natl. Acad. Sci. USA *88*, 9578-9582.

Choi,J.Y., Shah,M., Lee,M.G., Schultheis,P.J., Shull,G.E., Muallem,S., and Baum,M. (2000). Novel amiloride-sensitive sodium-dependent proton

secretion in the mouse proximal convoluted tubule. J. Clin. Invest *105*, 1141-1146.

Chow,C.W., Khurana,S., Woodside,M., Grinstein,S., and Orlowski,J. (1999). The epithelial Na^+/H^+ exchanger, NHE3, is internalized through a clathrin-mediated pathway. J. Biol. Chem. *274*, 37551-37558.

Clayton-Smith,J. and Laan,L. (2003). Angelman syndrome: a review of the clinical and genetic aspects. J. Med. Genet. *40*, 87-95.

Condeelis,J. (1993). Life at the leading edge: the formation of cell protrusions. Annu. Rev. Cell Biol. *9*, 411-444.

Conti,L.R., Radeke,C.M., and Vandenberg,C.A. (2002). Membrane targeting of ATP-sensitive potassium channel. Effects of glycosylation on surface expression. J. Biol. Chem. *277*, 25416-25422.

Cooper,E.M., Hudson,A.W., Amos,J., Wagstaff,J., and Howley,P.M. (2004). Biochemical analysis of Angelman syndrome-associated mutations in the E3 ubiquitin ligase E6-associated protein. J. Biol. Chem. *279*, 41208-41217.

Cordat,E. and Casey,J.R. (2009). Bicarbonate transport in cell physiology and disease. Biochem. J. *417*, 423-439.

Counillon,L., Franchi,A., and Pouysségur,J. (1993a). A point mutation of the Na^+/H^+ exchanger gene (*NHE1*) and amplification of the mutated allele confer amiloride resistance upon chronic acidosis. Proc. Natl. Acad. Sci. USA *90*, 4508-4512.

Counillon,L., Noël,J., Reithmeier,R.A., and Pouysségur,J. (1997). Random mutagenesis reveals a novel site involved in inhibitor interaction within the fourth transmembrane segment of the Na^+/H^+ exchanger-1. Biochemistry *36*, 2951-2959.

Counillon,L., Pouysségur,J., and Reithmeier,R.A.F. (1994). The Na^+/H^+ exchanger NHE-1 possesses N- and O-linked glycosylation restricted to the first N-terminal extracellular domain. Biochemistry *33*, 10463-10469.

Counillon,L., Scholz,W., Lang,H.J., and Pouysségur,J. (1993b). Pharmacological characterization of stably transfected Na^+/H^+ antiporter isoforms using amiloride analogs and a new inhibitor exhibiting anti-ischemic properties. Mol. Pharmacol. *44*, 1041-1045.

Cox,G.A., Lutz,C.M., Yang,C.L., Biemesderfer,D., Bronson,R.T., Fu,A., Aronson,P.S., Noebels,J.L., and Frankel,W.N. (1997). Sodium/hydrogen exchanger gene defect in slow-wave epilepsy mutant mice. Cell *91*, 139-148.

Coyle,S.M., Gilbert,W.V., and Doudna,J.A. (2009). Direct link between RACK1 function and localization at the ribosome in vivo. Mol. Cell Biol. *29*, 1626-1634.

D'Souza,S., Garcia-Cabado,A., Yu,F., Teter,K., Lukacs,G.L., Skorecki,K., Moore,H.P., Orlowski,J., and Grinstein,S. (1998). The epithelial sodium-hydrogen antiporter Na^+/H^+ exchanger 3 accumulates and is functional in recycling endosomes. J. Biol. Chem. *273*, 2035-2043.

D'Souza-Schorey,C. and Chavrier,P. (2006). ARF proteins: roles in membrane traffic and beyond. Nat. Rev. Mol. Cell Biol. *7*, 347-358.

Danielsen,E.M. and van,D.B. (1995). A transferrin-like GPI-linked iron-binding protein in detergent-insoluble noncaveolar microdomains at the apical surface of fetal intestinal epithelial cells. J. Cell Biol. *131*, 939-950.

Darley,C.P., Van Wuytswinkel,O.C.M., Van der Woude,K., Mager,W.H., and De Boer,A.H. (2000). *Arabidopsis thaliana* and *Saccharomyces cerevisiae NHX1* genes encode amiloride sensitive electroneutral Na^+-/H^+ exchangers. Biochem. J. *351*, 241-249.

de Silva,M.G., Elliott,K., Dahl,H.H., Fitzpatrick,E., Wilcox,S., Delatycki,M., Williamson,R., Efron,D., Lynch,M., and Forrest,S. (2003). Disruption of a novel member of a sodium/hydrogen exchanger family and DOCK3 is associated with an attention deficit hyperactivity disorder-like phenotype. J. Med. Genet. *40*, 733-740.

Demaurex,N. (2002). pH Homeostasis of cellular organelles. News Physiol Sci. *17*, 1-5.

Demaurex,N., Furuya,W., D'Souza,S., Bonifacino,J.S., and Grinstein,S. (1998). Mechanism of acidification of the *trans*-Golgi network (TGN) - *In situ* measurements of pH using retrieval of TGN38 and furin from the cell surface. J. Biol. Chem. *273*, 2044-2051.

Demaurex,N., Romanek,R.R., Orlowski,J., and Grinstein,S. (1997). ATP dependence of Na^+/H^+ exchange - Nucleotide specificity and assessment of the role of phospholipids. J. Gen. Physiol. *109*, 117-128.

Denker,S.P. and Barber,D.L. (2002). Cell migration requires both ion translocation and cytoskeletal anchoring by the Na-H exchanger NHE1. J. Cell Biol. *159*, 1087-1096.

Denker,S.P., Huang,D.C., Orlowski,J., Furthmayr,H., and Barber,D.L. (2000). Direct binding of the Na-H exchanger NHE1 to ERM proteins regulates the cortical cytoskeleton and cell shape independently of H^+ translocation. Mol. Cell *6*, 1425-1436.

Dent,E.W., Kwiatkowski,A.V., Mebane,L.M., Philippar,U., Barzik,M., Rubinson,D.A., Gupton,S., Van Veen,J.E., Furman,C., Zhang,J., Alberts,A.S., Mori,S., and Gertler,F.B. (2007). Filopodia are required for cortical neurite initiation. Nat. Cell Biol. *9*, 1347-1359.

Dhariwala,F.A. and Rajadhyaksha,M.S. (2008). An unusual member of the Cdk family: Cdk5. Cell Mol. Neurobiol. *28*, 351-369.

Diering,G.H., Church,J., and Numata,M. (2009). Secretory Carrier Membrane Protein 2 Regulates Cell-surface Targeting of Brain-enriched Na^+/H^+ Exchanger NHE5. J. Biol. Chem. *284*, 13892-13903.

Dindot,S.V., Antalffy,B.A., Bhattacharjee,M.B., and Beaudet,A.L. (2008). The Angelman syndrome ubiquitin ligase localizes to the synapse and nucleus, and maternal deficiency results in abnormal dendritic spine morphology. Hum. Mol. Genet. *17*, 111-118.

Donowitz,M., Mohan,S., Zhu,C.X., Chen,T.E., Lin,R., Cha,B., Zachos,N.C., Murtazina,R., Sarker,R., and Li,X. (2009). NHE3 regulatory complexes. J. Exp. Biol. *212*, 1638-1646.

Erler,I., Al-Ansary,D.M., Wissenbach,U., Wagner,T.F., Flockerzi,V., and Niemeyer,B.A. (2006). Trafficking and assembly of the cold-sensitive TRPM8 channel. J. Biol. Chem. *281*, 38396-38404.

Fafournoux,P., Noël,J., and Pouysségur,J. (1994). Evidence that Na^+/H^+ exchanger isoforms NHE1 and NHE3 exist as stable dimers in membranes with a high degree of specificity for homodimers. J. Biol. Chem. *269*, 2589-2596.

Fanger,G.R., Widmann,C., Porter,A.C., Sather,S., Johnson,G.L., and Vaillancourt,R.R. (1998). 14-3-3 proteins interact with specific MEK kinases. J. Biol. Chem. *273*, 3476-3483.

Fernandez-Chacon,R., Achiriloaie,M., Janz,R., Albanesi,J.P., and Sudhof,T.C. (2000). SCAMP1 function in endocytosis. J. Biol. Chem. *275*, 12752-12756.

Flanigan,K., Gardner,K., Alderson,K., Galster,B., Otterud,B., Leppert,M.F., Kaplan,C., and Ptacek,L.J. (1996). Autosomal dominant spinocerebellar ataxia with sensory axonal neuropathy (SCA4): clinical description and

genetic localization to chromosome 16q22.1. Am. J. Hum. Genet. *59*, 392-399.

Forgac,M. (2007). Vacuolar ATPases: rotary proton pumps in physiology and pathophysiology. Nat. Rev. Mol. Cell Biol. *8*, 917-929.

Fukura,N., Ohgaki,R., Matsushita,M., Nakamura,N., Mitsui,K., and Kanazawa,H. (2010). A membrane-proximal region in the C-terminal tail of NHE7 is required for its distribution in the trans-Golgi network, distinct from NHE6 localization at endosomes. J. Membr. Biol. *234*, 149-158.

Fuster,D., Moe,O.W., and Hilgemann,D.W. (2008a). Steady-state function of the ubiquitous mammalian Na/H exchanger (NHE1) in relation to dimer coupling models with 2Na/2H stoichiometry. J. Gen. Physiol *132*, 465-480.

Fuster,D.G., Zhang,J., Shi,M., Bobulescu,I.A., Andersson,S., and Moe,O.W. (2008b). Characterization of the sodium/hydrogen exchanger NHA2. J. Am. Soc. Nephrol. *19*, 1547-1556.

Gahwiler,B.H., Capogna,M., Debanne,D., McKinney,R.A., and Thompson,S.M. (1997). Organotypic slice cultures: a technique has come of age. Trends Neurosci. *20*, 471-477.

Garbern,J.Y., Neumann,M., Trojanowski,J.Q., Lee,V.M., Feldman,G., Norris,J.W., Friez,M.J., Schwartz,C.E., Stevenson,R., and Sima,A.A. (2010). A mutation affecting the sodium/proton exchanger, SLC9A6, causes mental retardation with tau deposition. Brain *133*, 1391-1402.

Garlid,K.D., Sun,X., Paucek,P., and Woldegiorgis,G. (1995). Mitochondrial cation transport systems. Methods Enzymol. *260*, 331-348.

Gattineni,J., Sas,D., Dagan,A., Dwarakanath,V., and Baum,M. (2008). Effect of thyroid hormone on the postnatal renal expression of NHE8. Am. J. Physiol Renal Physiol *294*, F198-F204.

Gawenis,L.R., Greeb,J.M., Prasad,V., Grisham,C., Sanford,L.P., Doetschman,T., Andringa,A., Miller,M.L., and Shull,G.E. (2005). Impaired Gastric Acid Secretion in Mice with a Targeted Disruption of the NHE4 Na^+/H^+ Exchanger. J. Biol. Chem. *280*, 12781-12789.

Gaxiola,R.A., Rao,R., Sherman,A., Grisafi,P., Alper,S.L., Fink, and GR (1999). The Arabidopsis thaliana proton transporters, AtNhx1 and Avp1, can function in cation detoxification in yeast. Proc. Natl. Acad. Sci. USA *96*, 1480-1485.

Gekle,M., Drumm,K., Mildenberger,S., Freudinger,R., Gassner,B., and Silbernagl,S. (1999). Inhibition of Na^+-H^+ exchange impairs receptor-mediated albumin endocytosis in renal proximal tubule-derived epithelial cells from opossum. J. Physiol. (Lond.) *520*, 709-721.

Gekle,M., Volker,K., Mildenberger,S., Freudinger,R., Shull,G.E., and Wiemann,M. (2004). NHE3 Na^+/H^+ exchanger supports proximal tubular protein reabsorption in vivo. Am. J. Physiol Renal Physiol *287*, F469-F473.

Gentzsch,M., Cui,L., Mengos,A., Chang,X.B., Chen,J.H., and Riordan,J.R. (2003). The PDZ-binding Chloride Channel ClC-3B Localizes to the Golgi and Associates with Cystic Fibrosis Transmembrane Conductance Regulator-interacting PDZ Proteins. J. Biol. Chem. *278*, 6440-6449.

Gerbasi,V.R., Weaver,C.M., Hill,S., Friedman,D.B., and Link,A.J. (2004). Yeast Asc1p and mammalian RACK1 are functionally orthologous core 40S ribosomal proteins that repress gene expression. Mol. Cell Biol. *24*, 8276-8287.

Gietz,R.D., Triggs-Raine,B., Robbins,A., Graham,K.C., and Woods,R.A. (1997). Identification of proteins that interact with a protein of interest: applications of the yeast two-hybrid system. Mol. Cell Biochem. *172*, 67-79.

Gilfillan,G.D., Selmer,K.K., Roxrud,I., Smith,R., Kyllerman,M., Eiklid,K., Kroken,M., Mattingsdal,M., Egeland,T., Stenmark,H., Sjoholm,H., Server,A., Samuelsson,L., Christianson,A., Tarpey,P., Whibley,A., Stratton,M.R., Futreal,P.A., Teague,J., Edkins,S., Gecz,J., Turner,G., Raymond,F.L., Schwartz,C., Stevenson,R.E., Undlien,D.E., and Stromme,P. (2008). SLC9A6 mutations cause X-linked mental retardation, microcephaly, epilepsy, and ataxia, a phenotype mimicking Angelman syndrome. Am. J. Hum. Genet. *82*, 1003-1010.

Glozman,R., Okiyoneda,T., Mulvihill,C.M., Rini,J.M., Barriere,H., and Lukacs,G.L. (2009). N-glycans are direct determinants of CFTR folding and stability in secretory and endocytic membrane traffic. J. Cell Biol. *184*, 847-862.

Goedert,M. and Jakes,R. (1990). Expression of separate isoforms of human tau protein: correlation with the tau pattern in brain and effects on tubulin polymerization. EMBO J. *9*, 4225-4230.

Goedert,M., Spillantini,M.G., Jakes,R., Rutherford,D., and Crowther,R.A. (1989). Multiple isoforms of human microtubule-associated protein tau: sequences and localization in neurofibrillary tangles of Alzheimer's disease. Neuron *3*, 519-526.

Goyal,S., Mentone,S., and Aronson,P.S. (2005). Immunolocalization of NHE8 in Rat Kidney. Am. J. Physiol Renal Physiol *288*, F530-F538.

Goyal,S., Vanden Heuvel,G., and Aronson,P.S. (2003). Renal Expression of Novel Na^+-H^+ Exchanger Isoform NHE8. Am. J. Physiol. Renal Physiol. *284*, F467-F473.

Greer,P.L., Hanayama,R., Bloodgood,B.L., Mardinly,A.R., Lipton,D.M., Flavell,S.W., Kim,T.K., Griffith,E.C., Waldon,Z., Maehr,R., Ploegh,H.L., Chowdhury,S., Worley,P.F., Steen,J., and Greenberg,M.E. (2010). The

Angelman Syndrome protein Ube3A regulates synapse development by ubiquitinating arc. Cell *140*, 704-716.

Grinstein,S., Woodside,M., Waddell,T.K., Downey,G.P., Orlowski,J., Pouysségur,J., Wong,D.C.P., and Foskett,J.K. (1993). Focal localization of the NHE-1 isoform of the Na^+/H^+ antiport: Assessment of effects on intracellular pH. EMBO J. *12*, 5209-5218.

Gruwel,M.L., Rauw,V.L., Loewen,M., and Abrams,S.R. (2001). Effects of Sodium Chloride on plant cells; a 31P and 23Na NMR system to study salt tolerance. Plant Sci. *160*, 785-794.

Guillemot,F., Billault,A., and Auffray,C. (1989). Physical linkage of a guanine nucleotide-binding protein-related gene to the chicken major histocompatibility complex. Proc. Natl. Acad. Sci. U. S. A *86*, 4594-4598.

Guo,Z., Liu,L., Cafiso,D., and Castle,D. (2002). Perturbation of a very late step of regulated exocytosis by a secretory carrier membrane protein (SCAMP2)-derived peptide. J. Biol. Chem. *277*, 35357-35363.

Haber,M., Zhou,L., and Murai,K.K. (2006). Cooperative astrocyte and dendritic spine dynamics at hippocampal excitatory synapses. J. Neurosci. *26*, 8881-8891.

Hacker,G. (2000). The morphology of apoptosis. Cell Tissue Res. *301*, 5-17.

Haltiwanger,R.S. and Lowe,J.B. (2004). Role of glycosylation in development. Annu. Rev. Biochem. *73*, 491-537.

Han,W., Kim,K.H., Jo,M.J., Lee,J.H., Yang,J., Doctor,R.B., Moe,O.W., Lee,J., Kim,E., and Lee,M.G. (2006). Shank2 associates with and regulates Na^+/H^+ exchanger 3. J. Biol. Chem. *281*, 1461-1469.

Hara-Chikuma,M., Wang,Y., Guggino,S.E., Guggino,W.B., and Verkman,A.S. (2005a). Impaired acidification in early endosomes of ClC-5 deficient proximal tubule. Biochem. Biophys. Res. Commun. *329*, 941-946.

Hara-Chikuma,M., Yang,B., Sonawane,N.D., Sasaki,S., Uchida,S., and Verkman,A.S. (2005b). ClC-3 chloride channels facilitate endosomal acidification and chloride accumulation. J. Biol. Chem. *280*, 1241-1247.

Hayashi,H., Szaszi,K., and Grinstein,S. (2002). Multiple modes of regulation of Na^+/H^+ exchangers. Ann. N. Y. Acad. Sci. *976*, 248-258.

He,P. and Yun,C.C. (2010). Mechanisms of the regulation of the intestinal Na^+/H^+ exchanger NHE3. J. Biomed. Biotechnol. *2010*, 238080.

Helenius,A. and Aebi,M. (2001). Intracellular functions of N-linked glycans. Science *291*, 2364-2369.

Henkel,J.R., Gibson,G.A., Poland,P.A., Ellis,M.A., Hughey,R.P., and Weisz,O.A. (2000). Influenza M2 proton channel activity selectively inhibits *trans*-Golgi network release of apical membrane and secreted proteins in polarized Madin-Darby canine kidney cells. J. Cell Biol. *148*, 495-504.

Hill,J.K., Brett,C.L., Chyou,A., Kallay,L.M., Sakaguchi,M., Rao,R., and Gillespie,P.G. (2006). Vestibular hair bundles control pH with $(Na^+, K^+)/H^+$ exchangers NHE6 and NHE9. J. Neurosci. *26*, 9944-9955.

Hisamitsu,T., Pang,T., Shigekawa,M., and Wakabayashi,S. (2004). Dimeric interaction between the cytoplasmic domains of the Na^+/H^+ exchanger NHE1 revealed by symmetrical intermolecular cross-linking and selective co-immunoprecipitation. Biochemistry *43*, 11135-11143.

Hisamitsu,T., Yamada,K., Nakamura,T.Y., and Wakabayashi,S. (2007). Functional importance of charged residues within the putative intracellular loops in pH regulation by Na^+/ H^+ exchanger NHE1. FEBS J. *274*, 4326-4335.

Hofstetter,W., Siegrist,M., Simonin,A., Bonny,O., and Fuster,D.G. (2010). Sodium/hydrogen exchanger NHA2 in osteoclasts: Subcellular localization and role in vitro and in vivo. Bone.

Honda,T., Knobel,S.M., Bulus,N.M., and Ghishan,F.K. (1993). Kinetic characterization of stably expressed novel Na^+/H^+ exchanger (NHE-2). Biochim. Biophys. Acta Bio-Membr. *1150*, 199-202.

Honkura,N., Matsuzaki,M., Noguchi,J., Ellis-Davies,G.C., and Kasai,H. (2008). The subspine organization of actin fibers regulates the structure and plasticity of dendritic spines. Neuron *57*, 719-729.

Huibregtse,J.M., Scheffner,M., and Howley,P.M. (1993). Localization of the E6-AP regions that direct human papillomavirus E6 binding, association with p53, and ubiquitination of associated proteins. Mol. Cell Biol. *13*, 4918-4927.

Hunte,C., Screpanti,E., Venturi,M., Rimon,A., Padan,E., and Michel,H. (2005). Structure of a Na^+/H^+ antiporter and insights into mechanism of action and regulation by pH. Nature *435*, 1197-1202.

Hurtado-Lorenzo,A., Skinner,M., El,A.J., Futai,M., Sun-Wada,G.H., Bourgoin,S., Casanova,J., Wildeman,A., Bechoua,S., Ausiello,D.A., Brown,D., and Marshansky,V. (2006). V-ATPase interacts with ARNO and Arf6 in early endosomes and regulates the protein degradative pathway. Nat. Cell Biol. *8*, 124-136.

Huynh,K.K. and Grinstein,S. (2007). Regulation of vacuolar pH and its modulation by some microbial species. Microbiol. Mol. Biol. Rev. *71*, 452-462.

Jefferies,K.C., Cipriano,D.J., and Forgac,M. (2008). Function, structure and regulation of the vacuolar (H^+)-ATPases. Arch. Biochem. Biophys. *476*, 33-42.

Jentsch,T.J. (2007). Chloride and the endosomal-lysosomal pathway: emerging roles of CLC chloride transporters. J. Physiol *578*, 633-640.

Jiang,Y.H., Armstrong,D., Albrecht,U., Atkins,C.M., Noebels,J.L., Eichele,G., Sweatt,J.D., and Beaudet,A.L. (1998). Mutation of the Angelman ubiquitin ligase in mice causes increased cytoplasmic p53 and deficits of contextual learning and long-term potentiation. Neuron *21*, 799-811.

Johnson,L.S., Dunn,K.W., Pytowski,B., and McGraw,T.E. (1993). Endosome acidification and receptor trafficking: bafilomycin A1 slows receptor externalization by a mechanism involving the receptor's internalization motif. Mol. Biol. Cell *4*, 1251-1266.

Jones,J., Krag,S.S., and Betenbaugh,M.J. (2005). Controlling N-linked glycan site occupancy. Biochim. Biophys. Acta *1726*, 121-137.

Kapus,A., Grinstein,S., Wasan,S., Kandasamy,R.A., and Orlowski,J. (1994). Functional characterization of three isoforms of the Na^+/H^+ exchanger stably expressed in Chinese hamster ovary cells: ATP dependence, osmotic sensitivity and role in cell proliferation. J. Biol. Chem. *269*, 23544-23552.

Karmazyn,M., Gan,X.H.T., Humphreys,R.A., Yoshida,H., and Kusumoto,K. (1999). The myocardial Na^+-H^+ exchange - Structure, regulation, and its role in heart disease. Circ. Res. *85*, 777-786.

Kerjaschki,D., Noronha-Blob,L., Sacktor,B., and Farquhar,M.G. (1984). Microdomains of distinctive glycoprotein composition in the kidney proximal tubule brush border. J. Cell Biol. *98*, 1505-1513.

Khadilkar,A., Iannuzzi,P., and Orlowski,J. (2001). Identification of sites in the second exomembrane loop and ninth transmembrane helix of the

mammalian Na^+/H^+ exchanger important for drug recognition and cation translocation. J. Biol. Chem. *276*, 43792-43800.

Khan,I. (2001). Topology of the C-terminus of sodium hydrogen exchanger isoform-1: Presence of an extracellular epitope. Arch. Biochem. Biophys. *391*, 25-29.

Kim,J.H., Johannes,L., Goud,B., Antony,C., Lingwood,C.A., Daneman,R., and Grinstein,S. (1998). Noninvasive measurement of the pH of the endoplasmic reticulum at rest and during calcium release. Proc. Natl. Acad. Sci. USA *95*, 2997-3002.

Klanke,C.A., Su,Y.R., Callen,D.F., Wang,Z., Meneton,P., Baird,N., Kandasamy,R.A., Orlowski,J., Otterud,B.E., Leppert,M., Shull,G.E., and Menon,A.G. (1995). Molecular-Cloning and Physical and Genetic-Mapping of a Novel Human Na^+/H^+ Exchanger (NHE5/Slc9A5) to Chromosome 16q22.1. Genomics *25*, 615-622.

Kurashima,K., Yu,F.H., Cabado,A.G., Szabó,E.Z., Grinstein,S., and Orlowski,J. (1997). Identification of sites required for down-regulation of Na^+/H^+ exchanger NHE3 activity by cAMP-dependent protein kinase. Phosphorylation-dependent and -independent mechanisms. J. Biol. Chem. *272*, 28672-28679.

Lalande,M. and Calciano,M.A. (2007). Molecular epigenetics of Angelman syndrome. Cell Mol. Life Sci. *64*, 947-960.

Lawrence,S.P., Bright,N.A., Luzio,J.P., and Bowers,K. (2010). The Sodium/Proton Exchanger NHE8 Regulates Late Endosomal Morphology and Function. Mol. Biol. Cell.

Lehoux,S., Abe,J., Florian,J.A., and Berk,B.C. (2001). 14-3-3 binding to Na^+/H^+ exchanger isoform-1 is associated with serum-dependent activation of Na^+/H^+ exchange. J. Biol. Chem. *276*, 15794-15800.

Levine,S.A., Montrose,M.H., Tse,C.M., and Donowitz,M. (1993). Kinetics and regulation of three cloned mammalian Na^+/H^+ exchangers stably expressed in a fibroblast cell line. J. Biol. Chem. *268*, 25527-25535.

Liliental,J. and Chang,D.D. (1998). Rack1, a receptor for activated protein kinase C, interacts with integrin beta subunit. J. Biol. Chem. *273*, 2379-2383.

Lin,P.J., Williams,W.P., Kobiljski,J., and Numata,M. (2007). Caveolins bind to $(Na^+, K^+)/H^+$ exchanger NHE7 by a novel binding module. Cell Signal. *19*, 978-988.

Lin,P.J., Williams,W.P., Luu,Y., Molday,R.S., Orlowski,J., and Numata,M. (2005). Secretory carrier membrane proteins interact and regulate trafficking of the organellar $(Na^+,K^+)/H^+$ exchanger NHE7. J. Cell Sci. *118*, 1885-1897.

Liu,L., Guo,Z., Tieu,Q., Castle,A., and Castle,D. (2002). Role of secretory carrier membrane protein SCAMP2 in granule exocytosis. Mol. Biol. Cell *13*, 4266-4278.

Liu,L., Liao,H., Castle,A., Zhang,J., Casanova,J., Szabo,G., and Castle,D. (2005). SCAMP2 interacts with Arf6 and phospholipase D1 and links their function to exocytotic fusion pore formation in PC12 cells. Mol. Biol. Cell *16*, 4463-4472.

Liu,Y.V. and Semenza,G.L. (2007). RACK1 vs. HSP90: competition for HIF-1 alpha degradation vs. stabilization. Cell Cycle *6*, 656-659.

Lundstrom,K., Abenavoli,A., Malgaroli,A., and Ehrengruber,M.U. (2003). Novel Semliki Forest virus vectors with reduced cytotoxicity and temperature sensitivity for long-term enhancement of transgene expression. Mol. Ther. *7*, 202-209.

Luo,L., Hensch,T.K., Ackerman,L., Barbel,S., Jan,L.Y., and Jan,Y.N. (1996). Differential effects of the Rac GTPase on Purkinje cell axons and dendritic trunks and spines. Nature *379*, 837-840.

Luo,S., Vacher,C., Davies,J.E., and Rubinsztein,D.C. (2005). Cdk5 phosphorylation of huntingtin reduces its cleavage by caspases: implications for mutant huntingtin toxicity. J. Cell Biol. *169*, 647-656.

Maccioni,R.B., Otth,C., Concha,I.I., and Munoz,J.P. (2001). The protein kinase Cdk5. Structural aspects, roles in neurogenesis and involvement in Alzheimer's pathology. Eur. J. Biochem. *268*, 1518-1527.

Malakooti,J., Dahdal,R.Y., Schmidt,L., Layden,T.J., Dudeja,P.K., and Ramaswamy,K. (1999). Molecular cloning, tissue distribution, and functional expression of the human Na^+/H^+ exchanger NHE2. Am. J. Physiol. Gastrointest. Liver Physiol. *277*, G383-G390.

Marshansky,V. and Futai,M. (2008). The V-type H^+-ATPase in vesicular trafficking: targeting, regulation and function. Curr. Opin. Cell Biol. *20*, 415-426.

Masereel,B., Pochet,L., and Laeckmann,D. (2003). An overview of inhibitors of Na^+/H^+ exchanger. Eur. J. Med. Chem. *38*, 547-554.

Matsuzaki,M. (2007). Factors critical for the plasticity of dendritic spines and memory storage. Neurosci. Res. *57*, 1-9.

Matsuzaki,M., Honkura,N., Ellis-Davies,G.C., and Kasai,H. (2004). Structural basis of long-term potentiation in single dendritic spines. Nature *429*, 761-766.

Mattila,P.K. and Lappalainen,P. (2008). Filopodia: molecular architecture and cellular functions. Nat. Rev. Mol. Cell Biol. *9*, 446-454.

Matus,A. (2000). Actin-based plasticity in dendritic spines. Science *290*, 754-758.

McCahill,A., Warwicker,J., Bolger,G.B., Houslay,M.D., and Yarwood,S.J. (2002). The RACK1 scaffold protein: a dynamic cog in cell response mechanisms. Mol. Pharmacol. *62*, 1261-1273.

Mellman,I. (1992). The importance of being acid: the role of acidification in intracellular membrane traffic. J. Exp. Biol. *172*, 39-45.

Mellman,I., Fuchs,R., and Helenius,A. (1986). Acidification of the endocytic and exocytic pathways. Annu. Rev. Biochem. *55*, 663-700.

Miura,K., Kishino,T., Li,E., Webber,H., Dikkes,P., Holmes,G.L., and Wagstaff,J. (2002). Neurobehavioral and electroencephalographic abnormalities in Ube3a maternal-deficient mice. Neurobiol. Dis. *9*, 149-159.

Miyazaki,E., Sakaguchi,M., Wakabayashi,S., Shigekawa,M., and Mihara,K. (2001). NHE6 protein possesses a signal peptide destined for endoplasmic reticulum membrane and localizes in secretory organelles of the cell. J. Biol. Chem. *276*, 49221-49227.

Mochly-Rosen,D., Khaner,H., and Lopez,J. (1991). Identification of intracellular receptor proteins for activated protein kinase C. Proc. Natl. Acad. Sci. U. S. A *88*, 3997-4000.

Morrow,E.M., Yoo,S.Y., Flavell,S.W., Kim,T.K., Lin,Y., Hill,R.S., Mukaddes,N.M., Balkhy,S., Gascon,G., Hashmi,A., Al-Saad,S., Ware,J., Joseph,R.M., Greenblatt,R., Gleason,D., Ertelt,J.A., Apse,K.A., Bodell,A., Partlow,J.N., Barry,B., Yao,H., Markianos,K., Ferland,R.J., Greenberg,M.E., and Walsh,C.A. (2008). Identifying autism loci and genes by tracing recent shared ancestry. Science *321*, 218-223.

Mukherjee,S., Kallay,L., Brett,C.L., and Rao,R. (2006). Mutational analysis of the intramembranous H10 loop of yeast Nhx1 reveals a critical role in ion homoeostasis and vesicle trafficking. Biochem. J. *398*, 97-105.

Murtazina,R., Booth,B.J., Bullis,B.L., Singh,D.N., and Fliegel,L. (2001). Functional analysis of polar amino-acid residues in membrane associated regions of the NHE1 isoform of the mammalian Na+/H+ exchanger. Eur. J. Biochem. *268*, 4674-4685.

Nakamura,N., Tanaka,S., Teko,Y., Mitsui,K., and Kanazawa,H. (2005). Four Na^+/H^+ exchanger isoforms are distributed to Golgi and post-Golgi compartments and are involved in organelle pH regulation. J. Biol. Chem. *280*, 1561-1572.

Nakayama,A.Y., Harms,M.B., and Luo,L. (2000). Small GTPases Rac and Rho in the maintenance of dendritic spines and branches in hippocampal pyramidal neurons. J. Neurosci. *20*, 5329-5338.

Nass,R., Cunningham,K.W., and Rao,R. (1997). Intracellular sequestration of sodium by a novel Na^+/H^+ exchanger in yeast is enhanced by mutations in the plasma membrane H^+-ATPase. Insights into mechanisms of sodium tolerance. J. Biol. Chem. *272*, 26145-26152.

Nass,R. and Rao,R. (1998). Novel localization of a Na^+/H^+ exchanger in a late endosomal compartment of yeast - Implications for vacuole biogenesis. J. Biol. Chem. *273*, 21054-21060.

Nass,R. and Rao,R. (1999). The yeast endosomal Na^+/H^+ exchanger, Nhx1, confers osmotolerance following acute hypertonic shock. Microbiology *145*, 3221-3228.

Newey,S.E., Velamoor,V., Govek,E.E., and Van Aelst,L. (2005). Rho GTPases, dendritic structure, and mental retardation. J. Neurobiol. *64*, 58-74.

Neystat,M., Rzhetskaya,M., Oo,T.F., Kholodilov,N., Yarygina,O., Wilson,A., El-Khodor,B.F., and Burke,R.E. (2001). Expression of cyclin-dependent kinase 5 and its activator p35 in models of induced apoptotic death in neurons of the substantia nigra in vivo. J. Neurochem. *77*, 1611-1625.

Ng,J., Nardine,T., Harms,M., Tzu,J., Goldstein,A., Sun,Y., Dietzl,G., Dickson,B.J., and Luo,L. (2002). Rac GTPases control axon growth, guidance and branching. Nature *416*, 442-447.

Nikolic,M., Chou,M.M., Lu,W., Mayer,B.J., and Tsai,L.H. (1998). The p35/Cdk5 kinase is a neuron-specific Rac effector that inhibits Pak1 activity. Nature *395*, 194-198.

Numata,M. and Orlowski,J. (2001). Molecular Cloning and Characterization of a Novel (Na^+,K^+)/H^+ Exchanger Localized to the *trans*-Golgi Network. J. Biol. Chem. *276*, 17387-17394.

Numata,M., Petrecca,K., Lake,N., and Orlowski,J. (1998). Identification of a mitochondrial Na^+/H^+ exchanger. J. Biol. Chem. *273*, 6951-6959.

Ohgaki,R., Fukura,N., Matsushita,M., Mitsui,K., and Kanazawa,H. (2008). Cell surface levels of organellar Na^+/H^+ exchanger isoform 6 are regulated by interaction with RACK1. J. Biol. Chem. *283*, 4417-4429.

Ohgaki,R., Matsushita,M., Kanazawa,H., Ogihara,S., Hoekstra,D., and Van IJzendoorn,S.C. (2010). The Na^+/H^+ exchanger NHE6 in the endosomal recycling system is involved in the development of apical bile canalicular surface domains in HepG2 cells. Mol. Biol. Cell *21*, 1293-1304.

Ohtsubo,K. and Marth,J.D. (2006). Glycosylation in cellular mechanisms of health and disease. Cell *126*, 855-867.

Olkhova,E., Hunte,C., Screpanti,E., Padan,E., and Michel,H. (2006). Multiconformation continuum electrostatics analysis of the NhaA Na^+/H^+

antiporter of Escherichia coli with functional implications. Proc. Natl. Acad. Sci. U. S. A *103*, 2629-2634.

Olkhova,E., Kozachkov,L., Padan,E., and Michel,H. (2009). Combined computational and biochemical study reveals the importance of electrostatic interactions between the "pH sensor" and the cation binding site of the sodium/proton antiporter NhaA of Escherichia coli. Proteins *76*, 548-559.

Olkhova,E., Padan,E., and Michel,H. (2007). The influence of protonation states on the dynamics of the NhaA antiporter from Escherichia coli. Biophys. J. *92*, 3784-3791.

Onishi,I., Lin,P.J., Diering,G.H., Williams,W.P., and Numata,M. (2007). RACK1 associates with NHE5 in focal adhesions and positively regulates the transporter activity. Cell Signal. *19*, 194-203.

Orlowski,J. (1993). Heterologous expression and functional properties of the amiloride high affinity (NHE-1) and low affinity (NHE-3) isoforms of the rat Na/H exchanger. J. Biol. Chem. *268*, 16369-16377.

Orlowski,J. and Grinstein,S. (2004). Diversity of the mammalian sodium/proton exchanger SLC9 gene family. Pflugers Arch. - Eur. J. Physiol. *447*, 549-565.

Orlowski,J. and Grinstein,S. (2007). Emerging roles of alkali cation/proton exchangers in organellar homeostasis. Curr. Opin. Cell Biol. *19*, 483-492.

Orlowski,J., Kandasamy,R.A., and Shull,G.E. (1992). Molecular cloning of putative members of the Na/H exchanger gene family. cDNA cloning, deduced amino acid sequence, and mRNA tissue expression of the rat Na/H exchanger NHE- 1 and two structurally related proteins. J. Biol. Chem. *267*, 9331-9339.

Otsu,K., Kinsella,J.L., Heller,P., and Froehlich,J.P. (1993). Sodium dependence of the Na^+-H^+ exchanger in the pre-steady state. Implications for the exchange mechanism. J. Biol. Chem. *268*, 3184-3193.

Otsu,K., Kinsella,J.L., Koh,E., and Froehlich,J.P. (1992). Proton dependence of the partial reactions of the sodium-proton exchanger in renal brush border membranes. J. Biol. Chem. *267*, 8089-8096.

Pang,T., Hisamitsu,T., Mori,H., Shigekawa,M., and Wakabayashi,S. (2004). Role of calcineurin B homologous protein in pH regulation by the Na^+/H^+ exchanger 1: tightly bound Ca2+ ions as important structural elements. Biochemistry *43*, 3628-3636.

Pang,T., Su,X., Wakabayashi,S., and Shigekawa,M. (2001). Calcineurin homologous protein as an essential cofactor for Na^+/H^+ exchangers. J. Biol. Chem. *276*, 17367-17372.

Pang,T., Wakabayashi,S., and Shigekawa,M. (2002). Expression of calcineurin B homologous protein 2 protects serum deprivation-induced cell death by serum-independent activation of Na^+/H^+ exchanger. J. Biol. Chem. *277*, 43771-43777.

Pardo,J.M., Cubero,B., Leidi,E.O., and Quintero,F.J. (2006). Alkali cation exchangers: roles in cellular homeostasis and stress tolerance. J. Exp. Bot. *57*, 1181-1199.

Parent,A., Laroche,G., Hamelin,E., and Parent,J.L. (2008). RACK1 regulates the cell surface expression of the G protein-coupled receptor for thromboxane A(2). Traffic *9*, 394-407.

Park,M., Penick,E.C., Edwards,J.G., Kauer,J.A., and Ehlers,M.D. (2004). Recycling endosomes supply AMPA receptors for LTP. Science *305*, 1972-1975.

Park,M., Salgado,J.M., Ostroff,L., Helton,T.D., Robinson,C.G., Harris,K.M., and Ehlers,M.D. (2006). Plasticity-induced growth of dendritic spines by exocytic trafficking from recycling endosomes. Neuron *52*, 817-830.

Paroutis,P., Touret,N., and Grinstein,S. (2004). The pH of the secretory pathway: measurement, determinants, and regulation. Physiology. (Bethesda.) *19*, 207-215.

Peti-Peterdi,J., Chambrey,R., Bebok,Z., Biemesderfer,D., St John,P.L., Abrahamson,D.R., Warnock,D.G., and Bell,P.D. (2000). Macula densa Na^+/H^+ exchange activities mediated by apical NHE2 and basolateral NHE4 isoforms. Am. J. Physiol. *278*, F452-F463.

Petrecca,K., Atanasiu,R., Grinstein,S., Orlowski,J., and Shrier,A. (1999). Subcellular localization of the Na^+/H^+ exchanger NHE1 in rat myocardium. Am. J. Physiol. Heart Circ. Physiol. *276*, H709-H717.

Pham,L., Purcell,P., Morse,L., Stashenko,P., and Battaglino,R.A. (2007). Expression analysis of nha-oc/NHA2: a novel gene selectively expressed in osteoclasts. Gene Expr. Patterns. *7*, 846-851.

Porter,K., Prescott,D., and Frye,J. (1973). Changes in surface morphology of Chinese hamster ovary cells during the cell cycle. J. Cell Biol. *57*, 815-836.

Pouysségur,J., Sardet,C., Franchi,A., L'Allemain,G., and Paris,S. (1984). A specific mutation abolishing Na^+/H^+ antiport activity in hamster fibroblasts precludes growth at neutral and acidic pH. Proc. Natl. Acad. Sci. USA *81*, 4833-4837.

Prior,C., Potier,S., Souciet,J.L., and Sychrova,H. (1996). Characterization of the *NHA1* gene encoding a Na^+/H^+- antiporter of the yeast *Saccharomyces cerevisiae*. FEBS Lett. *387*, 89-93.

Pulakat,L., Cooper,S., Knowle,D., Mandavia,C., Bruhl,S., Hetrick,M., and Gavini,N. (2005). Ligand-dependent complex formation between the Angiotensin II receptor subtype AT2 and Na^+/H^+ exchanger NHE6 in mammalian cells. Peptides *26*, 863-873.

Putney,L.K. and Barber,D.L. (2003). Na-H exchange-dependent increase in intracellular pH times G2/M entry and transition. J. Biol. Chem. *278*, 44645-44649.

Qiu,Q.S., Barkla,B.J., Vera-Estrella,R., Zhu,J.K., and Schumaker,K.S. (2003). Na^+/H^+ exchange activity in the plasma membrane of Arabidopsis. Plant Physiol *132*, 1041-1052.

Qiu,Q.S., Guo,Y., Quintero,F.J., Pardo,J.M., Schumaker,K.S., and Zhu,J.K. (2004). Regulation of vacuolar Na^+/H^+ exchange in Arabidopsis thaliana by the salt-overly-sensitive (SOS) pathway. J. Biol. Chem. *279*, 207-215.

Reiter,L.T., Seagroves,T.N., Bowers,M., and Bier,E. (2006). Expression of the Rho-GEF Pbl/ECT2 is regulated by the UBE3A E3 ubiquitin ligase. Hum. Mol. Genet. *15*, 2825-2835.

Rockwell,N.C. and Fuller,R.S. (2002). Specific modulation of Kex2/furin family proteases by potassium. J. Biol. Chem. *277*, 17531-17537.

Rodriguez-Rosales,M.P., Galvez,F.J., Huertas,R., Aranda,M.N., Baghour,M., Cagnac,O., and Venema,K. (2009). Plant NHX cation/proton antiporters. Plant Signal. Behav. *4*, 265-276.

Ron,D., Chen,C.-H., Caldwell,J., Jamieson,L., Orr,E., and Mochly-Rosen,D. (1994). Cloning of an intracellular receptor for protein kinase C: A homolog of the β subunit of G proteins. Proc. Natl. Acad. Sci. USA *91*, 839-843.

Roos,A. and Boron,W.F. (1981). Intracellular pH. Physiol. Rev. *61*, 296-434.

Rosskopf,D., Scholz,W., Lang,H.J., Schölkens,B.A., and Siffert,W. (1995). HOE 694 blocks Na^+/H^+ exchange in human B lymphoblasts without influencing proliferation. Cell. Physiol. Biochem. *5*, 269-275.

Rossmann,H., Sonnentag,T., Heinzmann,A., Seidler,B., Bachmann,O., Vieillard-Baron,D., Gregor,M., and Seidler,U. (2001). Differential expression and regulation of Na^+/H^+ exchanger isoforms in rabbit parietal and mucous cells. Am. J. Physiol. Gastrointest. Liver Physiol. *281*, G447-G458.

Rotin,D. and Grinstein,S. (1989). Impaired cell volume regulation in Na^+-H^+ exchange-deficient mutants. Am. J. Physiol. *257*, C1158-C1165.

Ruan,Y., Guo,L., Qiao,Y., Hong,Y., Zhou,L., Sun,L., Wang,L., Zhu,H., Wang,L., Yun,X., Xie,J., and Gu,J. (2009). RACK1 associates with CLEC-2 and promotes its ubiquitin-proteasome degradation. Biochem. Biophys. Res. Commun. *390*, 217-222.

Samuels,B.A., Hsueh,Y.P., Shu,T., Liang,H., Tseng,H.C., Hong,C.J., Su,S.C., Volker,J., Neve,R.L., Yue,D.T., and Tsai,L.H. (2007). Cdk5 promotes synaptogenesis by regulating the subcellular distribution of the MAGUK family member CASK. Neuron *56*, 823-837.

Sardet,C., Franchi,A., and Pouysségur,J. (1989). Molecular cloning, primary structure, and expression of the human growth factor-activatable Na/H antiporter. Cell *56*, 271-280.

Sato,Y., Ariyoshi,N., Mihara,K., and Sakaguchi,M. (2004). Topogenesis of NHE1: direct insertion of the membrane loop and sequestration of cryptic glycosylation and processing sites just after TM9. Biochem. Biophys. Res. Commun. *324*, 281-287.

Schapiro,F.B. and Grinstein,S. (2000). Determinants of the pH of the Golgi complex. J. Biol. Chem. *275*, 21025-21032.

Scheffner,M., Huibregtse,J.M., Vierstra,R.D., and Howley,P.M. (1993). The HPV-16 E6 and E6-AP complex functions as a ubiquitin-protein ligase in the ubiquitination of p53. Cell *75*, 495-505.

Scholz,W., Albus,U., Counillon,L., Gögelein,H., Lang,H.-J., Linz,W., Weichert,A., and Schölkens,B.A. (1995). Protective effects of HOE642, a selective sodium-hydrogen exchange subtype 1 inhibitor, on cardiac ischaemia and reperfusion. Cardiovasc. Res. *29*, 260-268.

Schoonderwoert,V.T., Holthuis,J.C., Tanaka,S., Tooze,S.A., and Martens,G.J. (2000). Inhibition of the vacuolar H+-ATPase perturbs the transport, sorting, processing and release of regulated secretory proteins. Eur. J. Biochem. *267*, 5646-5654.

Schultheis,P.J., Clarke,L.L., Meneton,P., Harline,M., Boivin,G.P., Stemmermann,G., Duffy,J.J., Doetschman,T., Miller,M.L., and Shull,G.E. (1998a). Targeted disruption of the murine Na^+/H^+ exchanger isoform 2 gene causes reduced viability of gastric parietal cells and loss of net acid secretion. J. Clin. Invest. *101*, 1243-1253.

Schultheis,P.J., Clarke,L.L., Meneton,P., Miller,M.L., Soleimani,M., Gawenis,L.R., Riddle,T.M., Duffy,J.J., Doetschman,T., Wang,T., Giebisch,G., Aronson,P.S., Lorenz,J.N., and Shull,G.E. (1998b). Renal and intestinal absorptive defects in mice lacking the NHE3 Na^+/H^+ exchanger. Nature Genet. *19*, 282-285.

Schwark,J.R., Jansen,H.W., Lang,H.-J., Krick,W., Burchardt,G., and Hropot,M. (1998). S3226, a novel inhibitor of Na^+/H^+ exchanger subtype 3 in various cell types. Pflügers Arch. *436*, 797-800.

Scott,D.B., Blanpied,T.A., Swanson,G.T., Zhang,C., and Ehlers,M.D. (2001). An NMDA receptor ER retention signal regulated by phosphorylation and alternative splicing. J. Neurosci. *21*, 3063-3072.

Sekino,Y., Kojima,N., and Shirao,T. (2007). Role of actin cytoskeleton in dendritic spine morphogenesis. Neurochem. Int. *51*, 92-104.

Sengupta,J., Nilsson,J., Gursky,R., Spahn,C.M., Nissen,P., and Frank,J. (2004). Identification of the versatile scaffold protein RACK1 on the eukaryotic ribosome by cryo-EM. Nat. Struct. Mol. Biol. *11*, 957-962.

Sklan,E.H., Podoly,E., and Soreq,H. (2006). RACK1 has the nerve to act: structure meets function in the nervous system. Prog. Neurobiol. *78*, 117-134.

Slepkov,E.R., Rainey,J.K., Sykes,B.D., and Fliegel,L. (2007). Structural and functional analysis of the Na^+/H^+ exchanger. Biochem. J. *401*, 623-633.

Soleimani,M., Singh,G., Bookstein,C., Rao,M.C., Chang,E.B., and Dominguez,J.H. (1996). Inhibition of glycosylation decreases Na^+/H^+ exchange activity, blocks NHE-3 transport to the membrane, and increases NHE-3 mRNA expression in LLC-PK_1 cells. J. Lab. Clin. Med. *127*, 565-573.

Soroka,C.J., Xu,S., Mennone,A., Lam,P., and Boyer,J.L. (2008). N-Glycosylation of the alpha subunit does not influence trafficking or functional activity of the human organic solute transporter alpha/beta. BMC. Cell Biol. *9*, 57.

Soto,A.G. and Trejo,J. (2010). N-linked glycosylation of protease-activated receptor-1 second extracellular loop: a critical determinant for ligand-induced receptor activation and internalization. J. Biol. Chem. *285*, 18781-18793.

Steele,M.R., McCahill,A., Thompson,D.S., MacKenzie,C., Isaacs,N.W., Houslay,M.D., and Bolger,G.B. (2001). Identification of a surface on the beta-propeller protein RACK1 that interacts with the cAMP-specific phosphodiesterase PDE4D5. Cell Signal. *13*, 507-513.

Sychrova,H., Ramirez,J., and Pena,A. (1999). Involvement of Nha1 antiporter in regulation of intracellular pH in Saccharomyces cerevisiae. FEMS Microbiol. Lett. *171*, 167-172.

Szabó,E.Z., Numata,M., Lukashova,V., Iannuzzi,P., and Orlowski,J. (2005). β-Arrestins bind and decrease cell-surface abundance of the Na^+/H^+ exchanger NHE5 isoform. Proc. Natl. Acad. Sci. U. S. A *102*, 2790-2795.

Szabó,E.Z., Numata,M., Shull,G.E., and Orlowski,J. (2000). Kinetic and pharmacological properties of human brain Na^+/H^+ exchanger isoform 5 stably expressed in Chinese hamster ovary cells. J. Biol. Chem. *275*, 6302-6307.

Szaszi,K., Paulsen,A., Szabó,E.Z., Numata,M., Grinstein,S., and Orlowski,J. (2002). Clathrin-mediated endocytosis and recycling of the neuron-specific Na^+/H^+ exchanger NHE5 isoform: regulation by phosphatidylinositol 3'-kinase and the actin cytoskeleton. J. Biol. Chem. *277*, 42623-42632.

Takahashi,E., Abe,J., Gallis,B., Aebersold,R., Spring,D.J., Krebs,E.G., and Berk,B.C. (1999). $p90^{RSK}$ is a serum-stimulated Na^+/H^+ exchanger isoform-1 kinase - Regulatory phosphorylation of serine 703 of Na^+/H^+ exchanger isoform-1. J. Biol. Chem. *274*, 20206-20214.

Thomson,R.B., Wang,T., Thomson,B.R., Tarrats,L., Girardi,A., Mentone,S., Soleimani,M., Kocher,O., and Aronson,P.S. (2005). Role of PDZK1 in membrane expression of renal brush border ion exchangers. Proc. Natl. Acad. Sci. U. S. A *102*, 13331-13336.

Tiffany,A.M., Manganas,L.N., Kim,E., Hsueh,Y.P., Sheng,M., and Trimmer,J.S. (2000). PSD-95 and SAP97 exhibit distinct mechanisms for regulating K(+) channel surface expression and clustering. J. Cell Biol. *148*, 147-158.

Tominaga,T. and Barber,D.L. (1998). Na-H exchange acts downstream of RhoA to regulate integrin-induced cell adhesion and spreading. Mol. Biol. Cell *9*, 2287-2303.

Tominaga,T., Ishizaki,T., Narumiya,S., and Barber,D.L. (1998). p160ROCK mediates RhoA activation of Na-H exchange. EMBO J. *17*, 4712-4722.

Tse,C.-M., Brant,S.R., Walker,M.S., Pouysségur,J., and Donowitz,M. (1992). Cloning and sequencing of a rabbit cDNA encoding an intestinal and kidney-specific Na^+/H^+ exchanger isoform (NHE-3). J. Biol. Chem. *267*, 9340-9346.

Tse,C.-M., Levine,S.A., Yun,C.H.C., Brant,S.R., Pouysségur,J., Montrose,M.H., and Donowitz,M. (1993a). Functional characteristics of a cloned epithelial Na^+/H^+ exchanger (NHE3): Resistance to amiloride and inhibition by protein kinase C. Proc. Natl. Acad. Sci. USA *90*, 9110-9114.

Tse,C.-M., Levine,S.A., Yun,C.H.C., Montrose,M.H., Little,P.J., Pouysségur,J., and Donowitz,M. (1993b). Cloning and expression of a rabbit cDNA encoding a serum- activated ethylisopropylamiloride-resistant epithelial Na^+/H^+ exchanger isoform (NHE-2). J. Biol. Chem. *268*, 11917-11924.

Van Buggenhout G. and Fryns,J.P. (2009). Angelman syndrome (AS, MIM 105830). Eur. J. Hum. Genet. *17*, 1367-1373.

Van Buggenhout,G. and Fryns,J.P. (2009). Angelman syndrome (AS, MIM 105830). Eur. J. Hum. Genet. *17*, 1367-1373.

van Weert,A.W., Dunn,K.W., Gueze,H.J., Maxfield,F.R., and Stoorvogel,W. (1995). Transport from late endosomes to lysosomes, but not sorting of integral membrane proteins in endosomes, depends on the vacuolar proton pump. J. Cell Biol. *130*, 821-834.

van Woerden,G.M., Harris,K.D., Hojjati,M.R., Gustin,R.M., Qiu,S., de Avila,F.R., Jiang,Y.H., Elgersma,Y., and Weeber,E.J. (2007). Rescue of neurological deficits in a mouse model for Angelman syndrome by reduction of αCaMKII inhibitory phosphorylation. Nat. Neurosci. *10*, 280-282.

Venema,K., Belver,A., Marin-Manzano,M.C., Rodriguez-Rosales,M.P., and Donaire,J.P. (2003). A novel intracellular K^+/H^+ antiporter related to Na^+/H^+ antiporters is important for K^+ ion homeostasis in plants. J. Biol. Chem. *278*, 22453-22459.

Venema,K., Quintero,F.J., Pardo,J.M., and Donaire,J.P. (2002). The arabidopsis Na^+/H^+ exchanger AtNHX1 catalyzes low affinity Na^+ and K^+ transport in reconstituted liposomes. J. Biol. Chem. *277*, 2413-2418.

Vermes,I., Haanen,C., Steffens-Nakken,H., and Reutelingsperger,C. (1995). A novel assay for apoptosis. Flow cytometric detection of phosphatidylserine expression on early apoptotic cells using fluorescein labelled Annexin V. J. Immunol. Methods *184*, 39-51.

von Andrian,U.H., Hasslen,S.R., Nelson,R.D., Erlandsen,S.L., and Butcher,E.C. (1995). A central role for microvillous receptor presentation in leukocyte adhesion under flow. Cell *82*, 989-999.

Wakabayashi,S., Bertrand,B., Ikeda,T., Pouysségur,J., and Shigekawa,M. (1994). Mutation of calmodulin-binding site renders the Na^+/H^+ exchanger (NHE1) highly H^+-sensitive and Ca^{2+} regulation- defective. J. Biol. Chem. *269*, 13710-13715.

Wakabayashi,S., Fafournoux,P., Sardet,C., and Pouysségur,J. (1992). The Na^+/H^+ antiporter cytoplasmic domain mediates growth factor signals and controls "H^+-sensing". Proc. Natl. Acad. Sci. USA *89*, 2424-2428.

Wakabayashi,S., Ikeda,T., Iwamoto,T., Pouysségur,J., and Shigekawa,M. (1997). Calmodulin-binding autoinhibitory domain controls "pH-sensing" in the Na^+/H^+ exchanger NHE1 through sequence-specific interaction. Biochemistry *36*, 12854-12861.

Wakabayashi,S., Pang,T., Su,X., and Shigekawa,M. (2000). A novel topology model of the human Na^+/H^+ exchanger isoform 1. J. Biol. Chem. *275*, 7942-7949.

Wang,D., King,S.M., Quill,T.A., Doolittle,L.K., and Garbers,D.L. (2003). A new sperm-specific Na^+/H^+ Exchanger required for sperm motility and fertility. Nat. Cell Biol. *5*, 1117-1122.

Wang,D., Lee,H.J., Cooper,D.S., Cebotaro,L., Walden,P.D., Choi,I., and Yun,C.C. (2006). Coexpression of MAST205 inhibits the activity of Na^+/H^+ exchanger NHE3. Am. J. Physiol Renal Physiol *290*, F428-F437.

Wang,Z., Orlowski,J., and Shull,G.E. (1993). Primary structure and functional expression of a novel gastrointestinal isoform of the rat Na/H exchanger. J. Biol. Chem. *268*, 11925-11928.

Watanabe,I., Zhu,J., Recio-Pinto,E., and Thornhill,W.B. (2004). Glycosylation affects the protein stability and cell surface expression of Kv1.4 but Not Kv1.1 potassium channels. A pore region determinant dictates the effect of glycosylation on trafficking. J. Biol. Chem. *279*, 8879-8885.

Watanabe,I., Zhu,J., Sutachan,J.J., Gottschalk,A., Recio-Pinto,E., and Thornhill,W.B. (2007). The glycosylation state of Kv1.2 potassium

channels affects trafficking, gating, and simulated action potentials. Brain Res. *1144*, 1-18.

Weeber,E.J., Jiang,Y.H., Elgersma,Y., Varga,A.W., Carrasquillo,Y., Brown,S.E., Christian,J.M., Mirnikjoo,B., Silva,A., Beaudet,A.L., and Sweatt,J.D. (2003). Derangements of hippocampal calcium/calmodulin-dependent protein kinase II in a mouse model for Angelman mental retardation syndrome. J. Neurosci. *23*, 2634-2644.

Weinman,E.J., Cunningham,R., and Shenolikar,S. (2005). NHERF and regulation of the renal sodium-hydrogen exchanger NHE3. Pflugers Arch. *450*, 137-144.

Weisz,O.A. (2003a). Acidification and protein traffic. Int. Rev. Cytol. *226*, 259-319.

Weisz,O.A. (2003b). Organelle acidification and disease. Traffic. *4*, 57-64.

Wells,K.M. and Rao,R. (2001). The yeast Na^+/H^+ exchanger Nhx1 is an N-linked glycoprotein - Topological implications. J. Biol. Chem. *276*, 3401-3407.

White,B.C., Sullivan,J.M., DeGracia,D.J., O'Neil,B.J., Neumar,R.W., Grossman,L.I., Rafols,J.A., and Krause,G.S. (2000). Brain ischemia and reperfusion: molecular mechanisms of neuronal injury. J. Neurol. Sci. *179*, 1-33.

Williams,K.A. (2000). Three-dimensional structure of the ion-coupled transport protein NhaA. Nature *403*, 112-115.

Wu,K.L., Khan,S., Lakhe-Reddy,S., Jarad,G., Mukherjee,A., Obejero-Paz,C.A., Konieczkowski,M., Sedor,J.R., and Schelling,J.R. (2004). The NHE1 Na^+/H^+ exchanger recruits ezrin/radixin/moesin proteins to regulate Akt-dependent cell survival. J. Biol. Chem. *279*, 26280-26286.

Wu,M.M., Grabe,M., Adams,S., Tsien,R.Y., Moore,H.P., and Machen,T.E. (2001). Mechanisms of pH regulation in the regulated secretory pathway. J. Biol. Chem. *276*, 33027-33035.

Xiang,M., Feng,M., Muend,S., and Rao,R. (2007). A human Na^+/H^+ antiporter sharing evolutionary origins with bacterial NhaA may be a candidate gene for essential hypertension. Proc. Natl. Acad. Sci. U. S. A *104*, 18677-18681.

Xu,H., Chen,H., Dong,J., Lynch,R., and Ghishan,F.K. (2008). Gastrointestinal distribution and kinetic characterization of the sodium-hydrogen exchanger isoform 8 (NHE8). Cell Physiol Biochem. *21*, 109-116.

Xu,H., Chen,R., and Ghishan,F.K. (2005). Subcloning, localization, and expression of the rat intestinal sodium-hydrogen exchanger isoform 8. Am. J. Physiol Gastrointest. Liver Physiol *289*, G36-G41.

Xu,H., Zhang,B., Li,J., Chen,H., Tooley,J., and Ghishan,F.K. (2010a). Epidermal growth factor inhibits intestinal NHE8 expression via reducing its basal transcription. Am. J. Physiol Cell Physiol *299*, C51-C57.

Xu,H., Zhang,B., Li,J., Chen,H., Wang,C., and Ghishan,F.K. (2010b). Transcriptional inhibition of intestinal NHE8 expression by glucocorticoids involves Pax5. Am. J. Physiol Gastrointest. Liver Physiol.

Yaka,R., Thornton,C., Vagts,A.J., Phamluong,K., Bonci,A., and Ron,D. (2002). NMDA receptor function is regulated by the inhibitory scaffolding protein, RACK1. Proc. Natl. Acad. Sci. U. S. A *99*, 5710-5715.

Yamaguchi,T., Aharon,G.S., Sottosanto,J.B., and Blumwald,E. (2005). Vacuolar Na+/H+ antiporter cation selectivity is regulated by calmodulin from within the vacuole in a Ca2+- and pH-dependent manner. Proc. Natl. Acad. Sci. U. S. A *102*, 16107-16112.

Yamaguchi,T., Apse,M.P., Shi,H., and Blumwald,E. (2003). Topological analysis of a plant vacuolar Na+/H+ antiporter reveals a luminal C terminus that regulates antiporter cation selectivity. Proc. Natl. Acad. Sci. U. S. A *100*, 12510-12515.

Yamaguchi,T., Fukada-Tanaka,S., Inagaki,Y., Saito,N., Yonekura-Sakakibara,K., Tanaka,Y., Kusumi,T., and Iida,S. (2001). Genes encoding the vacuolar Na^+/H^+ exchanger and flower coloration. Plant Cell Physiol *42*, 451-461.

Yamashiro,D.J. and Maxfield,F.R. (1984). Acidification of endocytic compartments and the intracellular pathways of ligands and receptors. J. Cell Biochem. *26*, 231-246.

Yan,W.H., Nehrke,K., Choi,J., and Barber,D.L. (2001). The Nck-interacting kinase (NIK) phosphorylates the Na^+-H^+ exchanger NHE1 and regulates NHE1 activation by platelet-derived growth factor. J. Biol. Chem. *276*, 31349-31356.

Yashiro,K., Riday,T.T., Condon,K.H., Roberts,A.C., Bernardo,D.R., Prakash,R., Weinberg,R.J., Ehlers,M.D., and Philpot,B.D. (2009). Ube3a is required for experience-dependent maturation of the neocortex. Nat. Neurosci. *12*, 777-783.

Ye,G., Chen,C., Han,D., Xiong,X., Kong,Y., Wan,B., and Yu,L. (2006). Cloning of a novel human NHEDC1 (Na^+/H^+ exchanger like domain containing 1) gene expressed specifically in testis. Mol. Biol. Rep. *33*, 175-180.

Yoshida,K., Kawachi,M., Mori,M., Maeshima,M., Kondo,M., Nishimura,M., and Kondo,T. (2005). The involvement of tonoplast proton pumps and $Na^+(K^+)/H^+$ exchangers in the change of petal color during flower opening of Morning Glory, Ipomoea tricolor cv. Heavenly Blue. Plant Cell Physiol *46*, 407-415.

Yu,F.H., Shull,G.E., and Orlowski,J. (1993). Functional properties of the rat Na/H exchanger NHE-2 isoform expressed in Na/H exchanger-deficient Chinese hamster ovary cells. J. Biol. Chem. *268*, 25536-25541.

Yun,C.H.C., Little,P.J., Nath,S.K., Levine,S.A., Pouysségur,J., Tse,C.M., and Donowitz,M. (1993). Leu143 in the putative fourth membrane spanning domain is critical for amiloride inhibition of an epithelial Na^+/H^+ exchanger isoform (NHE-2). Biochem. Biophys. Res. Commun. *193*, 532-539.

Zaun,H.C., Shrier,A., and Orlowski,J. (2008). Calcineurin B homologous protein 3 promotes the biosynthetic maturation, cell surface stability, and optimal transport of the Na+/H+ exchanger NHE1 isoform. J. Biol. Chem. *283*, 12456-12467.

Zerbini,G., Maestroni,A., Breviario,D., Mangili,R., and Casari,G. (2003). Alternative Splicing of NHE-1 Mediates Na-Li Countertransport and Associates With Activity Rate. Diabetes *52*, 1511-1518.

Zhang,J., Bobulescu,I.A., Goyal,S., Aronson,P.S., Baum,M.G., and Moe,O.W. (2007). Characterization of Na^+/H^+ Exchanger NHE8 in Cultured Renal Epithelial Cells. Am. J. Physiol Renal Physiol *293*, F761-F766.

Zhao,H., Wiederkehr,M.R., Fan,L.Z., Collazo,R.L., Crowder,L.A., and Moe,O.W. (1999). Acute inhibition of Na/H exchanger NHE-3 by cAMP - Role of protein kinase A and NHE-3 phosphoserines 552 and 605. J. Biol. Chem. *274*, 3978-3987.

Zheng,J.Q., Wan,J.J., and Poo,M.M. (1996). Essential role of filopodia in chemotropic turning of nerve growth cone induced by a glutamate gradient. J. Neurosci. *16*, 1140-1149.

Zhu,L., Jang,G.F., Jastrzebska,B., Filipek,S., Pearce-Kelling,S.E., Aguirre,G.D., Stenkamp,R.E., Acland,G.M., and Palczewski,K. (2004). A naturally occurring mutation of the opsin gene (T4R) in dogs affects glycosylation and stability of the G protein-coupled receptor. J. Biol. Chem. *279*, 53828-53839.

Zielinski,R.E. (1998). CALMODULIN AND CALMODULIN-BINDING PROTEINS IN PLANTS. Annu. Rev. Plant Physiol Plant Mol. Biol. *49*, 697-725.

Zito,K., Knott,G., Shepherd,G.M., Shenolikar,S., and Svoboda,K. (2004). Induction of spine growth and synapse formation by regulation of the spine actin cytoskeleton. Neuron *44*, 321-334.

APPENDIX

Candidate interacting proteins of NHE6 identified by yeast two-hybrid screening of a human brain cDNA library

CYTOSKELETON	SIGNALLING	SCAFFOLDING PROTEINS	CHANNELS/TRANSPORTERS	CELL METABOLISM	MISCELLANEOUS
RAC1	Cyclin-dependent kinase 5 (CDK5)	RACK1	Solute carrier organic anion transporter 2B1 (SLCO2B1)	Aldolase A	V-ATPase lysosomal accessory protein 2
Actin-like 6B (ACTL6B)	Se/Thr kinase receptor associated protein (STRAP)	DOK4	Chloride intracellular channel 1 (CLIC-1)		Ubiquitin-activating enzyme E1 (UBE1)
Tubulin, β2	Erbb2 interacting protein (ERBB2IP)	Ankyrin repeat and SOCS box-containing 3 (ASB3)	Apolipoprotein D		Stabilin1
	STAT3	SH3 domain binding glutamic acid-rich protein (SH3BGR)	Alpha-2-macroglobulin receptor		Ataxin 2-binding protein
	WD repeat domain 18				Cyclin B1 interacting protein 1 (CCB1P1)
					Phospholypase A2, group IVB (cytosolic)
					Atrophin 1